



HAL
open science

Elaboration of anti-inflammatory textiles based on eco-friendly microcapsules

Thi Chinh Thuy Dao

► **To cite this version:**

Thi Chinh Thuy Dao. Elaboration of anti-inflammatory textiles based on eco-friendly microcapsules. Materials. Université de Lyon; Institut Polytechnique (Hanoi), 2018. English. NNT : 2018LYSE1025 . tel-01967337v2

HAL Id: tel-01967337

<https://theses.hal.science/tel-01967337v2>

Submitted on 8 Jan 2019

HAL is a multi-disciplinary open access archive for the deposit and dissemination of scientific research documents, whether they are published or not. The documents may come from teaching and research institutions in France or abroad, or from public or private research centers.

L'archive ouverte pluridisciplinaire **HAL**, est destinée au dépôt et à la diffusion de documents scientifiques de niveau recherche, publiés ou non, émanant des établissements d'enseignement et de recherche français ou étrangers, des laboratoires publics ou privés.



N°d'ordre NNT : 2018LYSE1025

THESE de DOCTORAT DE L'UNIVERSITE DE LYON

opérée au sein de

l'Université Claude Bernard Lyon 1

Ecole Doctorale N° 34

Ecole Doctorale Matériaux de Lyon

Spécialité de doctorat :

Matériaux

Soutenue publiquement le 08/02/2018, par :

DAO Thi Chinh Thuy

Elaboration de texticaments à visée anti-inflammatoire contenant des microcapsules respectueuses de l'environnement

Devant le jury composé de :

- | | |
|--|------------------------------|
| 1. Assoc. Prof. VU Thi Hong Khanh, Hanoi University of Science and Technology | Examineur |
| 2. Prof. PONCELET Denis, Ecole Nationale Vétérinaire, Agroalimentaire et de l'Alimentation Nantes-Atlantique | Rapporteur |
| 3. Prof. TRAN Nhat Chuong, Vietnam Textile and Garment Association | Rapporteur |
| 4. Prof. BUI Chuong, Hanoi University of Science and Technology | Examineur |
| 5. Dr. DAO Anh Tuan, Hanoi University of Science and Technology | Examineur |
| 6. Assoc. Prof. GOUANVÉ Fabrice, Université Claude Bernard Lyon 1 | Examineur |
| 7. Assoc. Prof. SINTES-ZYDOWICZ Nathalie, Université Claude Bernard Lyon 1 | Co-directrice de thèse |
| 8. Assoc. Prof. CHU Dieu Huong, Hanoi University of Science and Technology | Directrice de thèse, Invitée |

UNIVERSITE CLAUDE BERNARD - LYON 1

Président de l'Université

Président du Conseil Académique

Vice-président du Conseil d'Administration

Vice-président du Conseil Formation et Vie Universitaire

Vice-président de la Commission Recherche

Directrice Générale des Services

M. le Professeur Frédéric FLEURY

M. le Professeur Hamda BEN HADID

M. le Professeur Didier REVEL

M. le Professeur Philippe CHEVALIER

M. Fabrice VALLÉE

Mme Dominique MARCHAND

COMPOSANTES SANTE

Faculté de Médecine Lyon Est – Claude Bernard

Faculté de Médecine et de Maïeutique Lyon Sud – Charles Mérieux

Faculté d'Odontologie

Institut des Sciences Pharmaceutiques et Biologiques

Institut des Sciences et Techniques de la Réadaptation

Département de formation et Centre de Recherche en Biologie Humaine

Directeur : M. le Professeur G.RODE

Directeur : Mme la Professeure C. BURILLON

Directeur : M. le Professeur D. BOURGEOIS

Directeur : Mme la Professeure C. VINCIGUERRA

Directeur : M. X. PERROT

Directeur : Mme la Professeure A-M. SCHOTT

COMPOSANTES ET DEPARTEMENTS DE SCIENCES ET TECHNOLOGIE

Faculté des Sciences et Technologies

Département Biologie

Département Chimie Biochimie

Département GEP

Département Informatique

Département Mathématiques

Département Mécanique

Département Physique

UFR Sciences et Techniques des Activités Physiques et Sportives

Observatoire des Sciences de l'Univers de Lyon

Polytech Lyon

Ecole Supérieure de Chimie Physique Electronique

Institut Universitaire de Technologie de Lyon 1

Ecole Supérieure du Professorat et de l'Education

Institut de Science Financière et d'Assurances

Directeur : M. F. DE MARCHI

Directeur : M. le Professeur F. THEVENARD

Directeur : Mme C. FELIX

Directeur : M. Hassan HAMMOURI

Directeur : M. le Professeur S. AKKOUCHE

Directeur : M. le Professeur G. TOMANOV

Directeur : M. le Professeur H. BEN HADID

Directeur : M. le Professeur J-C PLENET

Directeur : M. Y.VANPOULLE

Directeur : M. B. GUIDERDONI

Directeur : M. le Professeur E.PERRIN

Directeur : M. G. PIGNAULT

Directeur : M. le Professeur C. VITON

Directeur : M. le Professeur A. MOUGNIOTTE

Directeur : M. N. LEBOISNE

PLEDGE

I assure that:

This thesis is my own research under the guidance and supervision of my thesis supervisors.

The information and results in this thesis are reported honestly, a part of them has been published in scientific journals with the permission of co-authors, and the rest has not been mentioned in any publications.

Hanoi, 26/03/2018

On behalf of supervisors

PhD Student

Assoc. Prof. CHU Dieu Huong

DAO Thi Chinh Thuy

ACKNOWLEDGEMENTS

Firstly, I would like to express my profound gratitude to the two supervisors: Ass. Prof. CHU Dieu Huong and Ass. Prof. SINTES-ZYDOWICZ Nathalie, for their support, motivation and review during my PhD course.

I would like to thank the Board of Directors and all my colleagues at School of Textile - Leather and Fashion (Hanoi University of Science and Technology), who helped me a lot with teaching works so that I could concentrate on my thesis.

I also would like to thank the staff of Ingénierie des Matériaux Polymères (IMP) at University Claude Bernard Lyon 1: Prof. CASSAGNAU Philippe - the Director, the teachers, the postdocs and the PhD students, who supported me a lot during the time I worked at IMP.

I would like to acknowledge the financial support of the research project France-Vietnam Hoasen Lotus N° 27917ZH "Research on producing medical textile based on microencapsulation technology" and of the French Ministry of Foreign Affairs and International Development through the Eiffel scholarship (No. 840683J). These valuable grants give me facilities for doing experiments and having five months to study at IMP.

I also would like to thank all people who have given time and dedication to carry out some of the analytical tests and provide me the necessary resources to complete my thesis. As for the staff of Hanoi University of Science and Technology: I thank Mr. PHAM Duc Duong and Ms. TRAN Thi Phuong Thao (Department of Textile Material and Chemistry Technology) for training me to use the laboratory conditioning chamber and the Kawabata system; I thank Mr. VU Toan Thang, Mr. VU Van Quang and their students (Department of Precision Mechanical & Optical Engineering) for technical improvements on coating equipment Mini Coater so that I could control the coating speed during finishing textile with microcapsules; I thank Mr. HA Vinh Hung (Cleaner Production Center) for training me to use the vacuum drier OV-11; I thank Mr. NGUYEN Huu Dung (Laboratory of Electron Microscopy and Microanalysis) for the SEM works on microcapsule-treated fabrics; I thank Ms. NGUYEN Thi Ha Hanh and Ms. CHU Thi Hai Nam (Laboratory of Petrochemical and Catalysis Adsorption Materials) for the analyses on microcapsule size distribution and FTIR; and I thank Ms. LE Lan Chi (Center for Research and Development in Biotechnology) for training me to use the centrifuge, the UV-Vis equipment and the optical microscope. As for the staff of Ingénierie des Matériaux Polymères (University Claude Bernard Lyon 1): I thank Mr. ALCOUFFE Pierre for ESEM and cryo-SEM analyses on microcapsules; I thank Mr. MÉLIS Flavien for gas chromatography analyses; I thank Ms. CREPET Agnes and Mr. HADDANE Ali for all technical assistances during my five months of working at IMP.

Finally, I would like to show my deepest gratefulness to the most important people in my life: my parents, my sisters, my husband and my daughters, who always encourage me to improve myself.

TABLE OF CONTENT

LIST OF ABBREVIATIONS	4
LIST OF FIGURES	6
LIST OF TABLES	10
INTRODUCTION	12
1. Chapter 1: Literature review	16
1.1. Microcapsules and their textile applications	16
1.1.1. Microcapsules	16
1.1.2. Applications and requirements of microcapsules in the textile field	20
1.1.3. Microcapsules prepared from environment-friendly materials for textile applications	24
1.2. Microencapsulation by the solvent evaporation technique	25
1.2.1. Techniques of microencapsulation.....	25
1.2.2. Microencapsulation by the solvent evaporation technique.....	26
1.2.2.1. Basic principle of the technique	26
1.2.2.2. Important parameters of the microencapsulation by the solvent evaporation technique ..	27
1.2.2.3. Using non-halogenated solvents in the microencapsulation by the solvent evaporation technique.....	31
1.2.2.4. The quillaja saponin bio-sourced surfactant	32
1.3. The textile substrates	38
1.3.1. Influence of the textile substrate on the microcapsule loading capability of microcapsule-treated fabrics.....	38
1.3.2. Influence of the textile substrate on the microcapsule distribution of microcapsule- treated fabrics	40
1.3.3. Influence of the textile substrate on the active release capability from the microcapsule-treated fabrics.....	41
1.3.4. The interlock knitted fabrics	42
1.4. Textile finishing with microcapsules	45
1.4.1. Techniques of finishing textiles with microcapsules.....	45
1.4.2. Influence of the drying conditions on the microcapsule morphology after finishing process	47
1.5. Conclusions of the literature review	49
2. Chapter 2: Experimental methods	50
2.1. Materials	50
2.1.1. Interlock knitted fabrics	50
2.1.2. Chemicals for microencapsulation.....	51
2.2. Research contents	53
2.3. Experimental techniques	54
2.3.1. Determining the suitable microcapsule size for textile application.....	54

2.3.2. Evaluating the surface-active properties of quillaja saponin.....	55
2.3.3. Investigating the influence of the microencapsulation parameters on microcapsule characteristics	56
2.3.3.1. Microencapsulation	56
2.3.3.2. Microcapsule characterization.....	58
2.3.4. Investigating the influence of textile substrate on the characteristics of microcapsule-treated fabric	61
2.3.4.1. Structural parameters of the interlock knitted fabrics	61
2.3.4.2. Influence of textile material on characteristics of microcapsule-treated fabric	63
2.3.4.3. Influence of the loop length on the characteristics of the microcapsule-treated fabric	67
2.3.4.4. Influence of the fabric extension on the transdermal drug release capability of fabric	72
2.3.5. Investigating the influence of the drying conditions on the microcapsule morphology after finishing process	74
3. Chapter 3: Results and discussions	75
3.1. Microencapsulation of ibuprofen	75
3.1.1. Determination of the microcapsule size for the targeted textile application.....	75
3.1.2. Surface-active properties of quillaja saponin S4521 (Sigma Aldrich).....	77
3.1.3. Influence of the microencapsulation parameters on the microcapsule size and morphology	79
3.1.3.1. Influence of the saponin concentration	79
3.1.3.2. Influence of the stirring rate.....	84
3.1.3.3. Influence of the volume of ethyl acetate added to the aqueous phase	86
3.1.4. Conclusions on the microencapsulation parameters suitable for textile applications	90
3.1.5. Other characteristics of C0.075 microcapsules	91
3.2. Influence of the drying conditions on the microcapsule morphology after textile finishing process	93
3.2.1. Influence of the humidity during the drying process	94
3.2.2. Influence of the drying temperature	95
3.3. Influence of the textile substrate on the characteristics of the microcapsule-treated fabrics.....	97
3.3.1. Influence of the textile material type	97
3.3.1.1. Influence on the microcapsule loading capability.....	97
3.3.1.2. Influence on the microcapsule distribution.....	99
3.3.1.3. Influence on the ibuprofen release capability of the microcapsule-treated fabric.....	102
3.3.1.4. Conclusion.....	104
3.3.2. Influence of the loop length	104
3.3.2.1. Influence on the microcapsule loading capability.....	105
3.3.2.2. Influence on the microcapsule distribution.....	114
3.3.2.3. Influence on the ibuprofen release capability of the fabric.....	126
3.3.2.4. Conclusion.....	127
3.3.3. Influence of the fabric extension.....	128
3.4. Conclusion of Chapter 3	130
4. Final conclusions and future outlook.....	134

4.1. Final conclusions	134
4.2. Future outlook	135
REFERENCES	136
LIST OF PUBLISHED WORKS OF THE THESIS	147
APPENDIX	148

LIST OF ABBREVIATIONS

Abbréviation	Explication
<i>Organizations</i>	
HUST	Hanoi University of Science and Technology
IMP	Ingénierie des Matériaux Polymères, UMR CNRS 5223
UCBL	University Claude Bernard Lyon 1
ASTM	American Society for Testing and Materials
ISO	International Organization for Standardization
TCVN	Vietnam National Standards
<i>Experimental techniques and equipments</i>	
FRSE	Microencapsulation by the solvent evaporation method with the fast rate of the solvent evaporation
NRSE	Microencapsulation by the solvent evaporation method with the normal rate of the solvent evaporation
FTIR	Fourier-Transform Infrared Spectroscopy
HPLC	High-performance liquid chromatography
SEM	Scanning electron microscopy
UV-Vis	UV visible spectroscopy
<i>Materials and their characteristics</i>	
CMC	Critical micellar concentration
E	Microencapsulation efficiency
Eudragit RSPO	Poly(ethyl acrylate-co-methyl methacrylate-co-triméthylammonioéthyl méthacrylate chlorure) 1:2:0.1
HLB	Hydrophilic-lipophilic balance
MLC	Microcapsule loading capability of the

	microcapsule-treated fabric
L	Drug loading ratio of microcapsule
PCL	Poly- ϵ -caprolactone
PCM	Phase change material
PLGA	Poly(lactic-co-glycolic acid)
PLLA	Poly (l-lactic acid)
PU	Polyurethane
PVA	Poly (vinyl alcohol)
γ	Surface tension of a solution
<i>Structural parameters of the interlock knitted fabric</i>	
l	loop length
L_u	Length of yarn in a structural knitted cell
P_d	Course density
P_n	Wale density
P_s	Area density
SKC	Structural knitted cell
S_u	Number of the structural knitted cells per unit area of the fabric
M_{fbr}	Mass per unit area of the fabric
t	Fabric thickness
D	Yarn diameter in the fabric
P	Fabric porosity
ρ	Fiber density

LIST OF FIGURES

Figure 1.1: Microcapsule classification on the basis of their morphology [31]	16
Figure 1.2: SEM image of PLGA microsphere containing progesterone [121]	17
Figure 1.3: An example of the size distribution curve of microcapsules [140].....	18
Figure 1.4: Four types of theoretical curves describing the release mechanisms of the active ingredients from the non-erodible microcapsules [104].....	19
Figure 1.5: Classification of microencapsulation methods	25
Figure 1.6: Diagram of basic principle of microencapsulation by solvent evaporation technique [76]	26
Figure 1.7: SEM images of microcapsules with different mass ratio of core/shell: 60:40 (A); 70:30 (B); 75:25 (C) [84].....	29
Figure 1.8: SEM images of microspheres made by FRSE (on the left) and NRSE (on the right) [26].....	31
Figure 1.9: Schematic illustration of a surfactant [49]	34
Figure 1.10: Determination of CMC by the curve surface tension-lnC [92].....	35
Figure 1.11: Illustration of a spherical micelle [93]	36
Figure 1.12: General molecular structure of quillaja saponin, in which R^1 , R^2 , R^3 groups depend on different molecules in the bark extract [98]	37
Figure 1.13: SEM images of fabrics padded with microcapsules: polyester fabric (A) and cotton fabric (B) [125]	40
Figure 1.14: SEM images of polyester fabric (A) and cotton fabric (B) coated with microcapsules containing flame - retardant agent [40]	41
Figure 1.15: Structure (A) and notation (B) of interlock knitted fabric [1].....	42
Figure 1.16: Structure of knitted loop [1].....	43
Figure 1.17: Model of interlock knitted loop by Dabiryan-Jeddi [27] (A) Front view; (B) Plane view; (C) Side view; (D) a plain structure.....	44
Figure 1.18: SEM images of wet-coated nylon fabrics with and without microcapsules: without microcapsules (a), with 10% (b), 20% (c) and 30% microcapsules (d) [66]	47
Figure 1.19: SEM images of dry-coated nylon fabrics with and without microcapsules: without microcapsules (a), with 10% (b), 20% (c) and 30% microcapsules (d) [66].....	47
Figure 1.20: SEM images of microcapsule padded cotton fabrics with different drying temperature 120 °(11.1-11.2); 140 °C (11.3-11.4); 160 °C (11.5-11.6) [88].....	48
Figure 2.1: Structural formula of ibuprofen ($C_{13}H_{18}O_2$) [14].....	51
Figure 2.2: Chemical structure of Miglyol 812 [58]	52
Figure 2.3: Chemical structure of eudragit RSPO [147]	53

Figure 2.4: Tensiometer SEO-DST30M (Surface & Electro-Optics)	55
Figure 2.5: Diagram of microencapsulation of eudragit RSPO loading ibuprofen by solvent evaporation method	56
Figure 2.6: Equipment system for microencapsulation	57
Figure 2.7: Centrifuge G-16KS of Sigma.....	57
Figure 2.8: Optical microscopy Olympus EX 41	58
Figure 2.9: Scanning electron microscopy QUANTA FEG 250.....	58
Figure 2.10: Mastersizer 2000, Malvern Instruments.....	59
Figure 2.11: Ultrasonic equipment Fisher biolock Scientific 750W	60
Figure 2.12: Spectrometer UV-Vis Lamda 35 (Perkin Elmer).....	60
Figure 2.13: Gas chromatograph Agilent Technology 6890N	61
Figure 2.14: Experimental washing machine Electrolux.....	62
Figure 2.15: Laboratory conditioning chamber M250-RH	62
Figure 2.16: Electronic scale OHAUS - PA413	63
Figure 2.17: Thickness gauge	63
Figure 2.18: Vacuum drier France Etuves.....	63
Figure 2.19: Fabric samples soaking in the microcapsule suspension	64
Figure 2.20: Scanning electron microscopy QUANTA FEG 250 – FEI company	65
Figure 2.21: Interface of Meander 3.1.2 during determining the area of microcapsule aggregate	65
Figure 2.22: Glass jar simulating Franz diffusion cell	66
Figure 2.23: Drug release in vitro experiment.....	66
Figure 2.24: HPLC system of SHIMADZU	67
Figure 2.25: Coating equipment Mini Coater (DaeLim Starlet Co.,Ltd)	68
Figure 2.26: Vacuum drier OV-11	68
Figure 2.27: Scanning electron microscopy JEOL JSM - 7600F	70
Figure 2.28: A step in the in vitro experiment of transdermal drug release	71
Figure 2.29: HPLC system of Merck Hitachi.....	72
Figure 2.30: Experimental design to create different levels of fabric extension.....	73
Figure 3.1: SEM image of the surface of fabric B3.....	75
Figure 3.2: Distance between fibers in the region of loop legs on cotton interlock fabric B3 ..	76
Figure 3.3: Distance between fibers in the region created by overlapping loops on cotton interlock fabric B3	76
Figure 3.4: Surface tension of aqueous saponin solutions according to saponin concentration	78

Figure 3.5: Size distributions of microcapsule lots C0.025, C0.050, C0.075 and C0.100	80
Figure 3.6: $A_{\text{dense}}/A_{\text{surf}}$ ratio depending on the saponin concentration	81
Figure 3.7: Optical microscope images of microcapsules C0.025 (A), C0.050 (B), C0.075 (C) and C0.100 (D)	83
Figure 3.8: Optical microscope images of microcapsules R700 (A), R650 (B) and R600 (C)	85
Figure 3.9: Size distributions of microcapsules R700, R650 and R600	86
Figure 3.10: Size distributions of microcapsule lots S0, S8 and S12	87
Figure 3.11: Optical microscope image of microcapsule S8	88
Figure 3.12: Optical microscope images of the cotton interlock fabrics coated with microcapsules S0 (A), S8 (B) and S12 (C) after 24 hours of vacuum drying at 25°C	90
Figure 3.13: SEM images of the C0.075 microcapsules (A): overall image; (B): image of the microcapsule surface	92
Figure 3.14: SEM image of cross-section of microcapsule C0.075	92
Figure 3.15: SEM image of the microcapsule coated fabric dried at 25°C with the drying humidity rate of 65%	94
Figure 3.16: SEM image of the microcapsule coated fabric dried at 25°C with the drying humidity rate of 20%	94
Figure 3.17: SEM image of the microcapsule coated fabric dried at 25°C with the drying humidity rate of 0%	95
Figure 3.18: SEM image of the cotton interlock fabric coated with microcapsules with vacuum drying at 25°C	96
Figure 3.19: SEM image of the cotton interlock fabric coated with microcapsules with vacuum drying at 35°C	96
Figure 3.20: SEM image of the cotton interlock fabric coated with microcapsules with vacuum drying at 45°C	96
Figure 3.21: SEM image of the cotton interlock fabric coated with microcapsules with vacuum drying at 60°C	96
Figure 3.22: SEM images of the microcapsule-treated fabrics Cot_1 (A), 6535_1 (B) and Pet_1 (C)	101
Figure 3.23: Chemical structure of polyester fiber	102
Figure 3.24: Chemical structure of cellulose (main component of cotton fiber)	102
Figure 3.25: Release rate of ibuprofen from microcapsule-treated fabrics according to the type of the textile material	103
Figure 3.26: Microcapsule loading capability of the fabrics according to the loop length with a microcapsule concentration of 14 mg/ml	107

Figure 3.27: Microcapsule loading capability of the fabrics according to the loop length with a microcapsule concentration of 24 mg/ml	108
Figure 3.28: Fabric density according to the loop length	111
Figure 3.29: Fabric porosity according to the loop length	112
Figure 3.30: SEM images of the lower surface of the fabrics B1 (A) and B5 (B)	113
Figure 3.31: SEM images of the fabrics after microcapsule application by the coating technique B1 (A), B2 (B), B3 (C), B4 (D) and B5 (E).....	117
Figure 3.32: SEM images of the fabrics after microcapsule application by the impregnating technique: B3 (A), B4 (B) and B5 (C).....	125
Figure 3.33: Weight percentage of ibuprofen released into the receptor fluid according to the fabric extension.....	129

LIST OF TABLES

Table 1.1: The values of K for different kinds of fabrics [17]	42
Table 2.1: Information of chemicals used for microencapsulation	51
Table 2.2: Some properties of ibuprofen [151]	51
Table 2.3: Doses of ibuprofen for adults and children [14, 65].....	52
Table 3.1: Surface tensions of saponin solutions in distilled water according to the concentration	77
Table 3.2: d(0.5) diameter and span values of microcapsule lots C0.025, C0.050, C0.075 and C0.100.....	80
Table 3.3: d(0.5) diameter and span values of microcapsule lots R700, R650 and R600.....	86
Table 3.4: d(0.5) diameter and span values of microcapsule lots S0, S8 and S12	87
Table 3.5: Structural parameters of the interlock knitted fabrics used to investigate the influence of the textile material type on the characteristics of the microcapsule-treated fabric.....	97
Table 3.6: Microcapsule loading capability of the fabrics knitted from different materials	98
Table 3.7: Results of two independent samples t tests for fabrics knitted from different materials.....	99
Table 3.8: Statistical results of the area of microcapsule aggregates on different kinds of fabrics	101
Table 3.9: Ibuprofen release rate from the microcapsule-treated fabrics having different textile materials.....	103
Table 3.10: Microcapsule loading capability of the fabrics according to the loop length with a microcapsule concentration of 14 mg/ml	105
Table 3.11: Microcapsule loading capability of the fabrics according to the loop length with a microcapsule concentration of 24 mg/ml	106
Table 3.12: Results of the t tests according to the loop length with a microcapsule concentration of 14 mg/ml.....	106
Table 3.13: Results of the t tests according to the loop length with a microcapsule concentration of 24 mg/ml.....	107
Table 3.14: Practical structural parameters of the fabrics according to the loop length	109
Table 3.15: Microcapsule loading capability of the fabrics according to the loop length with a microcapsule concentration of 20 mg/ml	113
Table 3.16: Results of the t tests according to the loop length with a microcapsule concentration of 20 mg/ml.....	114

Table 3.17: Area of the microcapsule aggregates according to the loop length with a microcapsule concentration of 14 mg/ml	117
Table 3.18: Total cross section area of all microcapsules per cm ² of fabrics with coating technique.....	120
Table 3.19: Calculated values of V, V ₁ , V ₂ and V ₃	121
Table 3.20: Area of the yarn surface might be coated with the microcapsules per cm ² of the fabrics	123
Table 3.21: Value of K according to the loop length with a microcapsule concentration of 14 mg/ml.....	123
Table 3.22: Area of the microcapsule aggregates according to the loop length with a microcapsule concentration of 20 mg/ml	125
Table 3.23: Total cross section area of all microcapsules in an unit area of the fabrics when the microcapsule concentration impregnated to the fabrics was equal to 20 (mg/ml)	126
Table 3.24: Value of K according to the loop length with a microcapsule concentration of 20 mg/ml.....	126
Table 3.25: Weight percentage of ibuprofen on the microcapsule-treated fabrics (by impregnating) released into the receptor fluid after 24 hours	126
Table 3.26: Weight percentage of ibuprofen in the microcapsule-treated fabrics released into the receptor fluid Ibu_{r1} according to the fabric extension	128
Table 3.27: Content of the microcapsules per cm ² of the fabrics according to the fabric extension.....	129

INTRODUCTION

The functional textiles have been researched and developed strongly in recent years, contributing to the growth of many industrial fields and the social economic development all over the world. The application of microcapsules is now one of the modern technologies to manufacture the functional textiles, as shown in a lot of researches and commercial products.

Microcapsules are tiny particles having size of from one to few hundred micrometers, containing active ingredient packaged within the core surrounded by the polymer shell. The main advantages of microcapsules are controlling the release of the active ingredient and protecting the active ingredient from the surrounding environment. Therefore, microcapsules have been applied in many textile fields such as thermo-regulating textiles, flame-retardant textiles, cosmetic textiles, fragrant textiles and medical textiles. In the field of medical textiles, by using microcapsules, many kinds of medical ingredients have been incorporated into textiles, including the anti-inflammatory agents such as ibuprofen, dexamethasone and some herbs.

Using eco-friendly products is a global trend nowadays, so the application of microcapsules in textile also needs to integrate with this development. The use of microcapsules made from eco-friendly materials for medical textiles has been mentioned in many researches with many kinds of natural active ingredients have been encapsulated in the bio-sourced polymers. However, aside from the polymers and the active ingredients, the surfactants and the solvents are also two essential components of the microencapsulations, but the effort to reduce their hazard has not been in concern in the field of textile. Meanwhile, the natural surfactant quillaja saponin has been approved for human health and been applied commonly in producing emulsions for food, pharmaceutical and cosmetic industry. Besides, in recent years, there have been some studies using less toxic non-halogenated solvent ethyl acetate to replace toxic halogenated solvents in microencapsulation by solvent evaporation method.

Beside the microcapsules, the textile substrate is also an important component of the microcapsule-treated fabric. The fabric structure has strong influence on the microcapsule loading capability and the microcapsule distribution on the fabric, and consequently affects the active release capability of the fabric. Due to many advantages such as the softness, the high elasticity, the ability of not curling at edges and the difficulty of unraveling, the interlock knitted fabric is very suitable for the substrate in the medical textiles using microcapsules, especially in compressive bandages. However so far in the knitting field in general and on the interlock fabric in specific, there have been very few researches about the influence of fabric structural parameters on the characteristics of the microcapsule-treated fabrics. It was reported that the loop length obviously affected the microcapsule loading capability of the fabric, but the scientific nature of the influence was not discussed. Moreover, up to now, there have not been any studies about the influence of other structural parameters yet.

Microcapsules either in wet (not dried yet) or in dry (dried completely) type can be applied to textiles by common finishing techniques such as padding and coating. The drying and curing steps, which are always required in finishing, may induce the deformation of microcapsules, resulting in lower active release capability of the fabric. Especially in the case of using wet microcapsules for the textile finishing, the residual water and solvent in the microcapsules makes the polymer shell still weak and easier to be deformed during the drying and curing steps. Therefore, in the progress of applying a new kind of microcapsule to textile, it is very necessary to investigate the influence of drying conditions on microcapsule morphology in order to determine the suitable drying condition that keeps the microcapsules from deformation.

According to the analyses above, this thesis will discuss about:

"Elaboration of textiles containing eco-friendly anti-inflammatory microcapsules oriented to medical application".

Research objectives of the thesis:

1. Elaborating the microcapsules suitable for textile application, containing an anti-inflammatory drug, by solvent evaporation technique, using a bio-sourced surfactant and a non-halogenated solvent.
2. Finding out the suitable drying conditions for textile finishing with obtained microcapsules to keep the microcapsules from deformation.
3. Figuring out the influences of fabric structural parameters (textile material, loop length, fabric extension) on the important characteristics of the knitted fabrics containing microcapsules (microcapsule loading capability, microcapsule distribution, active release capability).

The following research contents were carried out:

1. Microencapsulation of the anti-inflammatory drug ibuprofen suitable for medical textile by solvent evaporation technique, using the bio-sourced surfactant quillaja saponin and the non-halogenated solvent ethyl acetate:
 - 1.1. Determining the range of microcapsule size that is appropriate for the cotton interlock fabric used in the thesis.
 - 1.2. Evaluating the surface active properties of quillaja saponin used in this thesis (the lot S4521 of Sigma Aldrich).
 - 1.3. Investigating the influence of microencapsulation parameters on the microcapsule size and their morphology. The parameters investigated were: the concentration of saponin, the stirring rate, the volume of the solvent added to the aqueous phase before the emulsification step.
 - 1.4. Choosing the suitable microencapsulation parameters for the application on anti-inflammatory textile.

-
2. Influence of the drying conditions on the microcapsule morphology after the finishing of textile with microcapsules:
 - 2.1. Influence of the humidity during drying process.
 - 2.2. Influence of the drying temperature.
 3. Influence of the fabric structural parameters on the main characteristics of the microcapsule-treated fabric:
 - 3.1. Influence of the textile material on the microcapsule loading capability, the microcapsule distribution and the active release capability of the fabric.
 - 3.2. Influence of the loop length on the microcapsule loading capability, the microcapsule distribution and the active release capability of the fabric.
 - 3.3. Influence of the fabric extension on the active release capability of the fabric.

New contributions of the thesis

1. This is the first study to use the bio-sourced surfactant quillaja saponin combining with the non-halogenated solvent ethyl acetate in the microencapsulation by solvent evaporation technique.
2. This is the first study in the knitting field to investigate the influences of textile material and loop length on the microcapsule loading capability, the microcapsule distribution and the active release capability of the microcapsule-treated fabrics.
3. The thesis presented a new concept, which was the microcapsule cover ratio, to explain the effect of the loop length on the microcapsule distribution on the fabrics.

Scientific values of the thesis

1. The thesis proves the surface-active properties of quillaja saponin S4521 (Sigma-Aldrich) according to the cmc value, the surface density and the interfacial area occupied by one saponin molecule. The suitable saponin concentration for microencapsulation of ibuprofen by the solvent evaporation technique, which is appropriate for the textile application, has been chosen according to the cmc value of quillaja saponin.
2. The thesis indicates scientific basis to choose the suitable drying conditions for finishing interlock cotton fabrics with elaborated microcapsules. The humidity during the drying process was selected basing on the hydration of microcapsules and the drying temperature was selected basing on the glass transition of polymer membrane.
3. This thesis indicates scientific basis that is the model interlock knitted loop and introduces a new concept that is the microcapsule cover ratio K to explain the influence of loop length on microcapsule loading capability and microcapsule distribution on fabric.

Practical values of the thesis

1. The thesis contributes to the development of the eco-friendly productions in the textile industry:
 - 1.1. The eco-friendly microencapsulation for the textile application by the solvent evaporation technique, using the bio-sourced surfactant quillaja saponin and non-halogenated solvent ethyl acetate.
 - 1.2. The eco-friendly finishing of textile with microcapsules without using binders and other auxiliaries.
2. The thesis contributes to the development of medical textile products using microcapsules:
 - 2.1. The results about the influence of textile material on the characteristics of the microcapsule-treated fabric orient the selection of the textile substrate in manufacturing medical textile products using microcapsules.
 - 2.2. The results about the influence of loop length on the characteristics of the microcapsule-treated fabric orient the selection of loop length for the textile substrate in manufacturing medical textile products using microcapsules.
 - 2.3. The results about the influence of fabric extension on the transdermal release of the microcapsule-treated fabric orient the selection of dimensional parameters for the textile substrate in manufacturing medical compressive bandages using microcapsules.

1. Chapter 1: Literature review

1.1. Microcapsules and their textile applications

1.1.1. Microcapsules

Definition and classification

Microcapsules are microparticles in which solid, liquid or gaseous active ingredients (the core) are packaged within a second material (the shell or the membrane) [31, 61].

Advantages of microcapsules [31]:

- Controlled release of active compounds.
- Separation of incompatible components.
- Conversion of liquids to free flowing solids.
- Increased stability (protection of encapsulated materials against oxidation or deactivation due to reaction in the environment).
- Masking of odour, taste and activity of encapsulated materials.

Microcapsules could be classified on the basis of their size or morphology [31, 61, 104].

By their size, microcapsules can be classified as:

- Microcapsules: range in size from 1 to few hundred micrometers.
- Nanocapsules: range in size below 1 μm (nanometer range).

By their morphology, microcapsules can be categorized into monocored, polycored and matrix types (Figure 1.1).

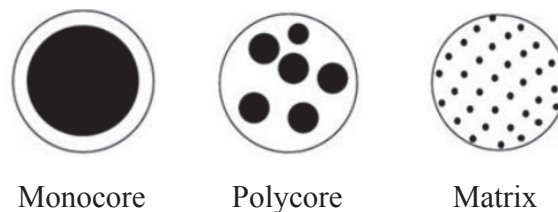


Figure 1.1: Microcapsule classification on the basis of their morphology [31]

- Monocored microcapsules (also called single-core microcapsules) have a single hollow chamber within the capsule.
- Polycored microcapsules (also called multiple-core microcapsules) have a number of different sized chambers within the shell.
- Matrix microcapsules (also called microspheres) have active ingredients integrated within the matrix of the shell materials.

Important characteristics of microcapsules and their determination

Some important characteristics of microcapsules that often mentioned in literatures are:

- The morphology
- The size

- The drug loading ratio and the microencapsulation efficiency
- The drug release profile

Microcapsule morphology

Microcapsule morphology expresses the shape, the features of membrane structure and the internal structure of a microcapsule [26, 36, 83, 84, 120]. In most studies, microcapsules have the spherical shapes (Figure 1.2), which help control the drug release much simpler than other shapes. Depending on microencapsulation parameters, the microcapsule shell could be smooth or rough, dense or porous, it often contains a system of tiny holes where active ingredients can be released gradually. The internal structure helps reveal the type of microcapsule (monocored, polycored or matrix type).

Microcapsule morphology is often observed by scanning electron microscope (SEM). At low magnification from x100 to x500, SEM images provide information about the shape and size of microcapsules, and at higher magnification, they give the feature of the shell such as porosity, the size and the density of tiny holes. The cryo-SEM technique, in which microcapsules are freezing to keep their original structures prior to observation, help look into the internal morphology of microcapsules [57, 120, 141]. Besides, the microcapsule samples using for SEM analysis are often dried microcapsules. For microcapsules suspended in water, the environmental mode of SEM (with pressure in sample chamber around 2÷3 Torr) is used in order not to deform microcapsules during observation [15].

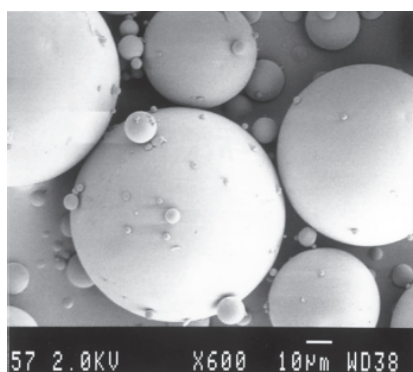


Figure 1.2: SEM image of PLGA microspheres containing progesterone [121]

Microcapsule size

The size is a very important characteristic of microcapsules, since it is in inverse proportion to surface area, it has very strong influence on the rate of drug release from microcapsules [31]. Microcapsule size and size distribution are determined by particle size analysis equipments, which often base on the effect of particle size on the spatial distribution of scattered light in the laser diffraction. The result of the particle size analysis is often expressed by the size distribution curve, which indicates the mean diameter of the microcapsules, the broadness of the size distribution and also provides other size information (Figure 1.3) [83, 138, 147].

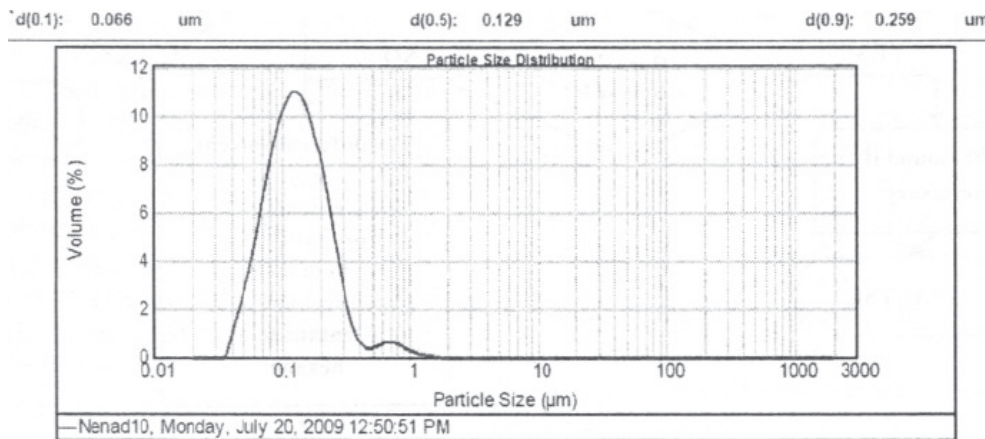


Figure 1.3: An example of the size distribution curve of microcapsules [140]

The drug loading ratio and the microencapsulation efficiency

The drug loading ratio is defined as the mass ratio of encapsulated active compound to microcapsule and often expressed by mass percentage [26, 55, 84, 147, 163]:

$$L (\%) = \frac{m_{ac}}{m_{mc}} \times 100 \% \quad (Eq 1.1)$$

In which:

L (%): the drug loading ratio

m_{ac} : the mass of encapsulated active compound

m_{mc} : the mass of microcapsule

The microencapsulation efficiency is defined as the ratio of encapsulated mass to initial mass used for microencapsulation of active compound, it is also expressed by mass percentage [26, 42, 55, 147, 163]:

$$E (\%) = \frac{m_{encap}}{m_{init}} \times 100\% \quad (Eq 1.2)$$

In which:

E (%): microencapsulation efficiency

m_{encap} : the mass of active compound that is successfully encapsulated into microcapsule

m_{init} : the total mass of active compound initially used for microencapsulation

In order to determine the drug loading ratio and the microencapsulation efficiency, the active compound needs to be separated from a certain mass of microcapsules and then be quantified. The separating process is often carried out by using a solvent that can dissolve the active compound only but can not dissolve the polymer shell of microcapsules. The dissolution is accelerated by ultrasonic [84, 147], or by using a solvent that can dissolve all the microcapsules and in this case, a suitable chemical is used to precipitate the polymer to remove it from the system [26, 42, 55, 163]. The drug loading ratio L(%) and the

microencapsulation efficiency E(%) can be deduced from the maximum concentration of active compound in solvent.

The drug release profile

The drug release rate of microcapsule is often represented by a curve that describes the change over time of the drug cumulative release. In the medical field, in order to build up the drug release curve, a certain amount of microcapsules are often immersed in a solvent that simulates the real release environment. Most studies used the phosphate buffer solution with pH=7÷7.4 at the temperature of $37 \pm 1^\circ\text{C}$ (for oral applications) or at $32 \pm 1^\circ\text{C}$ (for topical and transdermal applications) as the release solvent. After a predetermined period of time, the drug concentration in release solvent is quantified by UV-Vis or HPLC equipment at suitable wavelengths and the cumulative release of drug at that time could be deduced [8, 17, 26, 42, 55, 106, 163].

The drug release curve is a very important base to predict the release mechanism of the active ingredient from the microcapsule [17, 42, 104]. Figure 1.4 represents the four types of theoretical curves describing the four types of release mechanisms of the active ingredients from the non-erodible microcapsules.

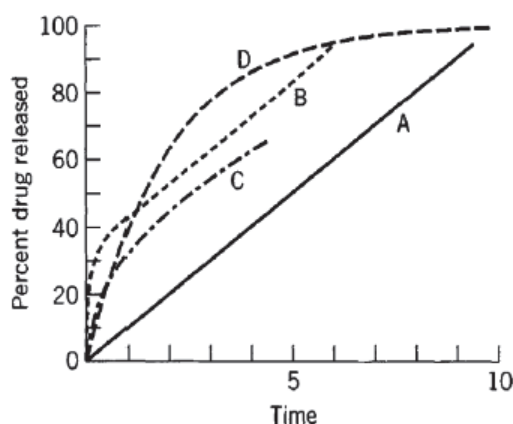


Figure 1.4: Four types of theoretical curves describing the release mechanisms of the active ingredients from the non-erodible microcapsules [104]

In which:

- The curve A describes the release behavior following zero order mechanism.
- The curve B describes the release behavior following zero order mechanism with the burst effect.
- The curve C describes the release behavior following the Fick law.
- The curve D describes the release behavior following the first order mechanism.

1.1.2. Applications and requirements of microcapsules in the textile field

Applications of microcapsules in textile

Microencapsulation technique dates back to 1950s when Green and Schleider produced microencapsulated dyes from gelatin and arabic gum for the manufacture of carbonless copying paper. Up to now, microcapsules have been applied widely in many industrial fields such as chemistry, medicine and pharmacy, agriculture, food, cosmetic, printing and textile [31]. Since 1990s, microencapsulation technique has been used in textile industry, mainly at the research and development stage but a few commercial applications. Moving into the 21st century, microcapsule applications in textile have developed more and more fast and extensively, especially in Western Europe, Japan and North America, helped produce textile materials with many new functions that conventional finishing techniques could not implement [97].

The following are some important applications of the microcapsules in textile:

Application of microcapsules in thermo-regulating textiles

Thermo-regulating fabric is an intelligent textile that offers suitable responses to changes in temperature of environment surrounding the body. The efficiency of thermal comfort depends on the heat exchange between the body and surrounding environment. An effective method that helps fabrics regulate the temperature is integrating phase change materials (PCMs) into them. The most used PCMs are some popular alkanes such as n-octadecane, n-hexadecane, n-eicosane and their mixtures. PCM materials absorb energy during the heating process as phase change takes place and release energy to the environment in the phase change during the reverse cooling process. Since PCMs could exist on fabrics in type of liquid when the environment temperature is higher than their melting point, they need to be microencapsulated [11, 25, 54, 66, 94, 95].

Application of microcapsules in flame-retardant textile

The mixture of polyurethane-phosphate is known to form an effective flame retardant intumescent system for textiles. But the intumescent formulation could not be permanent due to the water solubility of the phosphate. In order to overcome this problem, many researches try to microencapsulate the phosphate into microcapsules, then apply the combination of microcapsules with polyurethane resin to fabrics by conventional finishing techniques such as padding, coating and printing [38-40, 77, 127, 149].

Application of microcapsules in cosmetic textiles

In the cosmetic textiles, microcapsules are often used to encapsulate vitamins, essential oils, skin moisturizing agents, skin cooling agents, anti-aging agents...to control the release properties of active ingredients extending the functionality of cosmetic textiles [9, 23, 137].

Application of microcapsules in fragrant textiles

Using microcapsules for aroma finishing of fabrics helps improve obviously the fragrant stability over time and washing cycles. There are many types of fragrance that have been added to textiles by microencapsulation technique, including mainly perfumes and essential oils (lemon, citronella, mint, apple, moxa, lavender, grape fruit seed, rose...). Along with the pleasant by fragrance, essential oils also possess other valuable characteristics such as antimicrobial and anti-inflammatory activity and insect repellent [41, 85, 87, 88, 139].

Application of microcapsules in printing and dyeing

Applying microcapsules helps overcome some disadvantages of printing techniques. Without microcapsules, the transfer printing technique was used only for the dyes volatilizing at the temperature lower than the melting point of textile. By using microencapsulation technique, two or more microencapsulated dyes can be applied to the surface of a transfer web that is then laid to the textile, physical pressure can be exerted on the capsules to rupture and deposit the dyes on the textile. Besides, microencapsulation of dye particles is considered as the technique most suitable for multicolored speck printing of fabrics [96]. A pigmented polymer system using sub-micron particles helps reduce the viscosity of the inks under high loading in a water-based vehicle system, so improves the efficiency of ink jet printing on a wide variety of textile substrate [74].

Microencapsulation technique has also opened a very fast growth of dyeing technology using liposomes, which is environmentally friendly, more cost effective than conventional dyeing technology and does not require specific equipment or skills [97]. Liposomes are vesicular structures that have an internal aqueous domain entrapped between lipid bilayers. Lecithin, a bio-sourced phospholipid, is most commonly used for the preparation of liposomes [115]. Dyeing process using liposomes helps reduce obviously the need of dyeing auxiliaries, so the dyeing waste flow can be handled simply. Liposomes now are applied widely to encapsulate dispersed dyes for dyeing of polyester and nylon [60, 153, 159], acid dyes for dyeing of leather and polyamide [114, 115], reactive dyes for dyeing of wool [34].

Application of microcapsules in medical textiles

Microencapsulation technique has contributed considerably to the development of medical textiles. Microcapsules help protect the therapeutic agents from the oxidation of environment, control the release and prolong the therapeutic effects by more washing cycles in comparison to applying therapeutic agents directly to textiles.

Using microcapsules to apply antimicrobial agents to textiles:

- Powder silver nanoparticles were successfully padded to cotton fabrics to give the fabrics antimicrobial, anti-inflammatory and wound healing capabilities [46].
- The microcapsules made from gum acacia that contain geranium leaves extract were used for combined antimicrobial and aroma finishing treatment of cotton fabrics [143].

- The microcapsules made by a natural encapsulation technique with yeast, containing a mixture of herbs, were applied to cotton and silk fabrics in the antimicrobial finishing processes [131].
- The chitosan microcapsules containing honey were used to elaborate antimicrobial medical dressings that are air permiable, promote the wound healong, protect the honey from the oxydation of surrounding environment and reduce the sticky nature of honey [32].
- Some antibacterials agents (clothianidin, poly(N,N-dimethyl-2-hydroxypropylammonium chloride and chlorhexidine gluconate) were encapsulated in PLA microcapsules for antimicrobial finishing of wool fabric [45].
- Ozonated red pepper seed oil was encapsulated in gelatin-arabic gum microcapsules for antimicrobial finishing of non-woven fabrics [102].
- The antifungal therapeutic agent, Terbinafine, was successfully encapsulated in melamine formaldehyde microcapsules to add the antifungal property to cotton fabrics [99].
- Triclosan was encapsulated in melamine formaldehyde microcapsules for antibacterial finishing of cotton fabrics [35].

Using microcapsules to apply anti-inflammatory agents to textiles:

- Traditional Chinese Herbs was successfully encapsulated in chitosan-sodium alginate microcapsules and grafted to cotton fabrics to aid the treatment of atopic dermatitis [50].
- The antimicrobial and anti-inflammatory finishing was applied to the cotton fabrics by an eco-friendly natural technique, using sodium alginate microcapsules that containing marine organisms [33].
- The anti-inflammatory drug Dexamethasone was encapsulated in PLGA microspheres and incorporated to absorbable surgical sutures [73].
- The PCL microspheres loading the anti-inflammatory drug, ibuprofen, were padded to cotton fabrics. The results of investigation showed that after 37 hours the content of ibuprofen that diffused through the pig skin to enter the receptor fluid from the fabrics was $5.11 \pm 0.86 \mu\text{g}/\text{cm}^2$ [17].
- The Eudragit RSPO microcapsules containing anti-inflammatory drug, ibuprofen, were deposited to cotton fabrics. The mechanical properties of microcapsules deposited on fabrics were studied thanks to *in vitro* compression tests and *in vivo* tests [146].

Requirements of microcapsules for textile applications

Requirements for microcapsule size

Requirements for microcapsule size in textile application depend on many factors, especially the use of end products and the structures of textile substrates. In general, microcapsules used in textile often have average diameters in range of $1 \div 100 \mu\text{m}$. Among

them, the microcapsules containing phase-change materials and flame retardant agents, which are often elaborated by chemical methods, have small size that in range of $1 \div 15 \mu\text{m}$ [25, 38, 94, 124, 126, 127, 149]. The microcapsules used in medical textile field, which are often elaborated by physico-chemical methods, have bigger size in range of $15 \div 100 \mu\text{m}$ [56, 79, 143, 147]. C.D. Huong et al. [52] have proposed the suitable size of microcapsules, which was in the range of $15 \div 20 \mu\text{m}$, for some popular knitted structures (Single, Rib1x1 and Interlock 1x1 fabrics). Their proposal based on the observation on the fabric structure by the optical microscopy and the scanning electron microscopy in order to determine the width and the height of the knitted loops.

Requirements for microencapsulation efficiency

According to the definition of microencapsulation efficiency presented at section 1.1.1, the microencapsulation efficiency exerts strong influence on the cost in the manufacture of medical textiles using microcapsules. All researches on microencapsulation always aim to get high microencapsulation efficiency. This value depends closely on the process and formulation parameters of the microencapsulation. In the field of medical textile, there are many researches that have reached high microencapsulation efficiency, such as the research on microencapsulation of ibuprofen from poly- ϵ -caprolactone by solvent evaporation technique with microencapsulation efficiency of 84% [17], the research on microencapsulation of ibuprofen from eudragit RSPO also by solvent evaporation technique with microencapsulation efficiency of 95% [147], the research on microencapsulation of jojoba oil from ethyl cellulose by solvent extraction method with microencapsulation of 99% [56]. However, there are still some researches that were not successful in getting high microencapsulation efficiency, such as the research on microencapsulation of tamoxifen from gelatin-arabic gum by complex coacervation technique with microencapsulation efficiency of $53 \div 65\%$ [79], the research on microencapsulation of dexamethasone from PLGA by solvent evaporation technique with microencapsulation efficiency of only 30% [73].

Requirements for user's safety

The safety for users is highly required for microcapsules applied in medical textiles. This problem was mentioned in the research of B. Ocepek et al. [99], in which the melamine formaldehyde microcapsules containing triclosan (an antibacterial agent) were printed to cotton fabrics. Since both the compositions of microcapsules and printing paste included formaldehyde, a toxic chemical that had to obey the safety regulations all over the world, the authors determined the amount of free formaldehyde on the microcapsule treated fabrics. Their results showed that both microcapsules and printing paste contributed to the presence of free formaldehyde on fabrics ($75 \div 250 \text{ ppm}$) but the content of formaldehyde decreased strongly after washing (below 50 ppm). According to Oeko-tex standard 100, the amount of free formaldehyde in the final fabric should not exceed 20 ppm for baby clothing, 75 ppm for

products that come in direct contact with the skin (with the exception of baby clothing) and 300 ppm for all other products. With regard to these regulations, all the samples that were analysed were suitable for products that were not in direct contact with the skin, all washed samples were suitable for clothes worn in direct contact with the skin and just one sample was appropriate for babies.

The issue of safety was also cared by P. C. Hui et al. [50], when the sodium alginate microcapsules containing the extract of Penta Herbs were applied to cotton fabrics to aid the treatment of atopic dermatitis. In order to determine if the microcapsules had toxic effects on skin, in vitro skin toxicity tests were performed, using the cell membrane integrity test and cell viability test. Their results showed that elaborated microcapsules did not appear to have toxic effects on cells and could be suitable for making garments for clinical care.

1.1.3. Microcapsules prepared from environment-friendly materials for textile applications

Using environment-friendly products is a global trend nowadays. Therefore, the application of microcapsules in textile also needs to integrate with this trend of development.

So far, there have been many researches in the textile field mentioning about the use of the bio-sourced active ingredients and bio-sourced polymers for the microencapsulations. Some bio-sourced active ingredients that have been used include: the herb extracts [33, 50, 131, 143], the plant oils [102, 136], the essential oils [75, 139] and honey [32]... Besides, some bio-sourced polymers and monomers have been used include: chitosan [32], gum acacia [143], gelatin - arabic gum [102], sodium alginate [33], silk fibroin [161], isosorbide [9], succinyl chloride and 1,4-butanediamine [136]...

Aside from polymers and active ingredients, surfactants and solvents are also two essential components of the microencapsulations. However, up to now, most of the researches on the microcapsule applications in the textile field have still used the synthetic surfactants (such as sodium sulphate [143], tween 20 [102], span 80 [50], polysorbate 80 [9]...) and the toxic solvents (such as cyclohexane [9, 128], dichloromethane [17, 73, 147], chloroform [128] and toluene [38]...).

Comment:

Microcapsules are very small particles having size in range from one to few hundred micrometers, with the active ingredients were packaged within the core surrounded by the polymer shells. They possess many advantages, especially the ability of controlling the release of the active ingredients and protecting the active ingredients from the surrounding environment. Therefore, microcapsules have been applied widely in many industrial sectors, including the textile industry. In the field of textile, medical textile using microcapsules has been received much care recently with many types of therapeutic agents have been applied to textiles, been controlled the release and prolonged the therapeutic effects by washing cycles.

The requirements for microcapsules used for textile in general and for medical textile in particular include: the size distribution is as narrow as possible, the average diameter is in the range of 1÷100 μm , the microencapsulation efficiency is as high as possible and the microcapsules need to be safe for users.

The application of microcapsules that made from eco-friendly materials has got much attention from textile industry. Up to now, many researches have tried to encapsulate the natural active ingredients in the bio-sourced polymers. Aside from polymers and active ingredients, surfactants and solvents are also two essential components of the microencapsulations, however the effort to reduce their hazard has not been concerned in the field of textile.

1.2. Microencapsulation by the solvent evaporation technique

1.2.1. Techniques of microencapsulation

Techniques of microencapsulation have got more and more diversified recently. The choice of a technique depends on the properties of active ingredients and the requirements of the end products. In general, techniques of microencapsulation are divided into three groups that are chemical, physico-chemical and physico-mechanical methods (Figure 1.5) [31, 61, 104].

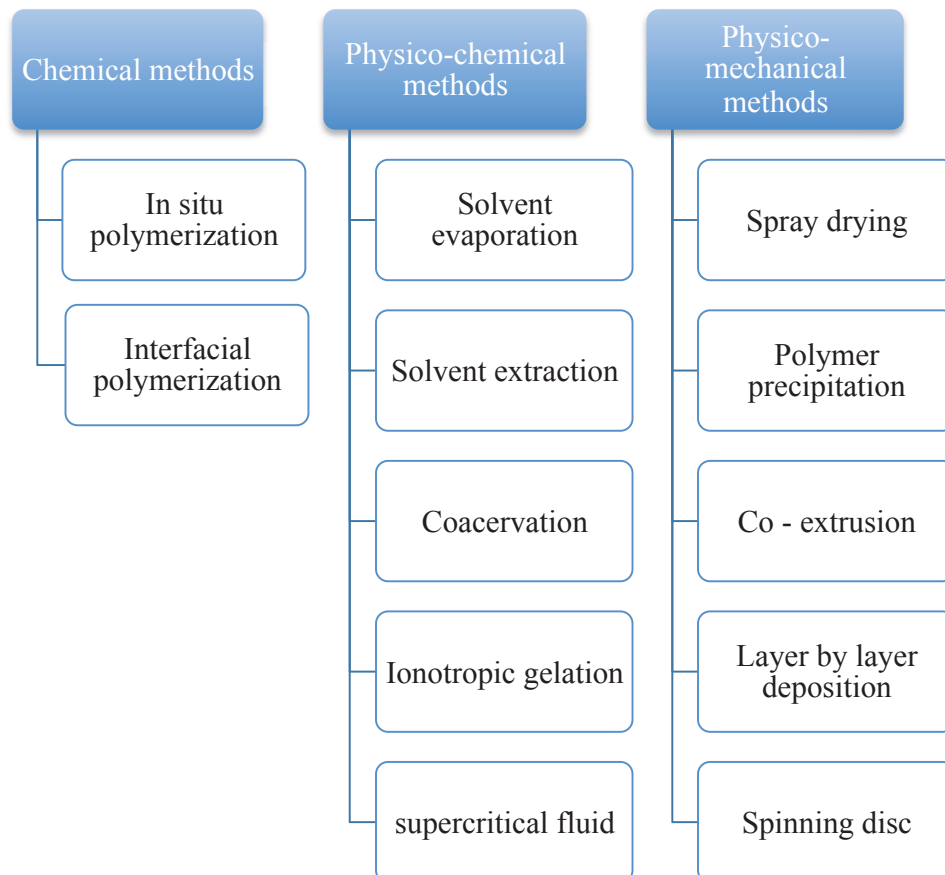


Figure 1.5: Classification of microencapsulation methods

In the chemical methods, the polymer shell is directly formed by the polycondensation of two reactive monomers surrounding the dispersed core material [36, 123, 160, 162]. The use of toxic monomers is a big disadvantage of these techniques because the residual monomers of chemical reactions could be hazardous to human and environment.

In the physico-mechanical methods, microcapsules are elaborated by the combination of physical and mechanical factors [13, 117]. The complicated system of microencapsulation equipment is a big disadvantage of these techniques.

The physico-chemical methods are based on the control of the solubility and precipitation conditions of the polymers under the influence of several factors that tend to reduce the solvation on the solvent [15-17, 83, 89, 120, 147]. In these techniques, the toxic monomers are not used, the equipment system is not so complicated, and the elaborated microcapsules have small and even size.

1.2.2. Microencapsulation by the solvent evaporation technique

1.2.2.1. Basic principle of the technique

Basic principle

Microencapsulation by solvent evaporation technique has some options that often depend on the solubility of active ingredients in the water [76].

- For insoluble or poorly water-soluble active ingredients: the oil in water (o/w) option is frequently used.
- For high hydrophilic active ingredients: the o/w option is not suitable because the hydrophilic active ingredients may not be dissolved in the organic solvents and the active ingredients will diffuse into the continuous phase during the emulsification, leading to a great loss of active ingredients. In this case, some other options will be used as the replacements, such as w/o/w double emulsion.

The basic principle of solvent evaporation technique from oil/water emulsion consists of two continuous stages, which can be described as below:

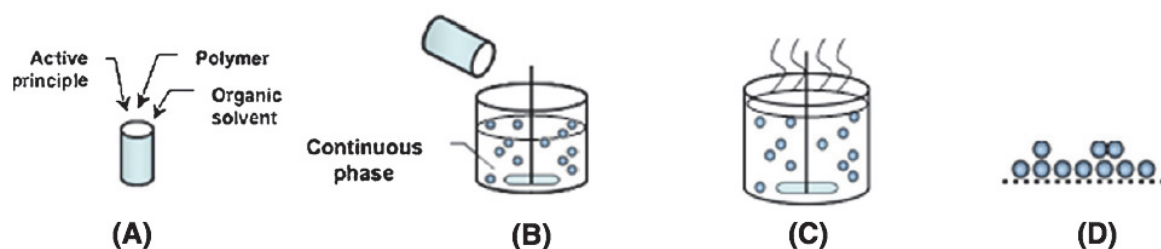


Figure 1.6: Diagram of basic principle of microencapsulation by solvent evaporation technique [76]

1. The emulsification stage:

- The oil phase (the dispersed phase, Figure 1.6A): is a homogenous mixture of polymer, active ingredients and a low-boiling good solvent for the polymer.

The amount of good solvent needs to be enough to ensure that the polymer is completely dissolved [30, 78].

- The aqueous phase (the continuous phase, Figure 1.6B): is the solution in water of a suitable surfactant.
2. The solvent evaporation stage (Figure 1.6C, D): the emulsion is then subjected to reduced pressure and elevated temperature to gradually remove the solvent from the droplets. Eventually, when the droplet composition reaches the bimodal boundary, the polymer phase separates as small droplets of liquid, which are rich in solvent and polymer (called a coacervate phase) within the emulsion droplets. These coacervate droplets are mobile and migrate to the oil/water interface where they fuse and spread to engulf the original oil droplet if the wetting conditions are correct. Further solvent removal causes the polymer to precipitate at the interface, forming the shell.

The advantage of this technique

Microencapsulation by solvent evaporation is one of physico-chemical methods so this technique could produce small and even microcapsules without the use of toxic monomers and intricate equipment. Besides, this technique is the most used for microencapsulation of anti-inflammatory drugs such as ibuprofen, naproxen and dexamethasone [17, 73, 108, 147]; the elaborated microcapsules have size in range of 1÷50 μm , which are suitable for textile application.

1.2.2.2. Important parameters of the microencapsulation by the solvent evaporation technique

In order to produce microcapsules suitable for textile application (as mentioned at section 1.1.2), the microencapsulation parameters should be selected appropriately. Some important parameters of microencapsulation by solvent evaporation technique are:

- the concentration of surfactant
- the concentration of polymer in the dispersed phase
- the molar mass of polymer
- the mass ratio of active ingredient to polymer
- the volume ratio of dispersed phase to continuous phase
- the stirring rate
- the solvent evaporation rate

The surfactant concentration

There is a general trend of many researches indicating that the microcapsule size will decrease when the surfactant concentration increases because of the reduced interfacial tension [31, 76, 138, 147]. In the study of P. Valot et al. [147] on the microencapsulation of ibuprofen by solvent evaporation technique, the concentration of the surfactant PVA ranged from 0.1 to

2.0 wt%. Their results showed that the mean diameter of microcapsules was not influenced by the surfactant concentration above 0.2 wt%, whereas it significantly decreased below 0.2 wt%, the variation suggested that the droplet cover was insufficient at this level, and could not prevent the droplet from coalescence. Besides, the PVA concentration also impacted the size distribution of microcapsules, which were relatively narrow only for the concentration of 0.2 wt%.

The polymer concentration in the dispersed phase

The polymer concentration in the dispersed phase also has obvious influence on the microcapsule size and size distribution. In general, the increase in polymer concentration makes the viscosity of dispersed phase also to increase, resulting in bigger microcapsules and broader size distribution. In the study of P. Valot et al. [147], the polymer concentration was varied in three levels of 37.5 g/l; 50 g/l and 62.5 g/l for both eudragit RSPO and ethyl cellulose. The effect of polymer concentration on the microcapsule size was different between two polymers due to the different intrinsic viscosity of polymers in the solvent (dichloromethane). Because of lower intrinsic viscosity in dichloromethane (40 ml/g at 25°C), the concentration of eudragit RSPO appeared to have little effect on the microcapsule size and size distribution. The mean diameter centred on the major population equal to 10, 28 and 20 µm for 37.5 g/l, 50 g/l and 62.5 g/l respectively. Meanwhile, thanks to much higher intrinsic viscosity (380 ml/g at 25°C), the concentration of ethyl cellulose obviously affected the microcapsule size and size distribution. The concentration of 50 g/l helped produce smallest microcapsules (64 µm) with the narrowest size distribution while the size distribution was quite broader and sizing on much higher diameter (150 µm) with the polymer concentration of 62.5 g/l. In another research on microencapsulation of aspirin by solvent evaporation method [155], the size of ethyl cellulose microcapsules also increased by the increase of polymer concentration. The average size of microcapsules was in order of 520, 1005 and 1342 µm corresponding to the polymer concentration of 4, 6 and 8 (wt%).

The mass ratio of active ingredient to polymer

The mass ratio of active ingredient to polymer is reported to have marked effects on microcapsule morphology, especially the structure of the shell [76, 84]. In the research of S. M. Merabedini et al. [84], in which the plant oils were encapsulated in ethyl cellulose microcapsules by solvent evaporation method, the mass ratio of active ingredient to polymer varied in three levels of 60:40 (Figure 1.7A), 70:30 (Figure 1.7B) and 75:25 (Figure 1.7C). The results showed that the increase of this ratio made the polymer shell more porous with much more tiny holes on the surface. According to the authors, too much of active ingredient may increase the risk of active ingredient leakage due to the limited space inside the microcapsule and the shrinkage of the microcapsule during its solidification, resulting in the more porous polymer shell with an increasing number of holes.

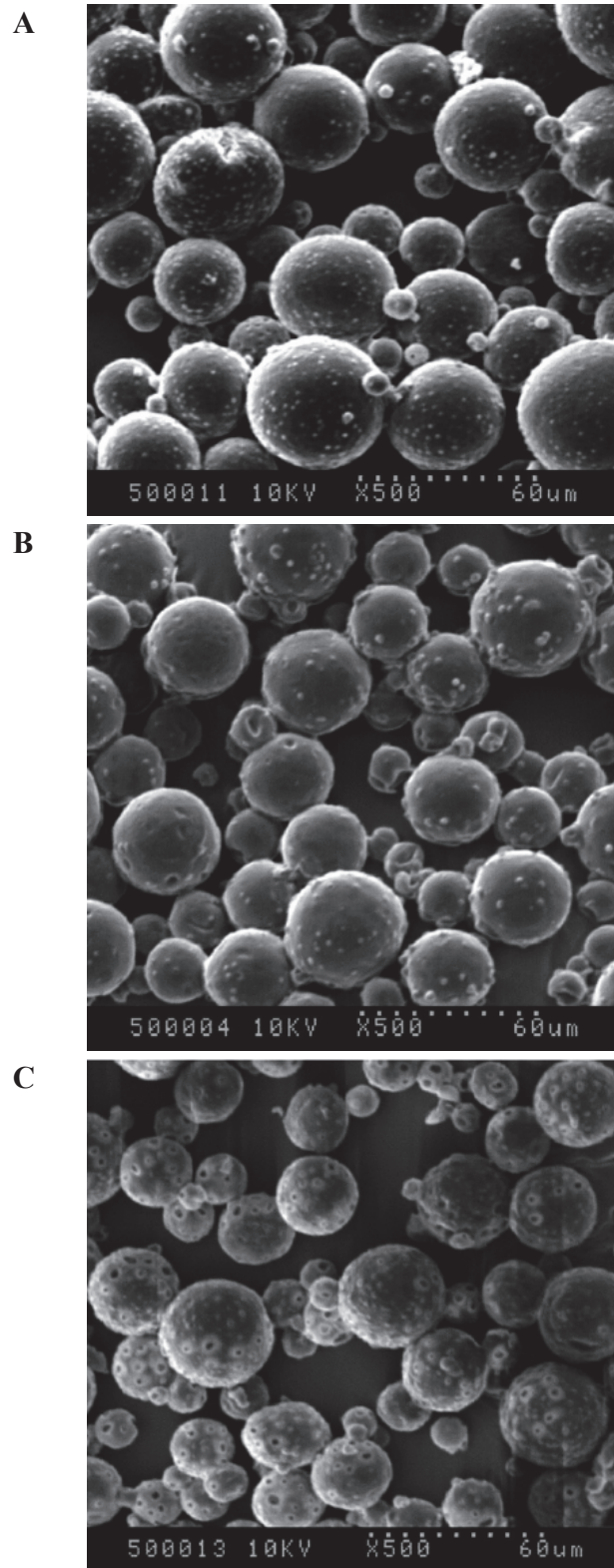


Figure 1.7: SEM images of microcapsules with different mass ratio of core/shell: 60:40 (A); 70:30 (B); 75:25 (C) [84]

The volume ratio of dispersed phase to continuous phase

The volume ratio of two phases affects obviously the microcapsule size with different trend in literatures [76, 147]. In the study of P. Valot et al. [147], the volume ratio was changed by fixing the volume of dispersed phase at 80 ml while the volume of continuous phase was varied in three levels of 400 ml, 800 ml and 1200 ml. For eudragit RSPO microcapsules, the mean diameter and the size distribution did not change when the volume of continuous phase increased from 800 ml to 1200 ml, whereas the size distribution became broader with two minor populations when the volume of continuous phase was 400 ml. For ethyl cellulose microcapsules, the mean diameter equal to 64 μm was observed with 800 ml of continuous phase, whereas the mean diameter was higher when this volume was 400 ml (90 μm) and 1200 ml (92 μm). The high viscosity of the emulsion with continuous phase volume of 400 ml combined with the high intrinsic viscosity of the dispersed phase may explain the increase of ethyl cellulose microcapsule size. The relatively higher volume of continuous phase at 1200 ml induced a non-uniform turbulence in the reactor that made elaborated microcapsules become bigger.

The stirring rate

The stirring rate also strongly affects the size of microcapsules with a common trend that at the higher stirring rate, the elaborated microcapsules are smaller due to the stronger shear stress in the emulsion system [76, 110, 147].

The solvent evaporation rate

The solvent evaporation rate also has significant effects on microcapsule characteristics, such as the size, the morphology and the microencapsulation efficiency [26, 55, 76].

T. W. Chung et al. [26] investigated the influence of solvent evaporation rate on the properties of PLLA microspheres containing lidocaine. Normal solvent evaporation (NRSE) was carried out at the atmospheric pressure (760 mmHg) and the fast solvent evaporation (FRSE) at reduced pressure (160 mmHg). The results showed that reducing pressure accelerated the solvent evaporation, which resulted in smaller microspheres. The mean diameter of microspheres made by FRSE were 0.75 μm whereas by NRSE 1.14 μm . According to the authors, the smaller size of FRSE microspheres could be explained by the Laplace equation that expressed as $dP = 2\gamma/r$ when a liquid droplet was formed in stable. In this equation, dP is the pressure difference between outside and inside of liquid film of a droplet, γ is the surface tension of interfacial liquid of the emulsion system, and r is the radius of a spherical droplet. By experiments, the author showed that the value of γ for the above-mentioned systems could be assumed as constants. Besides, the pressure differences between outside and inside of liquid film of a droplet during solvent evaporation period, dP of the Laplace equation, would be larger for FRSE process compared with that for NRSE process.

Therefore, it could be deduced from the Laplace equation that the mean radius of microspheres elaborated by FRSE process should be smaller than that by NRSE process.

Besides, FRSE microspheres possessed smooth surfaces while NRSE ones were rougher and more porous (Figure 1.8). Furthermore, the microencapsulation efficiency fell from 70.6% to 45.6% because of the reduced pressure.

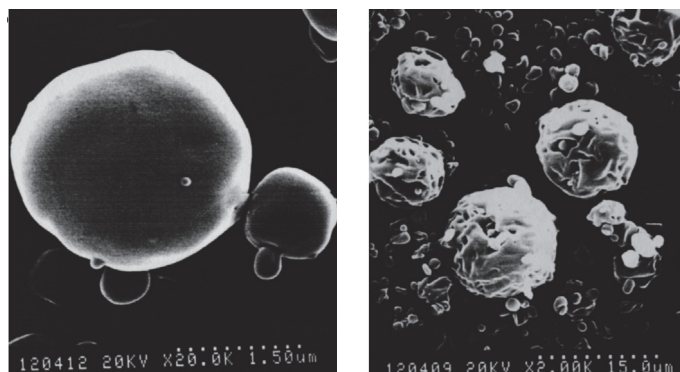


Figure 1.8: SEM images of microspheres made by FRSE (on the left) and NRSE (on the right) [26]

In the research of S. Imuzikawa et al. [55], the PLLA microspheres loading progesterone made at reduced pressure also had smoother surface in comparison to ones made at normal pressure, but contrary to the result of T. W. Chung et al. [26], the microencapsulation efficiency was higher. As explained by T. W. Chung et al., the different results between two studies might be due to different droplet forming methods. T. W. Chung et al. used o/w emulsification process to form PLLA droplets while S. Imuzikawa et al. used mechanical stirred method.

1.2.2.3. Using non-halogenated solvents in the microencapsulation by the solvent evaporation technique

For a more environment-friendly microencapsulation, a solvent with low toxicity but still meets the requirements of the solvent evaporation technique should be in consideration. The suitable solvent for solvent evaporation technique needs to fulfill the following criteria [76]:

- being able to dissolve the chosen polymer
- being poorly soluble in the continuous phase
- having a high volatility and a low boiling point
- having low toxicity

So far, the halogenated solvents such as methylene chloride and chloroform have been the most used solvents for the solvent evaporation technique because of its high volatility, quite low boiling temperature and very low solubility in water. For example, methylene chloride exhibits the vapor pressure of 453 mbar at 20°C, the boiling temperature of 39.7°C and the solubility in water of 20 g/l at 20°C. However, these solvents are confirmed carcinogenic

according to EPA (Environmental Protection Agency) data and many researchers are making great efforts to find less toxic replacements [76].

Ethyl acetate is a nonhalogenated solvent that has been used recently for microencapsulation by solvent evaporation method in the attempt to cut down the use of methylene chloride. The volatility of ethyl acetate is not as good as that of methylene chloride, its vapor pressure is 100 mbar at 20°C and its boiling temperature is 77°C. Because of its high solubility in water (90 g/l at 20°C, which is 4.5 times higher than that of methylene chloride), ethyl acetate has been often used for microencapsulation by solvent extraction technique rather than by solvent evaporation one [83, 120], but the solvent extraction technique requires a large amount of water to make the solvent diffuse completely from the droplets into the aqueous phase. H. Sah et al. [120] were successful in producing PLGA microspheres by solvent evaporation method that used ethyl acetate as the solvent. The elaborated microspheres have the average diameter of 44 µm, which were obviously smaller than that of microspheres made by solvent extraction technique (93 µm). Moreover, the amount of residual solvent in the microspheres made by solvent evaporation technique, which was 2.62 wt%, was also much lower than that in the microspheres made by solvent extraction technique (6 wt%). S. M. Merabedini et al. [84] also made successfully ethyl cellulose microcapsules containing plant oils by solvent evaporation method with the solvent ethyl acetate, the microcapsule size and the microencapsulation efficiency were equal to those of microcapsules made from the solvent chloroform.

1.2.2.4. *The quillaja saponin bio-sourced surfactant*

Some basic theories about surfactants

Surface phenomena [67]

Forces holding the molecules of a condensed phase together (cohesive forces) become anisotropic in the phase boundary region, and their normal component becomes smaller compared to the parallel component. To simplify the description and facilitate theoretical treatment, the properties of the boundary region of a condensed phase are projected to a two-dimensional surface (Gibbs “dividing surface”). The tensile stress resulting from the anisotropic forces in the boundary region is then termed the surface tension. This quantity corresponds to the reversible work required to bring particles from the volume phase to the interface during enlargement of the former, and thus corresponds to the increase in free enthalpy of the system per unit surface area.

$$\left(\frac{dG}{dF}\right)_{P,T} = \gamma \quad (\text{Eq 1.3})$$

Where G is the free enthalpy, F is the surface area, and γ the surface tension.

In the equilibrium state only very small energy interactions occur between the molecules at the surface of a condensed phase and those of the gaseous phase. The surface tension can therefore be regarded simply as an expression of the interactions between the particles in the

surface of the condensed phase. When examining the interactions between the molecules of condensed phases a distinction has to be made between London dispersion forces and polar forces. Accordingly, the surface tension comprises components that may be attributed to pure dispersion forces γ_d and to polar interactions γ_p .

$$\gamma = \gamma_d + \gamma_p \quad (\text{Eq 1.4})$$

The surface tension between two liquid phases 1 and 2 at their interface (interfacial tension) can be calculated by the equation (Eq 1.5):

$$\gamma_{12} = \gamma_1 + \gamma_2 - 2(\sqrt{\gamma_{d1}\gamma_{d2}} + \sqrt{\gamma_{p1}\gamma_{p2}}) \quad (\text{Eq 1.5})$$

In which:

γ_{12} : the interfacial tension at the interface of two liquid phases 1 and 2

γ_1, γ_2 : the surface tension of the phases 1 and 2

γ_{d1}, γ_{d2} : the dispersion components in the surface tensions of the phases 1 and 2

γ_{p1}, γ_{p2} : the polar components in the surface tensions of the phases 1 and 2

If a droplet of a liquid is brought into contact with the surface of a first liquid and the two liquids being immiscible then two phenomena can occur, depending on the magnitude of γ_{12} . If $\gamma_{12} < (\gamma_1 - \gamma_2)$, the second liquid spreads over the surface of the first liquid in the form of a thin film. If $\gamma_{12} > (\gamma_1 - \gamma_2)$, the applied droplet remains in the form of a lens in the surface of the underlying liquid.

Therefore, in order to increase the interfacial area between two immiscible liquid phases (in the formation of emulsion, for example), the interfacial tension needs to be reduced to meet the rule of $\gamma_{12} < (\gamma_1 - \gamma_2)$.

The adsorption of a solute at the liquid surface [142]

The adsorption of solutes from a liquid phase at its surface is described by the Gibbs equation (Eq 1.6):

$$\frac{d\gamma}{d \ln C} = -\Gamma_{max} RT \quad (\text{Eq 1.6})$$

where γ denotes the surface tension, C is the concentration of the solute in the solution (mol/l), Γ_{max} is the maximum surface density that is the maximum amount of solute adsorbed at the surface (mol/m²), R is the gas constant ($R = 8.314 \text{ J/mol K}$) and T is the absolute temperature.

If Γ is negative, the increase in the concentration of dissolved substance makes the surface tension increase. Inversely, if Γ is positive, the increase in the concentration of dissolved substance will reduce the surface tension of liquid phase. A dissolved substance that helps reduce the surface tension of the liquid phase is termed a surfactant.

Basic structure and classification of surfactant

All surfactant molecules consist of at least two parts, one is soluble in a specific fluid (the lyophilic part) and the other is insoluble (the lyophobic part). When the fluid is water, the two parts are often called the hydrophilic and hydrophobic parts, respectively. The hydrophilic part is referred as the head group and the hydrophobic part as the tail (Figure 1.9) [49]:

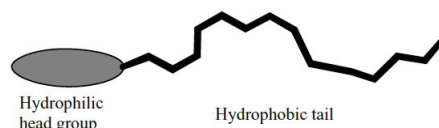


Figure 1.9: Schematic illustration of a surfactant [49]

In aqueous systems, the hydrophobic group can be composed of a long-chain aliphatic or aromatic hydrocarbon group or fluorinated or oxygenated hydrocarbon or siloxane chains. The hydrophilic head will be an ionic or highly polar group that can impart some water solubility to the molecule. The most useful chemical classification of surface-active agents is based on the nature of the hydrophile, with subgroups based on the nature of the hydrophobe or tail. The four basic classes of surfactants are defined as follows [92]:

- Anionic surfactants: the head group is a negatively charged group such as carboxyl ($\text{RCOO}^- \text{M}^+$), sulfonate ($\text{RSO}_3^- \text{M}^+$), sulfate ($\text{ROSO}_3^- \text{M}^+$), or phosphate ($\text{ROPO}_3^- \text{M}^+$).
- Cationic surfactants: the hydrophile bears a positive charge, as for example, the quaternary ammonium halides ($\text{R}_4\text{N}^+ \text{X}^-$), and the four R -groups may or may not be all the same.
- Nonionic surfactants: the head group has no charge, but derives its water solubility from highly polar groups such as polyoxyethylene (POE or $\text{R-OCH}_2\text{CH}_2\text{O-}$) or R-polyol groups including sugars.
- Amphoteric (or zwitterionic) surfactants: the surfactant molecule contains, or can potentially contain, both a negative charge and a positive charge, such as the sulfobetaines $\text{RN}^+(\text{CH}_3)_2\text{CH}_2\text{CH}_2\text{SO}_3^-$.

The critical micelle concentration (CMC) of a surfactant

In highly dilute aqueous solutions, surfactants exist in monodispersed form and are concentrated at the interfaces by hydrophilic – hydrophobic oriented adsorption. With a rise in volume concentration, the surface density Γ increases until the surface is completely covered by the surfactant molecules or ions. Further surfactant molecules can not be accommodated at the surface and Gibbs' equation (Eq 1.6) is no longer valid [67].

An entropy effect is extremely important for the interfacial activity. The hydrophobic groups of the surfactant molecules or ions are hydrophobically solvated in aqueous solution. Thus the water molecules are highly ordered in the immediate vicinity of the hydrophobic species, which is associated with a decrease in entropy. If the hydrophobic group is displaced from the aqueous phase, the state of disorder of the water and thus the entropy of the system increases. This effect is also termed the hydrophobic effect. If, under total occupancy of the

surface, the volume concentration of the surfactant in equilibrium with the surface concentration prevailing in this case is exceeded, the surfactant molecules or ions, which up to this concentration are mainly present in the volume phase in individual form, congregate in an entropy-governed manner to form aggregates (micelles) in which they are oriented with the hydrophilic groups pointing towards the aqueous volume phase and the hydrophobic groups towards the interior of the micelles [67].

The aggregation of surfactant molecules or ions into micelles takes place in a strictly limited concentration range characteristic of each surfactant; if the surfactant concentration rises further, the number of micelles per unit volume increases, but not, however, the number of individual– dissolved surfactant molecules or ions. Since micelle formation occurs at the volume concentration of the surfactant at which the water-air interface is completely covered the surface tension becomes independent of any increase in volume concentration, measurement of the surface tension as a function of the concentration represents a simple method of determining the so-called critical micelle concentration (CMC) at which micellization or micelle formation begins [67] (Figure 1.10).

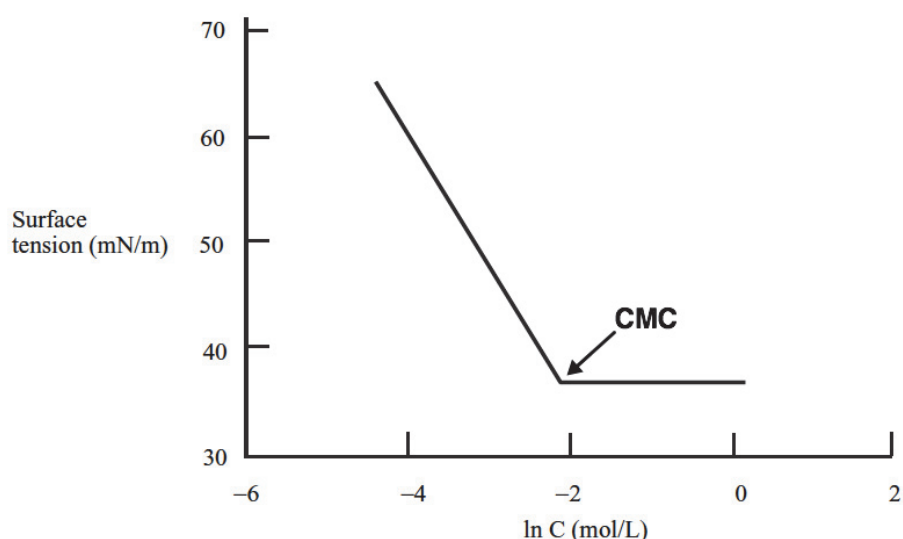


Figure 1.10: Determination of CMC by the curve surface tension- $\ln C$ [92]

The CMC value depends strongly on the molecular structure of a surfactant, it is also affected by the temperature and the cosolutes [49].

The increase in the number of molecules in a surfactant solution with concentration suddenly drops at the critical micelle concentration due to micelle formation, and consequently the concentration dependence of all colligative properties such as vapor pressure and osmotic pressure, and in the case of ionic surfactants also the equivalent conductance, changes at this concentration [67].

Micelles are dynamic structures that are in equilibrium with the surrounding individual surfactant molecules; their average aggregation number fluctuates in purely aqueous solutions at the critical micelle concentration around a mean value characteristic of each surfactant. This value is between 100 and 1000 in simple nonionic surfactants, and is generally below 100 in

ionic surfactants; with the latter, the electrostatic repulsion acting between the ionic head groups opposes further aggregation [67].

The shape of the micelle is related to molecular packing parameter p , which is defined as $V/(Al)$, where V and l are the volume and the length of the surfactant tail and A is the surface area of the hydrophobic core of the micelle expressed per molecule in the aggregate (hereafter referred to as the area occupied per molecule). The following well-known connection between the molecular packing parameter and the micelle shape: $0 \leq p \leq 1/3$ for sphere (Figure 1.11), $1/3 \leq p \leq 1/2$ for cylinder, and $1/2 \leq p \leq 1$ for lamellar [93].



Figure 1.11: Illustration of a spherical micelle [93]

Choice of surfactant based on the HLB system

A surfactant used for the formation of o/w emulsion should be poorly soluble in oil but well soluble in water, and its solubility depends closely on the molecular structure. To make the selection of surfactants easier, Griffin assigned a dimensionless number between 0 and 20 to each surfactant to give information on water and oil solubility. Numbers between 0 and 10 characterize oil-soluble hydrophobic surfactants, whereas numbers between 11 and 20 are used for water-soluble hydrophilic compounds. The HLB value of a surfactant can be calculated by equation (Eq 1.7) [48]:

$$HLB = 20 \frac{M_H}{M} \quad (Eq 1.7)$$

Where M_H and M are the mass of the hydrophilic part and the total surfactant molecule, respectively. In order to stabilize the o/w emulsion, the HLB value of the surfactant needs to be not only higher than 10 but also as near the HLB value of the oil phase as possible [48].

The quillaja saponin bio-sourced surfactant

An increasing trend in the food, pharmaceutical, and cosmetic industry is the utilization of natural plant extracts or plant-derived compounds, as an alternative to the application of chemical surfactants. Some bio-sourced surfactants that have been mentioned in the literatures are the derived Dodecylamino Diglycidyl Ether of Isosorbide surfactant [2], the fully bio-sourced lauroyl oligoester surfactants [4] and the quillaja saponin surfactants [101, 157]. The nontoxic nature of chemicals in plants, positive healthy properties, consumer perception and acceptance of their use has opened a good future.

Quillaja saponins are surfactants that originate from the bark of the tree *quillaja saponaria monila* (most popular in Chile and Peru). They are high molecular weight glycoside, consisting of a sugar moiety linked to a triterpene aglycol [81].

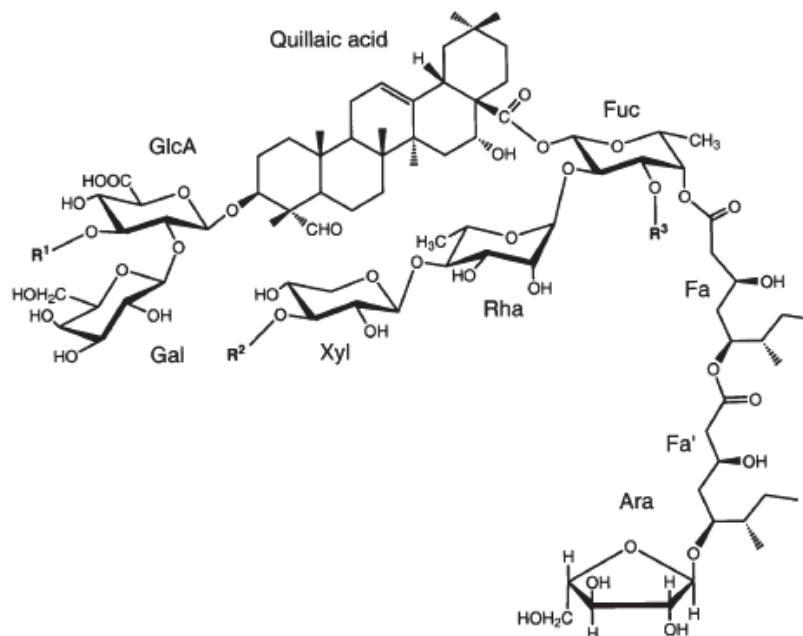


Figure 1.12: General molecular structure of quillaja saponin, in which R^1 , R^2 , R^3 groups depend on different molecules in the bark extract [98]

The bark extracts from tree *quillaja saponaria monila* contain a complex mixture of saponins that are difficult to separate into individual components. The most common basic structure reported for quillaja saponin is quillaic acid substituted at C-3 with a trisaccharide, and at C-28 with an oligosaccharide through a fucose residue. This fucose residue is usually substituted by an acyl group consisting of two 3,5-dihydroxy-6-methyloctanoic acid groups (C-9) terminated by an L-arabinofucranosyl group (Figure 1.12) [98]. The saponins are surface active substances because they contain both hydrophilic regions (such as rhamnose, xylose, arabinose, galactose, fucose and glucuronic acid) and hydrophobic ones (such as quillaic acid and gypsogenic acid) [156]. The average molecular weight of saponin fluctuates around 1650 Da, depending on the origin and extraction process [86].

The HLB value of quillaja saponin is round 13.5 [18], so it is well soluble in water that is suitable for the formation of o/w emulsion [101, 152, 156, 157]. The CMC value of this surfactant is in range of 0.01÷0.07 wt%, and the area per head group at the maximum surface adsorption $83\div96 \text{ \AA}^2$, depending on the origin and the extraction conditions [86, 152, 156].

There have been some researches using quillaja saponin as the surfactant in forming o/w emulsions recently, especially in food industry [101, 152, 156, 157]. The quillaja extracts are approved for human consumption by countries such as United State, Europe and Japan [81].

Comment:

Microencapsulation by solvent evaporation technique has been applied to encapsulate ibuprofen and the created microcapsules had the size of $1 \div 50 \mu\text{m}$, which was appropriate for textile application.

However, a big disadvantage of this technique is the use of toxic halogenated solvents to dissolve the polymers. The trend of replacing those toxic solvents with non-halogenated solvents, which are less toxic for human and environment, has been taken interest of some researchers.

Besides, quillaja saponins are bio-sourced surfactants that are approved for human health and have been applied in producing emulsions for food, pharmaceutical and cosmetic industry. However up to now, there have been not any studies on using quillaja saponin for the microencapsulation by solvent evaporation technique.

1.3. The textile substrates

Beside the microcapsule, the textile substrate is an important component of the microcapsule-treated fabric too because it could affect many characteristics of the microcapsule-treated fabric, including the active release capability.

1.3.1. Influence of the textile substrate on the microcapsule loading capability of microcapsule-treated fabrics

Definition and determination of microcapsule loading capability of the fabrics

The microcapsule loading capability (MLC) of the microcapsule-treated fabric is a very important value because it determines the dose of active released from the fabrics [40, 41, 94]. Therefore, it is necessary to find out the factors that can affect strongly the microcapsule loading capability of fabrics and figure out the trend of influence.

According to the literatures, there are two methods of determining the fabric microcapsule loading capability, which are direct and indirect ones.

The direct determination of microcapsule loading capability used more commonly, is defined by the amount of microcapsules deposited to fabrics and equal to the increase in weight of fabrics after the microcapsule treatment [17, 53, 72, 80, 124]. The increase in weight is often expressed by the percentage ratio (Eq 1.8):

$$\text{MLC (\%)} = \frac{M_2 - M_1}{M_1} \times 100\% \quad (\text{Eq 1.8})$$

In which MLC (%) is the microcapsule loading capability of fabric, M_1 and M_2 the weight of fabric before and after the microcapsule treatment, respectively.

In the indirect method, the amount of deposited microcapsules is deduced from the amount of active ingredient in fabric, which is quantified by UV-Vis [75] or FTIR equipments [88] after the complete extraction of active ingredient from the microcapsule-treated fabrics.

Influence of structural parameters on microcapsule loading capability of woven fabrics

It was reported that the textile material had strong influence on the microcapsule loading capability of the woven fabrics. N. Carreras et al. [17] studied the influence of textile material on the microcapsule loading capability of four kinds of woven fabrics that were cotton, polyamide, acrylic and polyester. Those fabrics were padded with PCL microspheres containing ibuprofen, the microcapsule loading capability of them were 4.30, 4.36, 4.64 and 5.65%, respectively. According to the authors, with the same pick-up value, the microcapsule loading capability of polyester fabric (5.65%) was higher than that of cotton fabric (4.30%) because the crystalline structure and the hydrophobicity of polyester fabric made it have higher affinity with microcapsules than cotton fabric.

The yarn count, the weft yarn density and the woven structure were also reported to affect the microcapsule loading capability of woven fabrics. In the research of L. Li et al. [75], three levels of yarn count investigated were Ne32, Ne20 and Ne10; three levels of weft yarn density investigated were 23, 19 and 15 yarns/cm; three kinds of woven structures investigated were 1/1 plain, 2/1 right twill and honey comb. The gelatin - arabic gum microcapsules containing moxa oil were padded to fabrics. Their results showed that the increase of yarn count and weft yarn density lowered the microcapsule loading capability of fabrics, but the influence was very slight. On the contrary, the woven structure exerted significant effect on the microcapsule loading capability, with the highest value belonged to the honey comb structure (2.059 mg/cm²). This result was explained by the differences in weaving mechanism of different structures. As for the honeycomb structure, an appropriate match of tight structure (numerous interlacing points) and slack (a few of interlacing points) forms quadrangle concave and convex decorative patterns in the surface of fabric, which is facilitates the adhesion for a large number of microcapsules.

Influence of structural parameters on microcapsule loading capability of knitted fabrics

Among the structural parameters of knitted fabrics, the knitted structure and the loop length were reported to influence the microcapsule loading capability of fabrics. According to C. D. Huong et al. [53], among three knitted structures that were single, rib 1x1 and interlock 1x1, the interlock fabric possessed the highest microcapsule loading capability, and this was thought to be due to its highest porosity. For single fabrics, the microcapsule loading capability changed with a not clearly trend when the loop length varied. For rib fabrics, the microcapsule loading capability increased when the loop length decreased, whereas for the interlock fabric, the microcapsule loading capability was in direct proportion to the loop length.

1.3.2. Influence of the textile substrate on the microcapsule distribution of microcapsule-treated fabrics

Along with the microcapsule loading capability, the microcapsule distribution on the fabrics also contributes to the control of drug release from the microcapsule-treated fabric. The influence of textile substrate on the microcapsule distribution has been mentioned in some papers literature.

The textile material was reported to affect the microcapsule distribution on the fabrics. According to F. Salaun et al. [125], the distribution of melamine formaldehyde microcapsules, which were padded to fabrics, depended on the textile materials with all three types of binders (Alcoprint PB-66, Dicrylan PMC and Airflex EN428). Due to the high wetting ability of polyester with the binder solutions, the binders wrapped the fibers homogenously throughout the fabric, so the microcapsules could enter the inner structure of the fabrics (Figure 1.13A). Contrarily, the low wetting ability of cotton with the binder solutions made the binders form a thin film over the fabric surface and could not penetrate the pores of the fabrics, therefore the microcapsules were only distributed on the surface of the fabrics (Figure 1.13B).

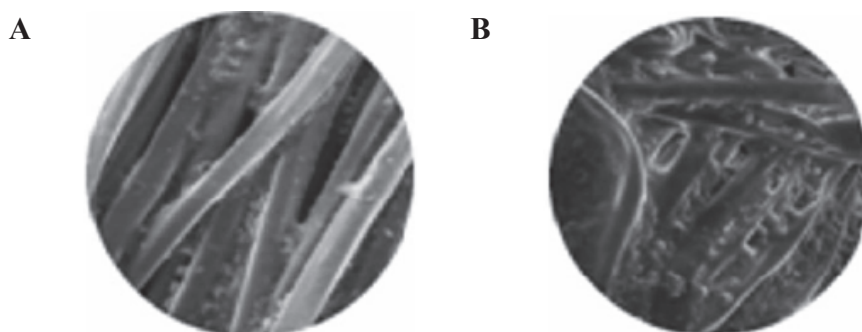


Figure 1.13: SEM images of fabrics padded with microcapsules: polyester fabric (A) and cotton fabric (B) [125]

Beside the textile material, the method of fabric construction also affected the microcapsule distribution on the fabrics. In the research of B. Golja et al. [40], the melamine formaldehyde microcapsules containing flame - retardant agent were coated to nonwoven polyester and woven cotton fabric. The woven cotton fabric was almost completely covered with microcapsules (Figure 1.14B) while on the nonwoven polyester fabric, most microcapsules were captured in the nooks among the fibers and only a few microcapsules were located on the fibers (Figure 1.14A). The difference in microcapsule distribution of these two fabrics was explained by the difference in the fabric construction; the polyester fabric was nonwoven kind with very porous structure that helped more microcapsules go inside the pores of fabric, while the cotton fabric was woven kind with rather tight structure that kept most microcapsules on the fabric surface.

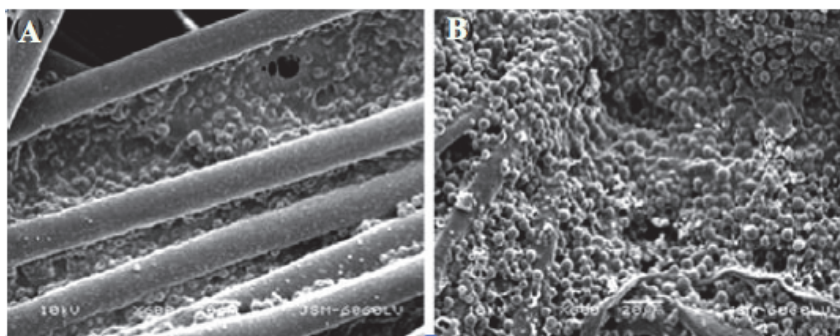


Figure 1.14: SEM images of polyester fabric (A) and cotton fabric (B) coated with microcapsules containing flame-retardant agent [40]

1.3.3. Influence of the textile substrate on the active release capability from the microcapsule-treated fabrics

Up to now, there have been only one research [17] about the influence of the textile material on the active release capability of the microcapsule-treated fabric. The effect of other fabric structural parameters has not been mentioned in any literatures yet.

N. Carreras et al. [17] evaluated the active release capability of four fabric types woven from different textile materials, which were cotton, polyamide, acrylic and polyester. The PCL microspheres were applied to these fabrics by padding. The microcapsule-treated fabrics were then submerged into the thermostated vessels filled with deionized water and physiological saline at temperature of 37°C in order to determine the release profile of ibuprofen from the fabrics. The release model of Higuchi, which was often used to describe the drug release from the polymer matrices, was applied in this research. The equation of Higuchi was as below:

$$\frac{M_t}{M_\infty} = K \times \sqrt{t} \quad (\text{Eq 1.9})$$

In which, $\frac{M_t}{M_\infty}$ is the percentage of drug released at each interval of time relative to the percentage of release at the equilibrium, K is the constant of drug release and t is time measured.

According to the equation (Eq 1.9), the higher value of K, the faster drug release rate from the polymer matrix. And the values of K for four kinds of fabrics investigated were listed in Table 1.1. It could be observed that cotton and polyamide had a similar trend, because in both cases the constant K had similar values in deionized water. In contrast, in the case of acrylic and polyester, the results were quite distant from cotton and polyamide but were similar to each other. It seemed that saline medium had no influence in the different systems, because the results obtained were similar in all cases.

Table 1.1: The values of K for different kinds of fabrics [17]

Fabric	Release medium	Value of K
Cotton	Deionized water	0.0355
	Physiological saline	0.1346
Polyamide	Deionized water	0.0383
	Physiological saline	0.1240
Acrylic	Deionized water	0.7678
	Physiological saline	0.1460
Polyester	Deionized water	0.7246
	Physiological saline	0.1373

1.3.4. The interlock knitted fabrics

Knitted fabrics are used very often in the field of medical textiles, especially in the high-tech products due to their soft and elastic features. Basing on the knitting principle, the knitted fabrics are divided into the two main groups that are the weft knitted and the waft knitted ones. Among those, the weft knitted fabrics with simple structures, including the interlock fabrics, are widely used as the textile substrates for the medical bandages.

The fabric structure and properties

Interlock is a derivative structure of the double-jersey structure (the rib structure), it is knitted on two-needle bed knitting machines with the opposite arrangement of needles on two needle beds. Each interlock pattern row (often termed an "interlock course") requires two feeder courses, each with a separate yarn that knits on separate alternate needles, producing two rib courses whose sinker loops cross over each other (Figure 1.15).

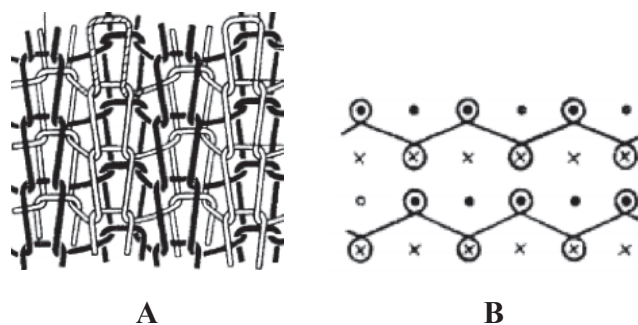


Figure 1.15: Structure (A) and notation (B) of interlock knitted fabric [1]

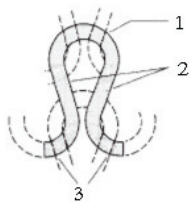
Because of the knitting technique, interlock fabrics are quite soft and elastic. The technical face of plain fabric on both sides provides smooth surface to the fabric. A structural knitted cell (SKC) consists of four loops in a same interlock course, in which two loops are in

the front side and two loops are in the back side of the fabric. The fabric could be unraveled only from the knitted last, but in fact the friction between layers of yarns makes it very difficult to be unraveled, the fabric is often torn by the abrasion rather than by the yarn rupture. It does also not curl at the edges because of the force balance here.

Due to the structure and properties described above, the interlock knitted fabric is very suitable for medical textile application, especially in the compressive bandages. If the microcapsule-treated fabric is used for a compressive bandage, it often is wrapped around a body part such as wrist and knee, so the fabric extension could affect the pressure exerting on microcapsules, altering the transdermal drug release capability of the fabric. But the influence of fabric extension on the transdermal release has been still not mentioned in any literatures.

Structure of knitted loops

The loop, which is the most basic unit of a knitted structure, consists of three main parts: one needle loop, two legs and one sinker loop (Figure 1.16).



1. Needle loop
2. Legs
3. Sinker loop

Figure 1.16: Structure of knitted loop [1]

The model of the knitted loop is the most basic tool to simulate all the knitted structure, supporting the fabric design process and the prediction of fabric properties such as the air permeability, the water adsorption... [3, 10, 29, 100, 134, 144]. Therefore, the model of knitted loop could be a scientific basis to explain the influence of knitted structure on the characteristics of microcapsule-treated fabric.

Basing on the principle of building the model, the models of knitted loop are classified into two main groups:

- The geometrical models: based on the observation, in which each part of the loop is simulated as a simple geometrical curve. This group includes the models of Pierce [109], Leaf-Glaskin [71], Suh [90] and Dabiryan-Jeddi [27, 132]... These models are quite simple and often used in geometrical design of fabric.
- The mechanical models: based on the analysis of the forces exerting on the loop at a certain mechanical state of fabric. This group includes the models of Postle-Munden [113], Shanahan-Postle [133] and Hepworth-Leaf [47]... These models are rather complicated and difficult to apply in geometrical design of fabric.

Most geometrical models describe the loop structure of single knitted fabrics, so far there have been only one model of Dabiryan-Jeddi [27] simulating the interlock knitted loop (Figure 1.17), which was based on the following assumptions:

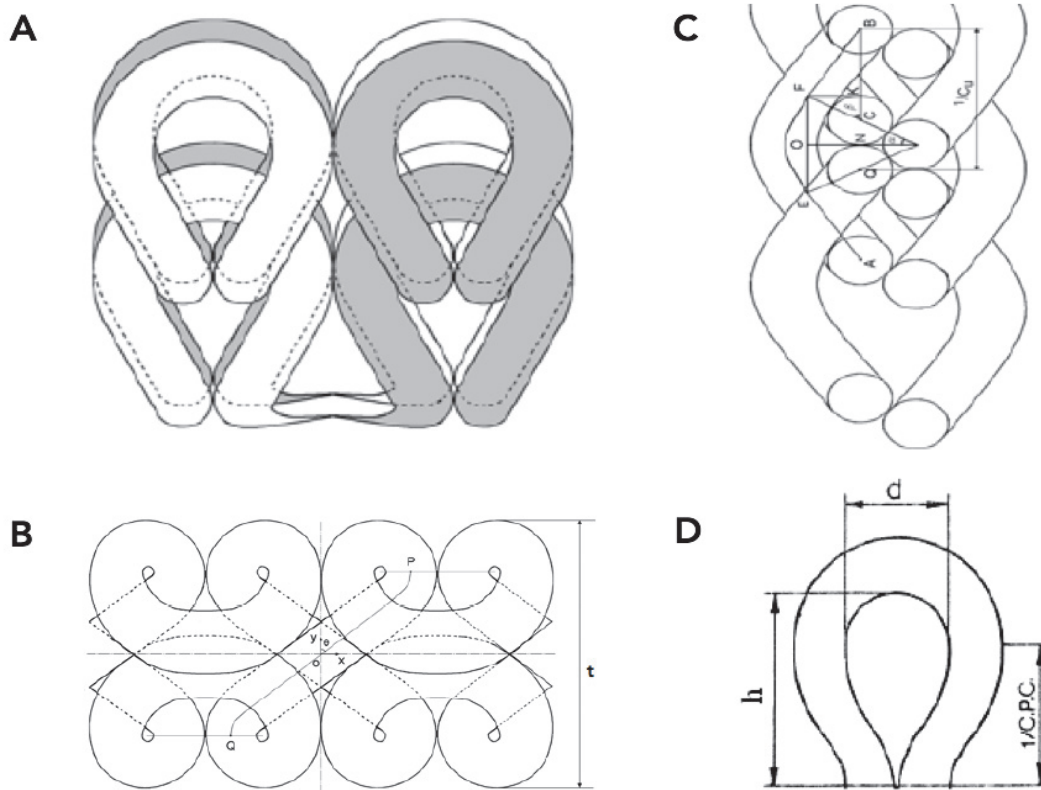


Figure 1.17: Model of interlock knitted loop by Dabiryani-Jeddi [27]
 (A) Front view; (B) Plane view; (C) Side view; (D) a plain structure

1. The yarn is assumed to behave as a cylindrical elastic rod having a uniform diameter D and follows the elastica property. The two ends of the needle loop are brought together so that the ratio of maximum height to minimum width (h/d) equals 2.08 (Figure 1.17D), irrespective of the type or length of yarn (according to Leaf [70]).
2. A structural knitted cell is divided into two segments, one segment being the needle loop and two legs of four plain-type face loops (one course described in Figure 1.17A), a plain-type face loop follows the mathematical based equation of improved Strophoid curve. Another segment is the linking portions between face and back loops (the sinker loop), which follows the parabolic equation of $y = ax^2$ (Figure 1.17B).
3. The narrowest and widest parts of any two interlocking loops in the same wale coincide (Figure 1.17A), which is in agreement with Munden's assumption [91].
4. Loops of adjacent wales touch at their widest parts. Also, the consecutive courses make contact with each other and the legs of the loop make contact at the point of minimum loop width, i.e. both length and width jamming of structure occurs in the fabric (Figure 1.17A).
5. In the side view (Figure 1.17C), it is assumed that $\alpha = \pi/6$ and $AE = FB$.
6. The ratio of the fabric thickness t to the yarn diameter D is 4.1 (Figure 1.17B), according to Postle [112].

According to the authors, if the assumptions mentioned above are met, the length of yarn within a structural knitted cell L_u will be calculated as below:

$$L_u = 9.38768 \times h + 19.889 \times D \quad (\text{Eq 1.10})$$

In which:

L_u (mm): the length of yarn within a structural knitted cell

h (mm): described in Figure 1.17

D (mm): the yarn diameter

And the relationship between the length of yarn within a structural knitted cell L_u (cm) with the number of structural knitted cells (SKCs) per unit area S_u (SKCs/cm²) is described by the following equation:

$$S_u \times L_u^2 = 169.44 \quad (\text{Eq 1.11})$$

Comment:

Due to many advantages such as the softness, the high elasticity, the ability of not curling at edges and the difficulty of unraveling, the interlock knitted fabric is very suitable for the substrate in the medical textiles using microcapsules, especially in compressive bandages.

The fabric structure has strong influence on the microcapsule loading capability, the microcapsule distribution and the active release capability of the fabric. However so far, there have been a few researches about these problems on the knitted fabrics in general and on the interlock fabric in specific. At our best knowledge, there has been no published research in the knitting field about the influence of textile material on the characteristics of microcapsule-treated fabric. Only one study reported that the loop length could affect the microcapsule loading capability of single, rib and interlock fabrics; but the scientific basis of the influences was not explained. There has been no study about the effects of loop length on the microcapsule distribution and the active release capability of the fabric. Besides, up to now, there has been no published research about the influence of fabric extension on the transdermal release capability of the microcapsule-treated fabric.

1.4. Textile finishing with microcapsules

1.4.1. Techniques of finishing textiles with microcapsules

The classification

Microcapsules were applied to textiles by conventional techniques such as padding [17, 72, 75, 85, 88], coating [25, 66, 79, 94, 95, 129, 130], impregnating [9, 56], printing [40, 94] or spraying [139]. In those techniques, in order to sustain the link between fabrics and microcapsules during use, the finishing formulations need to consist of cross-linking agents, which, after polymerization, create a film on fabric surface, hindering the active release from microcapsules.

To overcome this problem, the production of functional textiles containing microcapsules by only one-step techniques was presented, in which the microencapsulation and the grafting of microcapsules on textiles were simultaneous [5, 6, 128]. Those techniques help eliminate the use of cross-linking agents but the need of complicated equipment systems is a big disadvantage of them.

Beside the only one-step techniques, the technique of integrating microcapsules directly with fibers during the fiber manufacturing process also helps produce functional textiles without cross-linking agents. However, this technique is only suitable for fibers produced by melting spinning such as polypropylene [54, 127].

Influence of finishing technique on characteristics of microcapsule-treated fabric

The finishing technique has strong influence on many characteristics of microcapsule-treated fabric, including the microcapsule loading capability and the microcapsule distribution.

B. Golja et al. [40] reported that the finishing technique could affect the microcapsule distribution on fabric and therefore, alter the microcapsule loading capability of fabric. In their research, by padding technique, a lot of microcapsules could go into the inner structure of the fabric while most microcapsules were just on the fabric surface in case of coating technique. In the coating process, the paste was applied to the fabric horizontally with a squeegee and the rheological properties of the paste prevented the microcapsules from passing through the yarn during coating. Padding, on the contrary, is a mechanical process that allowed the products to pass through a yarn, so it seems that most of the microcapsules were located in the inner part of the fabric. Consequently, padding technique helped apply more microcapsules to fabric than coating one.

The research of K. Koo et al. [66] demonstrated that the microcapsule distribution in fabrics depends closely on the finishing technique. In this research, microcapsules loading phase change material were applied on the nylon fabrics by wet coating and dry coating methods, using polyurethane (PU) resin as the binder. The SEM images of cross-sections of coated fabrics showed that for the wet coating finish without microcapsules, a large number of micropores in the PU resin layer could be seen. As the amount of microcapsules was increased, the pores of the PU resin became closely compacted with the microcapsules (Figure 1.18). On the contrary, micropores could not be observed in the dry-coated fabrics without microcapsules, but with the addition of microcapsules the pore size of the coating layer increased gradually that might result from the breaking of microcapsules during the dry coating process (Figure 1.19).

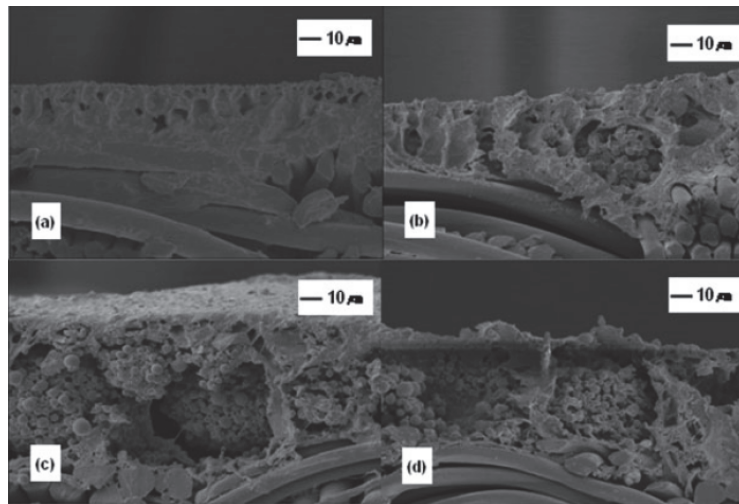


Figure 1.18: SEM images of wet-coated nylon fabrics with and without microcapsules: without microcapsules (a), with 10% (b), 20% (c) and 30% microcapsules (d) [66]

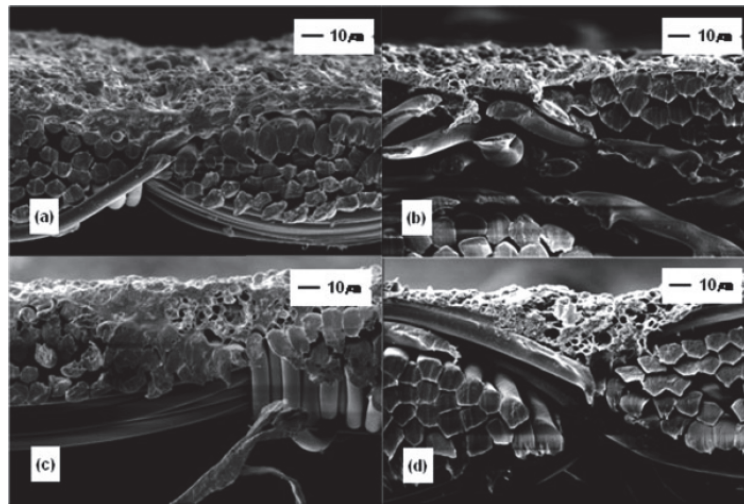


Figure 1.19: SEM images of dry-coated nylon fabrics with and without microcapsules: without microcapsules (a), with 10% (b), 20% (c) and 30% microcapsules (d) [66]

1.4.2. Influence of the drying conditions on the microcapsule morphology after finishing process

The deformation of microcapsules after finishing processes is a real problem in many researches on microcapsule application in textile, since most finishing processes require the drying step, which could make the microcapsules deflate significantly [9, 85, 88, 118, 139, 158]. However so far, at our best knowledge, there have been only one research [88] investigating the influence of drying condition on microcapsule morphology after finishing of microcapsule-treated fabrics.

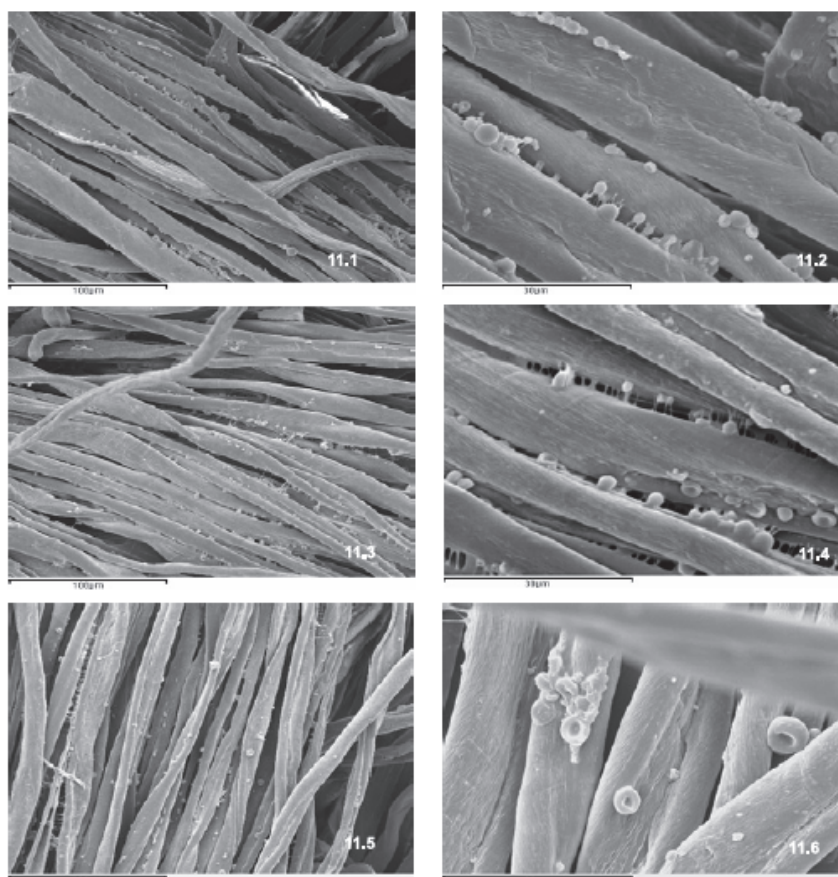


Figure 1.20: SEM images of microcapsule padded cotton fabrics with different drying temperature 120 °C (11.1-11.2); 140 °C (11.3-11.4); 160 °C (11.5-11.6) [88]

P. Mollor et al. [88] studied the influence of drying temperature on the deformation of melamine formaldehyde microcapsules containing peppermint fragrance after being applied to cotton fabrics by padding technique. Three levels of drying temperatures investigated were 120, 140 and 160°C (all for 10 minutes). Their results showed that the presence of apparently unaltered microcapsules could be observed on the fabric treated by air at 120°C, some deflated microcapsules appeared when heated at 140°C and the swelling was reduced considerably in each microcapsule at drying temperature of 160°C (Figure 1.20). By FTIR spectrum and of microcapsule padded fabrics at different drying temperatures, together with thermal analysis of microcapsules, the authors confirmed that microcapsule deformation was due to the fragrance loss from microcapsules during the drying step.

Comment:

There are many techniques of finishing microcapsule - treated textile, in which the padding and the coating one are the two most used technique. In the padding technique, most microcapsules could go inside the fabric structure while in the coating one, most microcapsules just locate at the fabric surface.

Most finishing processes include the drying step, which may induce the microcapsule deformation. Then in the research of microcapsule application in textile, it is very necessary to choose a suitable drying condition that does not affect the microcapsule morphology on the treated fabrics.

1.5. Conclusions of the literature review

1. A modern and effective method to produce medical textiles is to use the microcapsules to apply many kinds of drugs and therapeutic agents, including anti-inflammatory drugs, to fabric. Microcapsules help to control the release of active ingredients and protect them.
2. Application of bio-sourced microcapsules has taken much interest in the field of medical textile, with many kinds of bio-sourced polymers and active ingredients were used. In a microencapsulation, besides the polymer and the active ingredient, the surfactant and the solvents are also very important components. However, up to now, there has little concern in the textile field to use bio-sourced surfactants and less toxic solvents for microencapsulation.
3. Microencapsulation by solvent evaporation technique was often used to elaborate the microcapsules containing anti-inflammatory drugs, could produce the microcapsules with suitable size for textile application (1÷50µm) and narrow size distribution.
4. In the finishing of textile with microcapsules, the drying conditions should be chosen carefully to protect the microcapsules from deformation.
5. There are three characteristics of microcapsule-treated fabrics often mentioned in the literature that are the microcapsule loading capability, the microcapsule distribution and the active release capability. They depend closely on the structural parameters of the fabric substrate. However, up to now, there have been very few researches on this problem in the knitting field.

According to the conclusions above, the research objectives of the thesis are figured out as following:

1. Elaborating the microcapsules suitable for textile application, containing an anti-inflammatory drug, by solvent evaporation technique, using a bio-sourced surfactant and a non-halogenated solvent.
2. Finding out the suitable drying conditions for textile finishing with obtained microcapsules to keep the microcapsules from deformation.
3. Figuring out the influences of fabric structural parameters (textile material, loop length, fabric extension) on the important characteristics of the knitted fabrics containing microcapsules (microcapsule loading capability, microcapsule distribution, active release capability).

2. Chapter 2: Experimental methods

2.1. Materials

2.1.1. Interlock knitted fabrics

As mentioned at section 1.3.4, the interlock knitted fabric is very suitable for the medical textile application, especially in the compressive bandages, so it was used as the substrate for the textiles containing microcapsules in this work.

Two collections of the interlock knitted fabrics were used in this thesis:

- The first collection was used in order to investigate the influence of the textile material on the characteristics of the microcapsule-treated fabrics.

It consists of three kinds of interlock fabrics knitted from three different kinds of textile materials often used for medical gauges, patches and bandages; they were cotton, peco 65/35 and polyester yarns, and all the yarns had the same yarn count of Ne20. The knitting processes were carried out on the flat knitting machine SSR-112 (knitting gauge R16) of Shima Seiki. The grey fabrics were then scoured and bleached at Doximex Knitting Company. The knitting, scouring and bleaching parameters were similar for all fabrics. The codes Cot, 6535 and Pet were applied for cotton, peco 65/35 and polyester fabric, respectively.

- The second collection was used in order to investigate the influence of the loop length on the characteristics of the microcapsule-treated fabrics.

It consists of five lots of interlock fabrics, which were knitted from cotton yarn having yarn count of Ne40. The knitting process was conducted on circular knitting machine Fukahara (knitting gauge E18) with the loop length varied over five levels of 2.81, 2.83, 2.87, 2.96 and 3.05 (mm). These values are the most popular loop lengths used by Doximex Knitting Company because they are qualified for the fabrics with high dimensional stability. Five fabric lots were coded by B1, B2, B3, B4 and B5, respectively. The grey fabrics were then scoured and bleached under similar conditions. All the knitting, scouring and bleaching processes were carried out at Doximex Knitting Company.

2.1.2. Chemicals for microencapsulation

Chemicals used for microencapsulation are presented at Table 2.1. All chemicals have been used as providing without any more purification.

Table 2.1: Information of chemicals used for microencapsulation

Chemical	Supplier	Technical information
Ibuprofen	BASF (Germany)	
Miglyol 812	SASOL (Germany)	
Eudragit RSPO	EVONIK Industry (Germany)	MW 33 800 (g/mol)
Quillaja saponin	Sigma-Aldrich (Germany)	Type S4521, Sapogenin content 20-35%
Ethyl acetate	CARLO ERRA Group (France)	Purity of 99.9%

The anti-inflammatory agent ibuprofen

Ibuprofen, the (2*RS*)-1[4-(2-methyl propyl) phenyl] propionic acid (Figure 2.1), was the first member of propionic acid derivatives to be introduced in 1969 in order to replace aspirin. Gastric discomfort, nausea and vomiting, though less than aspirin or indomethacin, are still the most common side effects.

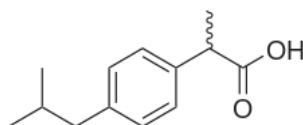


Figure 2.1: Structural formula of ibuprofen ($C_{13}H_{18}O_2$) [14]

Ibuprofen is the most commonly used and most frequently prescribed non-steroid (NSAID). It is a non-selective inhibitor of cyclooxygenase-1 (COX-1) and cyclooxygenase-2 (COX-2), which are involved in the synthesis of prostaglandins. Prostaglandins have an important role in the production of pain, inflammation and fever [14]. The short biological half-life of 1.8 ÷ 2 hours following oral dosing (Table 2.2) makes ibuprofen an ideal candidate for microencapsulation.

Table 2.2: Some properties of ibuprofen [151]

CAS number	15687-27-1
Molecular weight	206.281 Da
Melting point	76°C
Boiling point	365°C/760 mmHg

<i>Solubility</i>	Insoluble in water. Soluble in most organic solvents
<i>Biological half-life</i>	1.8 ÷ 2 hours

Table 2.3: Doses of ibuprofen for adults and children [14, 65]

Patients	The treatment	Doses
Adults	Analgesia	200 - 400 mg, every 4 - 6 hours
	Anti-inflammatory	300 mg, every 6 - 8 hours or 400 - 800 mg, 3 - 4 times daily
Children	Anti pyretic	5 - 10 mg/kg, every 6 hours (max. 40 mg/kg per day)
	Anti-inflammatory	20 - 40 mg/kg/day in 3 - 4 divided dose

Ibuprofen has been often microencapsulated by the solvent evaporation technique, in which methylene chloride was mostly used as the solvent [17, 147, 163]. Up to now, there have been not any researches concerned about using less toxic and more environment-friendly solvent as an alternative.

Miglyol 812

Miglyol 812 is the trade name of caprylic/capric triglycerides (Figure 2.2), which are fully saturated triglycerides having excellent emolliency and good user properties e.g. easy spreading and no occlusive feeling. It is entirely derived from vegetable resources and offers a stable alternative to mineral or vegetable oil. They are non-toxic and non-irritating to skin so often used as solvent and vehicle for vitamins and nutritional actives [19, 58].

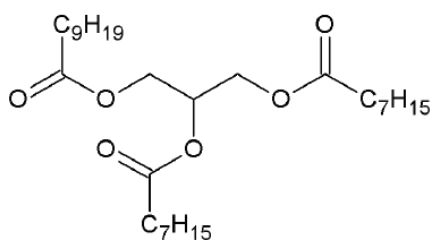


Figure 2.2: Chemical structure of Miglyol 812 [58]

Miglyol 812 is used widely in pharmaceutical field [103, 107, 119], cosmetic [20, 59, 62] and food industry [82]. In the pharmaceutical field, miglyol has very low reactivity with chemically sensitive pharmaceutical actives so it is often selected as the oil phase in microemulsion O/W, used as the drug delivery system to transport ketoprofen [103], lidocaine [119] and danazol [107]. The use of miglyol 812 to dissolve ibuprofen helped produce core-shell microcapsules containing ibuprofen, furthermore it could prevent the drug from

crystallizing at the microcapsule surface, implying a better efficiency of the drug delivery system [147].

The polymer eudragit RSPO

Eudragit RSPO is the trade name of poly(ethyl acrylate-co-methyl methacrylate-co-trimethylammonioethyl methacrylate chloride) 1:2:0.1 from EVONIK (Figure 2.3):

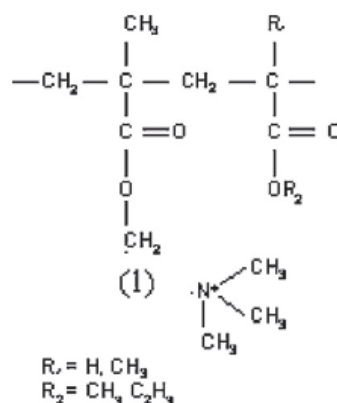


Figure 2.3: Chemical structure of eudragit RSPO [147]

Eudragit RSPO is a biocompatible polymer in type of white powder, having low permeability and the T_g of 61 - 67°C [44, 164], it is often used in the controlled drug delivery systems [7, 22, 37, 89, 108, 135, 147, 148]. Due to the dependence of swelling on the pH value of release environment, this polymer is mainly used in the oral drug delivery systems [37, 89, 108, 135], in transdermal drug delivery systems eudragit RSPO is often mixed with other types of eudragit to form the polymer substrate containing the drug. P. Valot et al. [147] used eudragit RSPO as the polymer for microencapsulation of ibuprofen, the elaborated microcapsules had spherical shape with the average diameter around 24 μm that was proposed to be suitable for textile applications.

2.2. Research contents

In order to meet the research objectives (figured out at section 1.5), the following research contents were carried out:

1. Microencapsulation of the anti-inflammatory drug ibuprofen suitable for medical textile by solvent evaporation technique, using the bio-sourced surfactant quillaja saponin and the non-halogenated solvent ethyl acetate:
 - 1.1. Determining the range of microcapsule size that is appropriate for the cotton interlock fabric used in this thesis.
 - 1.2. Evaluating the surface-active property of quillaja saponin used in this thesis (the lot S4521 of Sigma Aldrich).

- 1.3. Investigating the influence of microencapsulation parameters on the microcapsule size and morphology. The parameters investigated were: the concentration of saponin, the stirring rate, the volume of solvent added to aqueous phase before emulsification.
- 1.4. Choosing the most suitable microencapsulation parameters for the application on anti-inflammatory textile.
2. Influence of drying condition on microcapsule morphology after the finishing of textile with microcapsules:
 - 2.1. Influence of humidity during drying process.
 - 2.2. Influence of drying temperature.
3. Influence of the structural parameters of interlock knitted fabric on the main characteristics of the microcapsule-treated fabric:
 - 3.1. Influence of textile material on the microcapsule loading capability, the microcapsule distribution and the active release capability of fabric.
 - 3.2. Influence of loop length on the microcapsule loading capability, the microcapsule distribution and the active release capability of fabric.
 - 3.3. Influence of fabric extension on the active release capability of fabric.

2.3. Experimental techniques

In order to execute the above research contents, the following experiment methods and techniques were applied:

2.3.1. Determining the suitable microcapsule size for textile application

Because the ibuprofen-loaded microcapsules will be applied to textile, the size of microcapsules should be appropriate to the textile substrate. The microcapsule size should be small enough so that they could be kept well by adjacent fibers in the textile substrate. Besides, because the microcapsule-treated textile will be used for transdermal treatment, the microcapsule size should be such as most of them will locate only on the yarn surface and not inside the inner structure of yarns. The microcapsule size should be bigger than the minimum distance and smaller than the maximum distance between adjacent fibers in the fabric.

So in order to conclude about the suitable size of microcapsules, the distance between adjacent fibers in the fabric B3 (the fabric lot having loop length in the center of investigated range) was observed and measured by the scanning electron microscope. Then the conclusion about the suitable microcapsule size could be drawn out by combining the measured distance between fibers with the related information in literatures.

2.3.2. Evaluating the surface-active properties of quillaja saponin

According to some literatures, the cmc value of quillaja saponin is in range of 0.01 ÷ 0.07 (wt%) [86, 156], so to evaluate the surface-active properties of quillaja saponin, the surface tension of a series of saponin solutions in water having concentrations varying from 0 to 1 (wt%) was determined.

The surface tension was measured with the du Noüy ring method by tensiometer SEO-DST30M (Surface & Electro Optics) at Laboratory of Petrochemical and Catalysis Adsorption Materials, Hanoi University of Science and Technology (HUST) (Figure 2.4). The measurements were referred to the testing standard ASTM D1331-11, each measurement was triplicated. Some main parameters of the measurement included: the temperature 25°C, the pressure 1atm, the ring parameter 6.1858 (mm); R/r = 54.7857; the density of air 1.1839.



Figure 2.4: Tensiometer SEO-DST30M (Surface & Electro-Optics)
(Laboratory of Petrochemical and Catalysis Adsorption Materials, HUST)

The cmc value was determined from the plot of the surface tension γ (mN/m) versus $\ln C$ (C was the saponin concentration in mol/L) [86].

The surface density Γ_{max} (mol/m²) of saponin at air/water interface could be determined from the Gibbs adsorption equation [142] in the linear part of the curve $\gamma = f(\ln C)$:

$$\Gamma_{max} = -\frac{1}{RT} \frac{\partial \gamma}{\partial \ln C} \quad (\text{Eq 2.1})$$

Where R was the gas constant (8.314 J/mol K), T was the absolute temperature (K), γ was the surface tension (N/m) and C was the saponin concentration (mol/l).

Further, the interfacial area occupied by one molecule of surfactant A (m²) could be found from the surface density using the equation [142]:

$$A = \frac{1}{\Gamma_{max} N_{Av}} \quad (\text{Eq 2.2})$$

Where N_{Av} was the Avogadro constant (6.023×10^{23}).

2.3.3. Investigating the influence of the microencapsulation parameters on microcapsule characteristics

2.3.3.1. Microencapsulation

Ibuprofen was encapsulated into eudragit RSPO microcapsules by the solvent evaporation method, described in Figure 2.5. The microencapsulation experiments were performed at Ingénierie des Matériaux Polymères (IMP), University Claude Bernard Lyon 1 (UCBL).

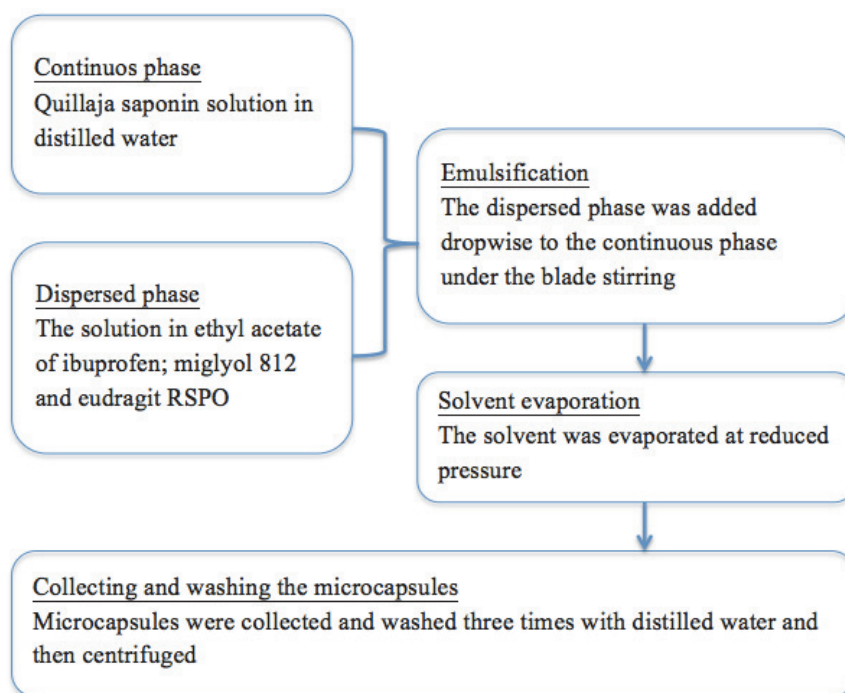


Figure 2.5: Diagram of microencapsulation of eudragit RSPO loading ibuprofen by solvent evaporation method

Step 1: Preparing the two phases of emulsion

The continuous phase was 100 ml of saponin solution in distilled water. In order to investigate the influence of saponin concentration on microcapsule characteristics, the saponin concentration varied with four levels: 0.025, 0.050, 0.075 and 0.100 (wt%), and the correlative microcapsule lots were coded as C0.025, C0.050, C0.075 and C0.100. In order to investigate the influence of the volume of solvent added to the continuous phase before emulsification on microcapsule characteristics, the volume of ethyl acetate added to the saponin solution was varied with three levels: 0, 8 and 12 ml, and the correlative microcapsule lots were coded as S0, S8 and S12.

The dispersed phase was 15 ml of ethyl acetate containing ibuprofen (8.33 mg/ml), miglyol 812 (33.33 mg/ml) and eudragit RSPO (116.67 mg/ml).

Step 2: Emulsifying

The dispersed phase was added dropwise to the continuous phase under the blade stirring for 5 minutes while the reactor was close in order to hinder the ethyl acetate evaporation. In order to investigate the influence of stirring rate on microcapsule characteristics, the stirring rate varied with three levels: 600, 650 and 700 rpm, and the correlative microcapsule lots were coded as R600, R650 and R700.

Step 3: Evaporating the solvent

The evaporation of ethyl acetate at reduced pressure (300 ÷ 350 Torr) was initiated 5 minutes after the emulsification start with a stirring rate of 600 rpm and lasted 5 hours. For microencapsulation batches, for which the continuous phase was saturated with ethyl acetate, 100 ml of distilled water was added to the system at the end of the organic phase addition and the evaporation of ethyl acetate was conducted similarly to that of microencapsulation without adding solvent.

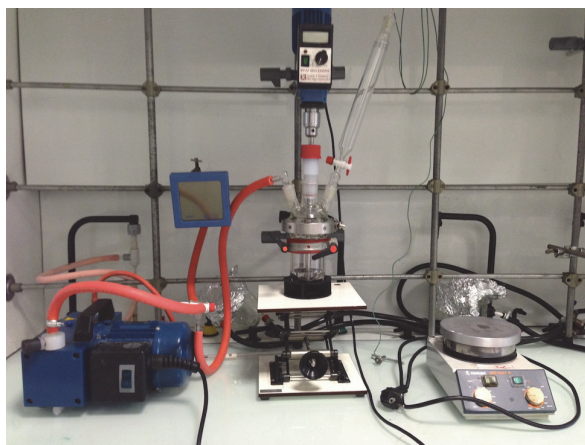


Figure 2.6: Equipment system for microencapsulation
(Ingénierie des Matériaux Polymères, UCBL)

Step 4: Collecting and washing the microcapsules

After 5 hours of solvent evaporation, microcapsules were collected and washed and centrifuged three times with centrifuge rate of 3000 rpm at 15°C for 15 minutes.



Figure 2.7: Centrifuge G-16KS of Sigma
(Ingénierie des Matériaux Polymères, UCBL)

In the microencapsulation described above: the scientific background, the equipment, the concentration of ibuprofen, miglyol 812 and eudragit RSPO in the dispersed phase, the phase volume ratio, the time of emulsification, the time and the pressure during evaporating solvent and the centrifuge conditions were referred and developed from the study of P. Valot et al. [147] and the research project France - Vietnam Hoa Sen Lotus N° 27917ZH "Research on producing medical textile based on microencapsulation technology" [51].

2.3.3.2. Microcapsule characterization

Microcapsule morphology

Microcapsule morphology was observed under the optical microscope Olympus EX 41 at IMP and the scanning electron microscope QUANTA FEG 250 (using the environmental mode) at Centre Technologique des Microstructures of UCBL.

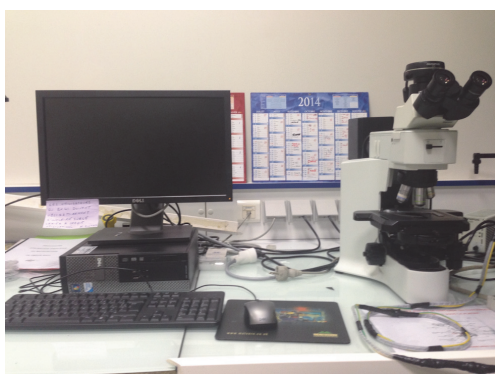


Figure 2.8: Optical microscopy
Olympus EX 41
(Ingénierie des Matériaux Polymères, UCBL)



Figure 2.9: Scanning electron microscopy
QUANTA FEG 250
Centre Technologique des Microstructures,
UCBL

Microcapsule size and size distribution

The average diameter and the size distribution of microcapsules were determined by static laser - light scattering on Mastersize 2000 (Malvern Instruments) at IMP, UCBL. The spatial distribution of scattered light is a function of the particle size of the analyzed sample [21, 116, 140].

The broadness of the size distribution curve is calculated as the Span value as follows:

$$Span = \frac{d(0.9) - d(0.1)}{d(0.5)} \quad (Eq 2.3)$$

Therefore, the smaller the span value, the narrower the size distribution.

The working conditions were:

- Dispersant: water (refractive index: 1.33)
- Sample material: default (refractive index: 1.52)
- Pump speed: 1600 (rpm)

- Sample measurement time: 5 seconds.
- Number of measurement cycles: 5, the result was the mean of 5 measured values.



Figure 2.10: Mastersizer 2000, Malvern Instruments
(Ingénierie des Matériaux Polymères, UCBL)

Hydration rate of microcapsules

The microcapsule hydration was determined by the procedure introduced by H. Sah [120]. At the end of each microencapsulation experiment, microcapsules were collected by centrifuge, weighted immediately (W_1) and after drying to a constant weight (W_2). The microcapsule hydration was then calculated by:

$$\text{Microcapsule hydration} = \frac{W_1 - W_2}{W_2} \times 100\% \quad (\text{Eq 2.4})$$

Drug loading ratio and microencapsulation efficiency

Sampling

The washed microcapsules were dried completely by a vacuum drier at 25°C for 24 hours, and then were weighed to determine the mass of dried microcapsules m_{lot} (mg).

300 mg of dried microcapsules were soaked in 55 ml of heptane, which dissolves only ibuprofen without affecting the other components of microcapsules according to P. Valot et al. [147]. The ultrasonic equipment Fisher biolock Scientific 750W (sonde 25 mm, amplitude 30%) (Figure 2.11) was used to accelerate the dissolution of ibuprofen from microcapsules. After a predetermined period of time, 5 ml of solution was withdrawn and filtered with pore size of 0.45 μm . Ibuprofen concentration in heptane was determined by UV-Vis spectrometer at wavelength $\lambda = 263 \text{ nm}$ (Figure 2.12). The calibration curve used to deduce ibuprofen concentration in heptane was built up from the absorbance values of 7 prepared standard solutions having concentrations varying from 0 to 2 mg/ml.

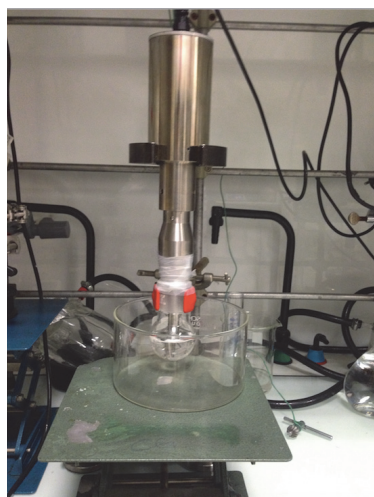


Figure 2.11: Ultrasonic equipment
Fisher biolock Scientific 750W

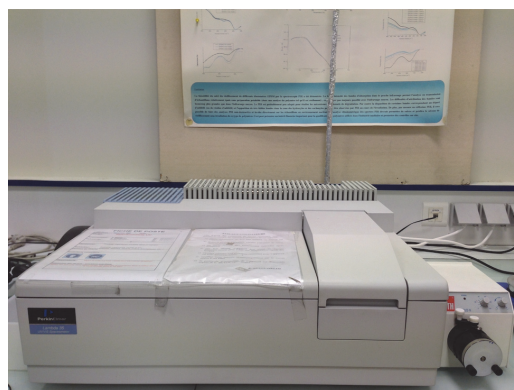


Figure 2.12: Spectrometer
UV-Vis Lamda 35 (Perkin Elmer)

(Ingénierie des Matériaux Polymères, UCBL)

The mass ratio of extracted ibuprofen to the microcapsules was deduced from the concentration of ibuprofen in heptane (Appendix 4). The maximum value of this mass ratio was exactly the ibuprofen loading ratio of the microcapsules, L (%).

Then the microencapsulation efficiency E (%) could be deduced from L (%) as below:

$$E (\%) = \frac{ibu_{exp}}{ibu_{init}} \times 100\% = \frac{L(\%) \times m_{lot}}{ibu_{init}} \times 100\% \quad (Eq 2.5)$$

In which ibu_{exp} and ibu_{init} are the mass of encapsulated and initial ibuprofen used for microencapsulation, respectively; m_{lot} is the mass of the whole microcapsule lot after the drying process.

Content of residual ethyl acetate

The content of residual ethyl acetate in dried microcapsules was determined by gas chromatograph Agilent Technology 6890N at IMP (UCBL), with a mass detector (Figure 2.13). 60 mg dried microcapsules were dissolved completely by 2 ml acetone, then the solution was injected to the gas chromatograph system. The initial oven temperature was set at 60°C for 0.5 minutes and then increased to the final temperature of 120°C at the rate of 10°C/min. The capillary column Agilent 19091S-577U was used as a stationary phase with hydrogen as the carrier gas. The concentration of ethyl acetate in acetone was deduced from the calibration curve that described the change in the number of ion $z = 70$ over the concentration, with six levels of concentrations ranging between 0 and 1.2 (μl Ethyl acetate /ml Acetone) were used to construct the calibration curve.



Figure 2.13: Gas chromatograph Agilent Technology 6890N
(Ingénierie des Matériaux Polymères, UCBL)

2.3.4. Investigating the influence of textile substrate on the characteristics of microcapsule-treated fabric

2.3.4.1. Structural parameters of the interlock knitted fabrics

From bleached fabric lots (see section 2.1.1 in this thesis), the initial samples were selected according to the testing standard TCVN 5791-1994. Those initial samples were then washed and dried until getting the fully-relaxed state.

The loop length l (mm) was determined according to the testing standard TCVN 5799-1994.

The length of yarn in a structural knitted cell L_u (mm) was calculated by:

$$L_u = 4 \times l \quad (\text{Eq 2.6})$$

The course density P_d (number of courses/10cm) and the wale density P_n (number of wales/10cm) were determined according to the testing standard ISO 7211-2.

The area density of fabric P_s (number of loops/cm²) was calculated by:

$$P_s = \frac{P_d \times P_n}{100} \quad (\text{Eq 2.7})$$

The number of structural knitted cells per unit area S_u (SKCs/cm²) was calculated by:

$$S_u = \frac{P_s}{2} \quad (\text{Eq 2.8})$$

The mass per area of fabric M_{fbr} (mg/mm²) was determined according to the testing standard ISO 3801:1997.

The thickness of fabric t (mm) was determined according to the testing standard ISO 5084:1997.

The average diameter of knitting yarn D (mm) was determined by observing the yarn unraveled from the fabric under an optical microscope, with the assumption that the knitting yarn has circular cross section.

The porosity of fabric $P(\%)$ was calculated by the equation proposed by R. Guidon [43]:

$$P(\%) = 100 \times \left[1 - \frac{M_{fbr}}{t \times \rho} \right] \quad (Eq\ 2.9)$$

With M_{fbr} is the mass per area of fabric (mg/mm^2), t the thickness of fabric (mm), ρ the fiber density (mg/mm^3). This equation has been applied in many researches on the porosity of knitted fabrics [3, 29, 134, 144]. In the case of this thesis, the density of cotton fiber is $\rho = 1.52$ (mg/mm^3).

The following equipments at Testing Center of Textile - Leather Materials (HUST) were used to determine the structural parameters of fabrics:



Figure 2.14: Experimental washing machine
Electrolux



Figure 2.15: Laboratory conditioning chamber
M250-RH



Figure 2.16: Electronic scale OHAUS - PA413



Figure 2.17: Thickness gauge

(Testing Center of Textile - Leather Materials, HUST)

2.3.4.2. Influence of textile material on characteristics of microcapsule-treated fabric

Applying microcapsules to fabric

Circle fabric sample having diameter of 2.5 cm was totally dried by the vacuum drier France Etuves (Figure 2.18) at 25°C, the weight of sample after drying was coded as M_1 . The sample was then placed into a plastic cup having the same diameter and containing 5 ml of the microcapsule suspension (in water) at concentration of 12.5 mg/ml (Figure 2.19). After 12 hours of soaking, the fabric sample was taken out and then dried in the vacuum drier at 25°C until totally dry. The sample weight right after the drying was coded as M_2 . M_1 and M_2 were determined by an electronic scale having accuracy of 0.1 mg.



Figure 2.18: Vacuum drier France Etuves
(Ingénierie des Matériaux Polymères, UCBL)

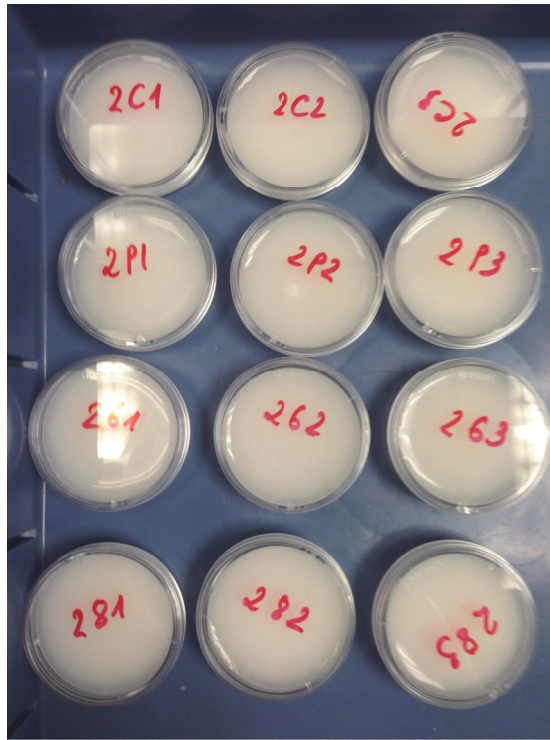


Figure 2.19: Fabric samples soaking in the microcapsule suspension

Calculating the microcapsule loading capability

The microcapsule loading capability of fabric was calculated as below:

$$MLC (\%) = \frac{M_2 - M_1}{M_1} \times 100\% \quad (Eq 2.10)$$

In which M_1 and M_2 were the weights of fabric sample before and after the fabric treatment with microcapsules (see above the description of applying microcapsules to fabric).

Statistical analysis to conclude about the difference in microcapsule loading capability of different fabric lots

In order to conclude the influence of textile material on fabric microcapsule loading capability, two independent samples t test was used to see if mean values of two population are equal or not [68].

For two samples having sample size of n_1 and n_2 , mean value of \bar{x}_1 and \bar{x}_2 , the variance of s_1^2 and s_2^2 , hypotheses were stated as:

Null hypothesis H_0 : $\mu_1 = \mu_2$

Alternative hypothesis H_a : $\mu_1 > \mu_2$ or $(\mu_1 < \mu_2)$

In case that $n_1 = n_2 < 30$, the t - statistic was calculated as below:

$$t = \frac{|\bar{x}_1 - \bar{x}_2| \sqrt{n_1}}{\sqrt{s_1^2 + s_2^2}} \quad (\text{Eq 2.11})$$

Null hypothesis H_0 was rejected if $t > t_\alpha$ with t_α was the critical value for one - tail t test. The confidence interval of the test was 95%.

Evaluating the microcapsule distribution on fabric

The microcapsule distribution on fabric was observed under the scanning electron microscope SEM QUANTA FEG 250 at IMP, UCBL (Figure 2.20). The area of microcapsule aggregates on fabric was determined by the software Meander 3.1.2 of peacock Media (Figure 2.21).

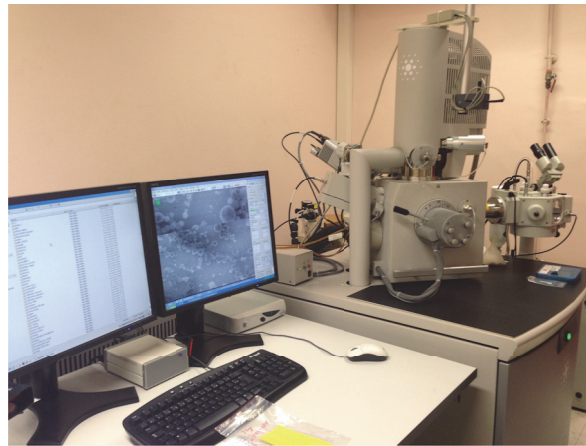


Figure 2.20: Scanning electron microscopy QUANTA FEG 250 – FEI company (Ingénierie des Matériaux Polymères, UCBL)

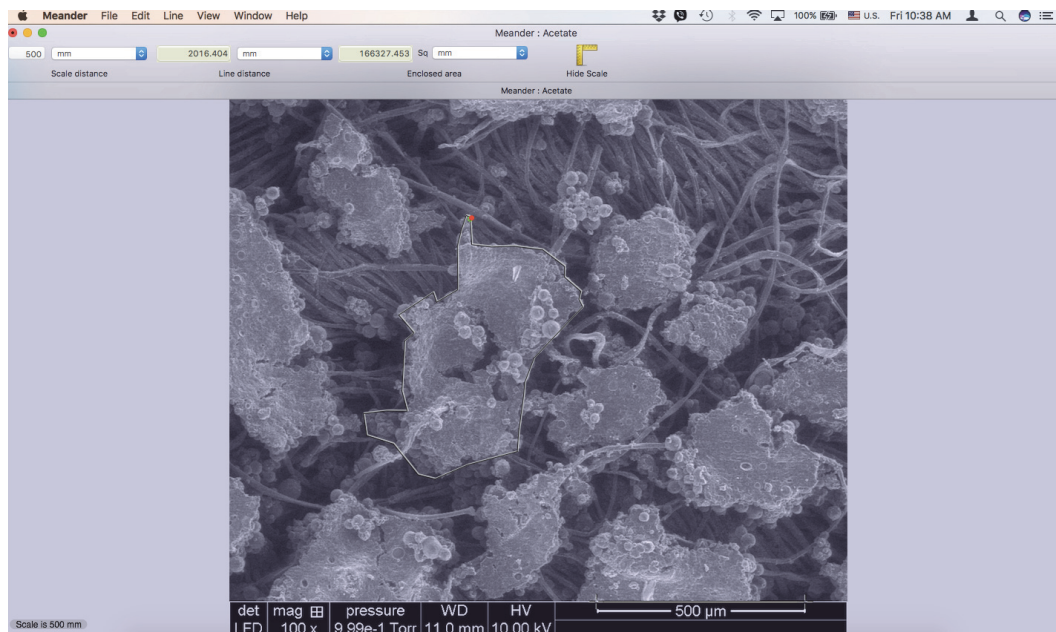


Figure 2.21: Interface of Meander 3.1.2 during determining the area of microcapsule aggregate

Drug release *in vitro* experiment

The drug release *in vitro* experiment was based on the procedure described in some literatures [63, 69, 145], using a glass jar having volume of 23 ml and the mouth diameter of 1 cm to simulate the Franz diffusion cell. The jar was filled with receptor fluid, which was the phosphate buffer solution pH 7.4. A nitrocellulose membrane having pore size of 0.22 μm was placed between the receptor fluid and the microcapsule-treated fabric sample. The membrane and the fabric sample both had the diameter similar to that of the mouth of glass jar (1 cm). It must be ensured that the nitrocellulose membrane contact with the phosphate buffer at its lower side and contact at its upper side with the fabric surface containing most microcapsules, and the fabric sample does not contact with the receptor fluid (Figure 2.22).



Figure 2.22: Glass jar simulating Franz diffusion cell

During the experiment, the receptor fluid was stirred by a magnetic stirrer at 100 rpm and the temperature of the fluid was maintained at $32 \pm 1^\circ\text{C}$ (in order to simulate the temperature of body skin).

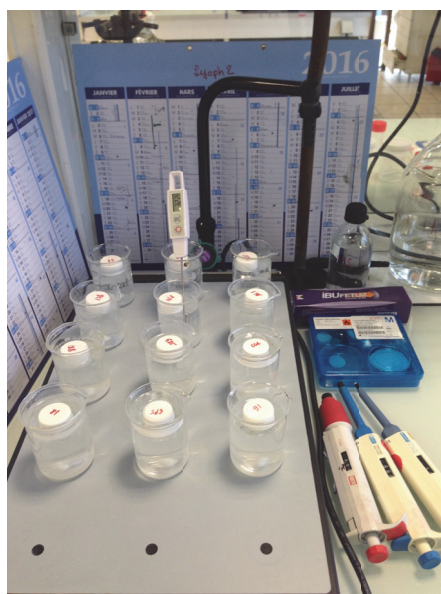


Figure 2.23: Drug release *in vitro* experiment

At predetermined times (8, 24, 32 and 48 hours), 3 ml of the receptor fluid was taken out and was compensated by 3 ml of fresh phosphate buffer solution.

Ibuprofen concentration in the receptor fluid was determined by HPLC equipment of SHIMADZU at IMP (UCBL) (Figure 2.24) under working conditions described in Appendix Table 4 (Appendix 6). The concentration of ibuprofen in the receptor fluid was deduced from the calibration curve that built up from the area of the typical peak according to the ibuprofen concentration, with seven levels of concentrations ranging from 0 to 0.2 mg/ml. Then the weight percentage of ibuprofen from the microcapsule-treated fabrics released into the receptor fluid after each period of time was deduced from the ibuprofen concentrations (according to the procedures described at Appendix 7).

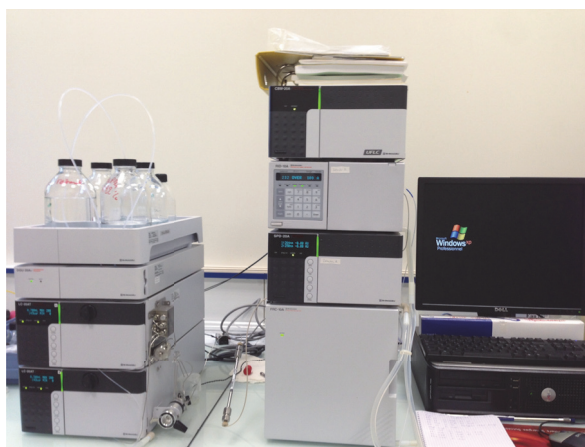


Figure 2.24: HPLC system of SHIMADZU
(Ingénierie des Matériaux Polymères, UCBL)

2.3.4.3. Influence of the loop length on the characteristics of the microcapsule-treated fabric

Applying microcapsules to the fabric

1. Coating technique

The coating formulation was the dispersion of wet microcapsules in distilled water. From initial fabric samples, which were completely relaxed, the experimental samples having dimension of 20 x 20 cm were cut out then were restored in standard atmosphere for 24 hours (according to the standard ISO 139:2005). The weight of sample right after the conditioning, which was coded as M_3 , was the weight of fabric before finishing with microcapsules.

The coating process was carried out on the experimental coating equipment Mini Coater (DaeLim Starlet Co.,Ltd - Korea) (Figure 2.25).



Figure 2.25: Coating equipment Mini Coater (DaeLim Starlet Co.,Ltd)
(The Laboratory of Knitting Technology, HUST)

The main coating parameters:

- Microcapsule concentration: 14 mg/ml; 24 mg/ml
- Coating rate: 40 mm/second
- Coating thickness: 0.5 mm

Microcapsule-coated fabric was vacuum dried at 45°C in the vacuum drier OV-11 of Jeio Tech Co., Inc (Korea) (Figure 2.26) until completely dried.



Figure 2.26: Vacuum drier OV-11
(Cleaner Production Center, HUST)

The dried microcapsule-coated fabric was restored again in standard atmosphere for 24 hours. The weight of fabric right after that, which was coded as M₄, was the weight of fabric after finishing with microcapsules. M₃ and M₄ were determined by an electronic scale having accuracy of 1 mg.

2. Impregnating technique

The impregnating formulation was the dispersion of wet microcapsules in water with concentration of 20 mg/ml. The circle fabric samples having diameter of 6 cm were restored in standard atmosphere for 24 hours (according to the standard ISO 139:2005). The weight of sample right after the conditioning, which was coded as M_5 , was the weight of fabric before finishing with microcapsules.

The fabric sample was then placed into a circle glass cup having the same diameter. 10 ml of microcapsule dispersion was gently poured into the glass cup and the fabric sample was soaked in the microcapsule dispersion for 12 hours. After that, the microcapsule-impregnated fabric was dried in a fridge at temperature of 8°C and humidity of 20% until totally dry. The dried sample was restored again in the standard atmosphere for 24 hours, the weight of sample right after that, which was coded as M_6 , was the weight of fabric after finishing with microcapsules. M_5 and M_6 were determined by an electronic scale having accuracy of 0.1 mg.

Calculating the microcapsule loading capability

The microcapsule loading capability MLC (%) was calculated as below:

As for the coating technique,

$$MLC (\%) = \frac{M_4 - M_3}{M_3} \times 100\% \quad (Eq 2.12)$$

In which M_3 and M_4 were the weights of the fabric sample before and after the fabric treatment with microcapsules (see the description above of applying the microcapsules to the fabric by coating).

As for the impregnating technique,

$$MLC (\%) = \frac{M_6 - M_5}{M_5} \times 100\% \quad (Eq 2.13)$$

In which M_5 and M_6 were the weights of the fabric sample before and after the fabric treatment with microcapsules (see the description above of applying the microcapsules to the fabric by impregnating).

The result of each fabric lot having certain loop length was the average of triplicated experiments. In order to conclude about the influence of loop length on microcapsule loading capability, the two independent samples t test (as described in section 2.3.4.2) was used, and in this case $n_1 = n_2 = n_0 = 3$.

Evaluating the microcapsule distribution on the fabric

1. Image analysis

The distribution of microcapsules on microcapsule-treated fabric was observed by the scanning electron microscope JEOL JSM - 7600F at Laboratory of Electron Microscopy and

Microanalysis (HUST) (Figure 2.27). The working conditions: the voltage 2kV; the low magnification (LM) mode; the working distance WD = 8.0 mm.

The area of microcapsule aggregates on fabric surface was determined by the software Meander 3.1.2 of Peacock Media.



Figure 2.27: Scanning electron microscopy JEOL JSM - 7600F (Laboratory of Electron Microscopy and Microanalysis, HUST)

2. Calculations based on the model of interlock knitted loop

In order to explain the microcapsule distribution observed by SEM, the microcapsule cover ratio of fabric K was first introduced in this thesis and was defined as the ratio of total cross section area of all microcapsules S_{mc} to the total yarn surface area might be coated with microcapsules S_{yar} in a unit area of fabric.

$$K = \frac{S_{mc}}{S_{yar}} \quad (Eq\ 2.14)$$

In which, the total cross section area of all microcapsules per unit area of fabric S_{mc} was calculated from the content of microcapsules on fabric and the size distribution of microcapsules. The total yarn surface area might be coated with microcapsules S_{yar} was calculated by:

$$S_{yar} = S_{\Sigma} - S_{ls} \quad (Eq\ 2.15)$$

With S_{Σ} was the total yarn surface area and S_{ls} was the area of yarn surface at lower side of fabric where only few microcapsules locate. These two values were calculated according to the model of interlock knitted loop proposed by Dabiryan-Jeddi.

In vitro experiment of transdermal drug release

In vitro experiment of transdermal drug release was based on some references about the transdermal drug release of medical patches [63, 69, 104, 145], in which the abdominal

pigskin was used. The receptor fluid was the phosphate buffer solution having pH of 7÷7.4. The temperature during experiment was maintained at 32±2°C.

The procedure of experiment:

- The microcapsule-treated fabric (prepared by impregnating technique above) was placed into the circle glass cup having the same diameter (6 cm) (Figure 2.28A). The wall of the cup was 1 cm in height.
- The abdominal pigskin was cleaned carefully and was then cut into circle pieces having diameter of 8 cm; the fat and hair in the skin were removed completely.
- The circle piece of pigskin was placed on the microcapsule-treated fabric in such a way that the fabric surface containing most microcapsules contacted to the stratum corneum layer of the skin, and the piece of skin covered both the bottom and the wall of the glass cup (Figure 2.28B).
- 10 ml of phosphate buffer solution was poured into the system. It must be ensured that the buffer contacted only to the pigskin but not to the microcapsule-treated fabric. The whole system was completely covered by aluminum foil in order to prevent the evaporation of the buffer and was restored in room conditions for 24 hours (temperature 29÷33°C, humidity 60÷85%).
- After 24 hours, the receptor fluid was collected to determined the concentration of ibuprofen in it.

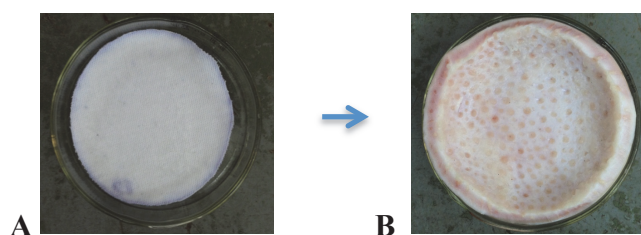


Figure 2.28: A step in the *in vitro* experiment of transdermal drug release
(A): sample of microcapsule-treated fabric was placed into a glass cup
(B): piece of pigskin was placed to the microcapsule-treated fabric sample

Calculating the weight percentage of ibuprofen in microcapsule-treated fabric dissolved into the receptor fluid

Determining the ibuprofen concentration in the receptor fluid

The concentration of ibuprofen released in the receptor fluid was determined by HPLC system of Merck Hitachi at National Institute of Drug Quality Control (Figure 2.29). The weight percentage of ibuprofen released into the receptor fluid was deduced from the ibuprofen concentration according to the procedure described at Appendix 10.



Figure 2.29: HPLC system of Merck Hitachi (National Institute of Drug Quality Control)

Some main conditions of HPLC analysis:

- Detector: L - 7455
- Pumping system: L - 7614
- Injection system: L - 7350
- Column: C18
- Eluent: 33% A (H₂O + 1.2% H₃PO₄); 67% B Methanol
- Flow: 1.2 ml/min
- Injection volume: 20 μ l
- Retention time: 10 min
- Wave length: 263 nm

2.3.4.4. Influence of the fabric extension on the transdermal drug release capability of fabric

Applying the microcapsules to the fabric

- Used a circle glass plate having flat bottom with diameter of 20 cm and enough high wall.
- From the initial samples of the B3 fabric lot (with loop length of 2.87 mm), a circle experimental sample having the diameter of 20 cm was severed.
- That experimental fabric sample was completely dried in a vacuum drier at 25°C and its dry weight was coded as m_{bf} (mg).
- Placed that fabric sample into the glass plate, added 150 ml of the microcapsule dispersion in water to the plate, the microcapsule concentration was 20 mg/ml.
- The fabric sample was taken out of the plate after 12 hours of soaking in the microcapsule dispersion and then was completely dried in the vacuum drier at 25°C, its dry weight was coded as m_{af} (mg).

In vitro experiment of transdermal drug release

- From the microcapsule treated fabric sample with the diameter $D_{tt} = 20$ cm, three circle samples with diameter (coded as d_{rl}) of 5, 6 and 8 cm were severed, they were coded as E1, E2 and E3 respectively.

- The abdominal pigskin was cleaned carefully and then divided into the circle pieces with diameter of 8 cm.

Three similar stainless sheets with half round shape were used to create the experimental systems as in Figure 2.30:

Sample E1	Sample E2	Sample E3
The experimental systems viewed from the bottom		
		
Sample diameter (d_{r1})/Fabric extension		
5 cm/60%	6 cm/33%	8 cm/0%
The experimental systems viewed from the top		
		

Figure 2.30: Experimental design to create different levels of fabric extension

- 15 ml of the phosphate buffer solution pH = 7 was used as the receptor fluid. It must be ensured that the buffer contact only with the pigskin and not with the fabric. The temperature was sustained in a range of $29 \div 33^{\circ}\text{C}$ during the experiment.
- After 24 hours, the receptor fluid was withdrawn and centrifuged to remove all supernatant materials.

Determining the concentration of ibuprofen in the receptor fluid

The concentration of ibuprofen in the receptor fluid was determined by HPLC system of Merck Hitachi (Figure 2.29) under the working conditions similar to which described at Appendix 6. According to this concentration, the weight percentage of ibuprofen in the microcapsule-treated fabric dissolved into the receptor fluid could be deduced as described at Appendix 11.

2.3.5. Investigating the influence of the drying conditions on the microcapsule morphology after finishing process

Applying microcapsules to fabric

The coating of microcapsules to interlock knitted fabrics was as described at section 2.3.4.3. For this research content, only the fabric B3 (the loop length of 2.87 mm) was used; and the microcapsule concentration used was 14 (mg/ml).

The microcapsule-coated fabrics were dried at different drying conditions:

- In order to investigate the influence of the humidity during the drying process on the microcapsule morphology, at drying temperature of 25°C, the humidity within drying chamber varied with three levels: 0% (vacuum drying), 20% and 65% (in the laboratory conditioning chamber M250-RH, Figure 2.15).
- In order to investigate the influence of drying temperature on the microcapsule morphology, during the vacuum drying, the temperature varied with four levels: 25, 35, 45 and 60°C.

Observing the microcapsule morphology on fabric

The microcapsule morphology on dried fabrics was observed by the scanning electron microscope JEOL JSM - 7600F with the same working conditions mentioned at section 2.3.4.3.

3. Chapter 3: Results and discussions

3.1. Microencapsulation of ibuprofen

3.1.1. Determination of the microcapsule size for the targeted textile application

The microcapsule size should be higher than the minimum distance and smaller than the maximum distance between adjacent fibers of the fabric. So in order to determine the suitable size of microcapsules, the fibers of the fabric B3 was observed under the scanning electron microscope. The fabric B3 belongs to the fabric collection used to investigate the influence of the loop length on the characteristics of microcapsule-treated fabric; this fabric collection contains five fabric lots having different loop lengths: B1 (2.81 mm), B2 (2.83 mm), B3 (2.87 mm), B4 (2.96 mm) and B5 (3.05 mm). The SEM image of the fabric surface at magnification x50 showed the tightly interlock of adjacent loops, two type of typical regions were observed: the region of loop legs and the region created by the overlap of the successive loops in a same wale (Figure 3.1).

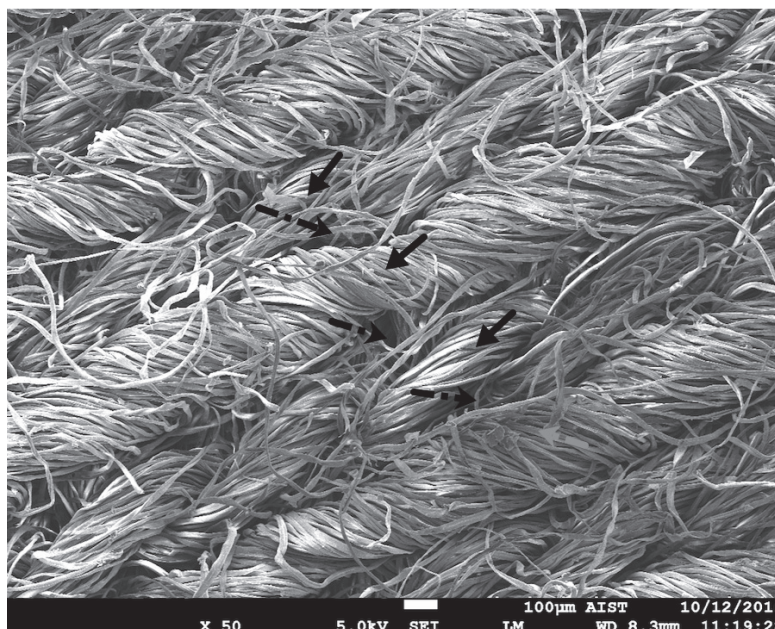


Figure 3.1: SEM image of the surface of fabric B3

→ The region of loop legs - - → The region created by overlapping loops

The fabric surface at those typical regions was observed in more detail under the magnification of x500. The average result of five observations for each region showed that in both the region of loop legs and the region created by overlapping loops, the distance between adjacent fibers was in range of 5÷60 µm (Figure 3.2, Figure 3.3).

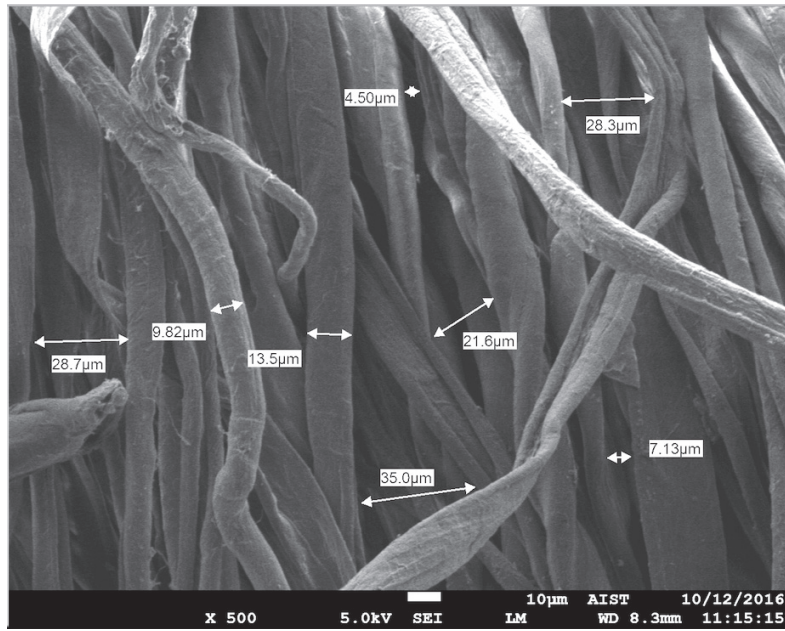


Figure 3.2: Distance between fibers in the region of loop legs on cotton interlock fabric B3

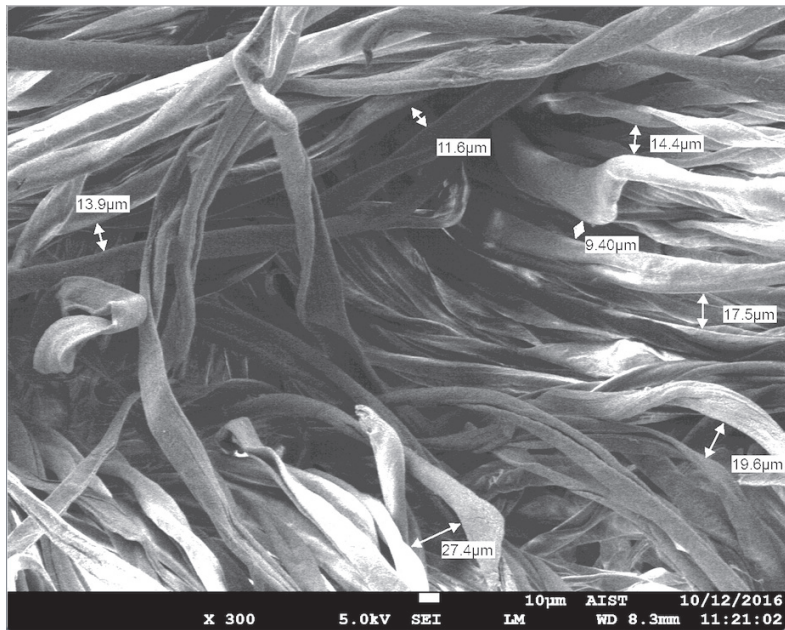


Figure 3.3: Distance between fibers in the region created by overlapping loops on cotton interlock fabric B3

Consequently, for the cotton interlock knitted fabrics with specifications presented at section 2.1.1, the suitable diameter of microcapsules should be $5\div 60\ \mu\text{m}$, which was in good agreement with the value reported in the literature concerning the application of microcapsules in medical textiles [52, 56, 79, 143, 147]. And to reach this range of size for the microcapsules, a suitable surfactant with a proper concentration should be chosen for the microencapsulation.

3.1.2. Surface-active properties of quillaja saponin S4521 (Sigma Aldrich)

Quillaja saponin has been used as the surfactant in the formation of o/w emulsions for a long time, and its surface-active properties has been reported in many researches [81, 86, 152]. However, quillaja saponin is a bio-sourced surfactant so the molecular structures and the ratio of impurities (not necessarily surface-active) could vary with the sources and the methods of purification. Therefore, before using the quillaja saponin S4521 of Sigma Aldrich as surfactant for microencapsulation in this work, it was very important to evaluate its surface-active properties. The surface tensions of a series of aqueous saponin solutions with concentrations ranging between 0 and 1 wt% were determined in order to find out the cmc value, the maximum surface density Γ_{max} and the interfacial area occupied by one molecule A. And as referred to the paper of S. Mitra et al. [86], in the thesis, the molecular weight of quillaja saponin S4521 from Sigma Aldrich was assumed equal to 1650 Da.

When the saponin concentration was lower than 0.05 wt%, the surface tension decreased significantly with increasing concentration (Table 3.1), indicating that saponin molecules could be absorbed at the air-water interface and helped reduce the surface tension of water. The cmc value of quillaja saponin (S4521 from Sigma-Aldrich) deduced from the break in the plot of surface tension γ (mN/m) versus $\ln C$ was found equal to 0.05 wt% ($\ln C = -8.17$) (Figure 3.4), which was in good agreement with the value reported for Sigma's quillaja saponin in literature (also 0.05 wt% at 25°C) [86] but higher than the value reported for quillaja saponin from National Starch LLC (0.01 wt%) [156]. The variation in the cmc value of saponin may be due to the differences in molecular structures and in the content of impurities contained within the source.

Table 3.1: Surface tensions of saponin solutions in distilled water according to the concentration

Saponin concentration (wt%)	Surface tension (mN/m) (the average of triplicated experiments)
0.000	73.60 ± 0.63
0.005	58.22 ± 0.74
0.010	55.15 ± 0.72
0.020	53.25 ± 0.46
0.030	51.51 ± 1.18
0.040	50.90 ± 0.06
0.050	50.53 ± 0.25
0.060	50.41 ± 0.55
0.070	50.63 ± 0.54

0.080	50.57 ± 0.35
0.090	50.35 ± 0.46
0.100	50.49 ± 0.70
0.500	50.55 ± 0.47
1.000	50.41 ± 0.69

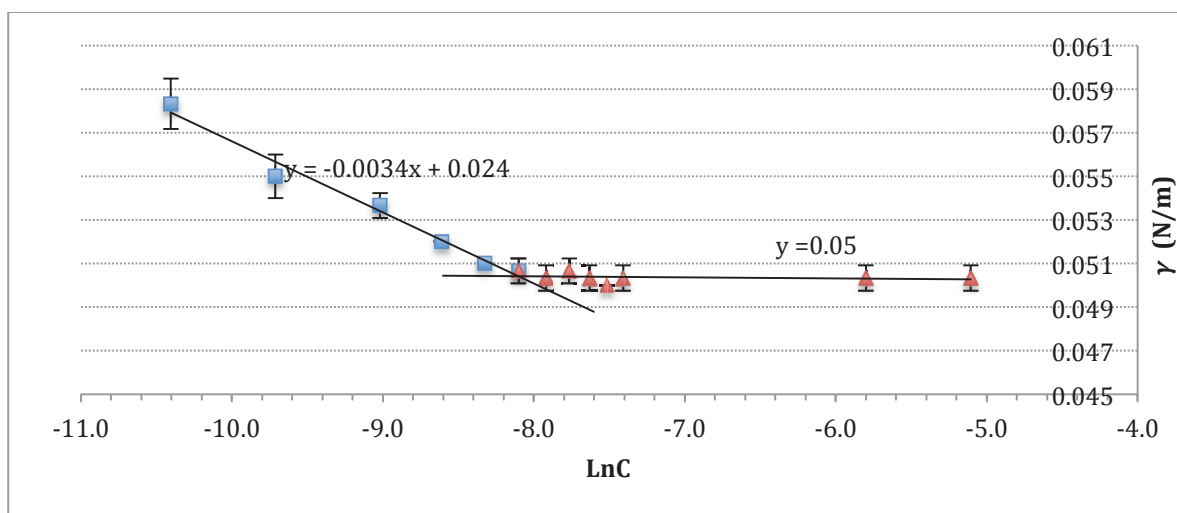


Figure 3.4: Surface tension of aqueous saponin solutions according to saponin concentration

The minimum surface tension of saponin solution (at the cmc value, 0.05 wt%) was 50.5 (mN/m) (Table 3.1, Figure 3.4), pointing out that saponin could help reduce 31 % the surface tension of pure water (73.6 mN/m). The minimum surface tension of hydrolyzed poly(vinyl acetate) solution, a synthetic polymeric surfactant often used in ibuprofen microencapsulation by the solvent evaporation method [17, 147, 163], varying with its molar mass and its degree of hydrolysis, was reported in the range of 47÷58 (mN/m) [12, 105]. Consequently, the capability of reducing water surface tension of quillaja saponin is nearly similar to that of that polymeric surfactant.

The linear regression performed on the data for the surface tension γ (N/m) as a function of $\ln C$ just below the cmc value (Figure 3.4) indicated that the slope of the curve γ - $\ln C$ just before the cmc value was - 0.0034. Then according to the Gibbs equation (Eq 2.1), it could be deduced that $\Gamma RT = 0.0034$, so the surface density of saponin $\Gamma = 1356$ (nmol/m²). According to the equation (Eq 2.2), the interfacial area occupied by one quillaja saponin molecule A was found equal to 121 Å². This value was higher than that reported by S. Mitra et al. (83÷96 Å²) [86], although the quillaja saponins used in two researches offered the same cmc values (0.05 wt%). Then saponin used in S. Mitra's work was more efficient at reducing water surface tension than saponin in our work, according to the surface tension observed at the cmc value.

The different composition of these two quillaja saponin samples may explain this difference.

In conclusion, quillaja saponin S4521 from Sigma-Aldrich allows reduce the surface tension of water to 50.5 (mN/m) at the cmc value of 0.05 wt%. Therefore, quillaja saponin appeared suitable as surfactant for microencapsulation by o/w emulsion solvent evaporation method.

3.1.3. Influence of the microencapsulation parameters on the microcapsule size and morphology

Ibuprofen-loaded microcapsules were elaborated by solvent evaporation method. 15 ml of ethyl acetate solution containing ibuprofen (125 mg), miglyol 812 (500 mg) and eudragit RSPO 1750 (mg) was added dropwise for 5 minutes to 100 ml of a quillaja saponin aqueous solution under blade stirring. The evaporation of ethyl acetate at reduced pressure (300 ÷ 350 Torr) was initiated 5 minutes after the emulsification start with a stirring rate of 600 rpm. Microcapsules collected after 5 hours were washed three times with distilled water.

The influence of the saponin concentration, the stirring rate during emulsification and the volume of ethyl acetate added to the aqueous phase on the microcapsule size and morphology will be discussed below.

3.1.3.1. Influence of the saponin concentration

The surfactant concentration strongly influences the average diameter and the size distribution of microcapsules [31, 76, 138, 147]. Besides, as mentioned at section 3.1.1, the suitable size of ibuprofen loaded microcapsules for the targeted textile application should be in range of 5÷60 µm. Therefore, we investigated the effect of the saponin concentration on the size distribution of microcapsules. The saponin concentration varied with four levels: 0.025, 0.05, 0.075 and 0.1 wt%, and the correlative microcapsule lots were signed as C0.025, C0.050, C0.075 and C0.100.

Within the scope of investigation, when the saponin concentration increased from 0.025 to 0.1 wt%, the d(0.5) diameter of microcapsules decreased respectively from 34.3 to 17.1 µm (Table 3.2, Figure 3.5).

Table 3.2: $d(0.5)$ diameter and span values of microcapsule lots C0.025, C0.050, C0.075 and C0.100

Lot	Saponin concentration wt%	$d(0.5)$ diameter μm	Volume ratio of microcapsules having diameter 5–60 μm	Span value
C0.025	0.025	34.3 ± 0.3	72 %	2.4
C0.500	0.050	23.2 ± 0.2	80 %	2.8
C0.075	0.075	21.5 ± 0.2	82 %	3.0
C0.100	0.100	17.1 ± 0.2	82 %	3.9

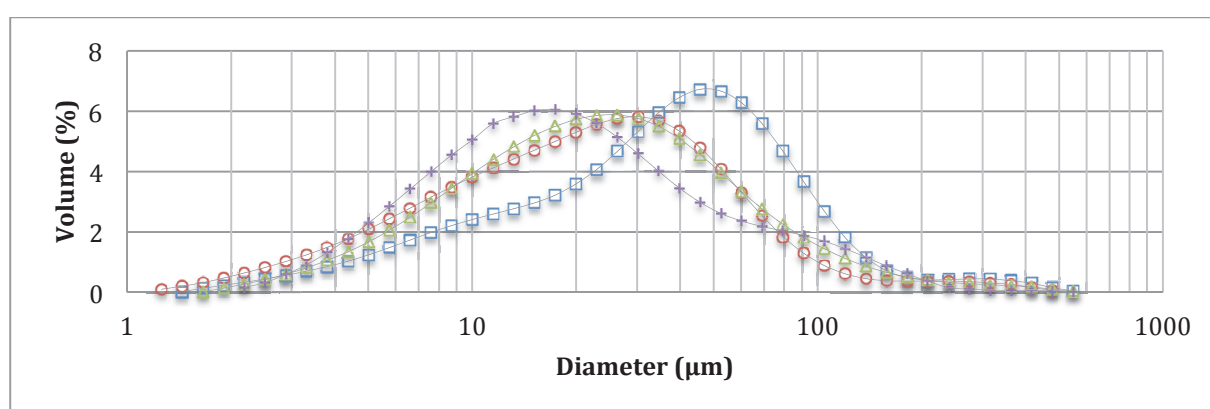


Figure 3.5: Size distributions of microcapsule lots C0.025, C0.050, C0.075 and C0.100

—□— C0.025 —○— C0.050 —△— C0.075 —×— C0.100

These results are in accordance with those reported in the literature for various surfactants, and especially for partially hydrolyzed poly(vinyl acetate) [138, 147] or polyoxyethylene octylphenyl ether [154]. At high concentration, more surfactant molecules could be oriented at the interface of two phases to reduce efficiently the interfacial tension, which resulted in the formation of smaller emulsion droplets, and then smaller microcapsules.

The decrease of the microcapsule $d(0.5)$ diameter is especially important when the saponin concentration increase from 0.025 to 0.05 wt%. The significant size decrease (from 34.3 to 23.2) may be connected to the cmc value of saponin found equal to 0.05 wt% (see section 3.1.2). With a saponin concentration lower than the cmc value, the droplet surface is only partially covered. Then the size of the emulsion is higher since the interfacial tension between the organic and aqueous phases is not reduced and coalescence phenomena are not hindered. When the saponin concentration reached the cmc value, the effect of the saponin concentration increase less significant on the interfacial tension, and then did not quite affect the microcapsule size. The total surface developed by the emulsion droplets (A_{dense}) as well as the theoretical surface covered by the surfactant if neglecting the saponin partition between

water and the oil/water interface (A_{surf}), calculated from the value of area occupied per molecule (121 \AA^2), were calculated for each batch. The values of the ratio $A_{\text{dense}}/A_{\text{surf}}$ versus saponin concentration (Figure 3.6) clearly evidenced the increase of the interface coverage efficiency by increasing saponin concentration and may suggest the reach of a plateau at 0.1 wt%, as largely described in the literature [138, 147]. Concurrently the volume ratio of microcapsules having a diameter in the range of $5\div 60 \mu\text{m}$ reach a plateau for saponin concentration above 0.05 wt%.

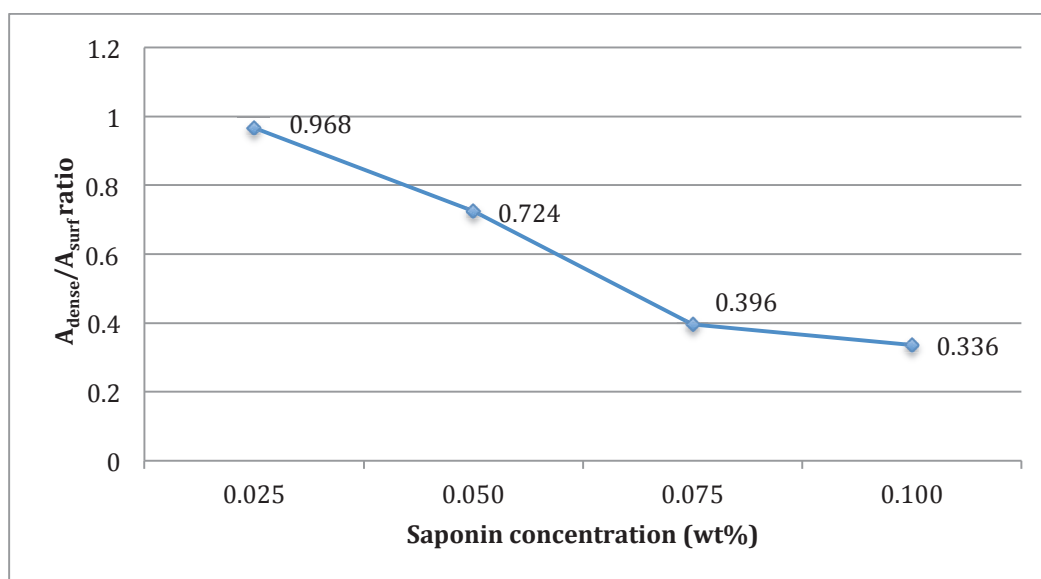
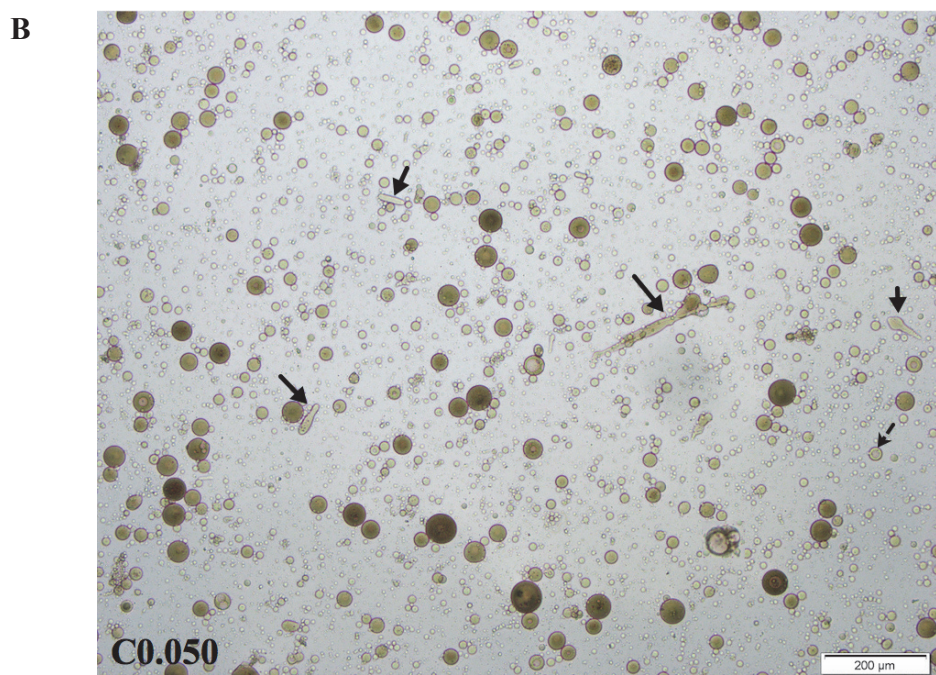
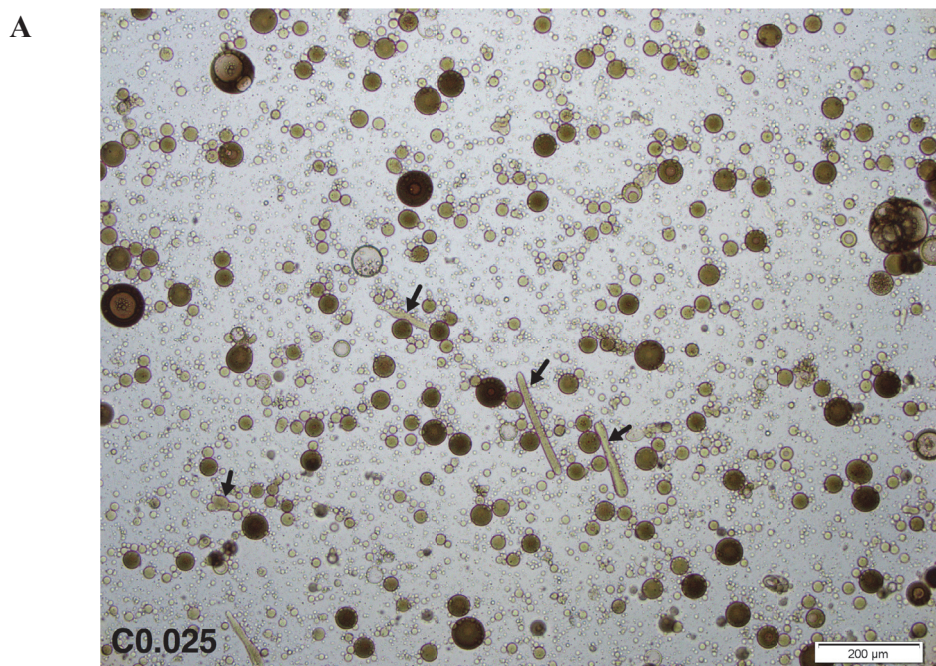


Figure 3.6: $A_{\text{dense}}/A_{\text{surf}}$ ratio depending on the saponin concentration

The optical microscope images confirmed the results of laser diffractometry. Moreover, the optical microscope images revealed the presence of no-spherical microparticles in the microcapsule lots, with elliptical and rod shapes (Figure 3.7). Since most equations used to predict the active release rate from microcapsules were only based on spherical ones so those irregular microparticles would be a big disadvantage in predicting the drug release capability of microcapsule-treated fabric.



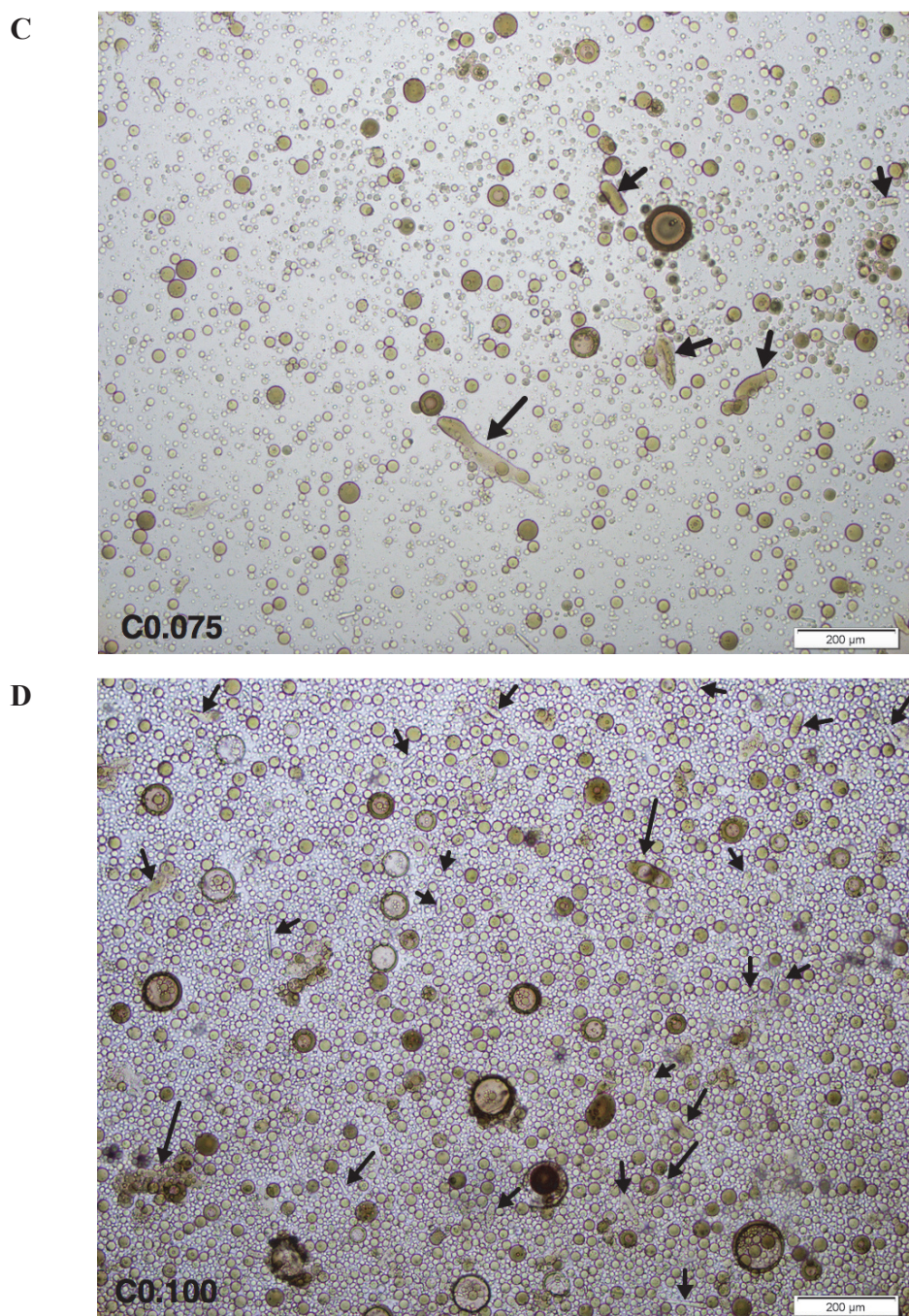


Figure 3.7: Optical microscope images of microcapsules C0.025 (A), C0.050 (B), C0.075 (C) and C0.100 (D)

→: irregular microparticles

The similar phenomenon was reported in some referred researches on the microencapsulation by solvent evaporation/extraction methods, using the solvent ethyl acetate. Since the solubility in water of ethyl acetate (90 g/l at 20°C) is much higher than that of other solvents most used in solvent evaporation method such as dichloromethane (20 g/l at 20°C), combining with the high stirring rate during the emulsification, ethyl acetate in oil droplets diffuses quickly from the droplets to the aqueous phase, inducing the fast precipitation of the

polymer. The elliptical or rod shape microparticles are the results of oil droplets hardening during the emulsification step [83, 120]. The fast precipitation of polymer also provides the broadening of the size distribution of microcapsules especially in the region above $d(0.5)$ with span value was in range of 2.4÷3.9 (Table 3.2). Furthermore, the diffusion rate of ethyl acetate from the oil droplets to the aqueous phase may increase according to the increase of saponin concentration, resulting in more no-spherical microparticles in the microcapsule batch and then the broader size distribution of the microcapsules. Especially when the saponin concentration increased from 0.075 to 0.1 wt%, the optical microscope images showed the important increase of the no-spherical microparticles (Figure 3.7), and the results of the laser diffractometry also pointed out the strong increase of the span value from 3.0 to 3.9 (Table 3.2).

Consequently, the elaborated microcapsules exhibited suitable size for their deposit on the interlock fabrics (5÷60 μm). However, the size distributions are still rather broad with span values in range of 2.4÷3.9 with some irregular microparticles in the microcapsule lots. Two ways may allow narrow the size distribution and reduce the number of irregular microparticles [83]: 1/ reducing the stirring rate during the emulsification; 2/ reducing the diffusion rate of ethyl acetate from the oil droplets to the aqueous phase by adding ethyl acetate to the aqueous phase before the emulsification step. The following are two correlative investigations.

3.1.3.2. Influence of the stirring rate

One of the reasons of irregular microparticles in the microcapsule lots produced by solvent evaporation method using the solvent ethyl acetate might be the high stirring rate during the emulsification step. During the emulsification, the high shear stress, which is the result of the high stirring rate, pulls long the oil droplets. At the same time, the high speed fluid of the external aqueous phase outside the interface of the deformed oil droplets accelerated the diffusion of the ethyl acetate near the surface layer, resulting in a rapid solidification of the polymer on the surface layer, and then the no-spherical microparticles [83]. So in order to reduce the number of the no-spherical microparticles and to get the narrower size distribution, the influence of stirring rate on microcapsule size and morphology was investigated. Because the rate of 700 rpm was nearly the upper limit of the stirrer, three levels of stirring rate were investigated: 700, 650 and 600 rpm. The correlative microcapsule lots were coded as R700, R650 and R600, with a saponin concentration equal to 0.075 wt%.

The lots were observed by optical microscopy. The images pointed out that reducing stirring rate did not help to decrease the number of irregular microparticles (Figure 3.8).

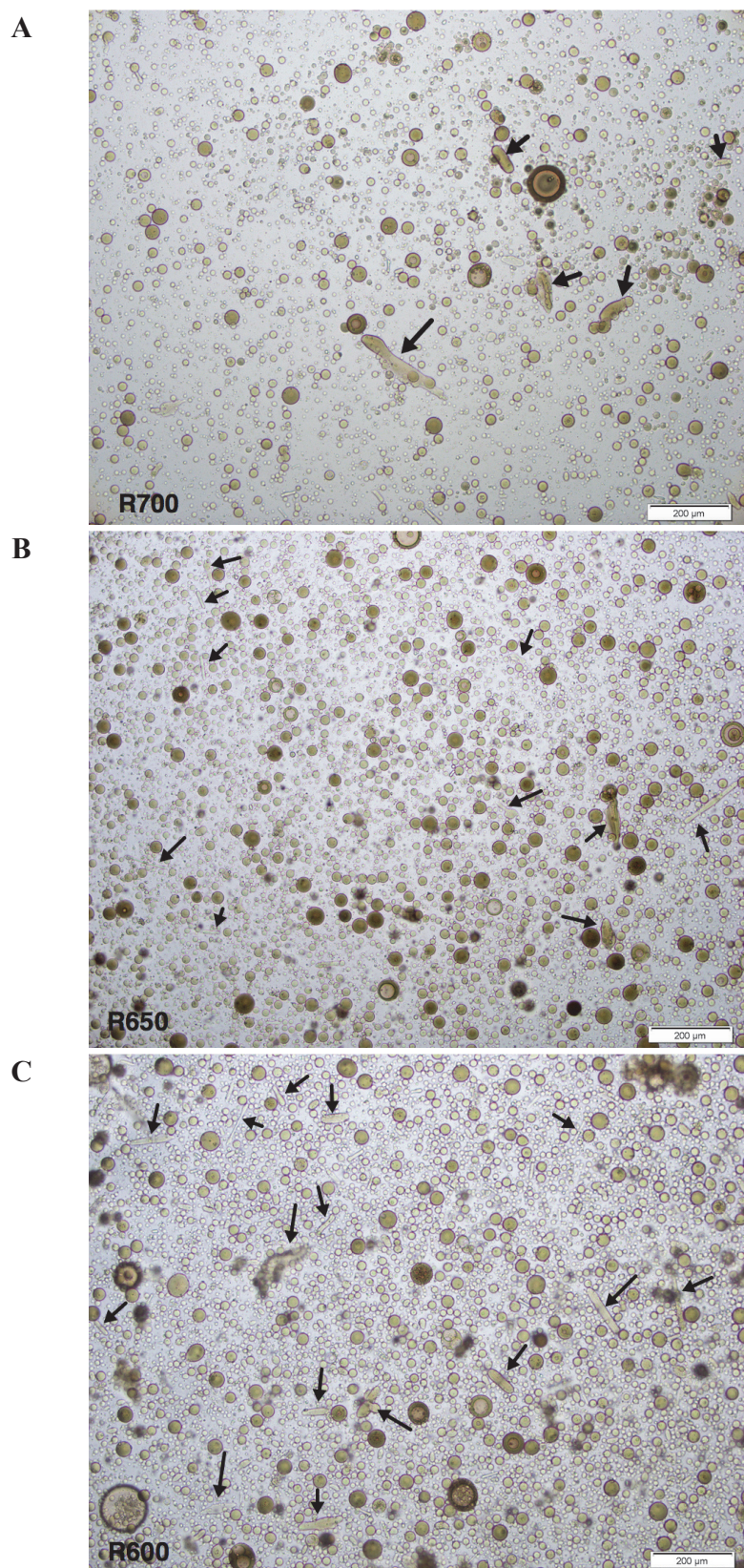


Figure 3.8: Optical microscope images of microcapsules R700 (A), R650 (B) and R600 (C)

→: irregular microparticle

Moreover, both the mean diameter and the span value increased when the stirring rate decreased (Table 3.3, Figure 3.9). In detail, when the stirring rate decreased in order of 700, 650 and 600 rpm, the $d(0.5)$ diameter of microcapsules increased in order of 21.5, 22.4 and 21.0 μm , and the span value also increased in relevant order of 3.0, 3.5 and 3.9.

Table 3.3: $d(0.5)$ diameter and span values of microcapsule lots R700, R650 and R600

Lot	Stirring rate (rpm)	$d(0.5)$ diameter (μm)	Volume ratio of microcapsules having diameter $5 \div 60 \mu\text{m}$	Span value
R700 (C0.075)	700	21.5 ± 0.2	82%	3.0
R650	650	22.4 ± 0.2	81%	3.5
R600	600	21.0 ± 0.1	80%	3.9

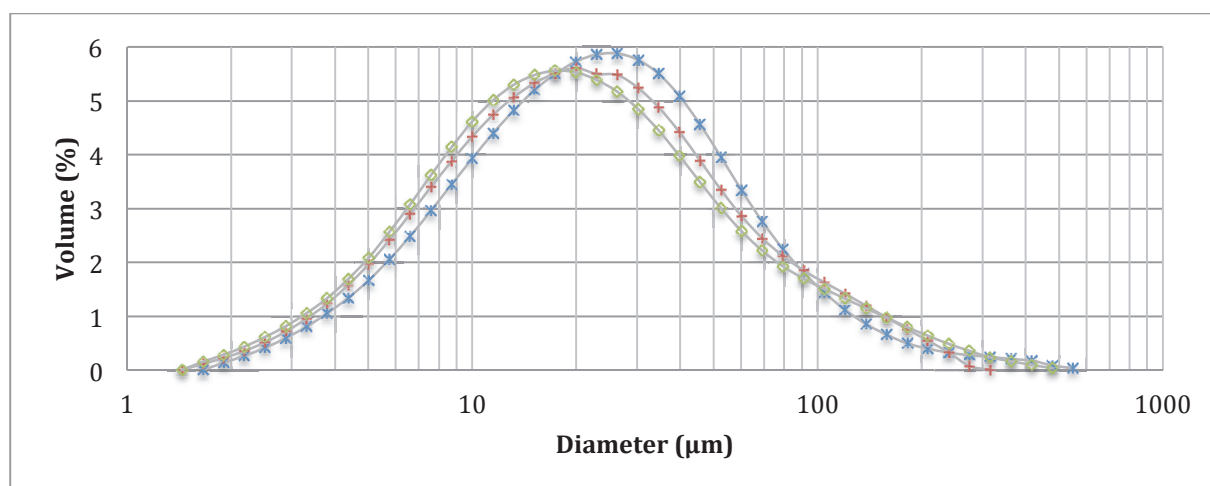


Figure 3.9: Size distributions of microcapsules R700, R650 and R600

—*— R700 —+— R650 —◇— R600

According to D. Perumal [110], the low stirring rate may decrease the uniformity of the mixing force throughout the emulsion mixture, hence resulting in higher diameters and a wider size distribution of the final microcapsules.

3.1.3.3. Influence of the volume of ethyl acetate added to the aqueous phase

As presented at section 3.1.3.1, the solubility in water of ethyl acetate (90g/l at 20°C) is higher than that of halogenated solvents commonly used in the solvent evaporation method such as dichloromethane (20g/l at 20°C), so the fast diffusion rate of ethyl acetate from oil droplets to aqueous phase may disturb the emulsification step and induce the formation of elliptical and rod shape microparticles and of the rather broad size distributions. H.K. Kim et al. [64] tried to slow down the diffusion rate by saturating the outer aqueous phase with ethyl

acetate prior to the emulsification step. So in order to reduce the number of no-spherical microparticles and narrow the size distribution of microcapsules, a certain volume of ethyl acetate was added to the aqueous phase before the emulsification. The influence of that volume on the microcapsule size and morphology was investigated within three levels: 0 ml (the lot S0 - without adding solvent, was also the lot C0.075 or R700), 8 ml (the lot S8) and 12 ml (the lot S12).

Influence on size distribution of microcapsules

The addition of ethyl acetate to the aqueous phase before emulsification really helped to narrow the microcapsule size distribution (Table 3.4, Figure 3.10). When 8 ml of ethyl acetate was added to the aqueous phase, the span value decreased obviously from 3.0 (the lot S0) to 1.3 (the lot S8) while the $d(0.5)$ diameter of microcapsules increased slightly from 21.5 μm (the lot S0) to 29.5 μm (the lot S8). When 12 ml of ethyl acetate was added (the lot S12), the microcapsule $d(0.5)$ diameter (27.5 μm) and the span value (1.1) did not change much in comparison to those of the lot S8. The addition of ethyl acetate to the aqueous phase also markedly favoured the increase of the volume ratio of microcapsules with diameter in range of 5–60 μm from 82% (in the lot S0) to 97 and 98% (the lot S8 and S12).

Table 3.4: $d(0.5)$ diameter and span values of microcapsule lots S0, S8 and S12

Lot	Volume of added ethyl acetate (ml)	Mean diameter (μm)	Volume ratio of microcapsules having diameter 5–60 μm	Span value
S0 (C0.075)	0	21.5 \pm 0.2	82%	3.0
S8	8	29.5 \pm 0.2	97%	1.3
S12	12	27.5 \pm 0.2	98%	1.1

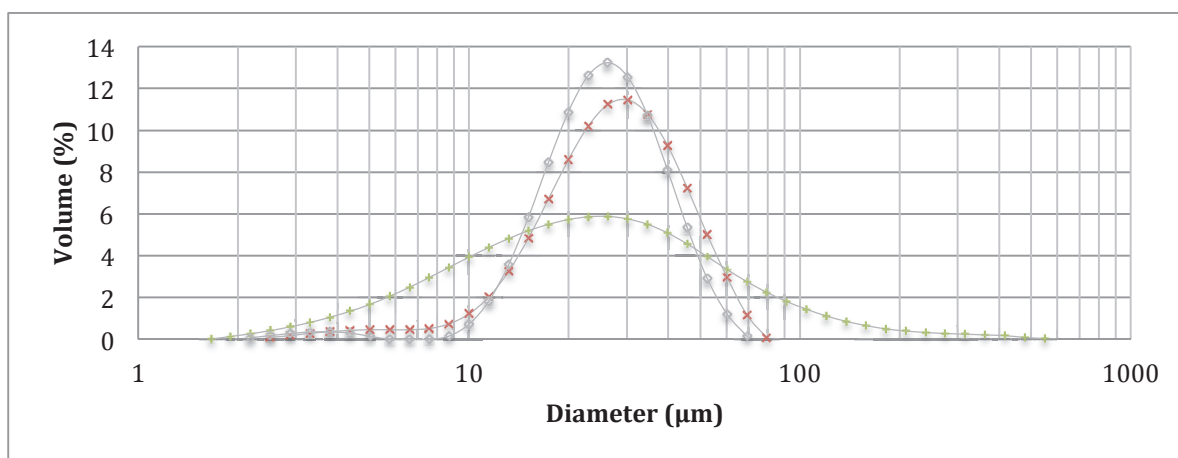


Figure 3.10: Size distributions of microcapsule lots S0, S8 and S12

—+— S0 —x— S8 —o— S12

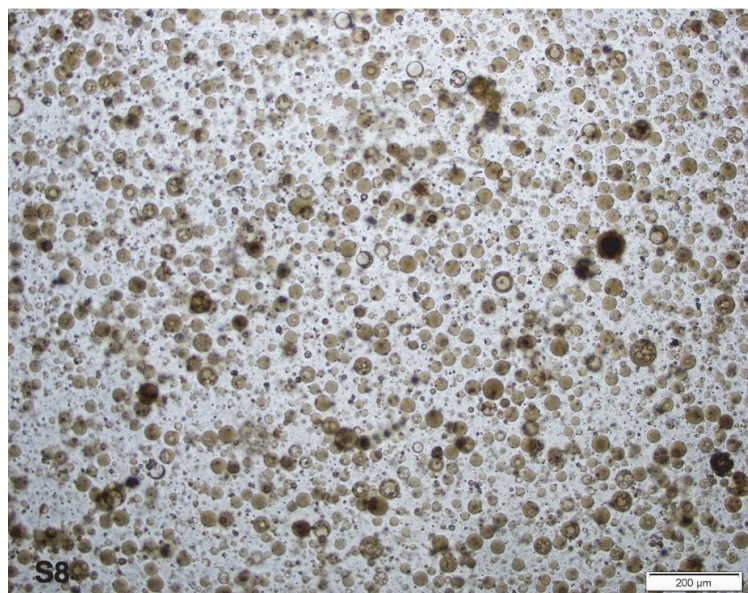


Figure 3.11: Optical microscope image of microcapsule S8

Since the solubility in water of ethyl acetate at 20°C is 90 g/l that equals to 100 (ml/l), when 8 ml of ethyl acetate was added to 100 ml of aqueous phase, the solvent was completely dissolved and almost reached the water saturation. The diffusion rate of ethyl acetate from the oil droplets to the aqueous phase was then significantly reduced, resulting in the delay of the polymer precipitation, increasing the efficiency of the emulsification step through the formation of smaller droplets with spherical shapes. In comparison to the lot S0, the size distribution of the lot S8 revealed the disappearance of the population of microcapsules with diameter higher than 80 μm (Figure 3.10). The optical microscope image of microcapsules S8 also confirmed this result and the disappearance of the irregular microparticles (Figure 3.11).

When 12 ml of ethyl acetate was added to the aqueous phase (the lot S12), the aqueous phase may be completely saturated by the solvent so the $d(0.5)$ diameter and the size distribution of microcapsules did not change much in comparison to the lot S8.

Influence on microcapsule morphology after drying

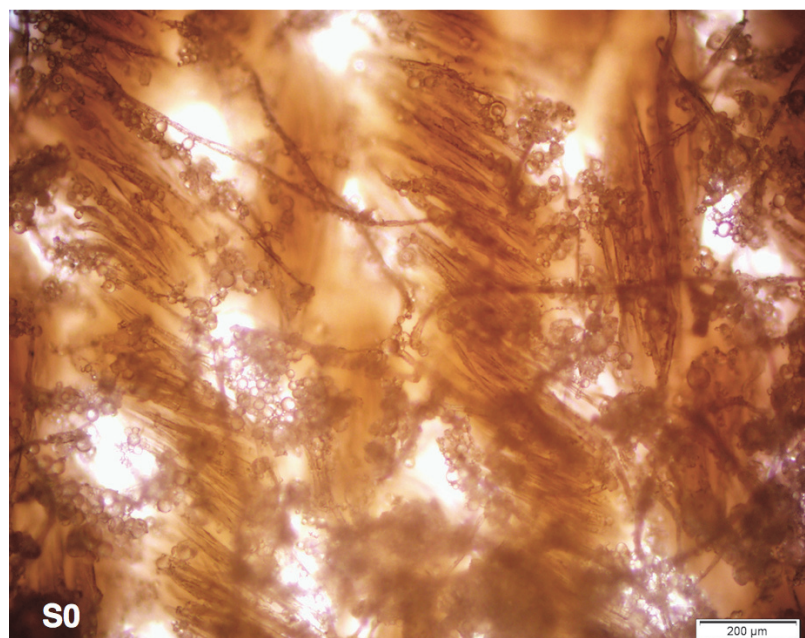
The addition of ethyl acetate to the aqueous phase really helped to narrow the size distribution of microcapsules. However, it was reported in the literature that the low diffusion rate of ethyl acetate from the oil droplets to the aqueous phase might then cause aggregation of the microcapsules during the drying step due to the high hydration rate. Since water solubility in ethyl acetate is 3.3 wt% at 20°C, the oil droplets can absorb a considerable amount of water during the microencapsulation processes. Therefore, before the drying step, microcapsules may be softened because of the residual ethyl acetate and water migrating into the surface of the microcapsules, leading to the aggregation of adjacent microcapsules during the drying step

[120]. The drying process is always necessary for the finishing of textiles. Therefore, the influence of the addition of ethyl acetate to the aqueous phase on the microcapsule morphology on the cotton interlock fabric after drying was investigated.

The washed microcapsules S0, S8 and S12 were redispersed in distilled water to the concentration of 15 (mg/ml) and then deposited to cotton interlock fabrics (code Cot, see section 2.1.1). The microcapsule deposited fabrics were observed by optical microscopy 24 hours after vacuum drying at 25°C, according to the amount of ethyl acetate added in the aqueous phase. The microcapsules S0 were still spherical (Figure 3.12A) while the microcapsules S8 and S12 deformed strongly, no clearly spherical microcapsules could be observed on the fabric surface (Figure 3.12B,C).

The addition of ethyl acetate to the aqueous phase decreased the diffusion rate of solvent from the oil droplets to the aqueous phase. After the same duration of solvent evaporation step (5 hours), the content of residual solvent in microcapsules S8 and S12 may be higher than that in microcapsules S0. Since the water solubility in ethyl acetate is equal to 3.3 wt% [120], the content of residual water in microcapsules S8 and S12 may be also higher than that of microcapsules S0. The hydration rate of S0, S8 and S12 determined by experiments (see section 2.3.3.2) was equal to 40, 85 and 97 wt% respectively. Because of the higher hydration rate, the polymer structure of microcapsules S8 and S12 was softer and weaker, resulting in stronger deformation after the drying process. The duration of the solvent evaporation step was prolonged to 8 hours. Nevertheless, S8 and S12 microcapsules still deformed significantly by drying.

A



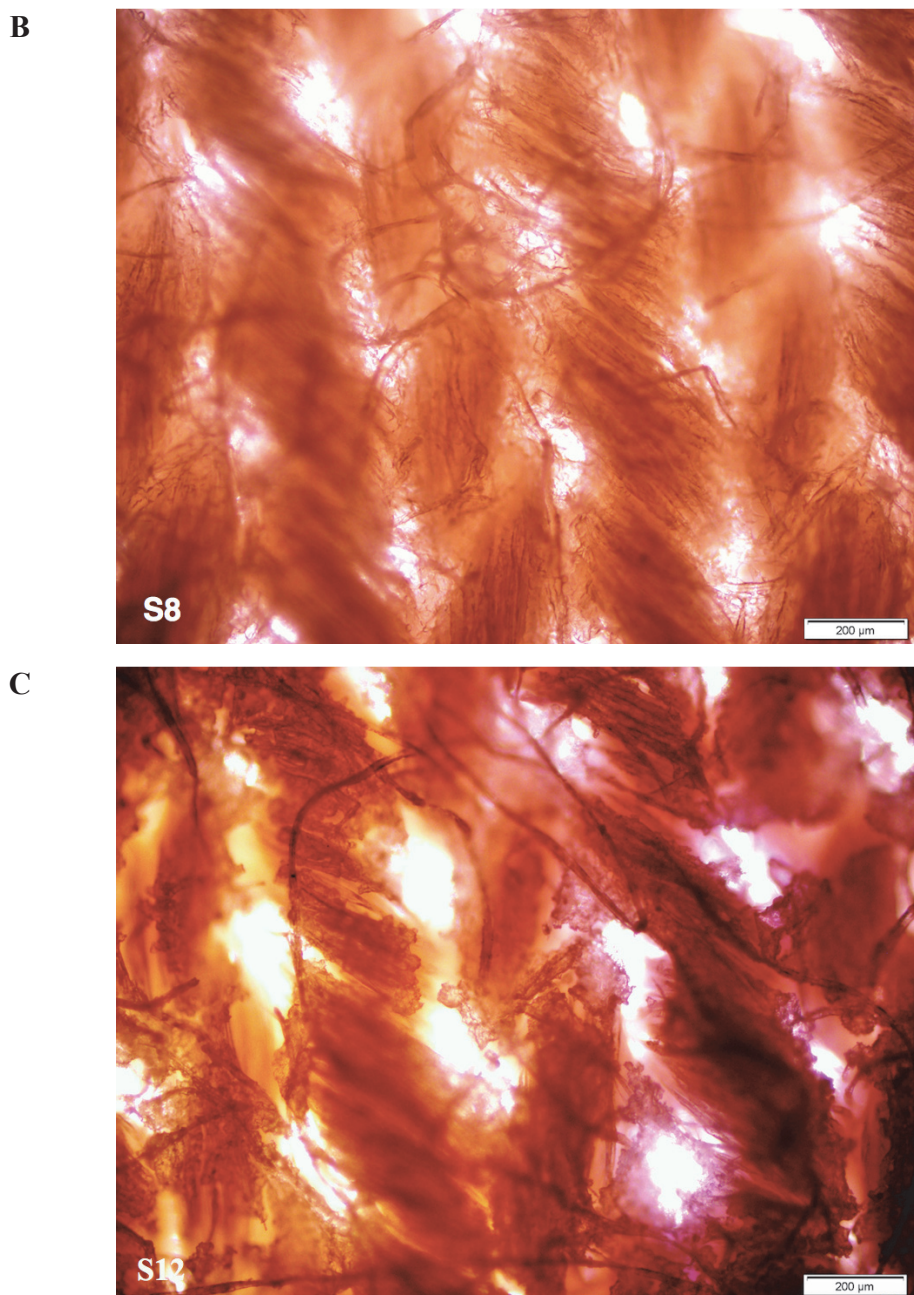


Figure 3.12: Optical microscope images of the cotton interlock fabrics coated with microcapsules S0 (A), S8 (B) and S12 (C) after 24 hours of vacuum drying at 25°C

3.1.4. Conclusions on the microencapsulation parameters suitable for textile applications

All the previous results express that the ibuprofen-loaded microcapsules can be elaborated successfully by the solvent evaporation method, using the bio-sourced surfactant quillaja saponin and the non-halogenated solvent ethyl acetate. Those microcapsules are spherical with more than 80% of the total volume exhibiting diameter in range of 5÷60 μm, in accordance with the targeted textile application. In order to narrow the size distribution, the addition of

ethyl acetate to the aqueous phase before the emulsification step helped to narrow the size distribution. Nevertheless, the recovered microcapsules were quite deformed during the drying process. In the manufacture of anti-inflammatory textile, the microcapsules always have to pass the drying process. Despite of the broad size distribution, the microcapsule lot C0.075 (R700 or S0) was chosen to be deposited to the fabrics since their capability of keeping their spherical shape during the drying step.

In conclusions, the appropriate microencapsulation parameters are as below:

- The continuous phase: the solution of quillaja saponin in water having concentration of 0.075 wt%.
- The dispersed phase: the mixture of ethyl acetate with ibuprofen (8.33 mg/ml), miglyol 812 (33.33 mg/ml) and eudragit RSPO (116.67 mg/ml).
- The volume ratio of the dispersed phase/continuous phase: 15/100
- The stirring rate during emulsification: 700 rpm
- The pressure during the solvent evaporation: 300÷350 Torr
- The time of solvent evaporation: 5 hours

3.1.5. Other characteristics of C0.075 microcapsules

The applicability of microcapsules on anti-inflammatory textiles also depends on some other characteristics of C0.075 microcapsules, such as the surface and inner morphology of the microcapsules, the drug loading ratio, the microencapsulation efficiency and the possible content of residual solvent.

The surface and inner morphology of the microcapsules

The surface and inner morphology exert strong influences on the drug release capability of microcapsules [26, 83]. These both characteristics are classically observed by SEM. The SEM images confirmed the results of the size and the size distribution of the microcapsules pointed out by the laser diffractometry and the optical microscopy (Figure 3.13A). Moreover, the C0.075 microcapsules exhibit many tiny spherical particles on their surface with diameters below 0.5 μm (Figure 3.13B).

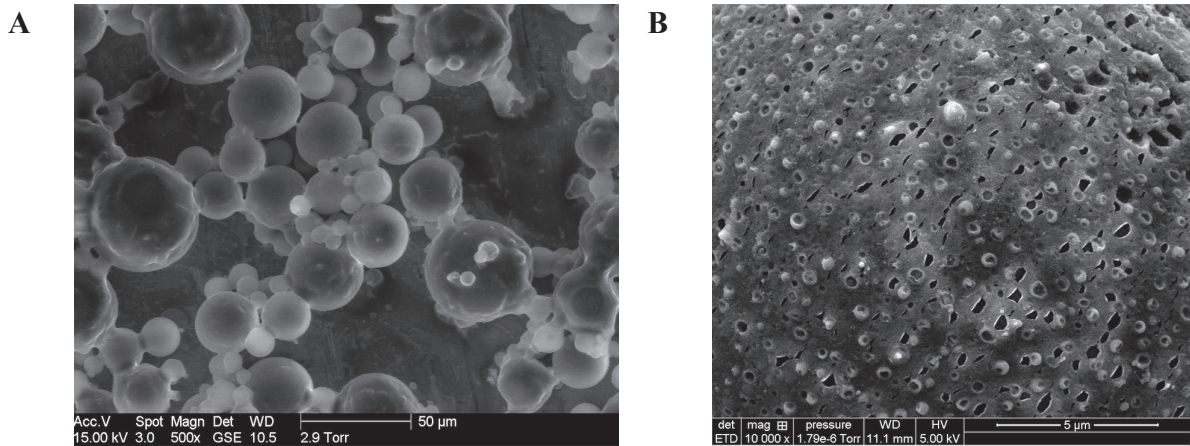


Figure 3.13: SEM images of the C0.075 microcapsules
(A): overall image; (B): image of the microcapsule surface

The image of microcapsule cross section (Figure 3.14) was obtained by cryo-SEM technique. The microcapsule dispersion in water was promptly frozen by liquid nitrogen at -80°C so that the microcapsules could keep their original morphology. The analysis of the cross section allow observe the internal morphology of the microcapsules, i.e. mono- or multiple one. The image showed the multiple core morphology of the microcapsules with alternate arrangement of the tiny cores and the pockets. The cores are spherical shaped with diameters smaller than $0.5\ \mu\text{m}$. They are the solutions of ibuprofen in miglyol 812 and surrounded by the polymer shells. The tiny spherical particles observed in the SEM image of the microcapsule surface (Figure 3.13B) may be the outermost cores of the microcapsules. The pockets contain the mixtures of the solvent and water with diameters in the range of $0.1\div 1.3\ \mu\text{m}$.

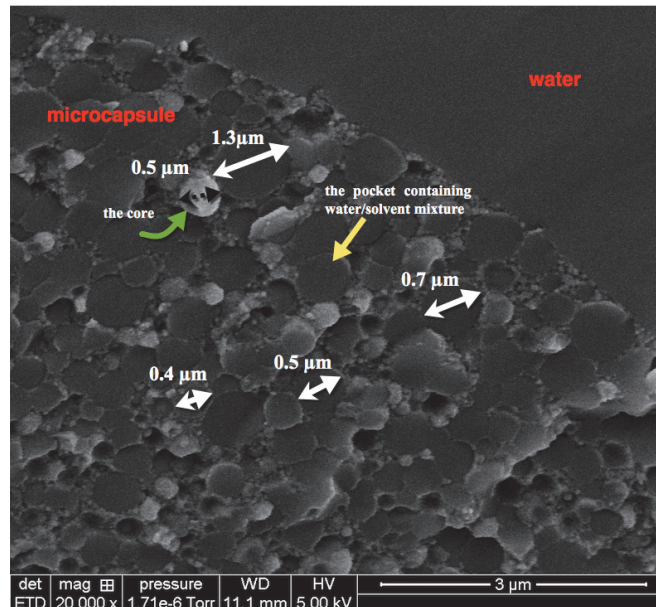


Figure 3.14: SEM image of cross-section of microcapsule C0.075

↗ The core → The pocket containing water/solvent mixture

The ibuprofen loading ratio and the microencapsulation efficiency

The ibuprofen loading ratio and the microencapsulation efficiency are closely related to the economic benefit of the manufacture of anti-inflammatory textile, and these values are expected to be as high as possible. In order to determine the ibuprofen loading ratio and the microencapsulation efficiency, ibuprofen was extracted from the microcapsules by heptane with the aid of sonication. Ibuprofen concentration was determined by the spectrometer UV-Vis.

After 60 minutes of sonication, the mass ratio of extracted ibuprofen/microcapsule reached the maximum value of 7.1% (Appendix Table 2 at Appendix 4), so it can be concluded that the drug loading ratio of microcapsules was $L = 7.1\%$.

The microencapsulation efficiency was calculated according to the equation (Eq 2.5):

$$E (\%) = \frac{L(\%) \times m_{lot}}{ibu_{init}} \times 100\% \quad (\text{Eq 2.5})$$

With the mass of the whole microcapsule lot after drying $m_{lot} = 1250$ (mg), and ibu_{init} is the mass of initial ibuprofen used for the microencapsulation that was equal to 125 (mg), the microencapsulation efficiency E was found equal to 71%, which was in average if compared with the values reported in other researches on the application of microcapsules in textile [17, 56, 73, 79].

The content of residual ethyl acetate

The anti-inflammatory textiles are in contact with the human skin. The content of residual solvent must be in the permitted level. According to the U.S.Pharmacopeia USP29 [111], the residual solvents in gauze bandages are limited to be lower than 0.5 wt%. In the thesis, the content of residual ethyl acetate was determined by gas chromatography, using a mass detector. According to the results by gas chromatography (the detail description was presented at Appendix 5, the mass ratio of residual ethyl acetate in the microcapsules was equal to 0.4 wt%. This value is below the permitted level according to the USP29 (0.5 wt%), proving that elaborated microcapsules are safe for users.

3.2. Influence of the drying conditions on the microcapsule morphology after textile finishing process

An advantage of the ibuprofen-loaded microcapsules in this thesis is the environmental friendly microencapsulation with the use of non-halogenated solvent ethyl acetate. This solvent is less toxic than commonly used chlorinated solvents such as chloroform and dichloromethane. However, due to the high solubility in water and the high boiling point of ethyl acetate, the wet microcapsules exhibit high hydration rate (40%) inducing a quite high sensitivity to drying process (see section 3.1.3.3 in this manuscript). Therefore, in order to find

out the suitable drying conditions for the manufacture of the medical textiles using microcapsules, the influences of the drying humidity and temperature on the microcapsule morphology were investigated.

3.2.1. Influence of the humidity during the drying process

The C0.075 microcapsules were coated to the interlock fabric B3 (having loop length of 2.87 mm) and then dried at 25°C with drying humidity rate varying between 0% (vacuum dried) and 65%.

When the drying humidity rate was 65%, the microcapsules on the fabric appeared completely melted, turning into a polymer film that covered the fabric surface (Figure 3.15).

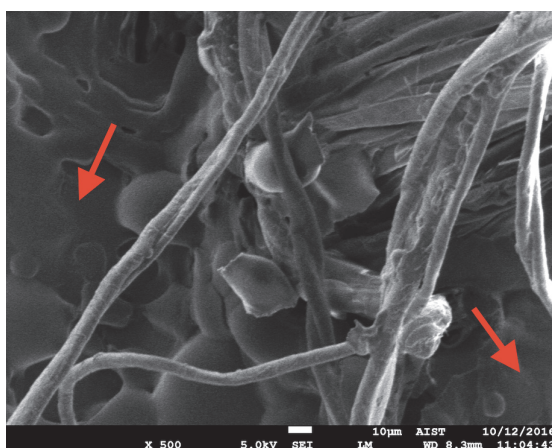


Figure 3.15: SEM image of the microcapsule coated fabric dried at 25°C with the drying humidity rate of 65%

→: polymer film created from melted microcapsules

When the drying humidity rate was decreased from 65% to 20%, the microcapsules were slightly deformed with elliptical shapes (Figure 3.16). And in the same observed area of 190 x 255 µm, 30 elliptical microcapsules could be seen. More microcapsules instead of polymer film observed in the SEM images pointing out that the microcapsule deformation was reduced.

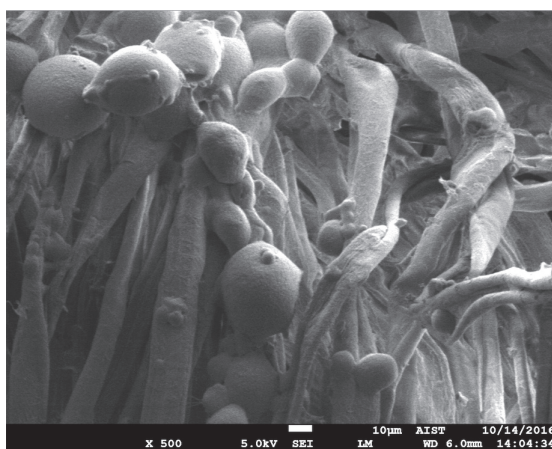


Figure 3.16: SEM image of the microcapsule coated fabric dried at 25°C with the drying humidity rate of 20%

When the drying humidity was reduced to 0% (vacuum drying), the deformation phenomenon dramatically decreased. The dried microcapsules on fabric were as spherical as before the drying. On the same fabric area of 190 x 255 μm , 96 microcapsules could be observed (Figure 3.17), which were more numerous than on the treated fabric dried at the humidity rate of 20%.

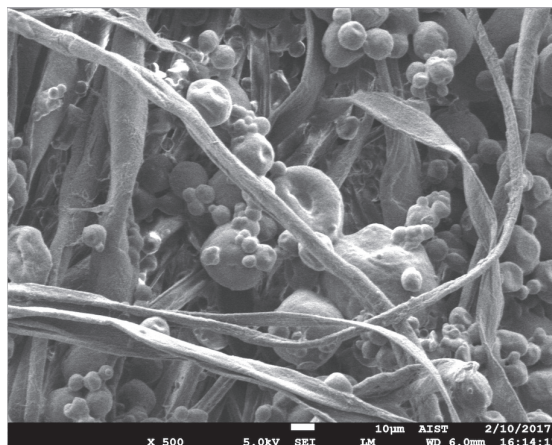


Figure 3.17: SEM image of the microcapsule coated fabric dried at 25°C with the drying humidity rate of 0%

Right after the coating process, the microcapsules deposited on the fabric were wet ones with a rather high hydration rate (40%). Then they were plasticized and easily deformed on the textile substrate by their own gravity. The lower the drying humidity, the faster the evaporation of water and the solvent during the drying step, resulting in less deformation of microcapsules.

In conclusion, within the scope of this research, the lower drying humidity is better for the keeping of microcapsule morphology during drying process. The vacuum drying should be applied in order to protect the original morphology of microcapsules from the deformation.

3.2.2. Influence of the drying temperature

The higher the drying temperature, the rapider the drying step, resulting in a shorter period of manufacturing the anti-inflammatory textiles. However, the high drying temperature may cause damage to the microcapsules. Then we investigated the influence of the vacuum drying temperature on the morphology of C0.075 microcapsules. The investigation began at 25°C, corresponding to the ambient temperature, then was gradually increased until the microcapsules were significantly deformed. The suitable drying temperature for the manufacture of the anti-inflammatory textiles should be the maximum temperature inducing no effect on the microcapsule morphology.

During the vacuum drying, when the temperature was increased from 25°C to 45°C, the microcapsules on the fabric still kept their spherical shapes and were almost not deformed (Figure 3.18-Figure 3.21).

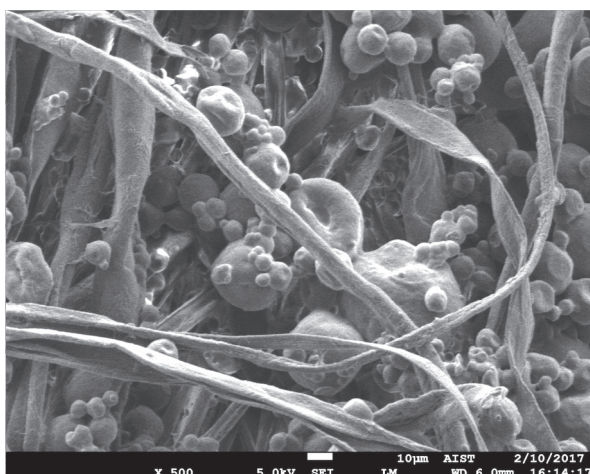


Figure 3.18: SEM image of the cotton interlock fabric coated with microcapsules with vacuum drying at 25°C

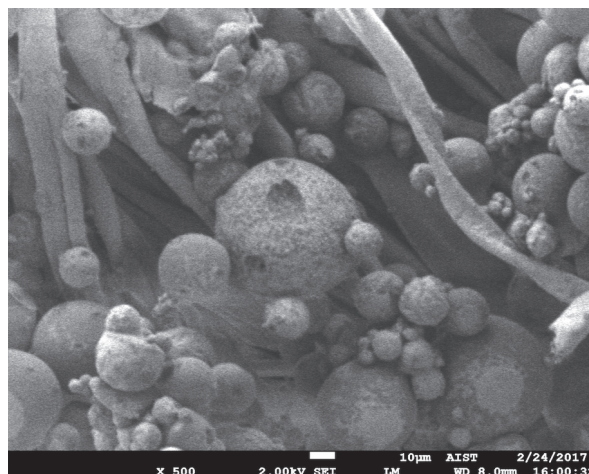


Figure 3.19: SEM image of the cotton interlock fabric coated with microcapsules with vacuum drying at 35°C

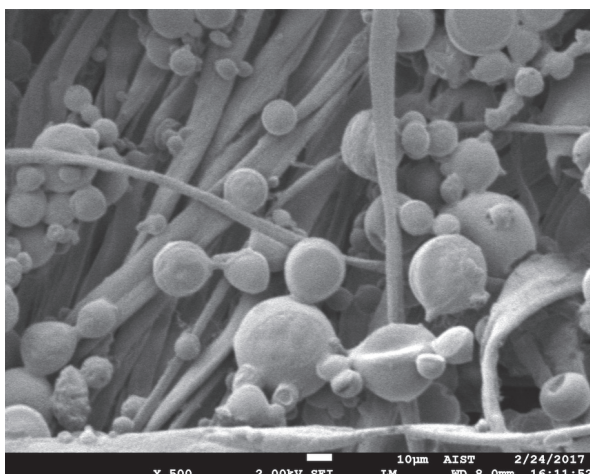


Figure 3.20: SEM image of the cotton interlock fabric coated with microcapsules with vacuum drying at 45°C

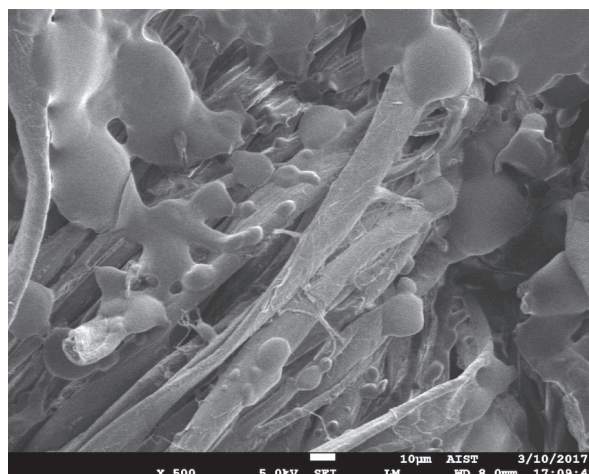


Figure 3.21: SEM image of the cotton interlock fabric coated with microcapsules with vacuum drying at 60°C

When the drying temperature was increased to 60°C, the microcapsules were significantly softened, turning into the polymer film that covered the fabric surface (Figure 3.21). That means the thermal stability of microcapsules declines obviously when the drying temperature is increase from 45°C to 60°C.

According to some literatures, the glass transition T_g of eudragit RSPO was reported to be 61 - 67°C [44, 164]. Around this range of temperature, the polymer changes from a hard and relatively brittle glassy state into a viscous or rubbery state, and this may be a reason for the microcapsule deformation observed when the drying temperature was increased to 60°C.

In conclusion, the appropriate drying conditions for the manufacture of the anti-inflammatory textiles using microcapsules in the thesis were fixed to vacuum drying at 45°C.

3.3. Influence of the textile substrate on the characteristics of the microcapsule-treated fabrics

3.3.1. Influence of the textile material type

As mentioned in the literature review, section 1.3, some researches about the application of microcapsules on woven fabrics reported that textile material type has a strong influence on the microcapsule loading capability, the microcapsule distribution and the active release capability of the microcapsule-treated fabrics [17, 40, 75, 125]. However up to now, there have been only few published researches investigating these effects in the knitting field; Therefore, we deposited C0.075 microcapsules on three kinds of interlock fabrics knitted from cotton, peco 65/35 and polyester having the same yarn count of Ne20, which are often used for the medical textile products. The structural parameters of these fabrics, which were determined by the techniques described at section 2.3.4.1, were reported in Table 3.5. Microcapsules were applied to fabrics by impregnating technique.

Table 3.5: Structural parameters of the interlock knitted fabrics used to investigate the influence of the textile material type on the characteristics of the microcapsule-treated fabric

Fabric Lot	Cotton	Peco 65/35	Polyester
Yarn count	Ne20	Ne20	Ne20
Loop length (mm)	3.78	3.72	3.76
Wale density (number of wales/10cm)	122	135	136
Course density (number of courses/10cm)	147	131	126
Area density (number of loops/cm²)	179	177	171

3.3.1.1. Influence on the microcapsule loading capability

In order to investigate the influence of textile material type on the microcapsule loading capability, five microcapsule-treated fabric samples were prepared for each lot of fabric. The results were shown in Table 3.6.

Table 3.6: Microcapsule loading capability of the fabrics knitted from different materials

Fabric lot	Sample	Microcapsule loading capability MLC (%)	
		For each sample	Average
Cotton	Cot_1	15.7	17.1 ± 0.8
	Cot_2	17.2	
	Cot_3	16.9	
	Cot_4	17.7	
	Cot_5	17.8	
Peco 65/35	6535_1	16.6	16.0 ± 1.1
	6535_2	14.2	
	6535_3	15.4	
	6535_4	16.5	
	6535_5	17.0	
Polyester	Pet_1	16.0	15.4 ± 1.1
	Pet_2	16.5	
	Pet_3	15.6	
	Pet_4	15.1	
	Pet_5	13.7	

The two independent samples t test was used to analyze the datas in Table 3.6 to conclude whether the microcapsule loading capability was affected by the textile material type or not. The results of t tests with a confidence interval of 95% were reported at Table 3.7.

Table 3.7: Results of two independent samples t tests for fabrics knitted from different materials

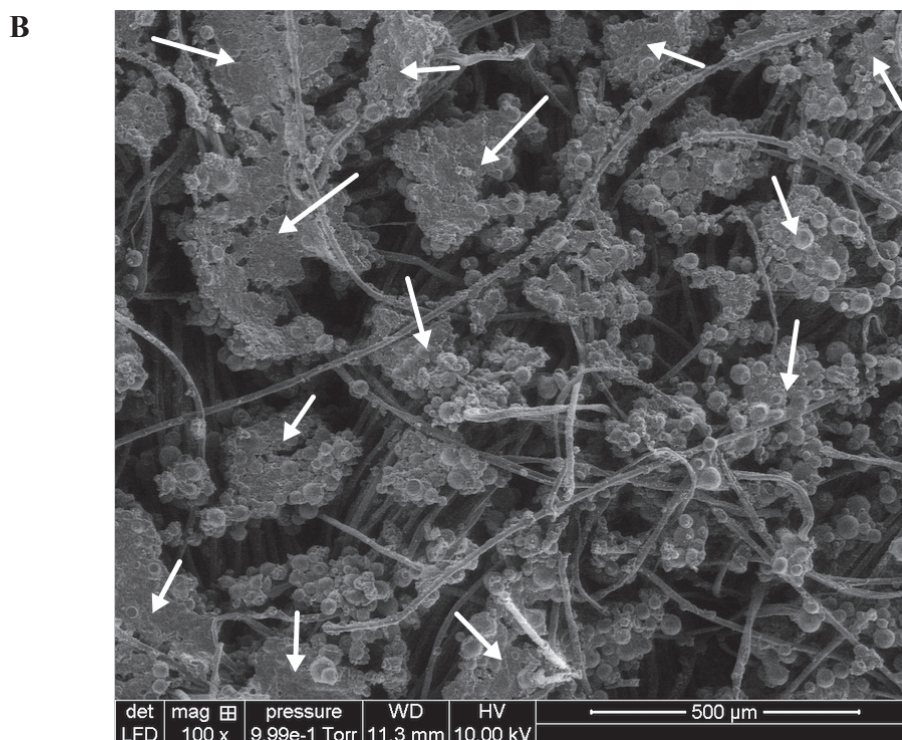
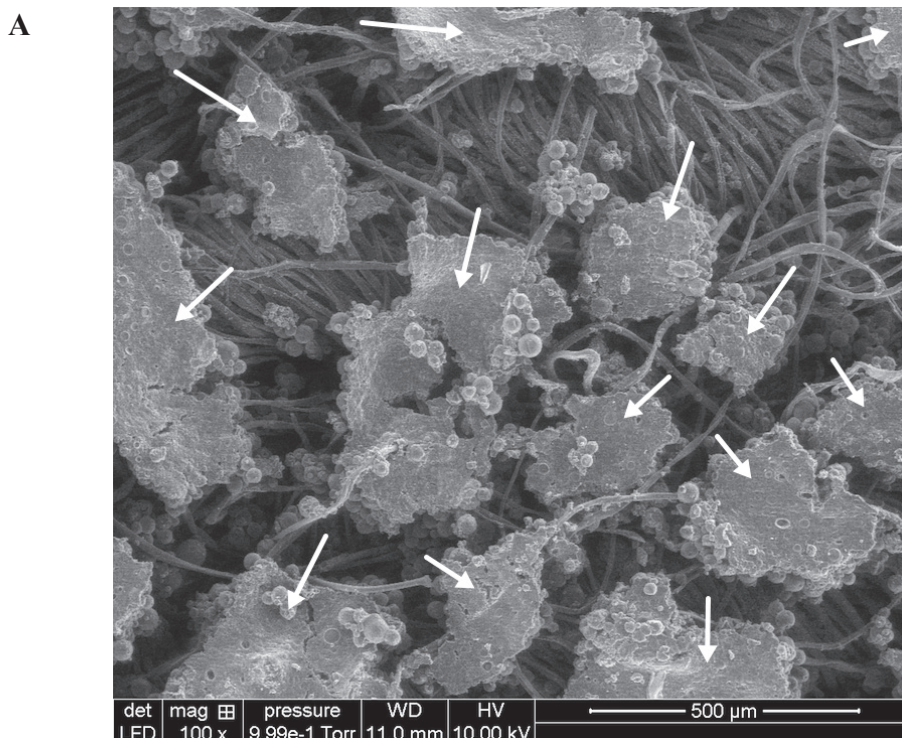
Comparison	Cotton vs. Peco 65/35	Peco 65/35 vs. Polyester
Sample size	$n_1 = n_2 = 5$	$n_1 = n_2 = 5$
Null hypothesis H_0	$\mu_1 = \mu_2$	$\mu_1 = \mu_2$
Alternative hypothesis H_a	$\mu_1 > \mu_2$	$\mu_1 > \mu_2$
t - statistic	1.8135	0.7892
t_α	1.8595	1.8595
Conclusion	$\mu_1 = \mu_2$	$\mu_1 = \mu_2$

According to the t-test, the textile material type had no influence on the microcapsule loading capability of the fabric. This result was different from the result obtained by N. Carreras et al. [17], in which the textile material type (including cotton and polyester) was reported to affect the microcapsule loading capability due to the different affinity of the textile substrates with the microcapsules. The differences of two researches could be due to the different techniques of finishing. In the research of N. Carreras et al. [17], the microcapsules were applied to the fabrics by padding whereas in this thesis, the microcapsules were applied by impregnating the fabric in the microcapsule suspension with a long time (12 hours). After such a long period of impregnating, the differences in the affinity of textile substrates with microcapsules were negligible to create the differences in the microcapsule loading capability of three kinds of fabrics.

3.3.1.2. Influence on the microcapsule distribution

In order to investigate the influence of the textile material type on the microcapsule distribution on the fabric, the microcapsule-treated fabric samples Cot_1, 6535_1 and Pet_1 (Table 3.6) were observed by scanning electron microscopy at the magnification of x100.

The SEM images showed the aggregate microcapsules in the three investigated fabrics (Figure 3.22). The microcapsule aggregation is a main disadvantage for the targeted application since it reduces the total surface area of microcapsules and may prevent the release of ibuprofen from the microcapsules deep inside the aggregate. Since the microstructure of the fabric surface is always bumpy, the microcapsules can certainly not be distributed evenly on the fabric, resulting in a number of microcapsules laying closely to each other after the coating process. Furthermore as mentioned at section 3.1.3.3, the high hydration rate of wet microcapsules (40%) favours the deformation of the microcapsules. Hence, the microcapsules lying closely to each other after the coating process could stick together to create large microcapsule aggregates, which were even weaker and easier to be deformed by drying than the smaller individual ones.



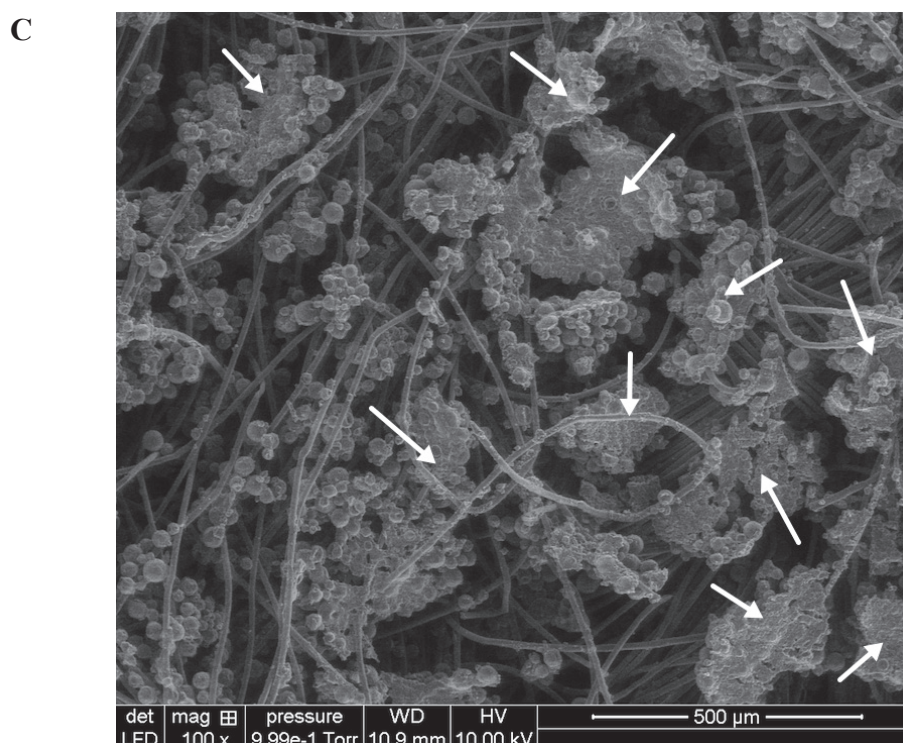


Figure 3.22: SEM images of the microcapsule-treated fabrics Cot_1 (A), 6535_1 (B) and Pet_1 (C)

→ aggregate microcapsules

To evaluate the microcapsule distribution at the fabric surface, the software Meander 3.1.2 of Peacock Media was used to determine the area of the microcapsule aggregates on the fabric surface. For each kind of fabric, three SEM images (at magnification x100) corresponding to the fabric area of 1290 x 1480 μm were analyzed. The statistical results of the area of the microcapsule aggregates were presented at Table 3.8. The results showed that the decrease of the weight ratio of the cotton fiber in textile material induced both the average area of microcapsule aggregates and the standard deviation decrease, suggesting that the microcapsules distributed more evenly on fabric.

Table 3.8: Statistical results of the area of microcapsule aggregates on different kinds of fabrics

Fabric lot	Average area of microcapsule aggregates (μm^2)
Cotton	78891 \pm 20324
Peco 65/35	49408 \pm 10693
Polyester	38850 \pm 8766

The wetting ability of the fabric by the binder solution [125] as well as the fabric structure [40] may induce some differences in the microcapsule distribution on the textile surface. In

this thesis, the three kinds of fabrics were all the knitted ones and had the similar structural parameters (Table 3.5), the finishing formulation was only the dispersion of microcapsules in distilled water without binder. Therefore, the difference of the microcapsule distribution between the three kinds of fabrics should be due to the difference in affinity with microcapsules of polyester and cotton fibers. Because the polymer shell of the microcapsule is eudragit RSPO (the chemical structure was described at Figure 2.3), which is a hydrophobic material, the affinity of the microcapsules with polyester (a hydrophobic fiber, Figure 3.23) would be higher than with cotton (a hydrophilic fiber, Figure 3.24). Consequently, the affinity with microcapsules of fabric was higher when the weight ratio of cotton fiber in the fabric was lower. If the affinity of the fabric with the microcapsules was lower than the attractive force between microcapsules, the microcapsules would stick together instead of distributing evenly on the fabric surface, resulting in microcapsule aggregates after finishing. The lower the affinity of the fabric with the microcapsules the less evenly the microcapsule distribution on the fabric.

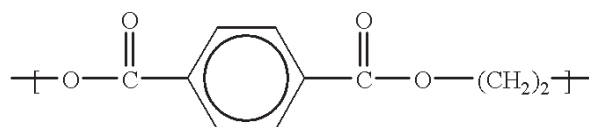


Figure 3.23: Chemical structure of polyester fiber

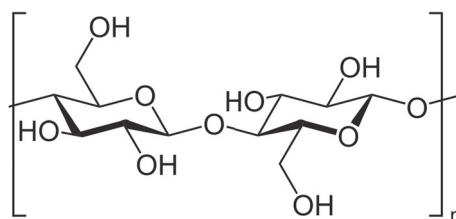


Figure 3.24: Chemical structure of cellulose (main component of cotton fiber)

3.3.1.3. Influence on the ibuprofen release capability of the microcapsule-treated fabric

The ibuprofen release capability from the microcapsule-treated fabrics was evaluated by *in vitro* experiments described at section 2.3.4.2. Two samples were used for each kind of fabric, the results were shown in Table 3.9 and Figure 3.25.

The chart at Figure 3.25 expressed that the textile material type had an obvious influence on the ibuprofen release rate from the microcapsule-treated fabrics. For a 8 hours release period, the weight percentage of ibuprofen dissolved into the receptor fluid was 37.3, 42.2 and 50.9% in case of cotton, peco 65/35 and polyester fabric, respectively. So within the scope of the investigation, the ibuprofen release rate from the microcapsule-treated fabric was higher when the weight ratio of cotton in the fabric was lower. This result could be explained by two factors: the first was the different affinity of ibuprofen with the different textile materials, the second was the different distribution of microcapsules on different kinds of fabrics.

Table 3.9: Ibuprofen release rate from the microcapsule-treated fabrics having different textile materials

Time	Weight percentage of ibuprofen dissolved into receptor fluid (%)								
	Cotton fabric			Peco 65/35 fabric			Polyester fabric		
	Cot_2	Cot_3	Average	6535_4	6535_5	Average	Pet_2	Pet_3	Average
8h	38.4	36.1	37.3 ± 1.2	41.3	43.0	42.2 ± 0.9	48.7	53.0	50.9 ± 1.1
24h	51.3	50.3	50.8 ± 0.5	54.3	55.6	55.0 ± 0.7	59.3	55.9	57.6 ± 1.7
32h	52.1	54.5	53.3 ± 1.2	53.5	56.1	54.8 ± 1.3	60.0	57.2	58.6 ± 1.4
48h	49.4	50.2	49.8 ± 0.5	52.5	57.6	55.1 ± 2.6	60.2	55.4	57.8 ± 2.4

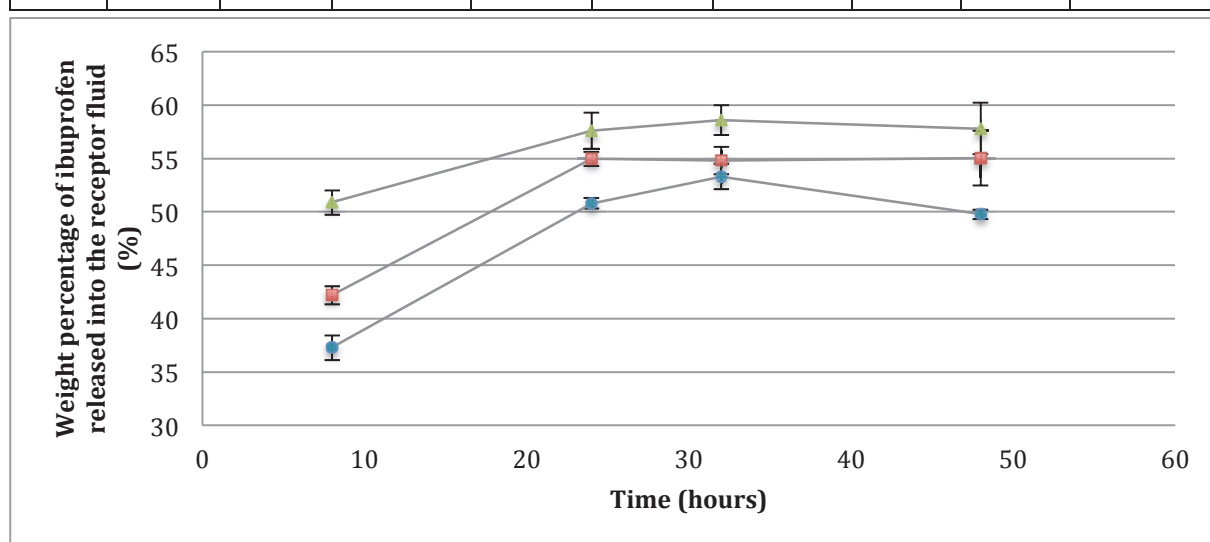


Figure 3.25: Release rate of ibuprofen from microcapsule-treated fabrics according to the type of the textile material

● Cotton ■ Peco 65/35 ▲ Polyester

Firstly, the chemical structures of cellulose (Figure 3.24), of polyester (Figure 3.23) and of ibuprofen (Figure 2.1) showed that the hydrogen bonds could be formed between the cotton fibers and ibuprofen whereas they could not be formed between the polyester fibers and ibuprofen, resulting in higher affinity with ibuprofen of cotton fibers and consequently, lower the ibuprofen release rate from the fabrics having higher content of cotton fibers.

Secondly, the results at section 3.3.1.2 showed that the average area of the microcapsule aggregates on the fabric surface decreased in order of cotton, peco 65/35 and polyester fabric. The bigger area of the microcapsule aggregates, the more difficult for ibuprofen deep inside

the aggregates to be released, resulting in lower release rate of ibuprofen from the fabrics having higher content of cotton fibers.

Figure 3.25 also showed that the release of ibuprofen from all three kinds of fabrics almost finished after 24 hours, and at that time the weight percentage of ibuprofen dissolved into the receptor fluid was 50.8, 55.0 and 57.6% in case of cotton, peco 65/35 and polyester fabric, respectively. This result once again expressed the disadvantage of the microcapsule aggregates. Ibuprofen encapsulated in the microcapsules deep inside those aggregates could not be released, resulting in the weight percentage of ibuprofen dissolved into the receptor fluid could not reach 100%.

3.3.1.4. Conclusion

Within the scope of investigation, which was carried out on three kinds of interlock fabrics knitted from cotton, peco 65/35 and polyester (with similar yarn count, loop length and fabric density), the textile material type had no influence on the microcapsule loading capability but had obvious effects on the microcapsule distribution and active release capability of the fabrics.

The microcapsule distribution was less even when the content of cotton fibers in fabric was higher. The average area of the microcapsule aggregates on cotton, peco 65/35 and polyester fabric were 78891, 49408 and 38850 (μm^2), respectively. This could be due to the lower affinity of the microcapsules with cotton fibers than polyester fibers. When the affinity of the microcapsules with the fabric was lower than the attractive force between microcapsules, the microcapsules were easy to stick together to form aggregates instead of evenly distributing on the fabric surface.

Due to the less even distribution of microcapsules on the fabric, together with higher affinity with ibuprofen of cotton fibers than polyester fibers, the release rate of ibuprofen from the microcapsule-treated fabric decreased when the content ratio of cotton fibers in the fabric increased. After 8 hours of release, the weight percentage of ibuprofen in the treated fabrics dissolved into the receptor fluid increased in order of 37.3, 42.2 and 50.9% corresponding to cotton, peco 65/35 and polyester fabric. Besides, the maximum weight ratio of ibuprofen dissolved into the receptor fluid, which was reached after 24 hours, also increased in order of 50.8, 55.0 and 57.6% corresponding to the cotton, the peco 65/35 and the polyester fabric.

3.3.2. Influence of the loop length

The loop is the most basic structural unit of the knitted fabrics. The loop length could be set directly on the knitting machine and it affects most of the fabric properties such as the dimensional properties, the bursting strength, the thermal properties and the air permeability [24, 28, 122]. However so far, there have been very few researches about the influence of the loop length on the characteristics of the microcapsule-treated fabrics. Therefore, we investigated the influence of the loop length in the interlock fabric on the microcapsule

loading capability, the microcapsule distribution and the active release capability of the microcapsule-treated fabrics.

Five investigated levels of the loop length in the cotton interlock knitted fabrics (with the yarn count of Ne40) were: 2.81 mm (B1 fabric); 2.83 mm (B2 fabric); 2.87 mm (B3 fabric); 2.96 mm (B4 fabric) and 3.05 mm (B5 fabric). These values were the most popular loop lengths used by Doximex Knitting Company, where the fabrics were made. The C0.075 microcapsules were deposited on the fabrics by the coating and impregnating techniques.

3.3.2.1. Influence on the microcapsule loading capability

1. Applications of the microcapsules by the coating technique

The microcapsules were applied on the textile by the coating technique, with two concentrations: 14 and 24 (mg/ml). The deposit was performed in triplicate. The microcapsule loading capability of the fabric lots having different loop lengths according to each microcapsule concentration were reported at Table 3.10 and Table 3.11.

Table 3.10: Microcapsule loading capability of the fabrics according to the loop length with a microcapsule concentration of 14 mg/ml

Fabric lot (loop length)	Fabric sample	Sample weight before finishing (mg)	Sample weight after finishing (mg)	Microcapsule loading capability MLC (%)	
				For each sample	Average
B1 (2.81 mm)	1	9312	9948	6.83	7.0 ± 0.2
	2	9216	9859	6.98	
	3	9888	10602	7.22	
B2 (2.83 mm)	1	9293	9934	6.90	7.2 ± 0.3
	2	9293	9973	7.32	
	3	9955	10690	7.38	
B3 (2.87 mm)	1	9025	9690	7.37	7.5 ± 0.2
	2	9522	10239	7.53	
	3	9347	10058	7.60	
B4 (2.96 mm)	1	8878	9555	7.62	7.8 ± 0.2
	2	9522	10277	7.93	
	3	9053	9763	7.85	
B5 (3.05 mm)	1	8580	9301	8.40	8.3 ± 0.1
	2	9020	9758	8.18	
	3	8659	9380	8.32	

Table 3.11: Microcapsule loading capability of the fabrics according to the loop length with a microcapsule concentration of 24 mg/ml

Fabric lot (loop length)	Fabric sample	Sample weight before finishing (mg)	Sample weight after finishing (mg)	Microcapsule loading capability MLC (%)	
				For each sample	Average
B1 (2.81 mm)	1	9427	10931	15.95	16.3 ± 0.3
	2	9936	11575	16.50	
	3	8640	10061	16.45	
B2 (2.83 mm)	1	9322	10890	16.83	17.1 ± 0.4
	2	9763	11472	17.50	
	3	8640	10101	16.91	
B3 (2.87 mm)	1	9016	10675	18.40	17.9 ± 0.5
	2	8924	10526	17.95	
	3	8961	10524	17.44	
B4 (2.96 mm)	1	9384	11115	18.45	18.3 ± 0.4
	2	9292	10955	17.90	
	3	9062	10743	18.55	
B5 (3.05 mm)	1	8518	10188	19.60	20.0 ± 0.4
	2	7480	9001	20.34	
	3	9152	10996	20.15	

In order to conclude about the influence of the loop length on the microcapsule loading capability, the two independent samples t test with confidence interval of 95% was used. The comparison was carried out for each lot of fabric: B1 vs. B2, B2 vs. B3, B3 vs. B4 and B4 vs. B5. The results of t tests were reported at Table 3.12 and Table 3.13.

Table 3.12: Results of the t tests according to the loop length with a microcapsule concentration of 14 mg/ml

Comparison	B1 vs. B2	B2 vs. B3	B3 vs. B4	B4 vs. B5
Sample size	$n_1 = n_2 = 3$			
Null hypothesis H_0	$\mu_1 = \mu_2$	$\mu_1 = \mu_2$	$\mu_1 = \mu_2$	$\mu_1 = \mu_2$
Alternative hypothesis H_a	$\mu_1 < \mu_2$	$\mu_1 < \mu_2$	$\mu_1 < \mu_2$	$\mu_1 < \mu_2$
t - statistic	1.0056	1.8113	2.6046	4.4252
t_α	2.1318	2.1318	2.1318	2.1318
Conclusion	$\mu_1 = \mu_2$	$\mu_1 = \mu_2$	$\mu_1 < \mu_2$	$\mu_1 < \mu_2$

Table 3.13: Results of the t tests according to the loop length with a microcapsule concentration of 24 mg/ml

Comparison	B1 vs. B2	B2 vs. B3	B3 vs. B4	B4 vs. B5
Sample size	$n_1 = n_2 = 3$			
Null hypothesis H_0	$\mu_1 = \mu_2$	$\mu_1 = \mu_2$	$\mu_1 = \mu_2$	$\mu_1 = \mu_2$
Alternative hypothesis H_a	$\mu_1 < \mu_2$	$\mu_1 < \mu_2$	$\mu_1 < \mu_2$	$\mu_1 < \mu_2$
t - statistic	2.8393	2.4382	1.0783	5.7645
t_α	2.1318	2.1318	2.1318	2.1318
Conclusion	$\mu_1 < \mu_2$	$\mu_1 < \mu_2$	$\mu_1 = \mu_2$	$\mu_1 < \mu_2$

When the microcapsule concentration deposited to the fabrics was equal to 14 mg/ml, the microcapsule loading capability of the five fabric lots increased in order of B1 = B2 = B3 < B4 < B5. When the microcapsule concentration deposited to the fabrics was equal to 24 mg/ml, the microcapsule loading capability of the five fabric lots increased in order of B1 < B2 < B3 = B4 < B5. The microcapsule loading capability tended to increase when the loop length increased. Furthermore, the average microcapsule loading capability of triplicated experiments in each fabric lot was proportional to the loop length for the both concentrations (Figure 3.26, Figure 3.27).

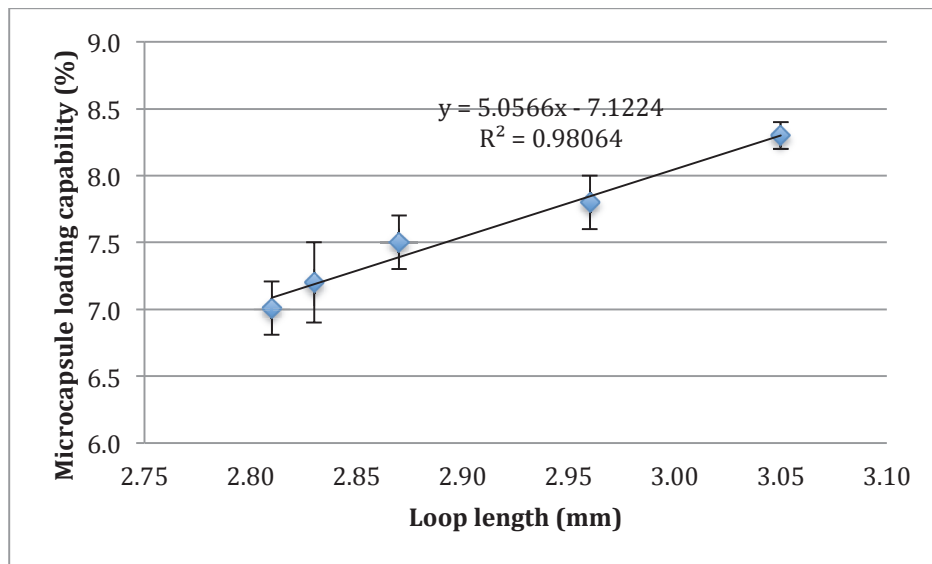


Figure 3.26: Microcapsule loading capability of the fabrics according to the loop length with a microcapsule concentration of 14 mg/ml

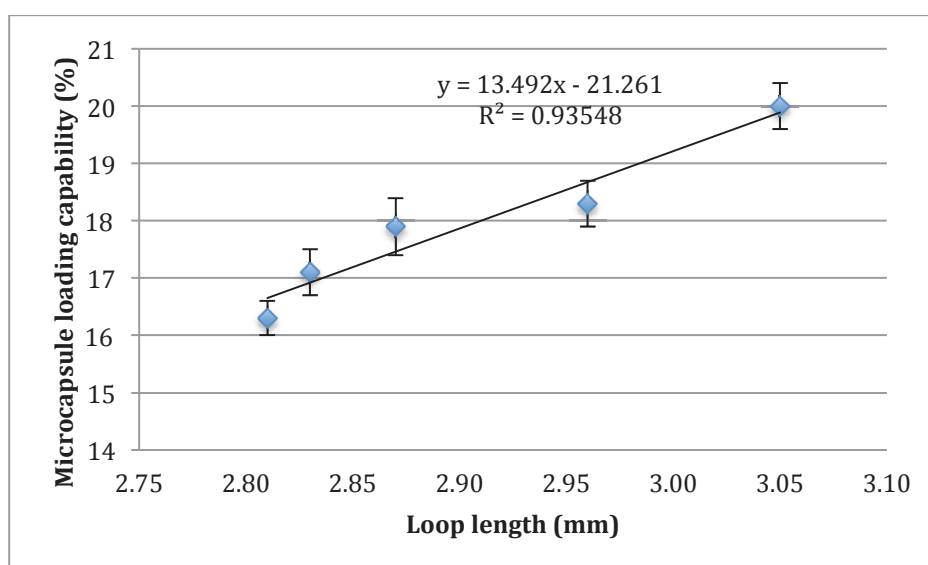


Figure 3.27: Microcapsule loading capability of the fabrics according to the loop length with a microcapsule concentration of 24 mg/ml

- When the microcapsule concentration was 14 (mg/ml) (Figure 3.26): the microcapsule loading capability was proportional to the loop length by the trend line $y = 5.0566x - 7.1224$ ($R^2 = 0.98$). When the loop length increased by 8.5% from 2.81 to 3.05 mm, the microcapsule loading capability increased by 18.4% from 7.0 to 8.3%.
- When the microcapsule concentration was 24 (mg/ml) (Figure 3.27): the microcapsule loading capability was proportional to the loop length by the trend line $y = 13.492x - 21.261$ ($R^2 = 0.94$). When the loop length increased by 8.5% from 2.81 to 3.05 mm, the microcapsule loading capability increased by 22.7% from 16.3 to 20.0%.

This tendency was similar to the result reported by C.D. Huong et al. [53], in which the microcapsule loading capability of the interlock cotton fabric was also proportional to the loop length. Hereinafter, the results will be explained according to the geometrical model of the interlock knitted loop. First of all, the suitability of the loop model proposed by Dabiryan-Jeddi [27] for the fabrics used in the thesis was checked.

The structural parameters of the fabric lots having different loop lengths were determined according to the techniques described at section 2.3.4.1. The results were reported at Table 3.14.

Table 3.14: Practical structural parameters of the fabrics according to the loop length

Fabric lot	B1	B2	B3	B4	B5
Loop length l (mm)	2.81	2.83	2.87	2.96	3.05
Length of yarn in a structural knitted cell L_u (mm)	11.24	11.32	11.48	11.84	12.20
Course density P_d (number of courses/10cm)	193	188	186	178	173
Wale density P_n (number of wales/10cm)	153	152	150	148	143
Area density P_s (number of loops/cm ²)	295	286	279	263	247
Number of structural knitted cells per unit area S_u (SKCs/cm ²)	147.5	143.0	139.5	131.5	123.5
Mass per unit area M_{fbr} (mg/mm ²)	0.240	0.240	0.230	0.230	0.220
Thickness t (mm)	0.83	0.83	0.83	0.83	0.83
Yarn diameter D (mm)	0.20	0.20	0.20	0.20	0.20
Porosity P (%)	81.0	81.0	81.8	81.8	82.6

As presented at section 1.3.4, in the loop model of Dabiryan-Jeddi [27], the length of yarn within a structural knitted cell L_u will be calculated by the equation (Eq 1.10) as below:

$$L_u = 9.38768 \times h + 19.889 \times D \quad (\text{Eq 1.10})$$

With the distance h is described in Figure 1.17D and D is the yarn diameter.

According to the assumption number 1 (see section 1.3.4), $h = 2.08 \times d$ with d is also described in Figure 1.17D. Besides, $d = 2 \times D$ basing on the assumption number 4 (see section 1.3.4). Then it could be deduced that:

$$L_u = 58.942 \times D \quad (\text{Eq 3.1})$$

Since the yarn diameter D determined by experiments was equal to 0.2 mm, the length of yarn in a structural knitted cell L_u in the model of Dabiryan-Jeddi calculated was $L_u = 58.942 \times D = 11.79$ (mm). In comparison to the real values of L_u in the fabric lots used in the thesis, the maximum difference of L_u in the model was 4.7% (in comparison to L_u of the B1 fabric). In the design process of manufacturing knitted fabrics, the difference between theoretical prediction and practical structural parameters should be in the limit of 5%. Therefore, it could be concluded that the loop model of Dabiryan-Jeddi was quite suitable for the real knitted fabrics used in the thesis. This model was accurate to explain the influence of the loop length on the microcapsule loading capability of fabrics.

According to this model, the number of structural knitted cells per unit area S_u (SKCs/cm²) was related to the length of yarn in a structural knitted cell L_u (cm) by the equation (Eq 1.11) as below:

$$S_u \times L_u^2 = 169.44 \quad (Eq 1.11)$$

Besides, as mentioned at section 2.3.4.1, the fabric porosity P (%) was calculated by the equation (Eq 2.9) as below:

$$P(\%) = 100 \times \left[1 - \frac{M_{fbr}}{t \times \rho} \right] \quad (Eq 2.9)$$

Basing on the assumption number 6 of the loop model, $t = 4.1 \times D$. Then it could be deduced from the equation (Eq 3.1) that:

$$t = \frac{L_u}{14.376} \quad (Eq 3.2)$$

On the other hand, the mass per area of fabric could be calculated by:

$$M_{fbr}(mg/mm^2) = \frac{2 \times P_s \times m_l}{100} \quad (Eq 3.3)$$

In which P_s (number of loops/cm²) is the area density of fabric and m_l (mg) is the weight of a knitted loop.

Because $P_s = 2 \times S_u$ (Eq 2.8), by the equation (Eq 1.11), it could be deduced as following:

$$P_s = \frac{338.88}{L_u^2} \quad (Eq 3.4)$$

The weight of a loop m_l (mg) is related to L_u (cm) by the following equation:

$$m_l = \frac{L_u}{40 \times Nm} \quad (Eq 3.5)$$

With Nm was yarn count.

According to equation (Eq 2.9) and equations (Eq 3.2)-(Eq 3.5), the relationship between fabric porosity P (%) and the length of yarn in a structural knitted cell L_u (cm) could be deduced as following:

$$P(\%) = 100 \times \left[1 - \frac{2435.8756}{L_u^2 \times Nm \times \rho} \right] \quad (Eq 3.6)$$

Therefore, when the loop length of interlock fabric increased:

- According to the equation (Eq 1.11) the fabric density decreased.
- According to the equation (Eq 3.6) the fabric porosity increased.

The decrease in the fabric density as well as the increase of the fabric porosity helped more microcapsules to locate at the inner structure of the fabric, resulting in higher microcapsule loading capability of the fabric.

The significant area density decrease as well as the slightly porosity increase observed with the increase of the loop length of the interlock fabrics (Figure 3.28, Figure 3.29) confirm the suitability of the experimental results to the loop model proposed by Dabiryan-Jeddi [27]

When the loop length increased in order of 2.81, 2.83, 2.87, 2.96 and 3.05 mm, the wale density decreased slightly in order of 153, 152, 150, 148 and 146 (wales/10 cm), while the course density decreased more rapidly in order of 193, 188, 186, 178 and 170 (courses/10 cm), resulting in the significant decrease of the area density over the order of 295, 286, 279, 263 and 247 (loops/cm²). Therefore, when the loop length increased by 8.5% from 2.81 to 3.05 (mm), the area density decreased by 16.6% from 295 to 247 (loops/cm²) (Figure 3.28).

When the loop length increased, the fabric porosity tended to slightly increase. In detail, when the loop length increased by 8.5% from 2.81 to 3.05 mm, the fabric porosity increased only by 2% from 81.0% (corresponding to loop length of 2.81 and 2.83 mm) to 82.6% (corresponding to loop length of 3.05 mm) (Figure 3.29).

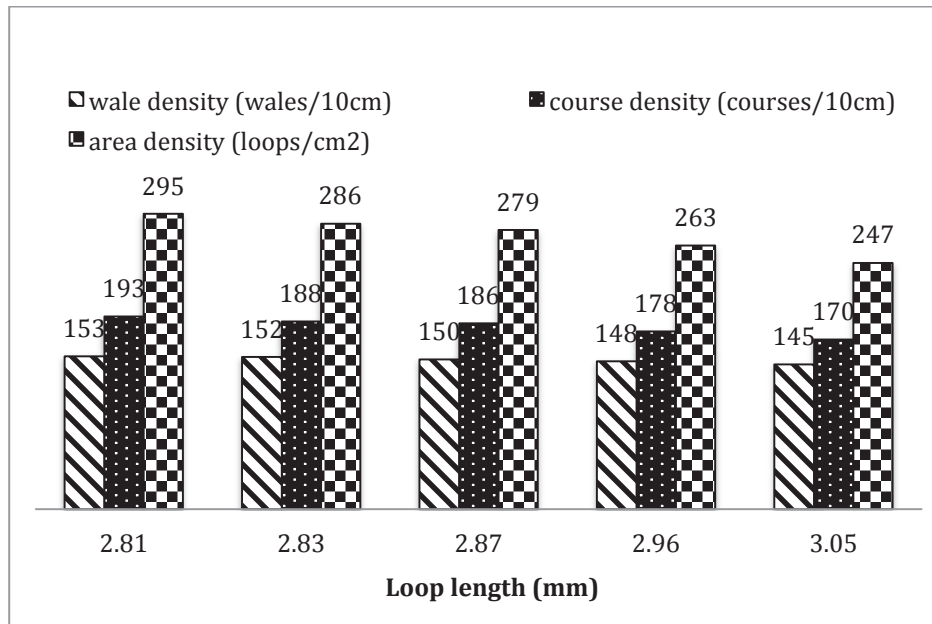


Figure 3.28: Fabric density according to the loop length

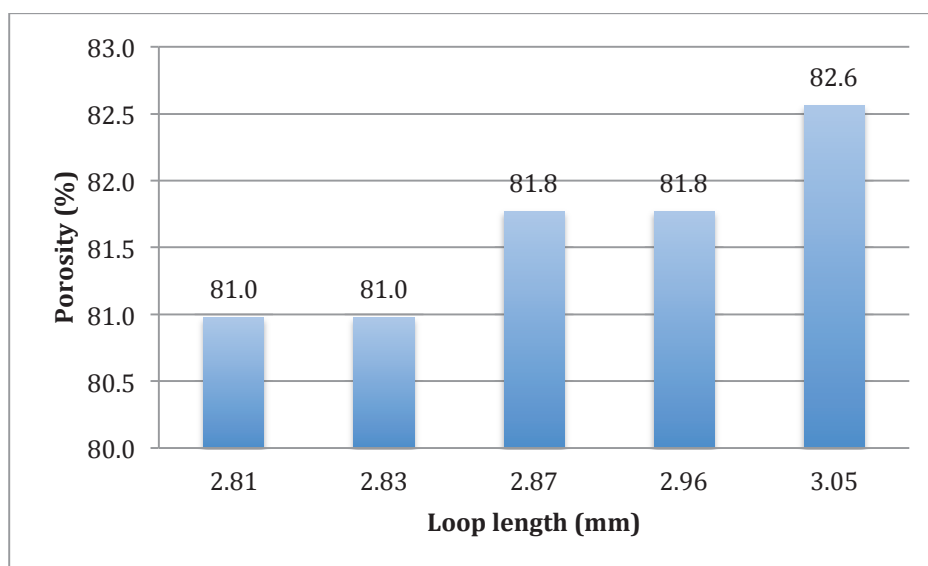


Figure 3.29: Fabric porosity according to the loop length

We previously suggested that the loop length increase should favour the deposit of the microcapsules inside the fabric structure. In order to check this hypothesis, the lower side of the microcapsule-coated fabric B1 (having the lowest loop length of 2.81 mm) and B5 (having the highest loop length of 3.05 mm) was observed by scanning electron microscopy. Five different areas corresponding to $318 \times 424 \mu\text{m}$ were observed for each fabric sample.

13 microcapsules having very small size (below $5 \mu\text{m}$) and 60 microcapsules with diameter higher than $10 \mu\text{m}$ were observed on the lower surface of B1 (Figure 3.30A) and B5 (Figure 3.30B) fabrics respectively. These observations confirm that a high loop length value favours the deposit of microcapsules inside the fabric and hence induces the increase of the microcapsule loading capability of the fabric.

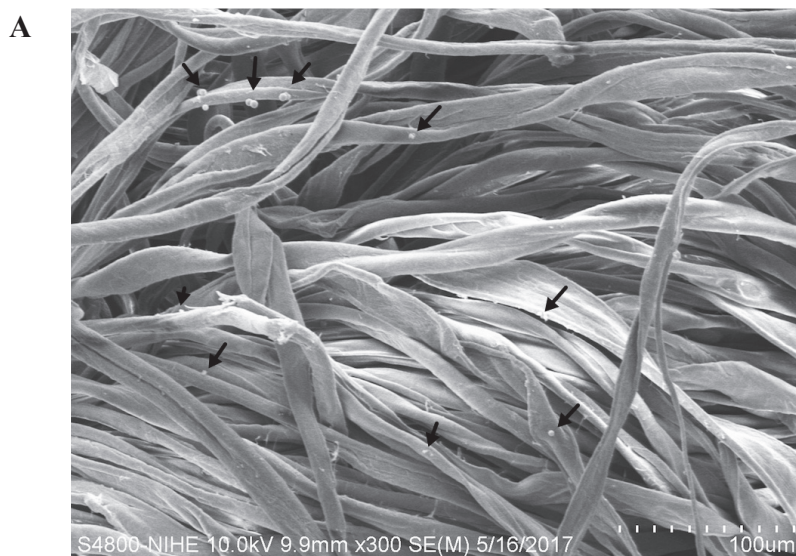




Figure 3.30: SEM images of the lower surface of the fabrics B1 (A) and B5 (B)

—→: microcapsules

2. Application of the microcapsules by the impregnating technique

The impregnating technique was used to apply microcapsules to the B3, B4 and B5 fabric lots with the microcapsule concentration of 20 (mg/ml). Triplicated experiments were carried out for each lot of fabric. The results of microcapsule loading capability were presented at Table 3.15.

Table 3.15: Microcapsule loading capability of the fabrics according to the loop length with a microcapsule concentration of 20 mg/ml

Fabric lot (loop length)	Fabric sample	Weight of sample before finishing (mg)	Weight of sample after finishing (mg)	Microcapsule loading capability MLC (%)	
				For each sample	Average
B3 (2.87 mm)	1	0.540	0.711	31.67	31.8 ± 1.4
	2	0.545	0.711	30.46	
	3	0.540	0.720	33.33	
B4 (2.96 mm)	1	0.509	0.662	30.06	31.8 ± 1.6
	2	0.512	0.678	32.42	
	3	0.506	0.673	33.00	
B5 (3.05 mm)	1	0.489	0.653	33.54	32.2 ± 1.4
	2	0.490	0.648	32.25	
	3	0.503	0.658	30.82	

As previously described for the study concerning the application of the microcapsules by the coating technique, the two independent samples t test was used to conclude about the influence of the loop length on the microcapsule loading capability of the fabrics. The results of sample t tests were reported at Table 3.16.

Table 3.16: Results of the t tests according to the loop length with a microcapsule concentration of 20 mg/ml

Comparison	B3 vs. B4	B4 vs. B5
Sample size	$n_1 = n_2 = 3$	$n_1 = n_2 = 3$
Null hypothesis H_0	$\mu_1 = \mu_2$	$\mu_1 = \mu_2$
Alternative hypothesis H_a	$\mu_1 < \mu_2$	$\mu_1 < \mu_2$
t - statistic	0.0054	0.3155
t_α	2.1318	2.1318
Conclusion	$\mu_1 = \mu_2$	$\mu_1 = \mu_2$

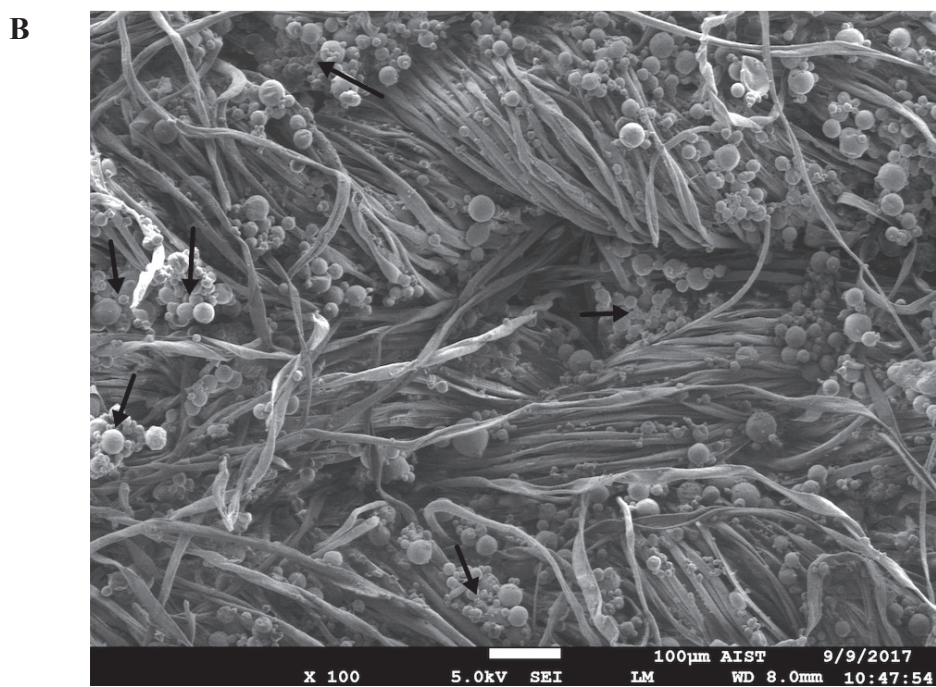
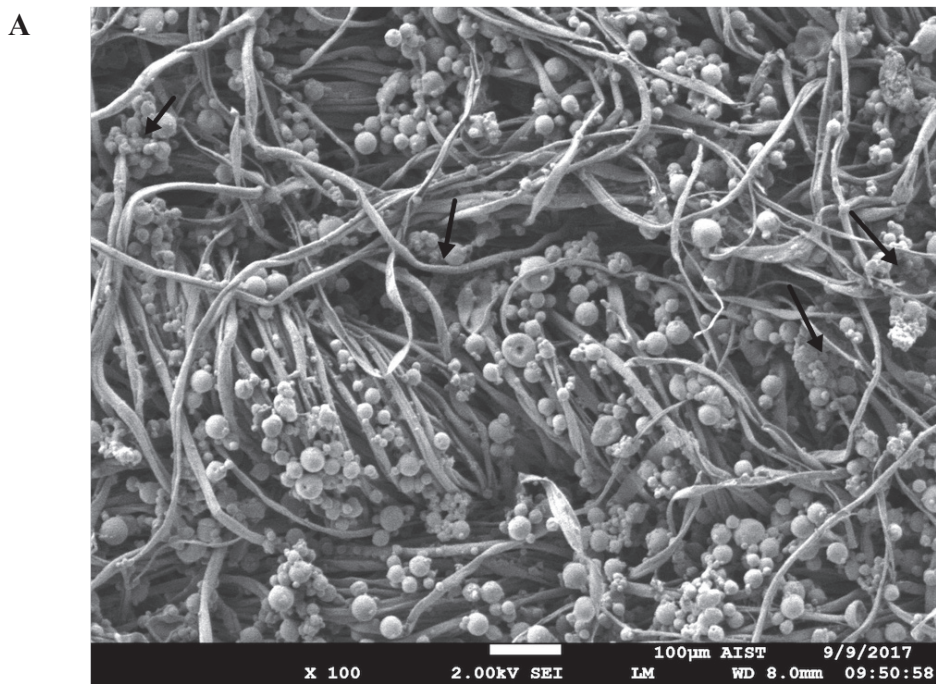
Contrarily to the results obtained in the case of application by the coating technique, the loop length of the interlock knitted fabric did not influence the microcapsule loading capability when the microcapsules were deposited by the impregnating technique.

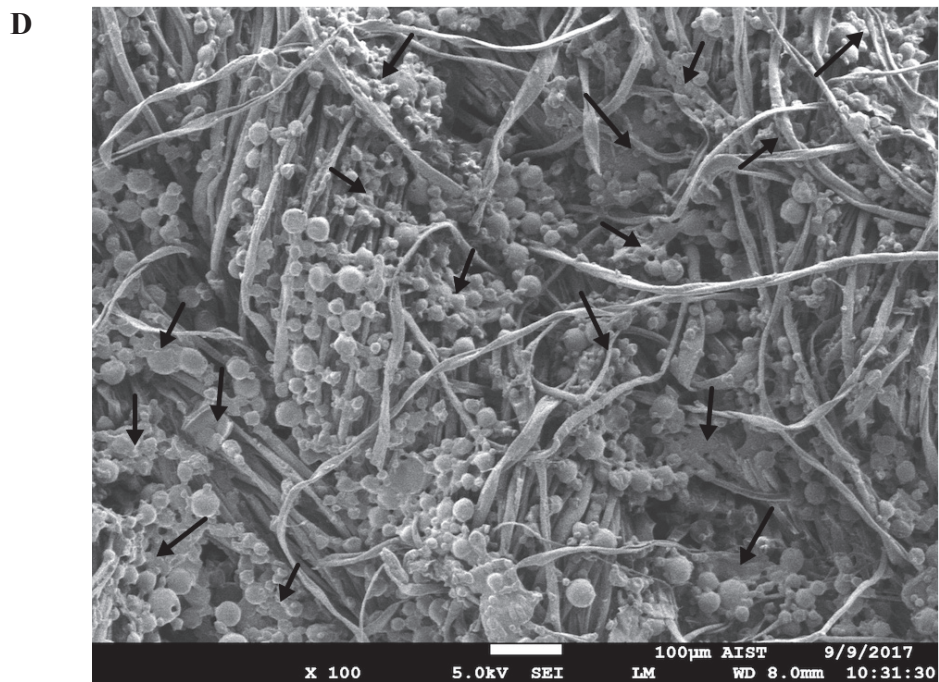
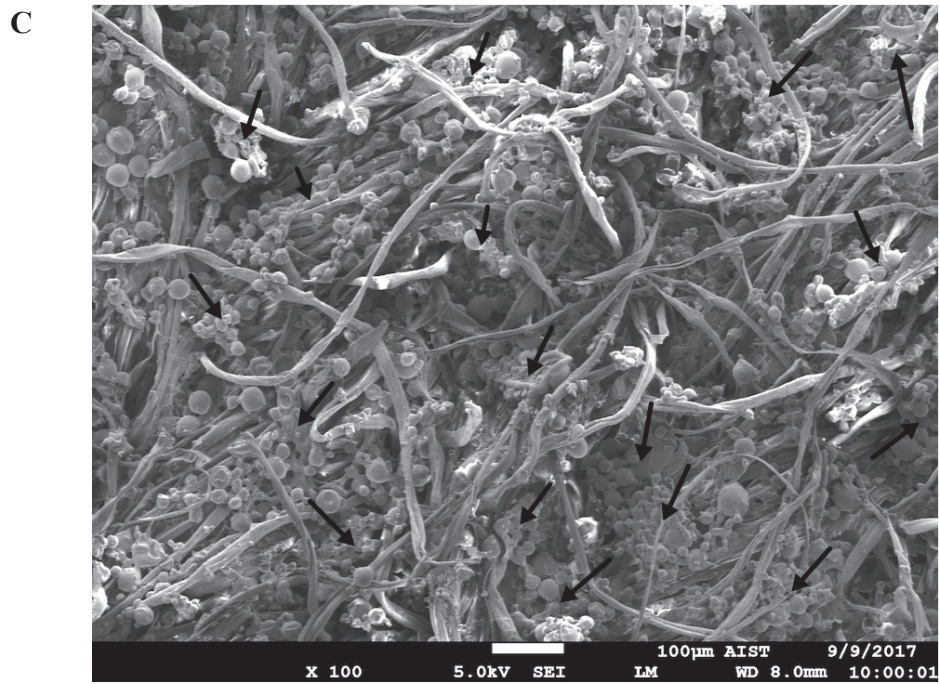
3.3.2.2. Influence on the microcapsule distribution

1. Application of the microcapsules by the coating technique

In order to evaluate the influence of the loop length on the microcapsule distribution in the case of the coating technique, the fabric samples coated with microcapsules at concentration of 14 (mg/ml) were analyzed by SEM and calculation based on the model of the knitted loop. The five fabric lots investigated were B1, B2, B3, B4 and B5 with the loop lengths of 2.81, 2.83, 2.87, 2.96 and 3.05 mm respectively.

The fabric samples finished with microcapsules by the coating technique were observed by scanning electron microscopy at magnification x100. All pictures pointed out individual and spherical microcapsules as well as some aggregates of many microcapsules bonded together and quite deformed (Figure 3.31).





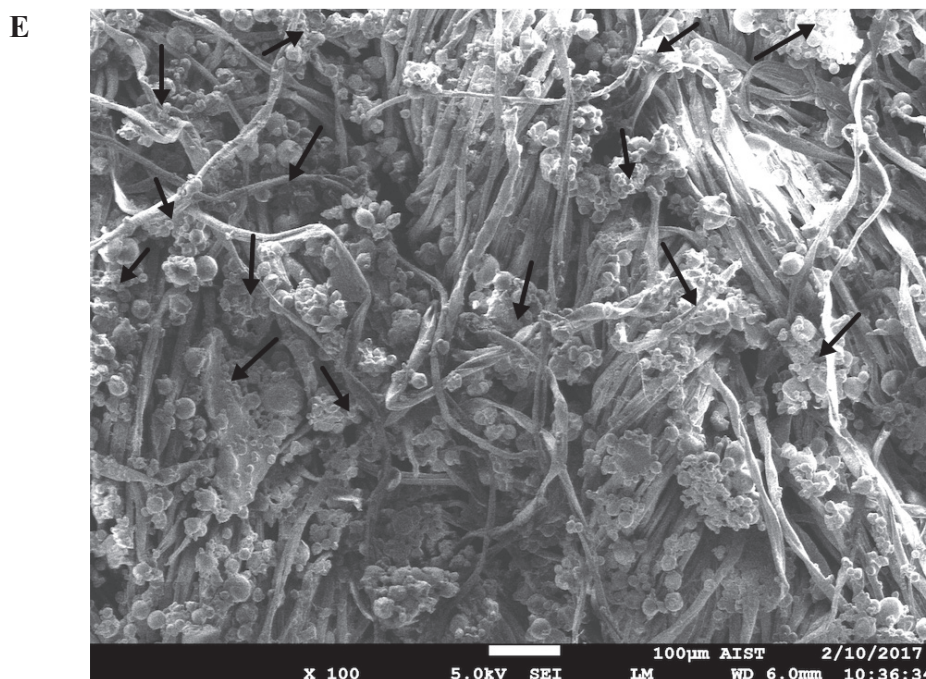


Figure 3.31: SEM images of the fabrics after microcapsule application by the coating technique B1 (A), B2 (B), B3 (C), B4 (D) and B5 (E)

→: microcapsule aggregates

As mentioned at section 3.3.1.2 and 3.3.1.3, the microcapsule aggregates are unwanted in textile applications since they lowered the active release capability of the fabric. The area of the microcapsule aggregates on SEM images was determined by the software Meander 3.1.2 of Peacock Media. Three different fabric areas with dimension of 840 x 1200 μm were analyzed. The statistical results on five fabric lots were presented at Table 3.17.

Table 3.17: Area of the microcapsule aggregates according to the loop length with a microcapsule concentration of 14 mg/ml

Fabric lot	Average area of microcapsule aggregates (μm^2)
B1	9439 \pm 2642
B2	7537 \pm 2110
B3	8600 \pm 2058
B4	13379 \pm 2806
B5	16020 \pm 3418

Statistical results in Table 3.17 indicated that both the average area and the standard deviation of microcapsule aggregates increased with the loop length increase.

The previous results pointed out that the microcapsule distribution became less even when the loop length increased. The microcapsule cover ratio K presented at section 2.3.4.3 and was defined as the ratio of total cross section area of all microcapsules S_{mc} to the total yarn surface area might be coated with microcapsules S_{yar} in a unit area of fabric, $K = \frac{S_{mc}}{S_{yar}}$, may help to explain the previous results. The higher value of K , the higher possibility of forming microcapsule aggregates on the fabric.

Hereinafter, we will calculate the values of S_{mc} and S_{yar} for the five fabric lots (from B1 to B5). Then the values of K will be deduced basing on the equation $K = \frac{S_{mc}}{S_{yar}}$

Calculation of S_{mc} (the total cross section area of all microcapsules in a unit area of fabric)

The total cross section area of all microcapsules in a unit area of fabric could be calculated as below:

$$S_{mc} = \frac{\pi}{4} \times \sum n_i \times d_i^2 \quad (Eq\ 3.7)$$

with n_i was the number of microcapsules having diameters of d_i coated to that fabric area.

On the other hand, the total volume of the microcapsule lot C0.075 could be calculated as below:

$$V_{lot} = V_{int} - V_{lost} + V_{hyd} \quad (Eq\ 3.8)$$

in which:

V_{lot} : the total volume of all microcapsules in the whole lot

V_{int} : the volume of initial components (ibuprofen, miglyol 812 and eudragit RSPO) in the dispersed phase

V_{lost} : the volume of initial components diffusing from the oil droplets to the aqueous phase during microencapsulation

V_{hyd} : the volume of solvent and water in the microcapsules because of the hydration (see section 3.1.3.3)

The volume of initial components in the dispersed phase V_{int} could be calculated as below:

$$V_{int} = V_{dis} - V_{sol} \quad (Eq\ 3.9)$$

with:

V_{dis} : the volume of the dispersed phase

V_{sol} : the volume of ethyl acetate used to prepare the dispersed phase

On the other hand:

$$\frac{V_{lost}}{V_{int}} = \frac{m_{lost}}{m_{int}} = \frac{m_{int} - m_{lot}}{m_{int}} \quad (Eq 3.10)$$

In the equation (Eq 3.10):

m_{lost} : the total weight of initial components diffusing from the oil droplets to the aqueous phase during microencapsulation

m_{int} : the total weight of initial components in the dispersed phase

m_{lot} : the total weight of the whole dried microcapsule lot

Besides, since the density of ethyl acetate is 0.9 g/ml that is approximate to the density of water (1 g/ml), the volume of solvent and water in the microcapsules V_{hyd} could be calculated approximately as below:

$$V_{hyd} = \frac{\text{the hydration} \times m_{lot}}{\text{the density of water}} \quad (Eq 3.11)$$

For the thesis, $V_{dis} = 17 (ml)$; $V_{sol} = 15 (ml)$; $m_{int} = 2375 (mg)$; $m_{lot} = 1250 (mg)$; and the hydration rate was 0.4.

According to equations (Eq 3.9)-(Eq 3.11), it could be calculated that $V_{hyd} = 0.5 (ml)$; $V_{int} = 2 (ml)$; $V_{lost} = 0.947 (ml)$.

Then according to equation (Eq 3.8), it could be calculated that $V_{lot} = 1.553 (ml)$. The number of microcapsules (n_i) having certain diameters (d_i) of the whole microcapsule lot and the size distribution of the microcapsule lot C0.075 were presented at Appendix 8 and Appendix 2 respectively.

Hereafter, according to the the total weight of the whole dried microcapsule lot m_{lot} , along with the content of microcapsules coated to a fabric area (mg/cm^2) (Table 3.18), the number of microcapsules (n_i) having certain diameters (d_i) in $1 cm^2$ of fabrics could be calculated and these results were presented at Appendix 9. Then the total cross section area of all microcapsules in $1 cm^2$ of fabrics S_{mc} was calculated according to equation (Eq 3.7), the results were summarized in Table 3.18:

Table 3.18: Total cross section area of all microcapsules per cm² of fabrics with coating technique

Fabric lot	B1	B2	B3	B4	B5
Loop length (mm)	2.81	2.83	2.87	2.96	3.05
Content of microcapsules coated to fabric (mg/cm ²)	1.682	1.728	1.725	1.794	1.826
Total cross section area of all microcapsules per cm ² of fabrics S _{mc} (μm ²)	209071344.2	214789109.8	214416212.1	222992860.6	226970436.7

Calculation of S_{var} (the total yarn surface area might be coated with microcapsules in a unit area of fabric)

The coating technique favours the deposition of the microcapsules mainly at the fabric upper surface instead of the lower one. The SEM images also showed that the number of microcapsules locating at the lower surface of the fabric was negligible in comparison to that at upper surface and inside the fabric. On the B5 fabric, for example, the microcapsules located so densely at the upper surface that they stuck together and formed big aggregates (Figure 3.31E), whereas there were only few microcapsules at the lower surface (Figure 3.30B).

The theoretical volume of the coating formulation in the different parts of the fabrics also confirms the negligible amount of the microcapsules at the fabric lower surface. When the microcapsules are applied on the fabric by the coating technique, the content of the microcapsules deposited on the fabric should be proportional to the total volume of the coating formulation retained by the fabric. If the microcapsule concentration in the coating formulation is N (mg/ml) and the total volume of the coating formulation retained by the fabric is V (ml), the amount of the microcapsules coated to the fabric, M (mg), would be as below:

$$M = N \times V \quad (Eq\ 3.12)$$

$$\Rightarrow V = \frac{M}{N} = \frac{MLC (\%) \times L \times B \times M_{fbr}}{100 \times N} \quad (Eq\ 3.13)$$

In the equation (Eq 3.13), MLC (%) is the fabric microcapsule loading capability, L (mm) is the length of the fabric sample, B (mm) is the width of the fabric sample and M_{fbr} (mg/mm^2) is the fabric mass per area.

The total volume of the coating formulation retained by the fabric V consists of three parts:

- The volume retained in the pores of the fabric, V_1 (ml)
- The volume retained on the fabric upper surface, laying between the fabric surface and the under side of coating blade, V_2 (ml)
- The volume retained at the fabric lower surface, V_3 (ml)

V_1 could be calculated as below:

$$V_1 = \frac{1}{1000} \times L \times B \times t \times \frac{P}{100} = \frac{1}{10^5} \times L \times B \times t \times P \quad (Eq 3.14)$$

With L (mm) is the length of the fabric sample, B (mm) is the width of the fabric sample, t (mm) is the fabric thickness and P (%) is the fabric porosity.

V_2 could be calculated as below:

$$V_2 = \frac{1}{1000} \times L \times B \times \theta \quad (Eq 3.15)$$

with θ (mm) was the coating thickness.

In the thesis, L = 200 (mm); B = 200 (mm); $\theta = 0.5$ (mm); N = 14 (mg/ml), then the calculated values of V, V_1 , V_2 and V_3 were as presented at Table 3.19:

Table 3.19: Calculated values of V, V_1 , V_2 and V_3

Fabric lot	B1	B2	B3	B4	B5
V (ml)	31.24	32.09	32.04	33.32	33.91
V_1 (ml)	17.91	17.89	18.04	18.02	18.17
V_2 (ml)	13.00	13.00	13.00	13.00	13.00
V_3 (ml)	0.33	1.20	0.99	2.30	2.74

The data in Table 3.19 showed that the coating formulation was mostly kept in the pores of the fabric (V_1 made up 54÷57% of V) and on the fabric upper surface (V_2 made up 38÷42% of V), while the volume of the coating formulation retained at the fabric lower surfaces was negligible (V_3 made up only 1÷8% of V).

Since the microcapsules mostly located on the upper side and inside the fabrics, the area of the yarn surface might be coated with microcapsules could be calculated as below:

$$S_{yar/skc} = S_{\Sigma/skc} - S_{ls/skc} \quad (Eq 3.16)$$

In which:

$S_{yar/skc}$: area of the the yarn surface might be coated with microcapsules in a structural knitted cell.

$S_{\Sigma/skc}$: total area of the yarn surface in a structural knitted cell.

$S_{ls/skc}$: area of the yarn surface at the fabric lower surface in a structural knitted cell.

The total area of yarn surface in a structural knitted cell could be calculated by:

$$S_{\Sigma/skc} = L_u \times \pi \times D \quad (Eq\ 3.17)$$

with L_u is the length of yarn in a structural knitted cell and D is the yarn diameter. According to the loop model of Dabiryan-Jeddi [27]:

$$L_u = 58.942 \times D \quad (Eq\ 3.18)$$

$$\rightarrow S_{\Sigma/skc} = \frac{L_u^2}{18.771} \quad (Eq\ 3.19)$$

The area of the yarn surface at the fabric lower side in a structural knitted cell could be calculated by:

$$S_{ls/skc} = L_{plain} \times \pi \times D \quad (Eq\ 3.20)$$

in which L_{plain} based on the loop model of Dabiryan-Jeddi [27] is:

$$L_{plain} = \frac{L_u}{5.389} \quad (Eq\ 3.21)$$

$$\rightarrow S_{ls/skc} = \frac{L_u^2}{101.158} \quad (Eq\ 3.22)$$

The area of the yarn surface might be coated with microcapsules in a structural knitted cell $S_{yar/skc}$ could be deduced from the equations (Eq 3.16), (Eq 3.19) and (Eq 3.22). After that, the area of the yarn surface might be coated with microcapsules per cm^2 of fabric S_{yar} could be deduced from $S_{yar/skc}$ and the number of the structural knitted cells in per cm^2 of fabric S_u . The results of S_{yar} for the five fabric lots were presented at Table 3.20.

Table 3.20: Area of the yarn surface might be coated with the microcapsules per cm^2 of the fabrics

Fabric lot	B1	B2	B3	B4	B5
Total area of yarn surface in a SKC $S_{\Sigma/skc}(\mu\text{m}^2)$	3538533.2	3580173.2	3670929.6	3795951.5	3958644.6
Area of yarn surface at lower side in a SKC $S_{ls/skc}(\mu\text{m}^2)$	277495.5	281449.6	289613.1	306342.9	324420.8
Area of yarn surface might be coated with microcapsules in a SKC $S_{yar/skc}(\mu\text{m}^2)$	3261037.7	3298723.6	3381316.5	3489608.6	3634223.8
Area of yarn surface might be coated with microcapsules per cm^2 of fabric $S_{yar}(\mu\text{m}^2)$	463317530.6	453529472.1	453331869.7	441829701.3	430297751.9

Calculation of the microcapsule cover ratio K

The microcapsule cover ratio K was calculated by the equation $K = \frac{S_{mc}}{S_{yar}}$ with the value of S_{mc} was presented at Table 3.18 and the value of S_{yar} was presented at Table 3.20. The calculated results of K were presented at Table 3.21.

Table 3.21: Value of K according to the loop length with a microcapsule concentration of 14 mg/ml

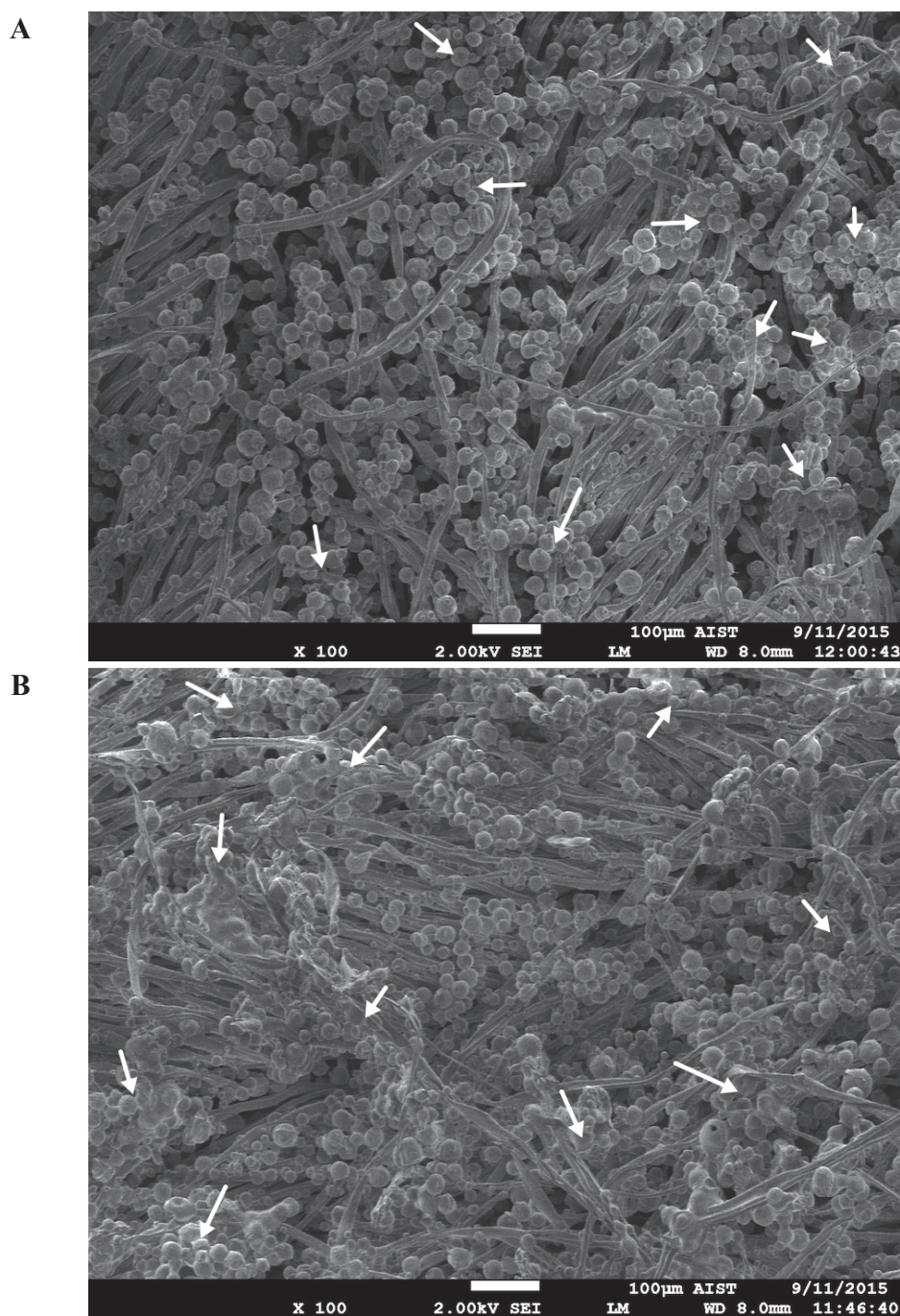
Fabric lot	B1	B2	B3	B4	B5
Loop length (mm)	2.81	2.83	2.87	2.96	3.05
Microcapsule cover ratio K	0.42	0.44	0.44	0.47	0.49

The results at Table 3.21 indicated that the microcapsule cover ratio K increased when the loop length increased. The increase in loop length induced a denser microcapsule distribution on the fabric, favouring the microcapsule aggregation. Therefore, these results helped to explain the trend of the microcapsule distribution observed by SEM.

2. Application of the microcapsules by the impregnating technique

The influence of the loop length on the microcapsule distribution when the microcapsules were applied on the fabrics by impregnating was investigated on the three fabric lots B3, B4 and B5 with the loop lengths of 2.87, 2.96 and 3.05 mm respectively.

As in the case of coating technique, the fabric samples finished by microcapsule impregnating were observed by scanning electron microscopy. Some microcapsule aggregates were observed on the surface of all fabric samples (Figure 3.32).



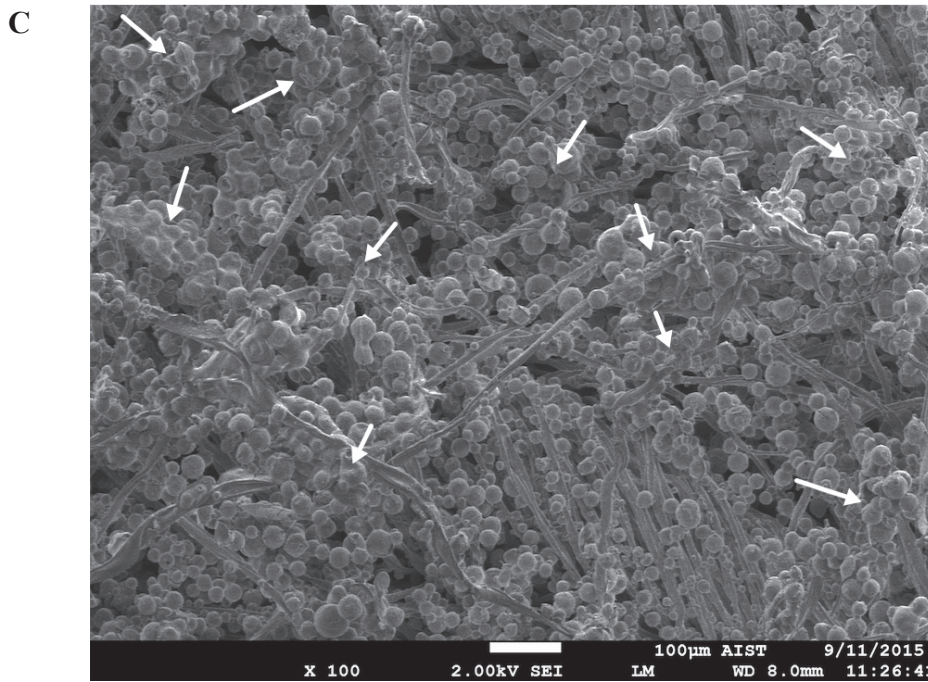


Figure 3.32: SEM images of the fabrics after microcapsule application by the impregnating technique: B3 (A), B4 (B) and B5 (C)

➡: microcapsule aggregates

For each fabric lot, the images of three different areas on the surface of the microcapsule-treated sample were captured under the magnification x100, and the area of the microcapsule aggregates in SEM images was determined by the software Meander 3.1.2. The statistical results were presented at Table 3.22.

Table 3.22: Area of the microcapsule aggregates according to the loop length with a microcapsule concentration of 20 mg/ml

Fabric lot	Average area of microcapsule aggregates (μm^2)
B3	30522 \pm 5640
B4	32562 \pm 6208
B5	44228 \pm 7350

The results in Table 3.22 showed that both the average area and the standard deviation of the microcapsule aggregates increased when the loop length increased, indicating a less even microcapsule distribution. This trend was similar to the case of the coating technique.

Similarly to the case of the coating technique, the microcapsule cover ratio K was calculated by the equation $K = \frac{S_{mc}}{S_{yar}}$. By the same calculations, the values of S_{mc} (the total cross section area of microcapsules per cm^2 of fabric) were found as presented at Table 3.23.

Table 3.23: Total cross section area of all microcapsules in an unit area of the fabrics when the microcapsule concentration impregnated to the fabrics was equal to 20 (mg/ml)

Fabric lot	B3	B4	B5
Loop length (mm)	2.87	2.96	3.05
Content of microcapsules on fabric (mg/cm ²)	5.874	5.874	5.803
Total cross section area of microcapsules per cm ² of fabrics S _{mc} (μm ²)	730133616.2	730133616.2	721308371.6

The values of S_{yar} (the area of the yarn surface might be coated with microcapsules per cm² of fabric) are equal to those in the case of the coating technique (Table 3.20) because by the impregnating technique, the microcapsules also mostly locate on the upper surface and inside the fabric. Therefore, the values of K were found as presented at Table 3.24.

Table 3.24: Value of K according to the loop length with a microcapsule concentration of 20 mg/ml

Fabric lot	B3	B4	B5
Loop length (mm)	2.87	2.96	3.05
Microcapsule cover ratio K	1.61	1.65	1.68

The results in Table 3.24 showed that the microcapsule cover ratio K increased when the loop length increased, which was in good agreement with the results of the image analysis and was similar to the case of the coating technique.

3.3.2.3. Influence on the ibuprofen release capability of the fabric

In order to evaluate the influence of the loop length on the ibuprofen release capability of the fabrics, *in vitro* experiments (described at section 2.3.4.3) were carried out on the three fabric lots B3, B4 and B5 with the loop lengths of 2.87, 2.96 and 3.05 mm respectively. The weight percentage of ibuprofen released into the receptor fluid after 24 hours Ibu_{rl} (%) was reported at Table 3.25 (the procedure of calculating was described at Appendix 10).

Table 3.25: Weight percentage of ibuprofen on the microcapsule-treated fabrics (by impregnating) released into the receptor fluid after 24 hours

Fabric lot	B3	B4	B5
Loop length (mm)	2.87	2.96	3.05
Ibu_{rl} (%)	5.43	5.68	2.06

The weight percentage of ibuprofen dissolved into the receptor fluid from the B3 fabric (5.43%) was almost equal to that from the B4 fabric (5.68%) and was more than twice as high as that from the B5 fabric (2.06%). Because the average area of the microcapsule aggregates on the B4 fabric was almost equal to that on the B3 fabric, the release rate of ibuprofen was similar for these two fabrics. The average area of the microcapsule aggregates on the B5 fabric was 1.45 times as big as that on the B3 fabric and was 1.36 times as big as that on the B4 fabric, so the release rate of ibuprofen from the B5 fabric was significantly lower than that from the B3 and B4 fabrics. Consequently, within the scope of investigation, the active release capability of the interlock fabric really depended on the loop length. When the loop length increased, the area of the microcapsule aggregates on the fabric increased, resulting in a lower release rate of ibuprofen from the fabric.

Moreover, the content of ibuprofen on the microcapsule-treated fabric released into the receptor fluid after 24 hours was in range of $0.0085 \div 0.0237$ (mg/cm²) (Appendix Table 5 at Appendix 10). The ibuprofen permeation amount of the commercial patch TEPI Patch Ibuprofen manufactured by Medherant (England), used to treat common painful conditions like chronic back pain, neuralgia and arthritis is reported to be $0.01 \div 0.1$ (mg/cm²) after 24 hours [150]. Therefore, within the scope of investigation, the B3 and B4 fabrics impregnated with the C0.075 microcapsules with a concentration of 20 mg/ml could meet the requirement for the dose of a medical patch containing ibuprofen used in transdermal treatment to relieve pain and arthritis.

3.3.2.4. Conclusion

Within the scope of investigations, the loop length of the interlock knitted fabrics significantly influences the microcapsule loading capability, the microcapsule distribution and the active release capability of the microcapsule-treated fabrics.

When microcapsules were applied to fabrics by the coating technique, the increase in the loop length induced the fabric porosity increase as well as a fabric quite density decrease, resulting in a higher microcapsule loading capability of the fabrics. The microcapsule loading capability was proportional to the loop length for two levels of microcapsule concentration used to finish the fabrics. Besides, the image analysis performed on SEM pictures showed that the microcapsule distribution on the fabric became less even when the loop length increased. That was confirmed by the increase of the average area and the standard deviation of the microcapsule aggregates on the fabric. The microcapsule cover ratio K , calculated according to the interlock knitted loop model proposed by Dabiryani-Jeddi, also increased when the loop length increased, indicating that microcapsules located on the fabric were more bonded together.

When the microcapsules were applied to the fabrics by the impregnating technique, the loop length did not affect the microcapsule loading capability but really affected the microcapsule distribution with the same trend in the case of the coating technique. Both the

results of the image analysis and the calculated microcapsule cover ratio K indicated that the microcapsule distribution became less even when the loop length increased. Due to the less even distribution of microcapsules, the release rate of ibuprofen from the microcapsule-treated fabric decreased when the loop length increased. Specifically, the average area of the microcapsule aggregates on the B3 and B4 fabrics were almost equal, leading to a similar weight percentage of ibuprofen released into the receptor fluid (5.43% from the B3 fabric and 5.68 % from the B4 fabric). The average area of the microcapsule aggregates on the B5 fabric was higher than that on the B4 fabric (1.36 times) and on the B3 fabric (1.45 times), inducing a significantly lower ibuprofen release rate from the B5 fabric than that from the B3 and B4 fabrics. The weight percentage of ibuprofen released into the receptor fluid after 24 hours from the B5 fabric was only 2.06%. Besides, the results showed that the B3 and B4 fabrics impregnated with the C0.075 microcapsules at the concentration of 20 mg/ml could meet the dose requirement of a medical patch containing ibuprofen used for the transdermal treatment of pain and arthritis relief.

3.3.3. Influence of the fabric extension

In order to deposit the elaborated microcapsules on the medical compressive bandages, the influence of the fabric extension on the active release capability of the microcapsule-treated fabric was investigated. The *in vitro* experiments to evaluate the active release capability of the fabric were described at section 2.3.4.4. The fabric extension was investigated for three values: 0% (sample E3), 33% (sample E2) and 60% (sample E1). The procedure of calculating the weight percentage of ibuprofen released into the receptor fluid $Ibu_{rl}(\%)$ was described at Appendix 11.

The results revealed that ibuprofen could be released successfully from the microcapsule-treated fabrics through the abdominal pigskin, and the transdermal release really depended on the fabric extension. When the fabric extension increased from 0% to 33%, the transdermal ibuprofen release capability increased from 35.76% to 38.87%. And when the fabric extension increased from 33 % to 60 %, the ibuprofen release increased from 38.87% to 44.78% (Table 3.26, Figure 3.33).

Table 3.26: Weight percentage of ibuprofen in the microcapsule-treated fabrics released into the receptor fluid Ibu_{rl} according to the fabric extension

Fabric sample	E1	E2	E3
Sample diameter (cm)	5	6	8
$Ibu_{rl}(\%)$	44.78	38.87	35.76

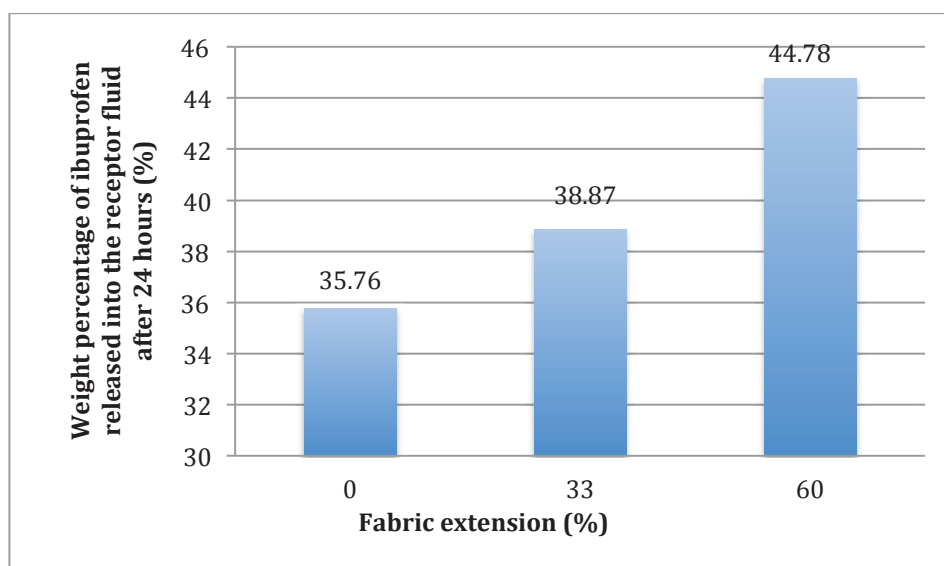


Figure 3.33: Weight percentage of ibuprofen released into the receptor fluid according to the fabric extension

The increase of the ibuprofen release rate by the increase of the fabric extension could be explained by two reasons:

- Firstly, when the fabric extension increased, the pressure that the fabric exerted on the pigskin also increased, maybe the microcapsules on the fabric were pressed more strongly, resulting in the faster release of ibuprofen.
- Secondly, when the fabric extension increased, the microcapsule content per fabric area decreased (Table 3.27). So with the same conditions of release (the volume, the pH and the temperature of the receptor fluid; the area and the thickness of the pigskin), the dissolution rate of ibuprofen would increase, resulting in its faster release.

Table 3.27: Content of the microcapsules per cm^2 of the fabrics according to the fabric extension

Fabric extension (%)	Area of elongated samples (cm^2)	Content of microcapsules on the sample M_{FI} (mg)*	Content of microcapsules per cm^2 of fabric (mg/cm^2)
0	12.56	185.43	14.76
33	9.42	104.30	11.07
60	7.85	72.43	9.22

(*): The calculation of M_{FI} was presented at Appendix 11

3.4. Conclusion of Chapter 3

1. In this chapter, the ibuprofen containing microcapsules were elaborated successfully with the uses of environment-friendly materials, suitable for textile application:
 - The eudragit RSPO microcapsules containing ibuprofen were prepared by the solvent evaporation method, using the non-halogenated solvent ethyl acetate and the bio-sourced surfactant quillaja saponin.
 - For the application in textiles, the requirements for the size and the size distribution of the microcapsules were considered as the most important ones. According to the determination of the distances between the fibers in the fabric substrate (the interlock cotton fabric with the loop length of 2.87 mm), along with the overview researches, the appropriate size of the microcapsules was proposed to be in range of 5÷60 μm .
 - Some surface active properties of quillaja saponin S4521 (Sigma-Aldrich) were evaluated. The cmc value of quillaja saponin was 0.05 wt%, the maximum surface density $\Gamma = 1356 \text{ (nmol/m}^2\text{)}$ and the interfacial area occupied by one saponin molecule $A = 121 \text{ \AA}^2$.
 - The influences of some microencapsulation parameters on the microcapsule characteristics were investigated:
 - o Influence of the saponin concentration: saponin concentration was varied with four levels of 0.025, 0.05, 0.075 and 0.1 wt%. The average diameter of the microcapsules decreased when saponin concentration increased. Especially, the $d(0.5)$ diameter of the microcapsules decreased strongly from 34.3 to 23.2 μm when the saponin concentration increased from 0.025 to 0.05 wt%. Above 0.05 wt%, the increase of the saponin concentration had no significant effect on the microcapsule size, and the volume ratio of the microcapsules having diameter in range of 5÷60 μm was higher than 80%. Besides, the size distribution became broader, with span values varying from 3.0 to 3.9 when the saponin concentration increased from 0.075 to 0.1 wt%. The optical microscope images revealed a number of irregular microparticles (with elliptical or rod shapes) in all four microcapsule lots. The broad size distribution of microcapsules and the irregular microparticles may arise from the high solubility of ethyl acetate in water combined with the high stirring rate during emulsification.
 - o Influence of the stirring rate: with the objective of reducing the number of irregular microparticles, the stirring rate was decreased gradually from 700 to 600 rpm. The decrease of the stirring rate did not help to reduce the number of the irregular microparticles but increased the microcapsule diameter and broadened the size distribution. Therefore, the stirring rate of 700 rpm was used for the further investigations.

- Influence of the ethyl acetate volume added to the continuous phase before the emulsification step: the addition of ethyl acetate to the continuous phase before emulsification quite reduced the number of the irregular microparticles. In addition, when 8 ml of ethyl acetate was added to the continuous phase, the d(0.5) diameter of the microcapsules increased slightly from 21.5 to 29.5 μm and the size distribution became quite narrower with the span value decreasing from 3.0 to 1.3, so the problems of the microcapsule shape and size were solved. Then the addition of ethyl acetate in the continuous phase before the emulsification step allowed solve the problems of the microcapsule shape and size. However, it significantly increased the microcapsule hydration rate, resulting in the strong deformation of the microcapsules during the drying process.
 - According to the above results, the C0.075 microcapsule lot (with saponin concentration of 0.075 wt%, stirring rate of 700 rpm, no addition of solvent to the aqueous phase) was considered as the most suitable one for the application on anti-inflammatory textile. Beside the shape and size, some other characteristics of this microcapsule lot were determined. The C0.075 microcapsules were in type of multiple-core, with the size of the cores was below 0.5 μm . The ibuprofen loading ratio was 7.1% and the microencapsulation efficiency was 71%. The content of the residual ethyl acetate in the dried microcapsules was 0.4 wt%, which was lower than the permitted value for the content of residual solvent in gauze bandage according to U.S. Pharmacopeia (0.5 wt%).
2. The elaborated microcapsules were successfully deposited on the interlock knitted fabrics with the suitable conditions of drying. The influences of the fabric structural parameters on the characteristics of the microcapsule-treated fabrics were revealed and the scientific basis of the influences was explained:
- Microcapsules were deposited on the fabrics by the coating and impregnating techniques. The finishing formulation was the dispersion of unwashed microcapsules in distilled water.
 - Within the scope of the research, the most suitable drying condition was the vacuum drying at 45°C.
 - Influence of the textile material: the investigations were carried out on three kinds of interlock fabrics knitted from cotton, peco 65/35 and polyester yarns, which often used for the medical textiles. Three kinds of yarns had the same count of Ne20; all fabrics were knitted, scoured and bleached under the same conditions. Except the textile material type, the other structural parameters (loop length and fabric density) of these three fabric lots were similar. Microcapsules were applied on the fabrics by impregnating. We observed that the textile material type had no

influence on the microcapsule loading capability but had significant effects on the microcapsule distribution and the active release capability of the fabrics. Microcapsule distribution was less even on the fabric knitted with higher content of cotton; the average area of the microcapsule aggregates on cotton, peco 65/35 and polyester fabrics were 78891, 49408 and 38850 (μm^2), respectively. This could be due to lower affinity of the microcapsules with the cotton fibers compared to the polyester fibers. Because of the less even distribution of the microcapsules on the fabrics, as well as the higher affinity of ibuprofen with the cotton fibers, the release rate of ibuprofen from the microcapsule-treated fabric decreased when the content ratio of cotton fibers in the fabric increased. After 8 hours of release at 32 ± 1 °C, the weight percentage of ibuprofen in the treated fabrics released into the receptor fluid increased in order of 37.3, 42.2 and 50.9% corresponding to cotton, peco 65/35 and polyester fabrics. Besides, the maximum weight ratio of ibuprofen released into the receptor fluid, which was reached after 24 hours, also increased in order of 50.8, 55.0 and 57.6% for cotton, peco 65/35 and polyester fabrics, respectively.

- Influence of the loop length: the influence of the loop length on the characteristics of the microcapsule-treated fabrics was investigated in the cases of two different finishing techniques.
 - o When microcapsules were deposited on the fabrics by the coating technique, the increase of the loop length induced the fabric porosity increase as well as the significant fabric density decrease, resulting in a higher microcapsule loading capability of the fabric. The microcapsule loading capability was in range of $7 \div 20\%$ and was proportional to the loop length for both levels of microcapsule concentration used to finish the fabrics. Besides, the image analysis performed on SEM pictures showed that the microcapsule distribution on fabric became less even when the loop length increased, in accordance with the increase of both the average area and the standard deviation of the microcapsule aggregates on the fabrics. The microcapsule cover ratio K , calculated according to the interlock knitted loop model proposed by Dabiryan-Jeddi, also increased when the loop length increased. The increase of the microcapsule cover ratio indicated that microcapsules located more closely on the fabrics, favouring the microcapsule aggregation as observed in SEM images.
 - o When microcapsules were applied to the fabrics by the impregnating technique, the loop length did not affect the microcapsule loading capability but really affected the microcapsule distribution with the same trend in the case of the coating technique. Both the results of image analysis and the calculations of the microcapsule cover ratio K indicated that the microcapsule distribution became less even when the loop length increased. Due to the less even distribution of the microcapsules, the

release rate of ibuprofen from the microcapsule-treated fabric decreased when the loop length increased. The weight percentage of ibuprofen released into the receptor fluid was 5.43, 5.68 and 2.06% for the loop length of 2.87, 2.96 and 3.05 mm, respectively. Moreover, the results showed that the microcapsule-treated fabrics could reach the dose requirement of a commercial medical patch containing ibuprofen used for the transdermal treatment of pain and arthritis relief.

- Influence of the fabric extension: the increase of the fabric extension helped to significantly increase the release of ibuprofen from the microcapsule-treated fabrics through the pigskin. After 24 hours of release, the content of ibuprofen in the receptor fluid made up 35.8, 38.9 and 44.8% of the ibuprofen content of the fabrics, corresponding to the fabric extensions of 0, 33 and 60%.

4. Final conclusions and future outlook

4.1. Final conclusions

1. The ibuprofen-loaded microcapsules suitable for the textile application have been successfully elaborated by the solvent evaporation technique, using the bio-sourced surfactant quillaja saponin (S4521 from Sigma Aldrich) and the non-halogenated solvent ethyl acetate. The microencapsulation parameters are chosen basing on the cmc value of saponin. The microcapsules exhibit the spherical shapes with the $d(0.5)$ diameter of 21.5 μm . The microencapsulation efficiency is 71%. The content of residual ethyl acetate in the dried microcapsules is 0.4 wt%, smaller than the permitted value for the content of residual solvent in gauze bandage according to U.S. Pharmacopeia USP 29.
2. In the finishing of the cotton interlock knitted fabrics with the microcapsules, in order to keep the microcapsules from deformation, the drying stage should be carried out in vacuum at 45°C.
3. Within the scope of research, when the microcapsules are applied to the cotton interlock knitted fabrics (with the loop length varies from 2.81 to 3.05 mm) by the coating technique, the microcapsule loading capability of the fabric is in the range of 7 ÷ 20% and is proportional to the loop length.
4. The microcapsule distribution on the interlock knitted fabric depends on both the textile material and the loop length. At the same loop length of 3.75 ± 0.03 mm, the microcapsule distribution is less even on the fabric knitted with higher content of cotton. And in the cotton interlock knitted fabrics with loop length ranging from 2.81 to 3.05 mm, the microcapsule distribution becomes less even due to the lower value of the microcapsule cover ratio K when the loop length increases.
5. The release rate of ibuprofen from microcapsule-treated interlock fabrics depends on both the textile material and the loop length. The weight percentage of ibuprofen released into the receptor fluid after 8 hours from cotton, peco 65/35 and polyester fabrics (with the same loop length of 3.75 ± 3 mm) are 37.3, 42.2 and 50.9%, respectively. And from the cotton interlock knitted fabrics with loop length ranging from 2.87 to 3.05 mm, the weight percentage of ibuprofen released into the receptor fluid after 8 hours ranges from 2.06 to 5.68% and tends to decrease with the higher value of loop length.
6. The increase of the fabric extension helped to significantly increase the release of ibuprofen from the microcapsule-treated fabrics through the pigskin. After 24 hours of

release, the content of ibuprofen in the receptor fluid was equal to 35.76, 38.87 and 44.78% of the ibuprofen content on the fabrics, according to the fabric extensions of 0, 33 and 60%.

4.2. Future outlook

In order to contribute more to the growth of the medical textiles using microcapsules, the research in the thesis should be continued along the following issues:

1. Higher quality of the microcapsules, such as a narrower size distribution and a higher microencapsulation efficiency.
2. More even microcapsule distribution on the fabrics (less and smaller microcapsule aggregates on the fabrics).
3. Microencapsulation of other kinds of active ingredients for the application in the medical textiles.

REFERENCES

References in Vietnamese

[1] H. V. Trí (2003) *Công nghệ dệt kim đan ngang*. NXB Đại học Quốc gia TP HCM.

References in English

[2] M. B. Abdelkader, N. Azizi, M. Chemli, Y. Chevalier, O. Boyron, M. Majdoub (2016), *Synthesis and emulsifier properties of a new bio-sourced surfactant based on isosorbide*. Colloids and Surfaces A: Physicochemical and Engineering Aspects, 492.Supplement C, pp. 1-11.

[3] S. Abdolmaleki, A. A. A. Jeddi, M. Amani (2012), *Estimation on the 3D porosity of plain knitted fabric under uniaxial extension*. Fibers and Polymers, 13.4, pp. 535-541.

[4] M. Agach, S. Delbaere, S. Marinkovic, B. Estrine, V. Nardello-Rataj (2013), *Synthesis, characterization, biodegradability and surfactant properties of bio-sourced lauroyl poly(glycerol-succinate) oligoesters*. Colloids and Surfaces A: Physicochemical and Engineering Aspects, 419.Supplement C, pp. 263-273.

[5] D. Alonso, M. Gimeno, J. D. Sepúlveda-Sánchez, K. Shirai (2010), *Chitosan-based microcapsules containing grapefruit seed extract grafted onto cellulose fibers by a non-toxic procedure*. Carbohydrate Research, 345.6, pp. 854-859.

[6] U. Angel, C. M. Silva, A. Cavaco-Paulo, A. Gedanken (2010), *Attaching Different Kinds of Proteinaceous Nanospheres to a Variety of Fabrics Using Ultrasound Radiation*. Israel Journal of Chemistry, 50.4, pp. 524-529.

[7] A. S. Apu, A. H. Pathan, D. Shrestha, G. Kibria, R.-u. Jalil (2009), *Investigation of In vitro release kinetics of Carbamazepine from Eudragit RSPO and RLPO Matrix Tablets*. TRopical Journal of Phamarceutical Research, 8.2, pp. 145-152.

[8] M. R. Avadi, A. M. M. Sadeghi, N. Mohammadpour, S. Abedin, F. Atyabi, R. Dinarvand, M. Rafiee-Tehrani (2010), *Preparation and characterization of insulin nanoparticles using chitosan and Arabic gum with ionic gelation method*. Nanomedicine: Nanotechnology, Biology and Medicine, 6.1, pp. 58-63.

[9] N. Azizi, Y. Chevalier, M. Majdoub (2014), *Isosorbide-based microcapsules for cosmeo-textiles*. Industrial Crops and Products, 52 pp. 150-157.

[10] S. Benltoufa, F. Fayala, M. Cheikhrouhou, S. B. Nasrallah (2007), *Porosity determination of Jersey structure*. AUTEK Research Journal, 7.1, pp. 63-69.

[11] D. Benmoussa, K. Molnar, H. Hannache, O. Cherkaoui (2016), *Novel Thermo-Regulating Comfort Textile Based on Poly(allyl ethylene diamine)/n-Hexadecane Microcapsules Grafted onto Cotton Fabric*. Advances in Polymer Technology, pp. n/a-n/a.

[12] A. Bhattacharya, P. Ray (2004), *Studies on surface tension of poly(vinyl alcohol): Effect of concentration, temperature, and addition of chaotropic agents*. Journal of Applied Polymer Science, 93.1, pp. 122-130.

[13] A. M. Borreguero, J. L. Valverde, J. F. Rodríguez, A. H. Barber, J. J. Cubillo, M. Carmona (2011), *Synthesis and characterization of microcapsules containing Rubitherm®RT27 obtained by spray drying*. Chemical Engineering Journal, 166.1, pp. 384-390.

-
- [14]R. Bushra, N. Aslam (2010), *An overview of clinical pharmacology of Ibuprofen*. Oman Med J, 25.3, pp. 155-1661.
- [15]C. Butstraen, F. Salatün (2014), *Preparation of microcapsules by complex coacervation of gum Arabic and chitosan*. Carbohydrate Polymers, 99 pp. 608-616.
- [16]F. Caballero, M. Foradada, M. Miñarro, P. Pérez-Lozano, E. García-Montoya, J. R. Ticó, J. M. Suñé-Negre (2014), *Characterization of alginate beads loaded with ibuprofen lysine salt and optimization of the preparation method*. International Journal of Pharmaceutics, 460.1–2, pp. 181-188.
- [17]N. Carreras, V. Acuña, M. Martí, M. J. Lis (2013), *Drug release system of ibuprofen in PCL-microspheres*. Colloid and Polymer Science, 291.1, pp. 157-165.
- [18]Catalog: *Quillaja*. Desert King International.
- [19]Catalog: *Information to product No. 3274 (miglyol 812)*. Caesar & Loretz GmbH.
- [20]Catalog: *Miglyol 810, 812*. CREMER OLEO GmbH.
- [21]Catalog: *A guidebook to Particle size analysis*. Horiba Scientific.
- [22]A. R. Chandak, P. R. Prasad Verma (2010), *Eudragit-based transdermal delivery system of pentazocine: Physico-chemical, in vitro and in vivo evaluations*. Pharm Dev Technol, 15.3, pp. 296-304.
- [23]S. Y. Cheng, C. W. M. Yuen, C. W. Kan, K. K. L. Cheuk (2008), *Development of cosmetic textiles using microencapsulation technology*. Research Journal of Textile and Apparel, 12.4, pp. 41-51.
- [24]P. Chidambaram, R. Govind, K. C. Venkataraman (2011), *The effect of loop length and yarn linear density on the thermal properties of bamboo knitted fabric*. Autex Research Journal, 11.4, pp. 102-105.
- [25]H. Chung, G. Cho (2004), *Thermal Properties and Physiological Responses of Vapor-Permeable Water-Repellent Fabrics Treated with Microcapsule-Containing PCMs*. Textile Research Journal, 74.7, pp. 571-575.
- [26]T. W. Chung, Y. Y. Huang, Y. Z. Liu (2001), *Effects of the rate of solvent evaporation on the characteristics of drug loaded PLLA and PDLLA microspheres*. International Journal of Pharmaceutics, 212.2, pp. 161-169.
- [27]H. Dabiryan, A. A. A. Jeddi (2007). *A geometrical assessment of the dimensional properties of interlock knitted structure*. The 9th Asian Textile Conference, Taiwan
- [28]Z. I. Değirmenci, E. Çoruh (2017), *The influences of loop length and raw material on bursting strength, air permeability and physical characteristics of single jersey knitted fabrics*. Journal of Engineered Fibers and Fabrics, 12.1, pp. 43-49.
- [29]G. B. Delkumburewatte, T. Dias (2009), *Porosity and capillarity of weft knitted spacer structures*. Fibers and Polymers, 10.2, pp. 226-230.
- [30]P. J. Dowding, R. Atkin, B. Vincent, P. Bouillot (2004), *Oil Core–Polymer Shell Microcapsules Prepared by Internal Phase Separation from Emulsion Droplets. I. Characterization and Release Rates for Microcapsules with Polystyrene Shells*. Langmuir, 20.26, pp. 11374-11379.
- [31]R. Dubey (2009), *Microencapsulation Technology and Applications*. Defence Science Journal, 59.1, pp. 82-95.
- [32]K. E. El-Nagar, N. M. Nagy, M. A. Elgamal (2012), *Medical Dressing Treated with Honey/Chitosan Microencapsules*. International Journal of Chemistry, 4.2, pp. 79-89.

-
- [33]H. M. El-Rafie, M. H. El-Rafie, H. M. Abdelsalam, W. A. El-Sayed (2016), *Antibacterial and anti-inflammatory finishing of cotton by microencapsulation using three marine organisms*. International Journal of Biological Macromolecules, 86 pp. 59-64.
- [34]M. M. El-Zawahry, S. El-Shami, M. H. El-Mallah (2007), *Optimizing a wool dyeing process with reactive dye by liposome microencapsulation*. Dyes and Pigments, 74.3, pp. 684-691.
- [35]G. Erkan, M. Sarişik, N. K. Pazarlioğlu (2010), *The microencapsulation of terbinafine via in situ polymerization of melamine-formaldehyde and their application to cotton fabric*. Journal of Applied Polymer Science, 118.6, pp. 3707-3714.
- [36]C. Fan, X. Zhou (2010), *Influence of operating conditions on the surface morphology of microcapsules prepared by in situ polymerization*. Colloids and Surfaces A: Physicochemical and Engineering Aspects, 363.1–3, pp. 49-55.
- [37]H. A. Garekani, Z. F. Moghaddam, F. Sadeghi (2013), *Organic solution versus aqueous dispersion of Eudragit RS in preparation of sustained release microparticles of theophylline using spray drying*. Colloids and Surfaces B: Biointerfaces, 108 pp. 374-379.
- [38]S. Giraud, S. Bourbigot, M. Rochery, I. Vroman, L. Tighzert, R. Delobel (2001), *Flame Behavior of Cotton Coated with Polyurethane Containing Microencapsulated Flame Retardant Agent*. Journal of Industrial Textiles, 31.1, pp. 11-26.
- [39]S. Giraud, S. Bourbigot, M. Rochery, I. Vroman, L. Tighzert, R. Delobel, F. Poutch (2005), *Flame retarded polyurea with microencapsulated ammonium phosphate for textile coating*. Polymer Degradation and Stability, 88.1, pp. 106-113.
- [40]B. Golja, B. Sumiga, B. Boh, L. Medved, T. Pusic, P. F. Tavcer (2014), *Application of flame retardant microcapsules to polyester and cotton fabrics*. Materials and technology, 48.1, pp. 105-111.
- [41]B. Golja, B. Šumiga, P. Forte Tavčer (2013), *Fragrant finishing of cotton with microcapsules: comparison between printing and impregnation*. Coloration Technology, 129.5, pp. 338-346.
- [42]R. A. Graves, S. Pamujula, R. Moiseyev, T. Freeman, L. A. Bostanian, T. K. Mandal (2004), *Effect of different ratios of high and low molecular weight PLGA blend on the characteristics of pentamidine microcapsules*. International Journal of Pharmaceutics, 270.1–2, pp. 251-262.
- [43]R. Guidoin, M. King, D. Marceau, A. Cardou, D. de la Faye, J. M. Legendre, P. Blais (1987), *Textile arterial prostheses: is water permeability equivalent to porosity?* J Biomed Mater Res, 21.1, pp. 65-87.
- [44]S. S. Gupta, N. Solanki, A. T. Serajuddin (2016), *Investigation of Thermal and Viscoelastic Properties of Polymers Relevant to Hot Melt Extrusion, IV: Affinisol HPMC HME Polymers*. AAPS PharmSciTech, 17.1, pp. 148-157.
- [45]M. M. Hassan, M. Sunderland (2015), *Antimicrobial and insect-resist wool fabrics by coating with microencapsulated antimicrobial and insect-resist agents*. Progress in Organic Coatings, 85 pp. 221-229.
- [46]A. Hebeish, M. H. El-Rafie, M. A. El-Sheikh, A. A. Seleem, M. E. El-Naggar (2014), *Antimicrobial wound dressing and anti-inflammatory efficacy of silver nanoparticles*. International Journal of Biological Macromolecules, 65 pp. 509-515.
- [47]B. Hepworth, G. A. V. Leaf (1976), *32—THE MECHANICS OF AN IDEALIZED WEFT-KNITTED STRUCTURE*. The Journal of The Textile Institute, 67.7-8, pp. 241-248.

-
- [48]R. Heusch, B. AG (2002) *Emulsions*. Wiley-VCH Verlag GmbH & Co. KGaA.
- [49]K. Holmberg, B. Jönsson, B. Kronberg, B. Lindman (2002) *Surfactants and Polymers in Aqueous Solution*. John Wiley & Sons, Ltd.
- [50]P. C.-L. Hui, W.-Y. Wang, C.-W. Kan, F. S.-F. Ng, E. Wat, V. X. Zhang, C.-L. Chan, C. B.-S. Lau, P.-C. Leung (2013), *Microencapsulation of Traditional Chinese Herbs—PentaHerbs extracts and potential application in healthcare textiles*. *Colloids and Surfaces B: Biointerfaces*, 111 pp. 156-161.
- [51]C. D. Huong (2015) "*Research on producing medical textile based on microencapsulation technology*". Research project France - Vietnam Hoa Sen Lotus No. 27917ZH.
- [52]C. D. Huong, V. T. H. Khanh, N. Sintes (2014), *Determination of size of Ibuprofen microcapsule using for textile application and research influence of stirring speed during microencapsulation on their dimension*. *Journal of Science and Technology Technical Universities*, 102 pp. 144-148.
- [53]C. D. Huong, N. T. B. Thuy (2014), *Research on the influence of structure of knitted fabrics on loading capability of microcapsule using for medical textile*. *Journal of Science and Technology Technical Universities*, 100 pp. 60-63.
- [54]K. Iqbal, D. Sun (2014), *Development of thermo-regulating polypropylene fibre containing microencapsulated phase change materials*. *Renewable Energy*, 71 pp. 473-479.
- [55]S. Izumikawa, S. Yoshioka, Y. Aso, Y. Takeda (1991), *Preparation of poly(l-lactide) microspheres of different crystalline morphology and effect of crystalline morphology on drug release rate*. *Journal of Controlled Release*, 15.2, pp. 133-140.
- [56]F. Jaâfar, M. A. Lassoued, M. Sahnoun, S. Sfar, M. Cheikhrouhou (2012), *Impregnation of ethylcellulose microcapsules containing jojoba oil onto compressive knits developed for high burns*. *Fibers and Polymers*, 13.3, pp. 346-351.
- [57]J. Jang, H. Sah (2011), *Nonhalogenated solvent-based solvent evaporation process useful in preparation of PLGA microspheres*. *J Microencapsul*, 28.6, pp. 490-498.
- [58]M. Jaworska, E. Sikora, J. Ogonowski (2014), *The influence of glicerides oil phase on O/W nanoemulsion formation by pic method*. *Periodica Polytechnica Chemical Engineering*, 58 pp. 43-48.
- [59]M. Jaworska, E. Sikora, M. Zielina, J. Ogonowski (2013), *Studies on the formation of O/W nano-emulsions, by low-energy emulsification method, suitable for cosmeceutical applications*. *Acta Biochim Pol*, 60.4, pp. 779-782.
- [60]J. Jun-Ling, C. Shui-Lin, Y. Xu-Jie, L. Lu-De, W. Xin, Y. Li-Min (2007), *The dyeing of nylon with a microencapsulated disperse dye*. *Coloration Technology*, 123.5, pp. 333-338.
- [61]N. V. Jyothi, P. M. Prasanna, S. N. Sakarkar, K. S. Prabha, P. S. Ramaiah, G. Y. Srawan (2010), *Microencapsulation techniques, factors influencing encapsulation efficiency*. *J Microencapsul*, 27.3, pp. 187-197.
- [62]T.-h. Kabri, E. Arab-Tehrany, N. Belhaj, M. Linder (2011), *Physico-chemical characterization of nano-emulsions in cosmetic matrix enriched on omega-3*. *Journal of Nanobiotechnology*, 9 pp. 41-41.
- [63]A. Kesarwani, A. K. Yadav, S. Singh, H. Gautam, H. N. Singh, A. Sharma, C. Yadav (2013), *Theoretical aspects of transdermal drug delivery system*. *Bulletin of Pharmaceutical Research*, 3.2, pp. 78-89.

-
- [64]H. K. Kim, T. G. Park (2001), *Microencapsulation of dissociable human growth hormone aggregates within poly(d,l-lactic-co-glycolic acid) microparticles for sustained release*. International Journal of Pharmaceutics, 229.1, pp. 107-116.
- [65]M. W. Konstan, J. E. Krenicky, M. R. Finney, H. L. Kirchner, K. A. Hilliard, J. B. Hilliard, P. B. Davis, C. L. Hoppel (2003), *Effect of ibuprofen on neutrophil migration in vivo in cystic fibrosis and healthy subjects*. J Pharmacol Exp Ther, 306.3, pp. 1086-1091.
- [66]K. Koo, Y. M. Park, J. D. Choe, E. A. Kim (2009), *Preparations of microencapsulated PCMs-coated nylon fabrics by wet and dry coating process and comparison of their properties*. Polymer Engineering & Science, 49.6, pp. 1151-1157.
- [67]K. Kosswig, in: *Ullmann's Encyclopedia of Industrial Chemistry*, Wiley-VCH Verlag GmbH & Co. KGaA: 2000.
- [68]N. V. Lân (2016) *Xử lý thống kê số liệu thực nghiệm và những ứng dụng trong ngành dệt may*. Nhà xuất bản Bách Khoa Hà Nội.
- [69]Latheeshj Lal.L, P. Phanitejaswini, Y.Soujanya, U.Swapna, V.Sarika, G.Moulika (2011), *Transdermal Drug Delivery Systems: An Overview*. International Journal of PharmTech Research, 4.4, pp. 2140-2148.
- [70]G. A. V. Leaf (1958), *A property of a buckled elastic rod*. British Journal of Applied Physics, 9.2, pp. 71.
- [71]G. A. V. Leaf, A. Glaskin (1955), *43—The Geometry of a Plain Knitted Loop*. Journal of the Textile Institute Transactions, 46.9, pp. T587-T605.
- [72]A. R. Lee, E. Yi (2013), *Investigating performance of cotton and lyocell knit treated with microcapsules containing Citrus unshiu oil*. Fibers and Polymers, 14.12, pp. 2088-2096.
- [73]D.-H. Lee, T.-Y. Kwon, K.-H. Kim, S.-T. Kwon, D.-H. Cho, S. H. Jang, J. S. Son, K.-B. Lee (2014), *Anti-inflammatory drug releasing absorbable surgical sutures using poly(lactic-co-glycolic acid) particle carriers*. Polymer Bulletin, 71.8, pp. 1933-1946.
- [74]S. Leelajariyakul, H. Noguchi, S. Kiatkamjornwong (2008), *Surface-modified and microencapsulated pigmented inks for ink jet printing on textile fabrics*. Progress in Organic Coatings, 62.2, pp. 145-161.
- [75]L. Li, S. Liu, T. Hua, M. W. Au, K. S. Wong (2013), *Characteristics of weaving parameters in microcapsule fabrics and their influence on loading capability*. Textile Research Journal, 83.2, pp. 113-121.
- [76]M. Li, O. Rouaud, D. Poncelet (2008), *Microencapsulation by solvent evaporation: State of the art for process engineering approaches*. International Journal of Pharmaceutics, 363.1–2, pp. 26-39.
- [77]M. Lin, Y. Yang, P. Xi, S.-I. Chen (2006), *Microencapsulation of water-soluble flame retardant containing organophosphorus and its application on fabric*. Journal of Applied Polymer Science, 102.5, pp. 4915-4920.
- [78]A. Loxley, B. Vincent (1998), *Preparation of Poly(methylmethacrylate) Microcapsules with Liquid Cores*. J Colloid Interface Sci, 208.1, pp. 49-62.
- [79]Z.-H. Ma, D.-G. Yu, C. J. Branford-White, H.-L. Nie, Z.-X. Fan, L.-M. Zhu (2009), *Microencapsulation of tamoxifen: Application to cotton fabric*. Colloids and Surfaces B: Biointerfaces, 69.1, pp. 85-90.
- [80]M. Martí, R. Rodríguez, N. Carreras, M. Lis, J. Valldeperas, L. Coderch, J. L. Parra (2012), *Monitoring of the microcapsule/liposome application on textile fabrics*. The Journal of The Textile Institute, 103.1, pp. 19-27.

-
- [81]R. S. Martín, R. Briones (1999), *Industrial uses and sustainable supply of Quillaja saponaria (Rosaceae) saponins*. Economic Botany, 53.3, pp. 302-311.
- [82]M. Matos, G. Gutiérrez, O. Iglesias, J. Coca, C. Pazos (2015), *Characterization, stability and rheology of highly concentrated monodisperse emulsions containing lutein*. Food Hydrocolloids, 49 pp. 156-163.
- [83]F. T. Meng, G. H. Ma, W. Qiu, Z. G. Su (2003), *W/O/W double emulsion technique using ethyl acetate as organic solvent: effects of its diffusion rate on the characteristics of microparticles*. Journal of Controlled Release, 91.3, pp. 407-416.
- [84]S. M. Mirabedini, I. Dutil, R. R. Farnood (2012), *Preparation and characterization of ethyl cellulose-based core-shell microcapsules containing plant oils*. Colloids and Surfaces A: Physicochemical and Engineering Aspects, 394 pp. 74-84.
- [85]M. M. Miró Specos, G. Escobar, P. Marino, C. Puggia, M. V. Defain Tesoriero, L. Hermida (2010), *Aroma Finishing of Cotton Fabrics by Means of Microencapsulation Techniques*. Journal of Industrial Textiles, 40.1, pp. 13-32.
- [86]S. Mitra, S. R. Dungan (1997), *Micellar Properties of Quillaja Saponin. 1. Effects of Temperature, Salt, and pH on Solution Properties*. Journal of Agricultural and Food Chemistry, 45.5, pp. 1587-1595.
- [87]P. Monllor, M. A. Bonet, F. Cases (2007), *Characterization of the behaviour of flavour microcapsules in cotton fabrics*. European Polymer Journal, 43.6, pp. 2481-2490.
- [88]P. Monllor, L. Sánchez, F. Cases, M. A. Bonet (2009), *Thermal Behavior of Microencapsulated Fragrances on Cotton Fabrics*. Textile Research Journal, 79.4, pp. 365-380.
- [89]A. Montes, M. D. Gordillo, C. Pereyra, D. M. De los Santos, E. J. Martínez de la Ossa (2014), *Ibuprofen-polymer precipitation using supercritical CO₂ at low temperature*. The Journal of Supercritical Fluids, 94 pp. 91-101.
- [90]Moon Won Suh (1967), *A Study of the Shrinkage of Plain Knitted Cotton Fabric, Based on the Structural Changes of the Loop Geometry Due to Yarn Swelling and Deswelling*. Textile Research Journal, 37.5, pp. 417-431.
- [91]D. L. Munden (1959), *26—THE GEOMETRY AND DIMENSIONAL PROPERTIES OF PLAIN-KNIT FABRICS*. Journal of the Textile Institute Transactions, 50.7, pp. T448-T471.
- [92]D. Myers (2006) *Surfactant science and technology*. A Jonh Wiley & Sons, Inc., Publication.
- [93]R. Nagarajan (2002), *Molecular Packing Parameter and Surfactant Self-Assembly: The Neglected Role of the Surfactant Tail*. Langmuir, 18.1, pp. 31-38.
- [94]A. Nejman, M. Cieślak, B. Gajdzicki, B. Goetzendorf-Grabowska, A. Karaszewska (2014), *Methods of PCM microcapsules application and the thermal properties of modified knitted fabric*. Thermochemica Acta, 589 pp. 158-163.
- [95]A. Nejman, B. Goetzendorf-Grabowska (2013), *Heat balance of textile materials modified with the mixtures of PCM microcapsules*. Thermochemica Acta, 569 pp. 144-150.
- [96]G. Nelson (1991), *Microencapsulates in textile coloration and finishing*. Review of Progress in Coloration and Related Topics, 21.1, pp. 72-85.
- [97]G. Nelson (2002), *Application of microencapsulation in textiles*. International Journal of Pharmaceutics, 242.1-2, pp. 55-62.
- [98]L. I. Nord, L. Kenne (2000), *Novel acetylated triterpenoid saponins in a chromatographic fraction from Quillaja saponaria Molina*. Carbohydrate Research, 329.4, pp. 817-829.

-
- [99] B. Ocepek, B. Boh, B. Šumiga, P. F. Tavčer (2012), *Printing of antimicrobial microcapsules on textiles*. *Coloration Technology*, 128.2, pp. 95-102.
- [100] R. T. Ogulata, S. Mavruz (2010), *Investigation of porosity and air permeability values of plain knitted fabrics*. *FIBERS & TEXTILES in Eastern Europe*, 18.5(82), pp. 71-75.
- [101] B. Ozturk, S. Argin, M. Ozilgen, D. J. McClements (2014), *Formation and stabilization of nanoemulsion-based vitamin E delivery systems using natural surfactants: Quillaja saponin and lecithin*. *Journal of Food Engineering*, 142 pp. 57-63.
- [102] F. Özyildiz, S. Karagönlü, G. Basal, A. Uzel, O. Bayraktar (2013), *Microencapsulation of ozonated red pepper seed oil with antimicrobial activity and application to nonwoven fabric*. *Letters in Applied Microbiology*, 56.3, pp. 168-179.
- [103] D. Paolino, C. A. Ventura, S. Nisticò, G. Puglisi, M. Fresta (2002), *Lecithin microemulsions for the topical administration of ketoprofen: percutaneous adsorption through human skin and in vivo human skin tolerability*. *International Journal of Pharmaceutics*, 244.1-2, pp. 21-31.
- [104] N. C. Parera, *Modelling drug delivery mechanisms for microencapsulated substances applied on textile substrates*, Universitat Politècnica De Catalunya, Terrassa (Spain), 2012.
- [105] J.-C. Park, T. Ito, K.-O. Kim, K.-W. Kim, B.-S. Kim, M.-S. Khil, H.-Y. Kim, I.-S. Kim (2010), *Electrospun poly(vinyl alcohol) nanofibers: effects of degree of hydrolysis and enhanced water stability*. *Polymer Journal*, 42.3, pp. 273-276.
- [106] S.-J. Park, S.-H. Kim (2004), *Preparation and characterization of biodegradable poly(L-lactide)/poly(ethylene glycol) microcapsules containing erythromycin by emulsion solvent evaporation technique*. *J Colloid Interface Sci*, 271.2, pp. 336-341.
- [107] D. P. Patel, P. Li, A. T. M. Serajuddin (2012), *Enhanced microemulsion formation in lipid-based drug delivery systems by combining mono-esters of medium-chain fatty acids with di- or tri-esters*. *Journal of Excipients and Food Chemicals*, 3.2, pp. 29-44.
- [108] S. Paul, S. Akhter, I. Hasan, S. S. Haider, M. S. Reza (2013), *Encapsulation of Naproxen in Eudragit RSPO Microsphere system: In vitro Characterization and Compatibility Studies*. 2013, 11.2, pp. 9.
- [109] F. T. Peirce (1947), *Geometrical Principles Applicable to the Design of Functional Fabrics*. *Textile Research Journal*, 17.3, pp. 123-147.
- [110] D. Perumal (2001), *Microencapsulation of ibuprofen and Eudragit® RS 100 by the emulsion solvent diffusion technique*. *International Journal of Pharmaceutics*, 218.1-2, pp. 1-11.
- [111] U. S. Pharmacopeia, *USP29 (USP Monograph for Gauge Bandage)*, 2007.
- [112] R. Postle (1974), *17—A GEOMETRICAL ASSESSMENT OF THE THICKNESS AND BULK DENSITY OF WEFT-KNITTED FABRICS*. *The Journal of The Textile Institute*, 65.4, pp. 155-163.
- [113] R. Postle, D. L. Munden (1967), *24—ANALYSIS OF THE DRY-RELAXED KNITTED-LOOP CONFIGURATION: PART I: TWO-DIMENSIONAL ANALYSIS*. *The Journal of The Textile Institute*, 58.8, pp. 329-351.
- [114] P. Prichystal, L. Burgert, R. Hrdina, N. Purev, M. Cerny (2013), *Encapsulation of textile dyes and textile auxiliary agents into liposome systems and their use for polyamide dyeing*. *Coloration Technology*, 129.1, pp. 64-68.

-
- [115] N. Purev, L. Burgert, P. Prichystal, R. Hrdina, J. Kühn, M. Cerny, J. Oyuntulkhuur (2013), *Dyeing of leather with microencapsulated acid dye*. *Coloration Technology*, 129.6, pp. 412-417.
- [116] A. Rawle: *Basic principles of particle size analysis*. Technical Paper of Malvern Instruments.
- [117] G. A. Rocha, C. S. Fávaro-Trindade, C. R. F. Grosso (2012), *Microencapsulation of lycopene by spray drying: Characterization, stability and application of microcapsules*. *Food and Bioproducts Processing*, 90.1, pp. 37-42.
- [118] S. N. Rodrigues, I. M. Martins, I. P. Fernandes, P. B. Gomes, V. G. Mata, M. F. Barreiro, A. E. Rodrigues (2009), *Scentfashion®: Microencapsulated perfumes for textile application*. *Chemical Engineering Journal*, 149.1–3, pp. 463-472.
- [119] N. Sadurní, C. Solans, N. Azemar, M. J. García-Celma (2005), *Studies on the formation of O/W nano-emulsions, by low-energy emulsification methods, suitable for pharmaceutical applications*. *European Journal of Pharmaceutical Sciences*, 26.5, pp. 438-445.
- [120] H. Sah (1997), *Microencapsulation techniques using ethyl acetate as a dispersed solvent: effects of its extraction rate on the characteristics of PLGA microspheres*. *Journal of Controlled Release*, 47.3, pp. 233-245.
- [121] H. Sah (2000), *Ethyl formate — alternative dispersed solvent useful in preparing PLGA microspheres*. *International Journal of Pharmaceutics*, 195.1–2, pp. 103-113.
- [122] J. C. Sakthivel, N. Anbumani (2012), *Dimensional properties of single jersey knitted fabrics made from new and regenerated cellulosic fibers*. *Journal of Textile and Apparel, Technology and Management*, 7.3, pp. 1-10.
- [123] F. Salaün, E. Devaux, S. Bourbigot, P. Rumeau (2009), *Influence of process parameters on microcapsules loaded with n-hexadecane prepared by in situ polymerization*. *Chemical Engineering Journal*, 155.1–2, pp. 457-465.
- [124] F. Salaün, E. Devaux, S. Bourbigot, P. Rumeau (2010), *Thermoregulating response of cotton fabric containing microencapsulated phase change materials*. *Thermochimica Acta*, 506.1–2, pp. 82-93.
- [125] F. Salaün, E. Devaux, S. Bourbigot, P. Rumeau (2009), *Application of Contact Angle Measurement to the Manufacture of Textiles Containing Microcapsules*. *Textile Research Journal*, 79.13, pp. 1202-1212.
- [126] F. Salaün, E. Devaux, S. Bourbigot, P. Rumeau (2010), *Development of Phase Change Materials in Clothing Part I: Formulation of Microencapsulated Phase Change*. *Textile Research Journal*, 80.3, pp. 195-205.
- [127] F. Salaün, M. Lewandowski, I. Vroman, G. Bedek, S. Bourbigot (2011), *Development and characterisation of flame-retardant fibres from isotactic polypropylene melt-compounded with melamine-formaldehyde microcapsules*. *Polymer Degradation and Stability*, 96.1, pp. 131-143.
- [128] F. Salaün, I. Vroman, I. Elmajid (2012), *A novel approach to synthesize and to fix microparticles on cotton fabric*. *Chemical Engineering Journal*, 213 pp. 78-87.
- [129] P. Sánchez, M. V. Sánchez-Fernandez, A. Romero, J. F. Rodríguez, L. Sánchez-Silva (2010), *Development of thermo-regulating textiles using paraffin wax microcapsules*. *Thermochimica Acta*, 498.1–2, pp. 16-21.

-
- [130] L. Sánchez-Silva, J. F. Rodríguez, A. Romero, P. Sánchez (2012), *Preparation of coated thermo-regulating textiles using Rubitherm-RT31 microcapsules*. Journal of Applied Polymer Science, 124.6, pp. 4809-4818.
- [131] R. Saraswathi, P. N. Krishnan, C. Dilip (2010), *Antimicrobial activity of cotton and silk fabric with herbal extract by micro encapsulation*. Asian Pacific Journal of Tropical Medicine, 3.2, pp. 128-132.
- [132] D. Semnani, M. Latifi, S. Hamzeh, A. A. A. Jeddi (2003), *A New Aspect of Geometrical and Physical Principles Applicable to the Estimation of Textile Structures: An Ideal Model for the Plain-knitted Loop*. The Journal of The Textile Institute, 94.3-4, pp. 202-211.
- [133] W. J. Shanahan, R. Postle (1973), *Jamming of Knitted Structures*. Textile Research Journal, 43.9, pp. 532-538.
- [134] M. O. R. Siddiqui, D. Sun (2015), *Porosity prediction of plain weft knitted fabrics*. Fibers, 3 pp. 1-11.
- [135] S. Singh, Neelam, S. Arora, Y. P. Singla (2015), *An overview of multifaceted significance of Eudragit polymers in drug delivery systems*. Asian Journal of Pharmaceutical and Clinical Research, 8.5, pp. 1-6.
- [136] E. M. Soares-Latour, J. Bernard, S. Chambert, E. Fleury, N. Sintès-Zydowicz (2017), *Environmentally benign 100% bio-based oligoamide microcapsules*. Colloids and Surfaces A: Physicochemical and Engineering Aspects, 524. Supplement C, pp. 193-203.
- [137] K. Son, D. I. Yoo, Y. Shin (2014), *Fixation of vitamin E microcapsules on dyed cotton fabrics*. Chemical Engineering Journal, 239 pp. 284-289.
- [138] X. Song, Y. Zhao, S. Hou, F. Xu, R. Zhao, J. He, Z. Cai, Y. Li, Q. Chen (2008), *Dual agents loaded PLGA nanoparticles: Systematic study of particle size and drug entrapment efficiency*. European Journal of Pharmaceutics and Biopharmaceutics, 69.2, pp. 445-453.
- [139] M. M. Specos, J. J. Garcia, J. Tornesello, P. Marino, M. D. Vecchia, M. V. Tesoriero, L. G. Hermida (2010), *Microencapsulated citronella oil for mosquito repellent finishing of cotton textiles*. Trans R Soc Trop Med Hyg, 104.10, pp. 653-658.
- [140] Z. Stojanovic, S. Markovic (2012), *Determination of Particle Size Distribution by Laser Diffraction*. Technics - New Materials, 21 pp. 11-20.
- [141] P. Sutaphanit, P. Chitprasert (2014), *Optimisation of microencapsulation of holy basil essential oil in gelatin by response surface methodology*. Food Chemistry, 150 pp. 313-320.
- [142] T. F. Tadros (2009) *Emulsion Science and Technology*. WILEY-VCH Verlag GmbH & Co. KGaA.
- [143] G. Thilagavathi, T. Kannaian (2010), *Combined antimicrobial and aroma finishing treatment for cotton, using microencapsulated geranium leaves extract*. Indian Journal of Natural Products and Resources, 1.3, pp. 348-352.
- [144] D. Tilak, G. B. Delkumburewatte (2007), *The influence of moisture content on the thermal conductivity of a knitted structure*. Measurement Science and Technology, 18.5, pp. 1304.
- [145] D. Vaja, A. K.Seth, G. U. Sailor, J. patel, J. patel, Krunal Pandya, M. Patel, T. K. Ghelani, U. Joshi (2011), *Formulation and evaluation of transdermal patch of Meloxicam*. Pharma Science Monitor, 2.4, pp. 89-103.

-
- [146] P. Valot, *Développement de nouveaux supports textiles contenant des microcapsules de principe actif médicamenteux pour orthèses*, Université Claude Bernard (Lyon), Lyon (France), 2007.
- [147] P. Valot, M. Baba, J. M. Nedelec, N. Sintès-Zydowicz (2009), *Effects of process parameters on the properties of biocompatible Ibuprofen-loaded microcapsules*. International Journal of Pharmaceutics, 369.1–2, pp. 53-63.
- [148] P. R. Verma, S. S. Iyer (2000), *Transdermal delivery of propranolol using mixed grades of Eudragit: design and in vitro and in vivo evaluation*. Drug Dev Ind Pharm, 26.4, pp. 471-476.
- [149] I. Vroman, S. Giraud, F. Salaün, S. Bourbigot (2010), *Polypropylene fabrics padded with microencapsulated ammonium phosphate: Effect of the shell structure on the thermal stability and fire performance*. Polymer Degradation and Stability, 95.9, pp. 1716-1720.
- [150] Web: <http://www.medherant.co.uk/drug-delivery-patches/tepi-patch-technology/ibuprofen-patch>, 2017, 2/10.
- [151] Web: <http://www.chemspider.com/Chemical-Structure.3544.html>, 2015, 02/5.
- [152] K. Wojciechowski (2013), *Surface activity of saponin from Quillaja bark at the air/water and oil/water interfaces*. Colloids and Surfaces B: Biointerfaces, 108 pp. 95-102.
- [153] L. Yan, Z. Yi, Z. Ben, D. Juan, C. Shuilin (2011), *Effect of microencapsulation on dyeing behaviors of disperse dyes without auxiliary solubilization*. Journal of Applied Polymer Science, 120.1, pp. 484-491.
- [154] N. Yan, M. Zhang, P. Ni (1992), *Size distribution and zeta-potential of polyamide microcapsules*. Journal of Membrane Science, 72.2, pp. 163-169.
- [155] C.-Y. Yang, S. Y. Tsay, R. C. C. Tsiang (2000), *An enhanced process for encapsulating aspirin in ethyl cellulose microcapsules by solvent evaporation in an O/W emulsion*. J Microencapsul, 17.3, pp. 269-277.
- [156] Y. Yang, M. E. Leser, A. A. Sher, D. J. McClements (2013), *Formation and stability of emulsions using a natural small molecule surfactant: Quillaja saponin (Q-Naturale®)*. Food Hydrocolloids, 30.2, pp. 589-596.
- [157] Y. Yang, D. J. McClements (2013), *Encapsulation of vitamin E in edible emulsions fabricated using a natural surfactant*. Food Hydrocolloids, 30.2, pp. 712-720.
- [158] Z. Yang, Z. Zeng, Z. Xiao, H. Ji (2014), *Preparation and controllable release of chitosan/vanillin microcapsules and their application to cotton fabric*. Flavour and Fragrance Journal, 29.2, pp. 114-120.
- [159] Z. Yi, F. Jihong, C. Shuilin (2005), *Dyeing of polyester using micro-encapsulated disperse dyes in the absence of auxiliaries*. Coloration Technology, 121.2, pp. 76-80.
- [160] H. Zhang, S. Sun, X. Wang, D. Wu (2011), *Fabrication of microencapsulated phase change materials based on n-octadecane core and silica shell through interfacial polycondensation*. Colloids and Surfaces A: Physicochemical and Engineering Aspects, 389.1–3, pp. 104-117.
- [161] L. Zhao, J. Luo, H. Wang, G. Song, G. Tang (2016), *Self-assembly fabrication of microencapsulated n-octadecane with natural silk fibroin shell for thermal-regulating textiles*. Applied Thermal Engineering, 99 pp. 495-501.
- [162] A. Zhu, F. Li, L. Ji (2012), *Poly(lactic acid)/N-maleoylchitosan core-shell capsules: preparation and drug release properties*. Colloids Surf B Biointerfaces, 91 pp. 162-167.

-
- [163] K. J. Zhu, Y. Li, H. L. Jiang, H. Yasuda, A. Ichimaru, K. Yamamoto, P. Lecomte, R. Jerome (2005), *Preparation, characterization and in vitro release properties of ibuprofen-loaded microspheres based on polylactide, poly(epsilon-caprolactone) and their copolymers*. J Microencapsul, 22.1, pp. 25-36.
- [164] Y. Zhu, N. H. Shah, A. W. Malick, M. H. Infeld, J. W. McGinity (2002), *Solid-state plasticization of an acrylic polymer with chlorpheniramine maleate and triethyl citrate*. International Journal of Pharmaceutics, 241.2, pp. 301-310.

LIST OF PUBLISHED WORKS OF THE THESIS

1. Dao Thi Chinh Thuy, Chu Dieu Huong (2014), *The influence of woven structure and yarn density on microcapsule loading capability of fabric*. Journal of Science and Technology Technical Universities, ISSN 0868-3980, No.100-2014, pp. 51-54.
2. Chu Dieu Huong, Dao Thi Chinh Thuy, Nathalie Sintès-Zydowicz (2015), *Influence of yarn type and yarn count on microcapsule loading capability of fabrics*. Magazine Textile and Clothing, ISSN 1310-912X, No. 5-2015, pp. 118-122.
3. Dao Thi Chinh Thuy, Chu Dieu Huong (2016), *Investigate the influence of loop length and fabric extension on transdermal drug release from knitted fabric containing ibuprofen-loaded microcapsules*. Journal of Science and Technology Technical Universities, ISSN 2354-1083, No.112-2016, pp. 51-54.
4. Dao Thi Chinh Thuy, Chu Dieu Huong (2017), *The influence of loop length on microcapsule loading capability of Interlock knitted fabric*. Journal of Science and Technology Technical Universities, ISSN 2354-1083, No.122-2017, pp. 67-72.

APPENDIX

Appendix 1

The surface tensions of saponin solutions

Saponin concentration: 0.005 (wt%)		
Experiment	m (g)	λ (dyn/cm)
1	0.621	58,153
2	0.629	58,940
3	0.618	57,567
Average	0.623	58,220
Saponin concentration: 0.010 (wt%)		
Experiment	m (g)	λ (dyn/cm)
1	0.578	54,185
2	0.592	55,751
3	0.590	55,527
Average	0.587	55,154
Saponin concentration: 0.020 (wt%)		
Experiment	m (g)	λ (dyn/cm)
1	0.569	53,513
2	0.569	53,513
3	0,562	52,708
Average	0.569	53,245
Saponin concentration: 0.030 (wt%)		
Experiment	m (g)	λ (dyn/cm)
1	0.561	52,487
2	0.555	51,832
3	0.539	50,201
Average	0.552	51,507
Saponin concentration: 0.040 (wt%)		
Experiment	m (g)	λ (dyn/cm)

1	0.545	50,933
2	0.544	50,826
3	0.545	50,933
Average	0.545	50,897
Saponin concentration: 0.050 (wt%)		
Experiment	m (g)	λ (dyn/cm)
1	0.541	50,503
2	0.539	50,291
3	0.553	50,790
Average	0.544	50,528
Saponin concentration: 0.060 (wt%)		
Experiment	m (g)	λ (dyn/cm)
1	0.536	50,197
2	0.534	49,989
3	0.544	51,030
Average	0.538	50,405
Saponin concentration: 0.070 (wt%)		
Experiment	m (g)	λ (dyn/cm)
1	0.539	50,494
2	0.546	51,228
3	0.536	50,180
Average	0.540	50,634
Saponin concentration: 0.080 (wt%)		
Experiment	m (g)	λ (dyn/cm)
1	0.540	50,372
2	0.540	50,375
3	0.542	50,972
Average	0.540	50,573
Saponin concentration: 0.090 (wt%)		

Experiment	m (g)	λ (dyn/cm)
1	0.537	50,878
2	0.531	50,190
3	0.529	49,993
Average	0.533	50,353
Saponin concentration: 0.100 (wt%)		
Experiment	m (g)	λ (dyn/cm)
1	0.533	50,186
2	0.531	49,985
3	0.543	51,290
Average	0.536	50,487
Saponin concentration: 0.500 (wt%)		
Experiment	m (g)	λ (dyn/cm)
1	0.530	50,141
2	0.533	50,444
3	0.539	51,054
Average	0.534	50,546
Saponin concentration: 1.000 (wt%)		
Experiment	m (g)	λ (dyn/cm)
1	0.533	50,237
2	0.541	51,169
3	0.529	49,826
Average	0.534	50,411

Appendix 2

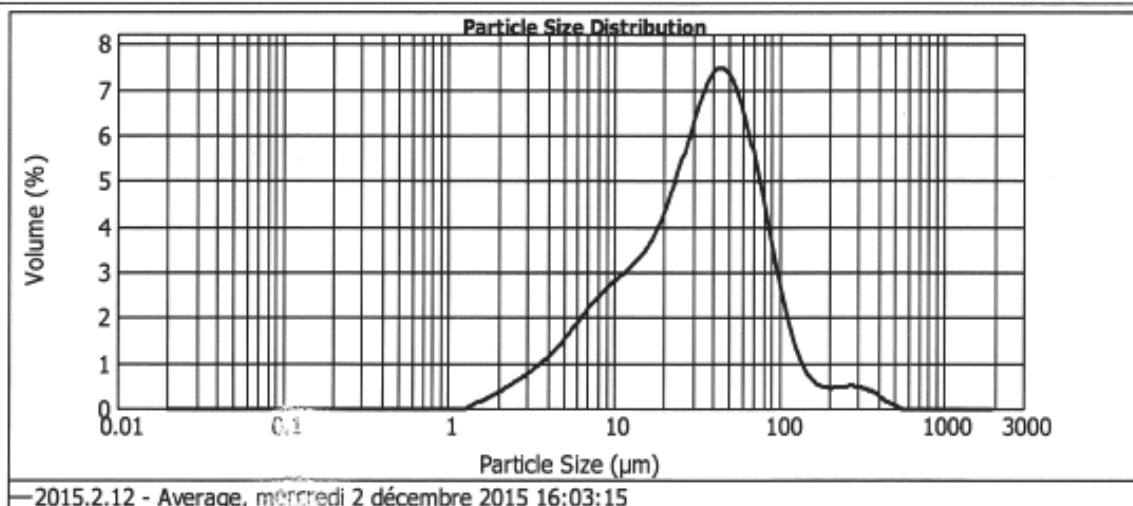
Mastersize reports of microcapsule lots

Mastersizer report of microcapsules C0.025

Particle Name: Défaut	Accessory Name: Hydro 2000MU (A)	Analysis model: General purpose	Sensitivity: Normal
Particle RI: 1.520	Absorption: 0.1	Size range: 0.020 to 2000.000 μm	Obscuration: 16.42 %
Dispersant Name: Eau	Dispersant RI: 1.330	Weighted Residual: 0.538 %	Result Emulation: Off

Concentration: 0.0410 %Vol	Span : 2.386	Uniformity: 0.862	Result units: Volume
Specific Surface Area: 0.348 m^2/g	Surface Weighted Mean D[3,2]: 17.232 μm	Vol. Weighted Mean D[4,3]: 46.383 μm	

d(0.1): 7.221 μm d(0.5): 34.271 μm d(0.9): 88.997 μm



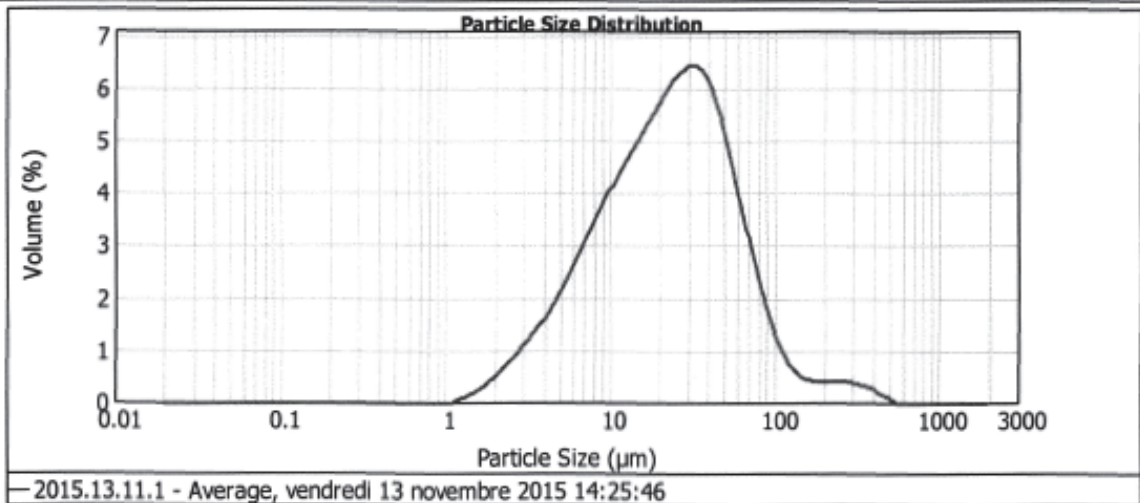
Size (μm)	Volume In %	Size (μm)	Volume In %	Size (μm)	Volume In %	Size (μm)	Volume In %	Size (μm)	Volume In %	Size (μm)	Volume In %
0.010	0.00	0.100	0.00	1.000	0.00	11.402	2.77	120.220	1.15	1258.925	0.00
0.011	0.00	0.120	0.00	1.259	0.02	13.183	2.96	138.038	0.71	1445.440	0.00
0.013	0.00	0.137	0.00	1.445	0.13	15.136	3.22	158.489	0.48	1689.587	0.00
0.015	0.00	0.158	0.00	1.660	0.23	17.378	3.59	181.970	0.41	1905.481	0.00
0.017	0.00	0.182	0.00	1.905	0.33	19.963	4.07	208.930	0.42	2187.762	0.00
0.020	0.00	0.209	0.00	2.188	0.44	22.909	4.67	239.803	0.44	2511.886	0.00
0.023	0.00	0.240	0.00	2.512	0.58	26.303	5.33	275.423	0.44	2884.032	0.00
0.026	0.00	0.276	0.00	2.884	0.70	30.200	5.96	316.228	0.38	3311.311	0.00
0.030	0.00	0.316	0.00	3.311	0.85	34.674	6.67	363.078	0.30	3801.894	0.00
0.035	0.00	0.360	0.00	3.802	1.03	39.811	7.33	416.869	0.15	4365.158	0.00
0.040	0.00	0.417	0.00	4.365	1.24	45.709	8.07	478.630	0.04	5011.872	0.00
0.046	0.00	0.479	0.00	5.012	1.48	52.481	8.88	549.541	0.00	5754.398	0.00
0.052	0.00	0.550	0.00	5.754	1.73	60.256	9.76	630.957	0.00	6606.934	0.00
0.060	0.00	0.631	0.00	6.607	1.98	69.183	10.71	724.436	0.00	7585.776	0.00
0.069	0.00	0.724	0.00	7.588	2.21	79.433	11.74	831.764	0.00	8709.636	0.00
0.079	0.00	0.832	0.00	8.710	2.41	91.201	12.86	954.993	0.00	10000.000	0.00
0.091	0.00	0.957	0.00	10.000	2.59	104.713	14.11	1095.478	0.00		
0.105	0.00	1.097	0.00	11.482		120.228		1258.925	0.00		

Mastersizer report of microcapsules C0.050

Particle Name: Défaut	Accessory Name: Hydro 2000MU (A)	Analysis model: General purpose	Sensitivity: Normal
Particle RI: 1.520	Absorption: 0.1	Size range: 0.020 to 2000.000 μm	Obscuration: 17.78 %
Dispersant Name: Eau	Dispersant RI: 1.330	Weighted Residual: 0.685 %	Result Emulation: Off

Concentration: 0.0340 %Vol	Span : 2.764	Uniformity: 1.05	Result units: Volume
Specific Surface Area: 0.456 m^2/g	Surface Weighted Mean D[3,2]: 13.171 μm	Vol. Weighted Mean D[4,3]: 36.109 μm	

d(0.1): 5.686 μm d(0.5): 23.241 μm d(0.9): 69.935 μm



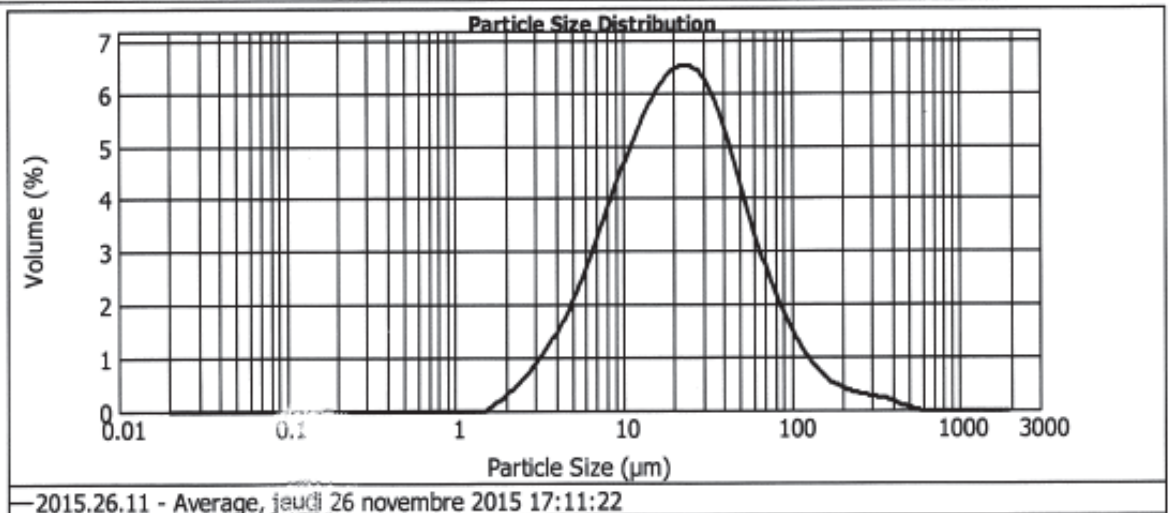
Size (μm)	Volume in %	Size (μm)	Volume in %	Size (μm)	Volume in %	Size (μm)	Volume in %	Size (μm)	Volume in %	Size (μm)	Volume in %
0.010	0.00	0.105	0.00	1.098	0.02	11.482	4.12	120.226	0.61	1258.925	0.00
0.011	0.00	0.120	0.00	1.259	0.10	13.183	4.42	138.038	0.45	1445.440	0.00
0.013	0.00	0.138	0.00	1.445	0.20	15.136	4.71	158.489	0.37	1659.567	0.00
0.015	0.00	0.158	0.00	1.660	0.32	17.378	5.00	181.970	0.37	1905.461	0.00
0.017	0.00	0.182	0.00	1.905	0.47	19.953	5.30	208.690	0.37	2187.762	0.00
0.020	0.00	0.209	0.00	2.188	0.64	22.909	5.57	239.893	0.37	2511.866	0.00
0.023	0.00	0.240	0.00	2.512	0.82	26.303	5.76	275.423	0.35	2894.032	0.00
0.026	0.00	0.275	0.00	2.884	1.02	30.200	5.82	316.228	0.31	3311.311	0.00
0.030	0.00	0.316	0.00	3.311	1.24	34.674	5.69	363.079	0.26	3801.894	0.00
0.035	0.00	0.363	0.00	3.802	1.49	39.811	5.34	416.869	0.16	4395.158	0.00
0.040	0.00	0.417	0.00	4.365	1.77	45.709	4.79	478.630	0.05	5011.872	0.00
0.046	0.00	0.479	0.00	5.012	2.09	52.481	4.08	549.541	0.00	5754.399	0.00
0.052	0.00	0.550	0.00	5.754	2.44	60.256	3.30	630.667	0.00	6606.934	0.00
0.060	0.00	0.631	0.00	6.607	2.79	69.183	2.53	724.436	0.00	7585.776	0.00
0.069	0.00	0.724	0.00	7.586	3.15	79.433	1.84	831.764	0.00	8709.836	0.00
0.079	0.00	0.832	0.00	8.710	3.49	91.201	1.29	954.993	0.00	10000.000	0.00
0.091	0.00	0.955	0.00	10.000	3.82	104.713	0.88	1096.478	0.00		
0.105	0.00	1.095	0.00	11.482		120.226		1258.925	0.00		

Mastersizer report of microcapsules C0.075 (R700, S0)

Particle Name: Défaut	Accessory Name: Hydro 2000MU (A)	Analysis model: General purpose	Sensitivity: Normal
Particle RI: 1.520	Absorption: 0.1	Size range: 0.020 to 2000.000 μm	Obscuration: 16.30 %
Dispersant Name: Eau	Dispersant RI: 1.330	Weighted Residual: 0.611 %	Result Emulation: Off

Concentration: 0.0331 %Vol	Span : 3.006	Uniformity: 1.07	Result units: Volume
Specific Surface Area: 0.429 m^2/g	Surface Weighted Mean D[3,2]: 13.986 μm	Vol. Weighted Mean D[4,3]: 34.495 μm	

d(0.1): 6.311 μm d(0.5): 21.488 μm d(0.9): 70.897 μm



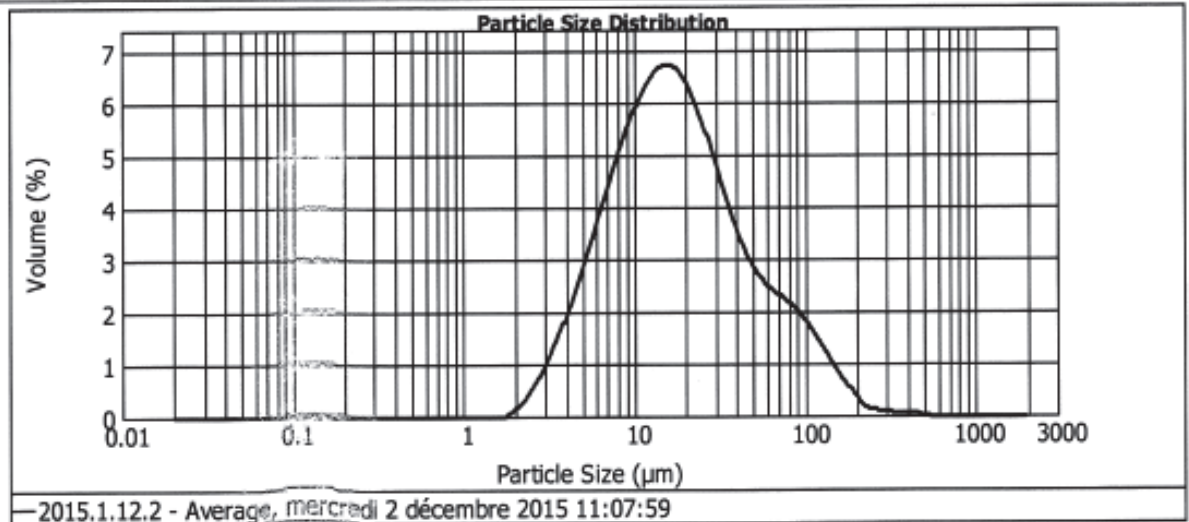
Size (μm)	Volume In %	Size (μm)	Volume In %	Size (μm)	Volume In %	Size (μm)	Volume In %	Size (μm)	Volume In %	Size (μm)	Volume In %
0.010	0.00	0.125	0.00	1.096	0.00	11.482	4.62	120.226	0.86	1258.925	0.00
0.011	0.00	0.138	0.00	1.258	0.00	13.183	5.20	138.038	0.65	1445.440	0.00
0.013	0.00	0.152	0.00	1.445	0.01	15.136	5.50	158.408	0.50	1650.587	0.00
0.015	0.00	0.167	0.00	1.650	0.14	17.378	5.73	181.970	0.40	1805.461	0.00
0.017	0.00	0.183	0.00	1.905	0.27	19.963	5.86	208.930	0.33	2187.762	0.00
0.020	0.00	0.200	0.00	2.188	0.42	22.909	5.88	239.883	0.28	2511.886	0.00
0.023	0.00	0.217	0.00	2.512	0.60	26.303	5.78	275.423	0.25	2884.032	0.00
0.026	0.00	0.235	0.00	2.884	0.81	30.200	5.50	318.228	0.21	3311.311	0.00
0.030	0.00	0.254	0.00	3.311	1.08	34.674	5.09	363.078	0.18	3601.894	0.00
0.035	0.00	0.275	0.00	3.802	1.34	39.811	4.66	419.889	0.09	4365.158	0.00
0.040	0.00	0.297	0.00	4.365	1.67	45.709	3.96	478.630	0.04	5011.872	0.00
0.046	0.00	0.320	0.00	5.012	2.08	52.481	3.34	548.541	0.00	5754.399	0.00
0.052	0.00	0.345	0.00	5.754	2.49	60.296	2.78	630.957	0.00	6608.934	0.00
0.060	0.00	0.371	0.00	6.607	2.96	69.183	2.25	724.436	0.00	7585.778	0.00
0.068	0.00	0.399	0.00	7.586	3.45	79.433	1.81	831.764	0.00	8709.636	0.00
0.078	0.00	0.428	0.00	8.710	3.93	91.201	1.44	954.993	0.00	10000.000	0.00
0.089	0.00	0.459	0.00	10.000	4.40	104.713	1.12	1096.478	0.00		
0.105	0.00	0.492	0.00	11.482		120.226		1258.925	0.00		

Mastersizer report of microcapsules C0.100

Particle Name: Défaut	Accessory Name: Hydro 2000MU (A)	Analysis model: General purpose	Sensitivity: Normal
Particle RI: 1.520	Absorption: 0.1	Size range: 0.020 to 2000.000 um	Obscuration: 16.34 %
Dispersant Name: Eau	Dispersant RI: 1.330	Weighted Residual: 0.698 %	Result Emulation: Off

Concentration: 0.0296 %Vol	Span : 3.854	Uniformity: 1.19	Result units: Volume
Specific Surface Area: 0.482 m ² /g	Surface Weighted Mean D[3,2]: 12.451 um	Vol. Weighted Mean D[4,3]: 30.003 um	

d(0.1): 5.698 um d(0.5): 17.126 um d(0.9): 71.697 um



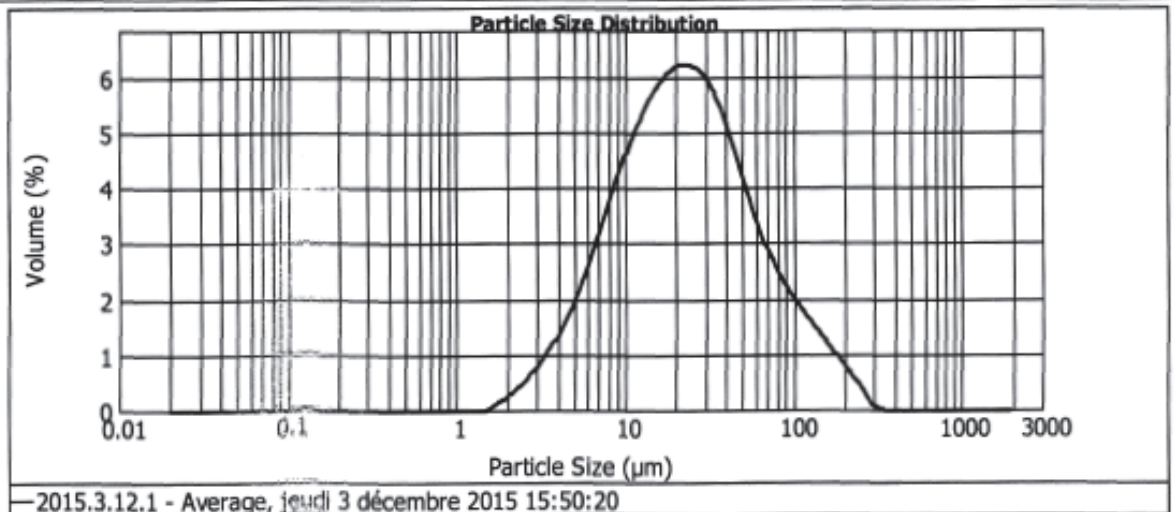
Size (µm)	Volume In %										
0.010	0.00	0.105	0.00	1.066	0.00	11.482	5.82	120.226	1.16	1258.925	0.00
0.011	0.00	0.120	0.00	1.259	0.00	13.183	6.02	138.036	0.87	1445.440	0.00
0.013	0.00	0.136	0.00	1.445	0.00	15.136	6.06	158.489	0.61	1659.587	0.00
0.015	0.00	0.155	0.00	1.660	0.00	17.378	5.91	181.970	0.36	1905.461	0.00
0.017	0.00	0.176	0.00	1.905	0.00	19.963	5.60	208.630	0.15	2187.762	0.00
0.020	0.00	0.200	0.00	2.188	0.15	22.909	5.14	238.893	0.10	2511.686	0.00
0.023	0.00	0.227	0.00	2.512	0.32	26.303	4.59	275.423	0.07	2884.032	0.00
0.026	0.00	0.257	0.00	2.884	0.59	30.200	4.01	316.228	0.05	3311.311	0.00
0.030	0.00	0.290	0.00	3.311	0.91	34.674	3.45	353.078	0.04	3801.894	0.00
0.035	0.00	0.327	0.00	3.802	1.32	39.811	2.98	418.899	0.03	4355.158	0.00
0.040	0.00	0.367	0.00	4.365	1.78	45.709	2.61	478.630	0.02	5011.872	0.00
0.046	0.00	0.410	0.00	5.012	2.30	52.481	2.36	549.541	0.01	5754.399	0.00
0.052	0.00	0.457	0.00	5.754	2.86	60.256	2.18	630.957	0.00	6609.934	0.00
0.060	0.00	0.508	0.00	6.607	3.42	69.183	2.03	724.436	0.00	7585.778	0.00
0.068	0.00	0.563	0.00	7.586	3.99	79.433	1.88	831.764	0.00	8709.636	0.00
0.079	0.00	0.622	0.00	8.710	4.55	91.201	1.69	954.968	0.00	10000.000	0.00
0.091	0.00	0.685	0.00	10.000	5.05	104.713	1.44	1096.478	0.00		
0.105	0.00	1.066	0.00	11.482	5.49	120.226		1258.925	0.00		

Mastersizer report of microcapsules R650

Particle Name: Défaut	Accessory Name: Hydro 2000MU (A)	Analysis model: General purpose	Sensitivity: Normal
Particle RI: 1.520	Absorption: 0.1	Size range: 0.020 to 2000.000 um	Obscuration: 15.98 %
Dispersant Name: Eau	Dispersant RI: 1.330	Weighted Residual: 0.563 %	Result Emulation: Off

Concentration: 0.0339 %Vol	Span : 3.464	Uniformity: 1.09	Result units: Volume
Specific Surface Area: 0.411 m ² /g	Surface Weighted Mean D[3,2]: 14.616 um	Vol. Weighted Mean D[4,3]: 36.471 um	

d(0.1): 6.566 um d(0.5): 22.410 um d(0.9): 84.183 um

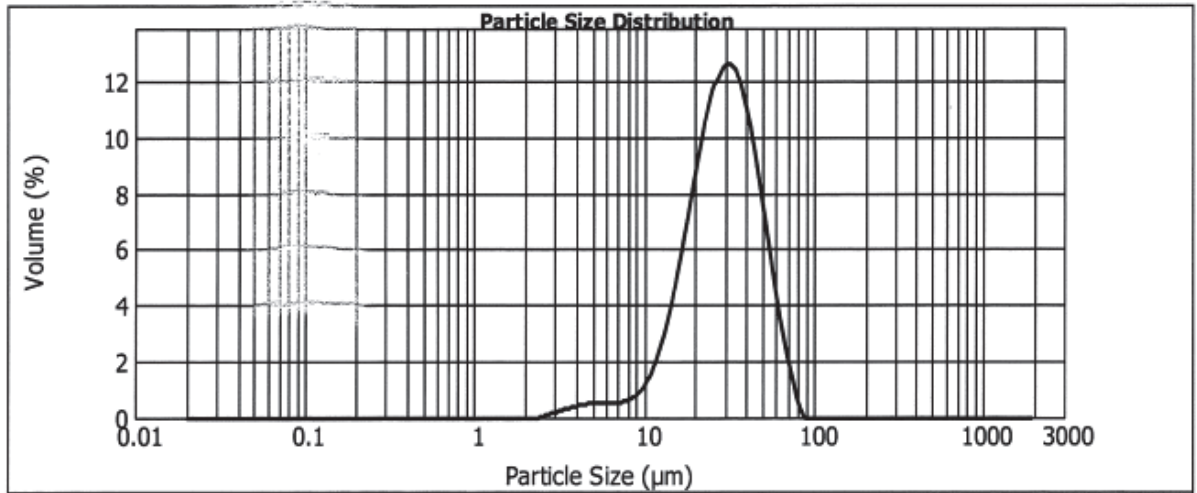


Size (µm)	Volume In %										
0.010	0.00	0.100	0.00	1.000	0.00	11.482	4.74	120.220	1.42	1258.925	0.00
0.011	0.00	0.120	0.00	1.250	0.00	13.183	5.07	138.030	1.29	1445.440	0.00
0.013	0.00	0.130	0.00	1.445	0.01	15.136	5.33	158.400	0.98	1658.587	0.00
0.015	0.00	0.150	0.00	1.660	0.12	17.378	5.51	181.970	0.78	1905.461	0.00
0.017	0.00	0.180	0.00	1.905	0.23	19.953	5.61	208.930	0.55	2187.782	0.00
0.020	0.00	0.200	0.00	2.188	0.36	22.909	5.60	239.880	0.33	2511.886	0.00
0.023	0.00	0.240	0.00	2.512	0.52	26.303	5.48	275.420	0.08	2884.032	0.00
0.026	0.00	0.275	0.00	2.884	0.72	30.200	5.24	316.220	0.01	3311.311	0.00
0.030	0.00	0.316	0.00	3.311	0.98	34.674	4.88	363.070	0.00	3801.894	0.00
0.035	0.00	0.363	0.00	3.802	1.24	39.811	4.42	416.800	0.00	4365.158	0.00
0.040	0.00	0.417	0.00	4.365	1.58	45.709	3.89	478.630	0.00	5011.872	0.00
0.046	0.00	0.479	0.00	5.012	1.97	52.481	3.35	549.541	0.00	5754.399	0.00
0.052	0.00	0.550	0.00	5.754	2.42	60.295	2.86	630.957	0.00	6606.934	0.00
0.060	0.00	0.631	0.00	6.607	2.90	69.183	2.45	724.430	0.00	7585.776	0.00
0.069	0.00	0.724	0.00	7.586	3.40	79.433	2.12	831.794	0.00	8709.636	0.00
0.079	0.00	0.832	0.00	8.710	3.88	91.201	1.85	954.900	0.00	10000.000	0.00
0.091	0.00	0.955	0.00	10.000	4.34	104.713	1.63	1096.470	0.00		
0.105	0.00	1.095	0.00	11.482		120.220		1258.925	0.00		

Mastersizer report of microcapsules S8

Concentration: 0.0584 %Vol	Span : 1.262	Uniformity: 0.395	Result units: Volume
Specific Surface Area: 0.258 m ² /g	Surface Weighted Mean D[3,2]: 23.262 um	Vol. Weighted Mean D[4,3]: 31.458 um	

d(0.1): 14.678 um d(0.5): 29.351 um d(0.9): 51.718 um



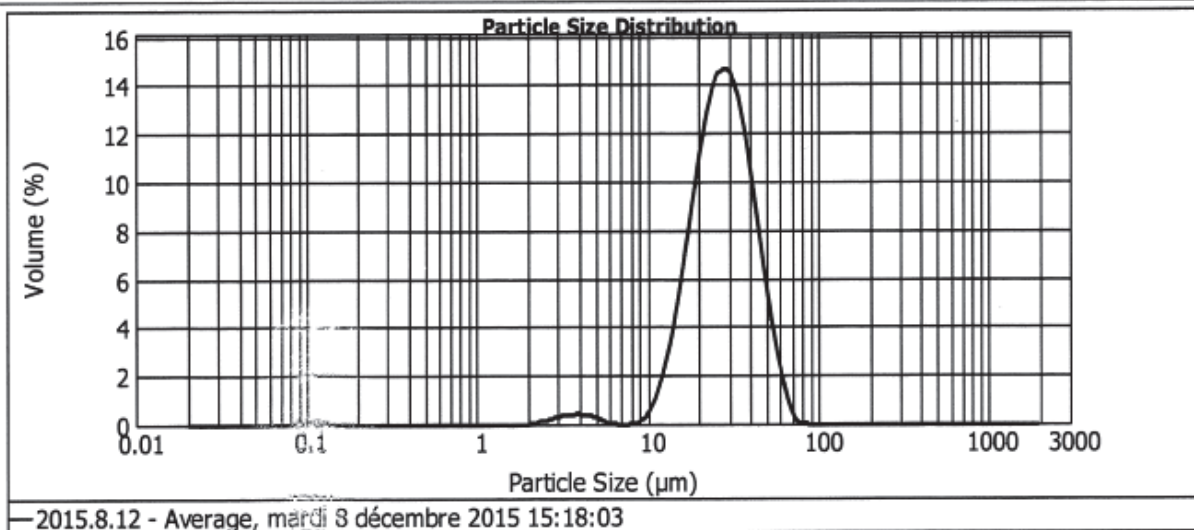
—2015.4.12_2nd measure - Average, vendredi 11 décembre 2015 14:59:29

Size (µm)	Volume In %										
0.010	0.00	0.105	0.00	1.066	0.00	11.482	2.10	120.226	0.00	1258.925	0.00
0.011	0.00	0.120	0.00	1.259	0.00	13.183	3.32	138.038	0.00	1445.440	0.00
0.013	0.00	0.138	0.00	1.445	0.00	15.136	6.73	158.489	0.00	1659.587	0.00
0.015	0.00	0.158	0.00	1.660	0.00	17.378	8.57	181.970	0.00	1905.461	0.00
0.017	0.00	0.182	0.00	1.905	0.00	19.963	10.15	208.930	0.00	2187.762	0.00
0.020	0.00	0.209	0.00	2.188	0.00	22.909	11.34	239.883	0.00	2511.886	0.00
0.023	0.00	0.240	0.00	2.512	0.10	26.303	9.16	275.423	0.00	2894.032	0.00
0.026	0.00	0.275	0.00	2.884	0.19	30.200	7.14	316.228	0.00	3311.311	0.00
0.030	0.00	0.316	0.00	3.311	0.29	34.674	4.95	363.078	0.00	3801.894	0.00
0.035	0.00	0.363	0.00	3.802	0.37	39.811	2.90	416.869	0.00	4355.158	0.00
0.040	0.00	0.417	0.00	4.365	0.44	45.709	1.37	478.630	0.00	5011.872	0.00
0.046	0.00	0.479	0.00	5.012	0.47	52.481	0.12	549.541	0.00	5754.399	0.00
0.052	0.00	0.550	0.00	5.754	0.47	60.256	0.00	630.957	0.00	6606.934	0.00
0.060	0.00	0.631	0.00	6.607	0.48	69.183	0.00	724.436	0.00	7585.776	0.00
0.069	0.00	0.724	0.00	7.586	0.56	79.433	0.00	831.764	0.00	8709.636	0.00
0.079	0.00	0.832	0.00	8.710	0.79	91.201	0.00	954.966	0.00	10000.000	0.00
0.091	0.00	0.958	0.00	10.000	1.26	104.713	0.00	1096.478	0.00		
0.105	0.00	1.096	0.00	11.482		120.226		1258.925			

Mastersizer report of microcapsules S12

Concentration: 0.0565 %Vol	Span : 1.069	Uniformity: 0.336	Result units: Volume
Specific Surface Area: 0.259 m ² /g	Surface Weighted Mean D[3,2]: 23.167 um	Vol. Weighted Mean D[4,3]: 29.202 um	

d(0.1): 15.972 um d(0.5): 27.480 um d(0.9): 45.340 um

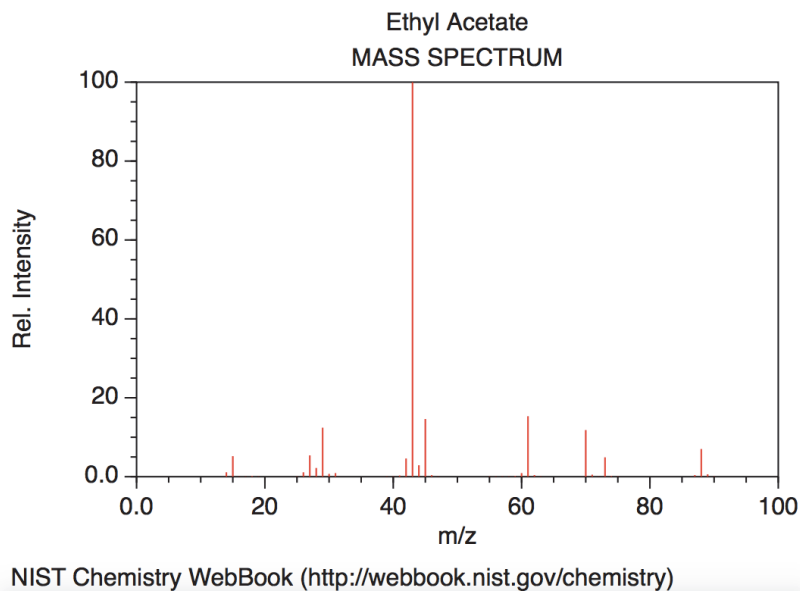


Size (µm)	Volume In %										
0.010	0.00	0.105	0.00	1.066	0.00	11.482	1.83	120.225	0.00	1258.925	0.00
0.011	0.00	0.120	0.00	1.259	0.00	13.183	3.58	138.038	0.00	1445.440	0.00
0.013	0.00	0.136	0.00	1.445	0.00	15.136	5.86	158.489	0.00	1659.587	0.00
0.015	0.00	0.153	0.00	1.660	0.00	17.378	8.46	181.970	0.00	1905.461	0.00
0.017	0.00	0.182	0.00	1.905	0.00	19.863	10.87	208.930	0.00	2187.762	0.00
0.020	0.00	0.209	0.00	2.188	0.08	22.909	12.61	239.883	0.00	2511.886	0.00
0.023	0.00	0.240	0.00	2.512	0.18	26.303	13.23	275.423	0.00	2884.032	0.00
0.026	0.00	0.275	0.00	2.884	0.28	30.200	12.55	316.228	0.00	3311.311	0.00
0.030	0.00	0.316	0.00	3.311	0.35	34.674	10.70	363.078	0.00	3801.894	0.00
0.035	0.00	0.363	0.00	3.802	0.38	39.811	8.10	416.869	0.00	4365.158	0.00
0.040	0.00	0.417	0.00	4.365	0.38	45.709	5.33	478.630	0.00	5011.872	0.00
0.046	0.00	0.478	0.00	5.012	0.30	52.481	2.91	549.541	0.00	5754.399	0.00
0.052	0.00	0.550	0.00	5.754	0.15	60.256	1.21	630.957	0.00	6606.934	0.00
0.060	0.00	0.631	0.00	6.607	0.00	69.183	0.15	724.436	0.00	7585.776	0.00
0.069	0.00	0.724	0.00	7.586	0.00	79.433	0.00	831.764	0.00	8709.636	0.00
0.079	0.00	0.832	0.00	8.710	0.00	91.201	0.00	954.968	0.00	10000.000	0.00
0.091	0.00	0.956	0.00	10.000	0.18	104.713	0.00	1096.478	0.00		
0.105	0.00	1.096	0.00	11.482	0.73	120.225	0.00	1258.925	0.00		

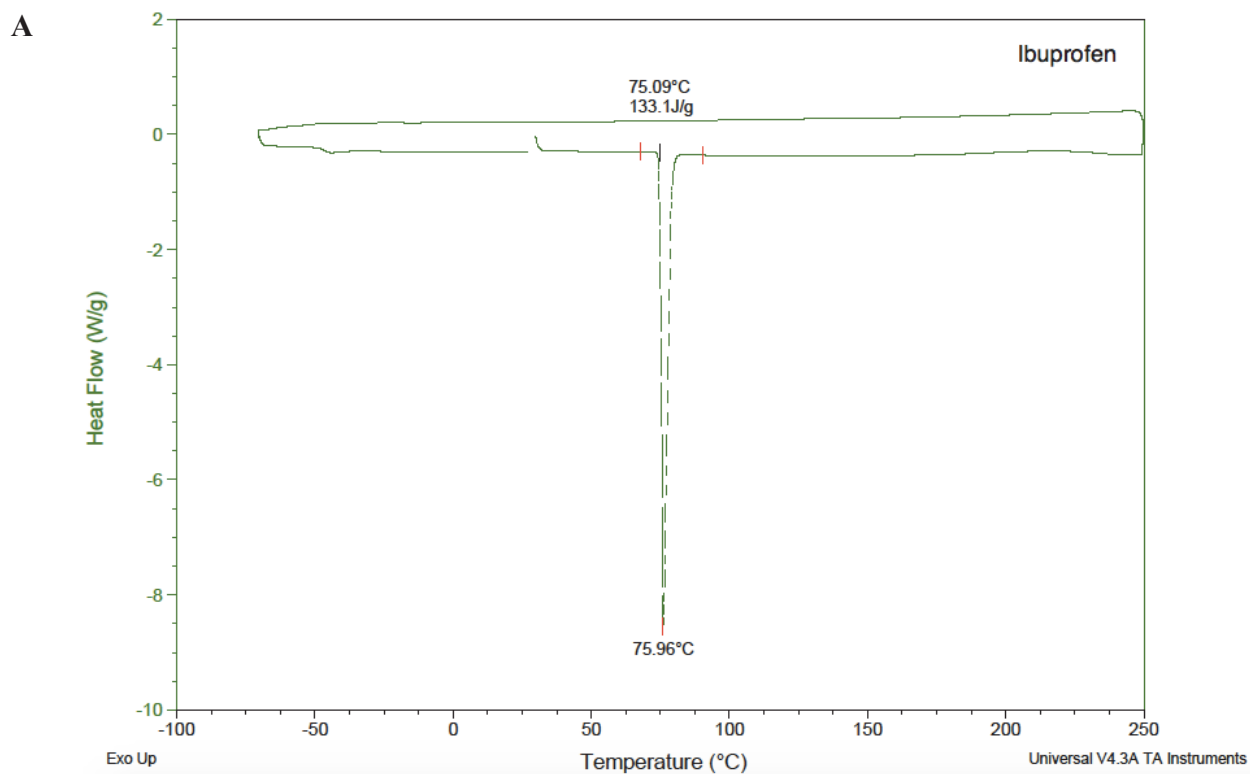
Appendix 3

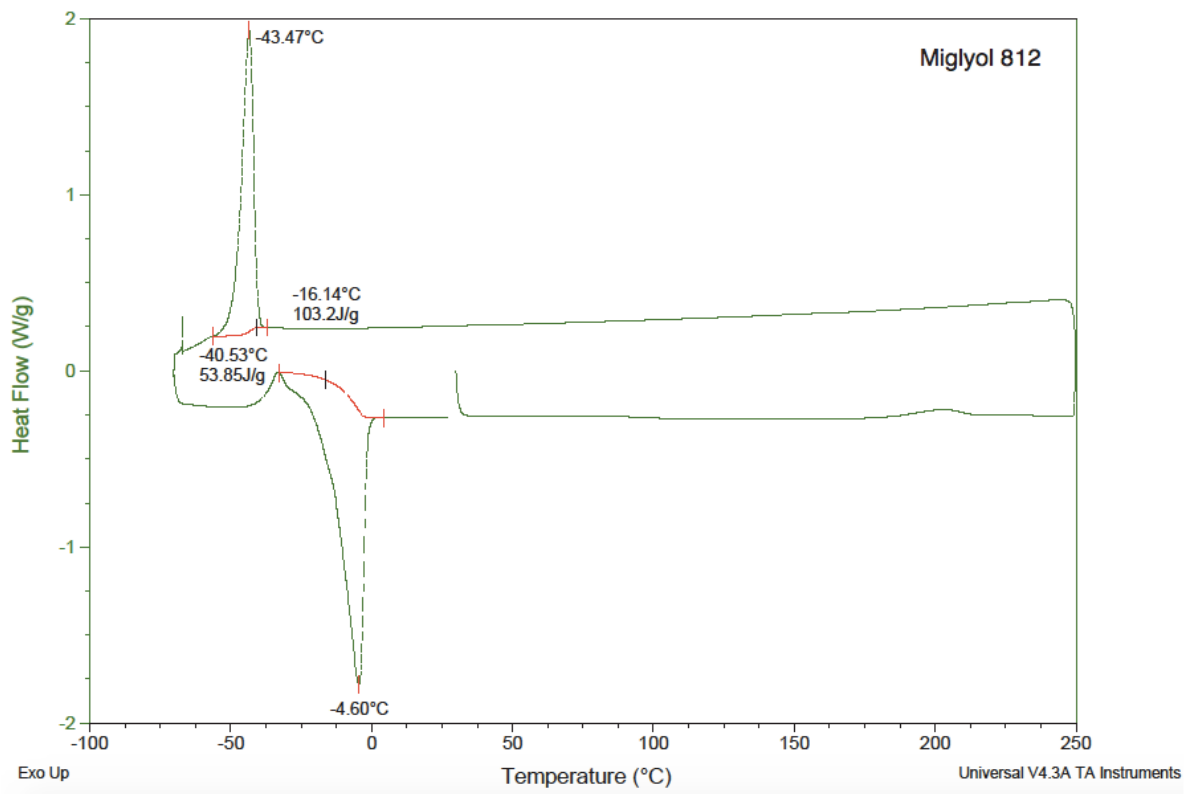
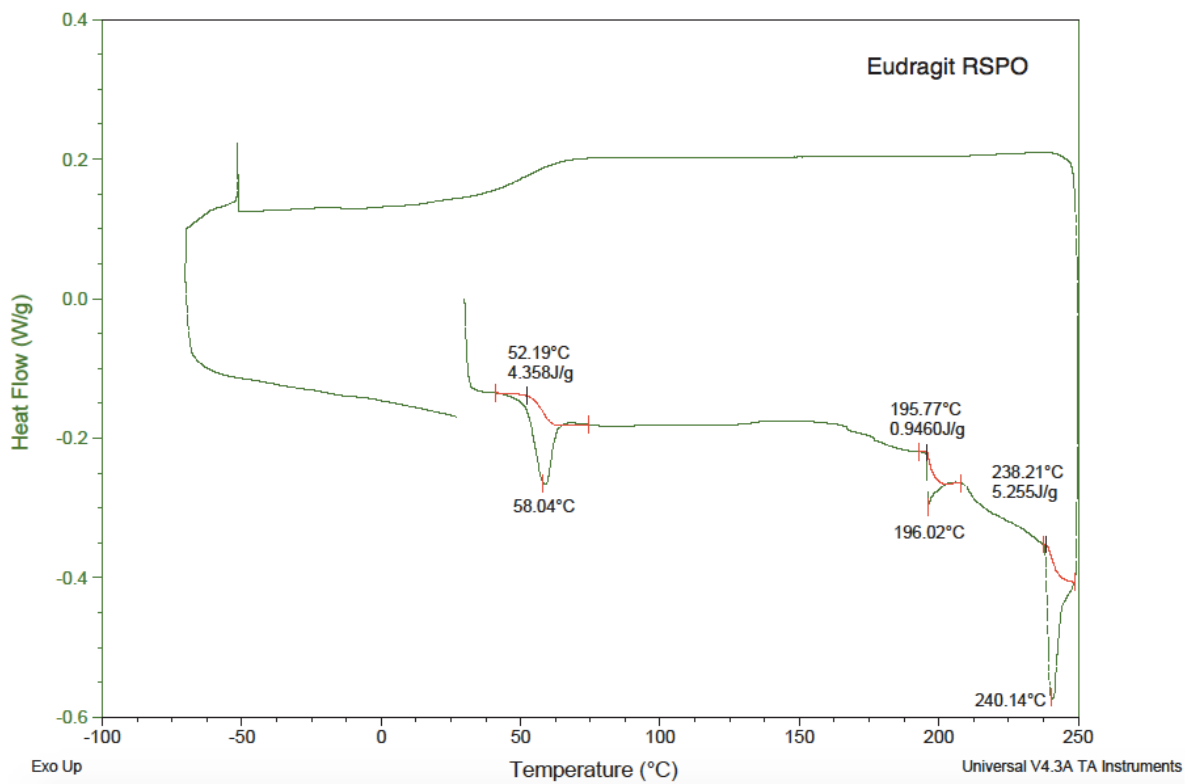
Physical and chemical properties of chemicals used for microencapsulation

The mass spectrum of ethyl acetate



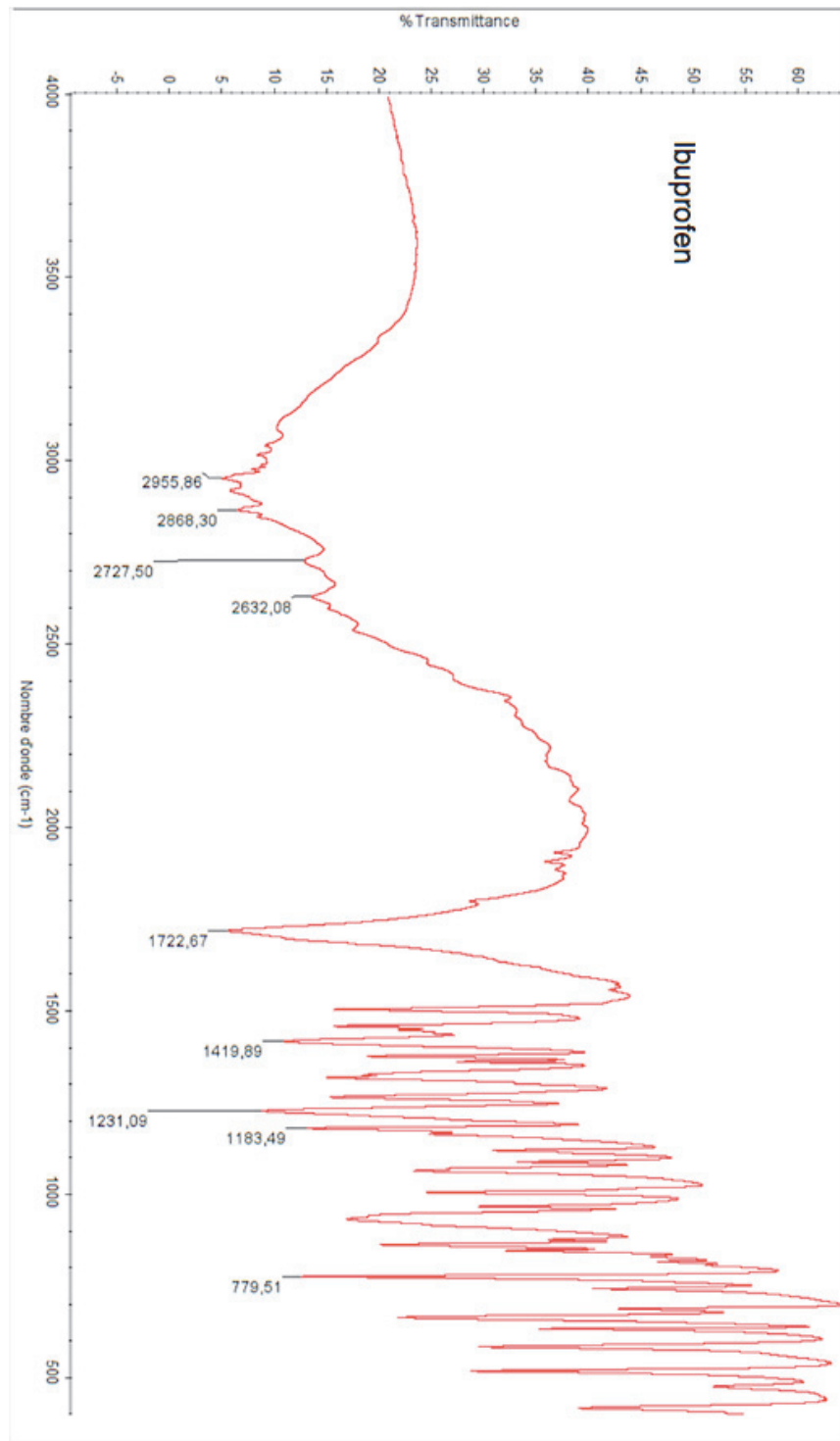
The DSC thermograms of Ibuprofen (A), Miglyol 812 (B), Eudragit RSPO (C)



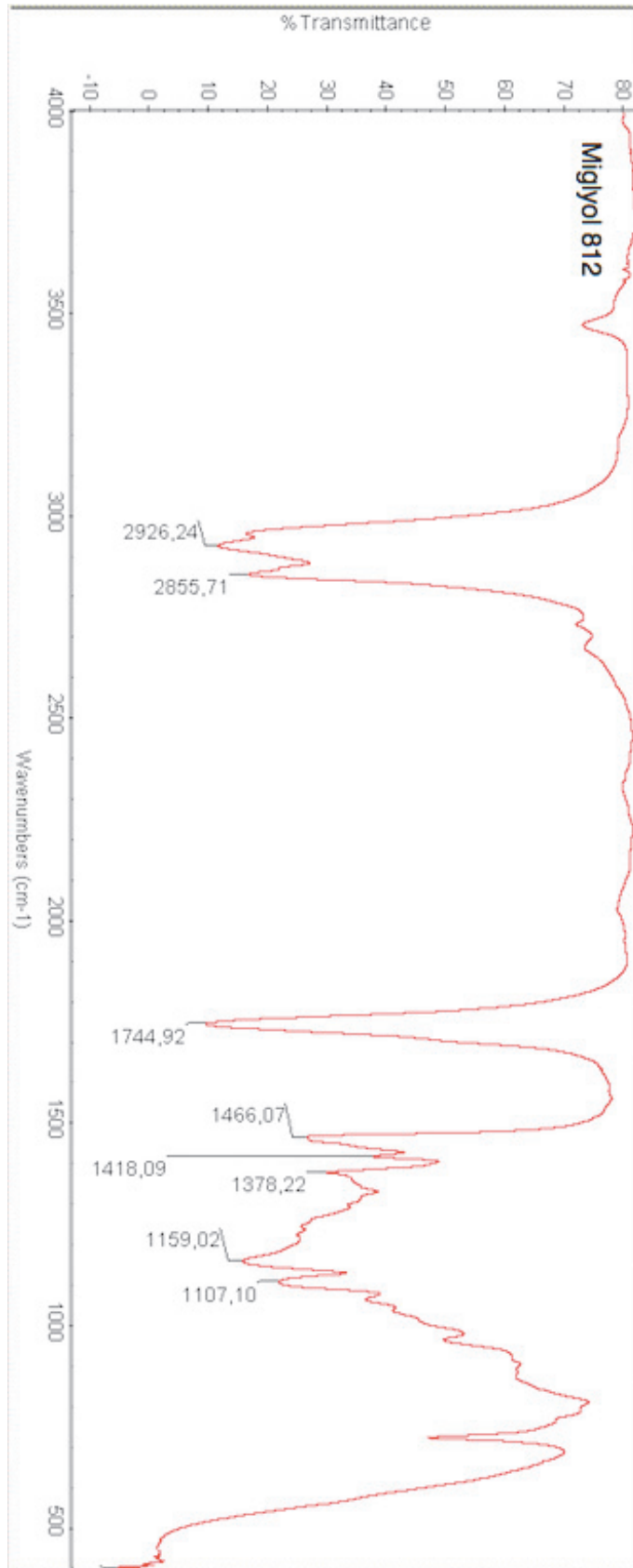
B**C**

**FTIR spectra of
Ibuprofen (A), Miglyol 812 (B), Eudragit RSPO (C), Quillaja Saponin (D)**

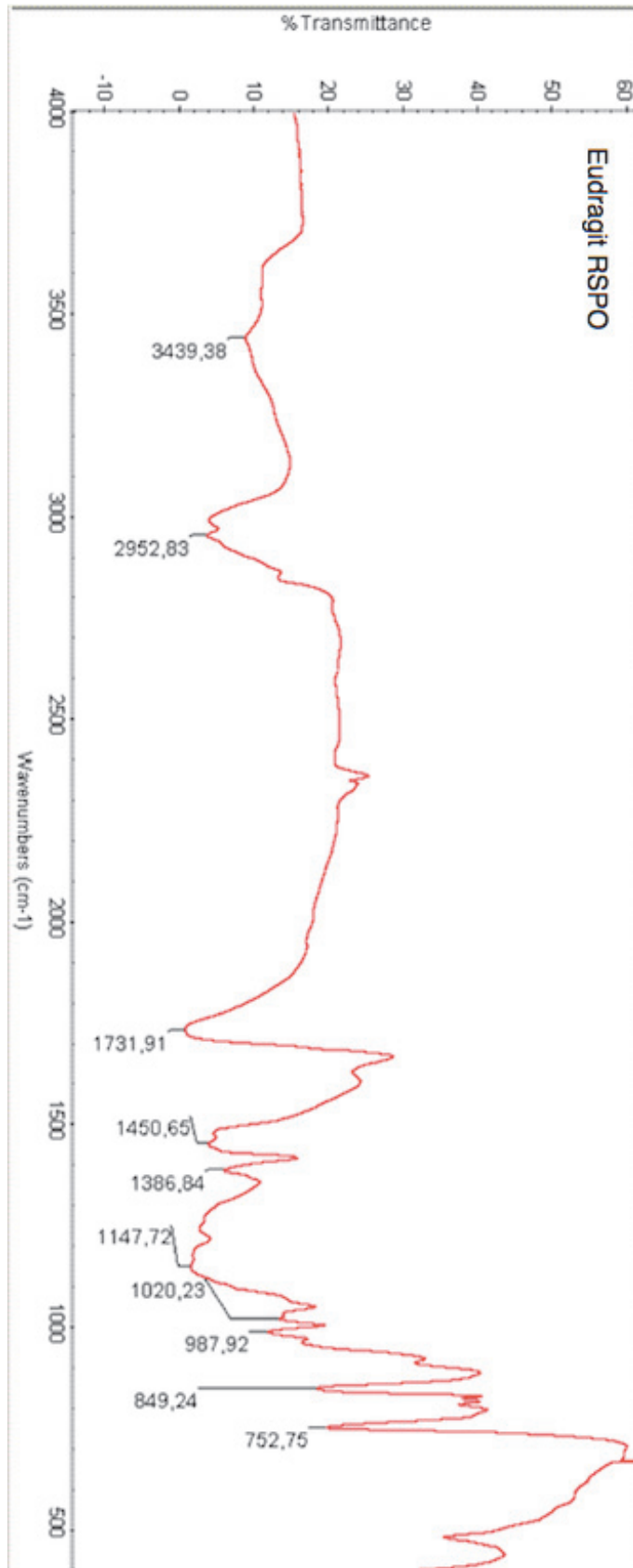
A



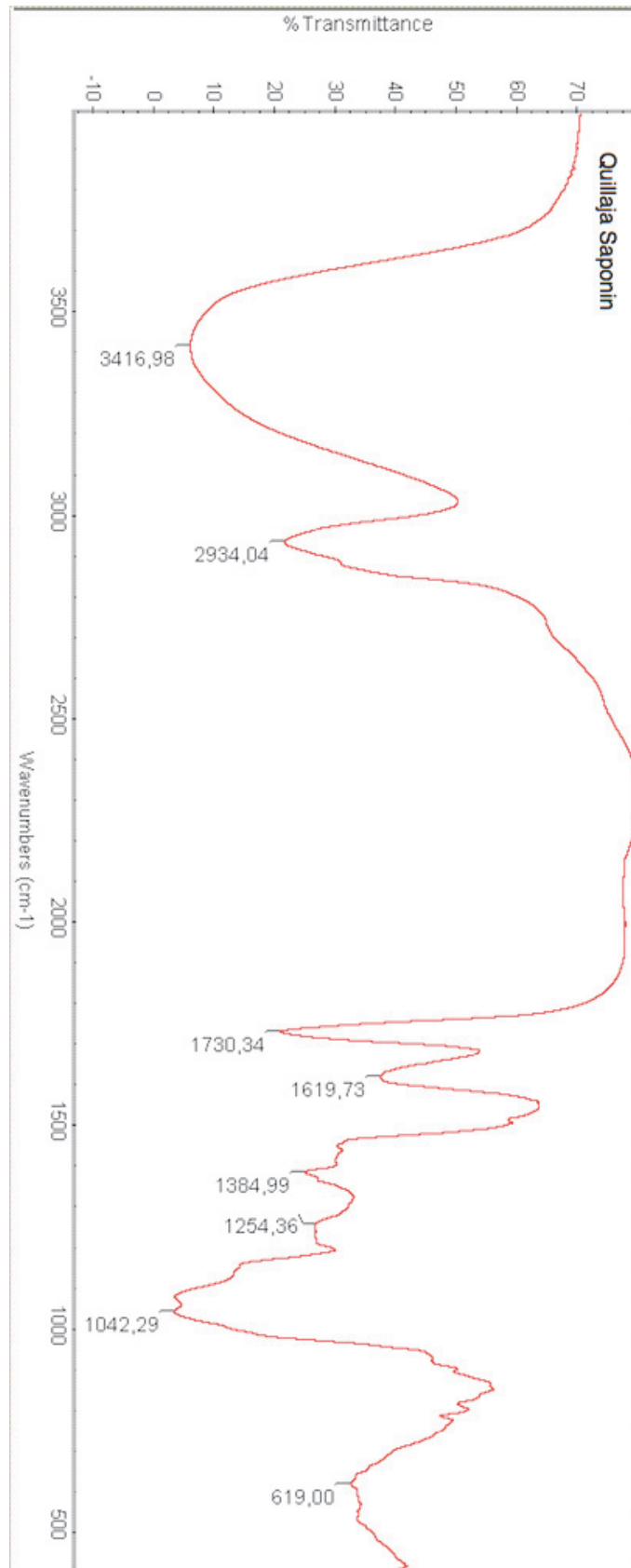
B



C



D



Appendix 4

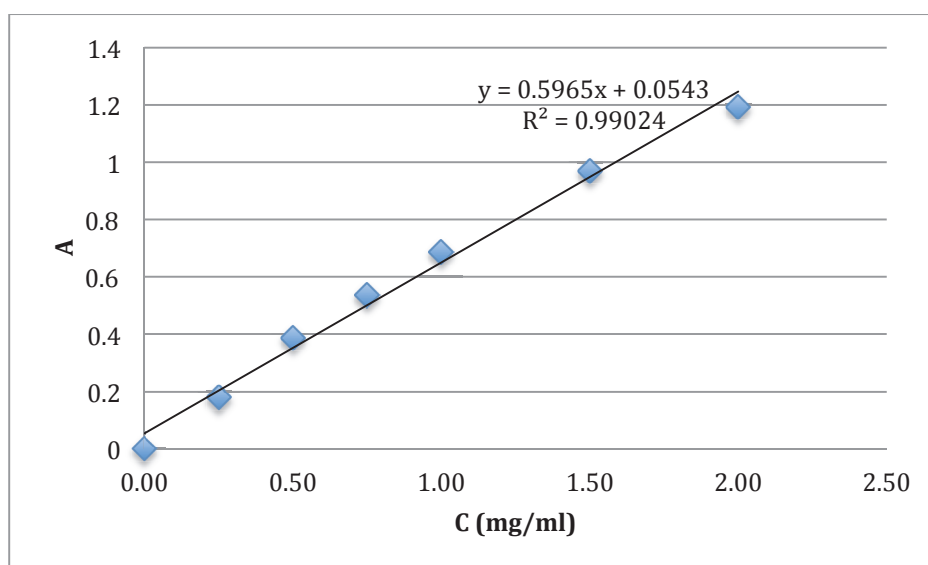
Procedure of calculating the drug loading ratio of the microcapsules

The calibration curve used to deduce ibuprofen concentration in heptane was built up from the absorbance values of 7 prepared standard solutions having concentrations varying from 0 to 2 mg/ml. The absorbance A of seven prepared calibration solutions were presented at Appendix Table 1.

Appendix Table 1: Absorbance of calibration solutions

C (mg/ ml)	0	0.25	0.5	0.75	1	1.5	2
A	0.0023	0.1799	0.3881	0.5365	0.6887	0.9697	1.1938

According to the data at Appendix Table 1, the calibration curve used to deduce ibuprofen concentration in heptane was built up, and the result was $y = 0.5965x + 0.0543$ (Appendix Figure 1).



Appendix Figure 1: Calibration curve expressing the influence of absorbance A on the concentration C of ibuprofen solutions in heptane

According to the absorbance of the collected solution A_i ($i = 1, 2, 3, \dots$), the concentration of ibuprofen in heptane C_i (mg/ml) was deduced from the calibration curve.

Then the content of ibuprofen in that solution ibu_i (mg) can be calculated by:

$$ibu_i \text{ (mg)} = C_i \times [55 - 5 \times (i - 1)] \quad (\text{Eq 0.1})$$

Then the mass ratio of extracted ibuprofen to microcapsules L_i (%) is defined as:

$$L_i \text{ (%) } = \frac{ibu_i}{300 \times \frac{55 - 5 \times (i - 1)}{55}} \times 100\% \quad (\text{Eq 0.2})$$

The results of A_i , C_i , ibu_i and L_i were presented at Appendix Table 2:

Appendix Table 2: Results of A_i , C_i , ibu_i and L_i according to the time of withdrawing the sonicated suspension

Calculations \ The time of sonication	45 minutes (i = 1)	60 minutes (i = 2)	75 minutes (i = 3)
The absorbance A_i (displayed on UV – Vis)	0.2312	0.2860	0.2847
The concentration of ibuprofen C_i (mg/ml), deduced from the calibration curve $y = 0.5965x + 0.0543$	0.2965	0.3885	0.3862
The content of ibuprofen ibu_i (mg) according to the equation (Eq 0.1)	16.3095	19.4234	17.3783
The mass ratio of extracted ibuprofen/microcapsule L_i (%) according to the equation (Eq 0.2)	5.44	7.12	7.10

Appendix 5

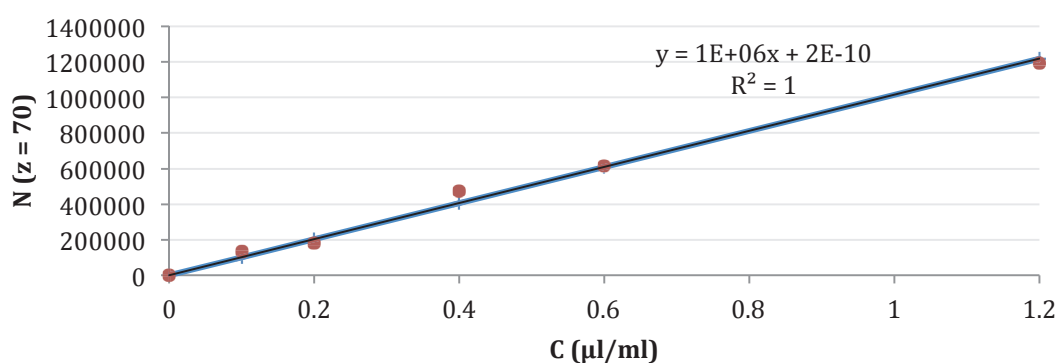
Procedure of calculating the mass ratio of the residual ethyl acetate in the microcapsules

The change in the number of ion $z = 70$ over the concentration of ethyl acetate in acetone was presented at Appendix Table 3:

Appendix Table 3: Number of ion $z=70$ in calibration solutions

C ($\mu\text{l/ml}$)	0	0.1	0.2	0.4	0.6	1.2
N ($z = 70$)	0	133697	180443	472408	616336	1195244

According to the data in Appendix Table 3, the calibration curve constructed was $y = 10^6x$ (Appendix Figure 2).



Appendix Figure 2: Calibration curve expressing the influence of the number of ion $z=70$ on the concentration of ethyl acetate in acetone

The solution containing 60 (mg) of dried microcapsules completely dissolved in 2 (ml) of acetone had 124598 ions $z = 70$, so according to the calibration curve, the concentration of ethyl acetate calculated was equal to 0.1246 ($\mu\text{l/ml}$). Since the density of ethyl acetate is 0.9 (kg/l), the content of ethyl acetate was equal to 0.2243 (mg). Then the mass ratio of residual ethyl acetate in the microcapsules was equal to 0.378 wt%.

Appendix 6

Working conditions of the HPLC system SHIMADZU

Appendix Table 4: Working conditions of the HPLC system SHIMADZU

Manufacture	SHIMADZU
Detector	SPD - 20A
Pumping system	LC - 20AT
Column	C18 (Agilent), pore size 3.5 μm
Eluent	33% A ($\text{H}_2\text{O} + 1.2\% \text{H}_3\text{PO}_4$); 67% B Methanol
Flow	1 ml/min
Injection volume	20 μl
Wavelength	263 nm

Appendix 7

Procedure of calculating the weight percentage of ibuprofen released from the microcapsule-treated fabric into the receptor fluid

(to investigate the influence of the textile material type on the active release capability of the microcapsule-treated fabric)

The content of microcapsules on the fabric sample in the drug release *in vitro* experiment, which was coded by M_{mc_fbr} (mg), was calculated by:

$$M_{mc_fbr} = \frac{M_2 - M_1}{2.5^2} (mg) \quad (Eq\ 0.3)$$

The content of ibuprofen on the fabric sample m_{Ibu_fbr} (mg) was calculated by:

$$m_{Ibu_fbr} = M_{mc_fbr} \times \frac{L}{100} (mg) \quad (Eq\ 0.4)$$

In which L(%) was the drug loading ratio of microcapsule.

Because at predetermined times (8, 24, 32 and 48 hours), 3 ml of the receptor fluid was taken out to determine the ibuprofen concentration in it and was compensated by 3 ml of fresh phosphate buffer solution, if the ibuprofen concentration in the receptor fluid after 8 hours of release, which was determined by HPLC, was coded as C_{rl_8} (mg/ml), then the content of ibuprofen in the receptor fluid at that time m_{Ibu_8} (mg) was calculated by:

$$m_{Ibu_8} = C_{rl_8} \times 23 (mg) \quad (Eq\ 0.5)$$

Therefore, the weight percentage of ibuprofen released from the microcapsule-treated fabric into the receptor fluid after 8 hours of release Ibu_{rl_8} (%) could be calculated by:

$$Ibu_{rl_8}(\%) = \frac{m_{Ibu_8}}{m_{Ibu_fbr}} \times 100\% \quad (Eq\ 0.6)$$

Similarly, if the ibuprofen concentration in the receptor fluid after 24 hours of release was coded as C_{rl_24} (mg/ml), then the content of ibuprofen in the receptor fluid at that time m_{Ibu_24} (mg) was calculated by:

$$m_{Ibu_24} = C_{rl_8} \times 3 + C_{rl_24} \times 23 (mg) \quad (Eq\ 0.7)$$

And the weight percentage of ibuprofen released from the microcapsule-treated fabric into the receptor fluid after 24 hours of release Ibu_{rl_24} (%) could be calculated by:

$$Ibu_{rl_24}(\%) = \frac{m_{Ibu_24}}{m_{Ibu_fbr}} \times 100\% \quad (Eq\ 0.8)$$

Similarly, when the ibuprofen concentration in the receptor fluid after 32 hours of release was C_{rl_32} (mg/ml), the correlative content of ibuprofen m_{Ibu_32} (mg) was calculated by:

$$m_{Ibu_32} = (C_{rl_24} + C_{rl_8}) \times 3 + C_{rl_32} \times 23 (mg) \quad (Eq\ 0.9)$$

And the weight percentage of ibuprofen in microcapsule-treated fabric dissolved into the receptor fluid after 32 hours of release Ibu_{rl_32} (%) could be calculated by:

$$Ibu_{rl_32}(\%) = \frac{m_{Ibu_32}}{m_{Ibu_fbr}} \times 100\% \quad (Eq\ 0.10)$$

Similarly, when the ibuprofen concentration in the receptor fluid after 48 hours of release was C_{rl_48} (mg/ml), the correlative content of ibuprofen m_{Ibu_48} (mg) was calculated by:

$$m_{Ibu_48} = (C_{rl_32} + C_{rl_24} + C_{rl_8}) \times 3 + C_{rl_48} \times 23 \text{ (mg)} \quad (Eq\ 0.11)$$

And the weight percentage of ibuprofen in microcapsule-treated fabric dissolved into the receptor fluid after 48 hours of release Ibu_{rl_48} (%) could be calculated by:

$$Ibu_{rl_48}(\%) = \frac{m_{Ibu_48}}{m_{Ibu_fbr}} \times 100\% \quad (Eq\ 0.12)$$

Appendix 8

The number of microcapsules having certain diameters in the microcapsule lot C0.075

The mean diameter d corresponding to the volume ratio (%) was presented at Appendix 2

The volume of a microcapsule having diameter of d : $V = \frac{4}{3} \pi \left(\frac{d}{2}\right)^3$

The total volume of all microcapsules having diameters of d :

$$\sum V = \text{The total volume of the whole lot} \times \text{The volume ratio (\%)}$$

The number of microcapsules having diameter of d : $n = \frac{\sum V}{V}$

Diameter (μm)	Volume ratio (%)	Volume of one microcapsule (μm^3)	Total volume of all microcapsules (μm^3)	Number of microcapsules
1.66	0.01	2.393881573	155300000	64873719
1.905	0.14	3.617956474	2174200000	600946975
2.188	0.27	5.481764205	4193100000	764917980
2.512	0.42	8.295399438	6522600000	786291251
2.884	0.6	12.55348089	9318000000	742264244
3.311	0.81	18.9957279	12579300000	662217319
3.802	1.06	28.76171213	16461800000	572351184
4.365	1.34	43.52423453	20810200000	478129029
5.012	1.67	65.88879797	25935100000	393619262
5.754	2.06	99.69834989	31991800000	320885953
6.607	2.49	150.9354723	38669700000	256200212
7.586	2.96	228.4635458	45968800000	201208468
8.71	3.45	345.8062694	53578500000	154937908
10	3.93	523.3333333	61032900000	116623376
11.482	4.4	792.1930451	68332000000	86256753
13.183	4.82	1199.005441	74854600000	62430576
15.136	5.2	1814.728897	80756000000	44500311
17.378	5.5	2746.488446	85415000000	31099712
19.953	5.73	4157.219975	88986900000	21405386
22.909	5.86	6292.117069	91005800000	14463463
26.303	5.88	9523.448828	91316400000	9588585
30.2	5.76	14414.48819	89452800000	6205756
34.674	5.5	21816.7589	85415000000	3915109
39.811	5.09	33020.80508	79047700000	2393876
45.709	4.56	49978.53918	70816800000	1416944
52.481	3.96	75645.77956	61498800000	812984
60.256	3.34	114493.0943	51870200000	453042

69.183	2.76	173291.224	42862800000	247345
79.433	2.25	262289.7343	34942500000	133221
91.201	1.81	396987.8348	28109300000	70806
104.713	1.44	600869.5614	22363200000	37218
120.226	1.12	909439.0368	17393600000	19126
138.038	0.86	1376494.158	13355800000	9703
158.489	0.66	2083414.936	10249800000	4920
181.97	0.5	3153390.703	7765000000	2462
208.93	0.4	4772883.242	6212000000	1302
239.883	0.33	7223984.613	5124900000	709
275.423	0.28	10933998.53	4348400000	398
316.228	0.25	16549289.82	3882500000	235
363.078	0.21	25048296.83	3261300000	130
416.869	0.18	37912043.95	2795400000	74
478.63	0.09	57382325.73	1397700000	24
549.541	0.04	86851774.63	621200000	7

Appendix 9

The detailed calculations of the total cross section area of all microcapsules in 1cm² of fabric

The diameter d of microcapsule presented at Appendix 2

The cross section area of one microcapsule: $S = \pi \times \frac{d^2}{4}$

The number of microcapsules in 1 cm² of fabric:

$$n = \frac{\text{The content of microcapsules in 1 cm}^2 \text{ of fabric } \left(\frac{\text{mg}}{\text{cm}^2}\right) \times \text{the number of microcapsules in the whole lot}}{\text{The mass of the dried whole lot}}$$

The total cross section area of all microcapsules having diameter of d in 1cm² of fabric:

$$\sum S = n \times S$$

The total cross section area of all microcapsules in 1cm² of fabric was calculated by equation (Eq 3.7).

1. Application of the microcapsules by the coating technique

Fabric B1 (loop length of 2.81 mm)			
Microcapsule diameter (μm)	Cross section area of one microcapsule (μm ²)	Number of microcapsules in 1 cm ² of fabric	Total cross section area of all microcapsules (μm ²)
1.66	2.163146	87294.08	188829.8313
1.905	2.848784625	808634.25	2303624.819
2.188	3.75806504	1029273.63	3868077.258
2.512	4.95346304	1058033.51	5240929.873
2.884	6.52920296	998790.77	6521307.628
3.311	8.605735985	891079.62	7668395.989
3.802	11.34733514	770155.75	8739215.445
4.365	14.95678163	643370.42	9622750.9
5.012	19.71931304	529654.08	10444414.57
5.754	25.99018506	431784.14	11222149.66
6.607	34.26717247	344743.01	11813368.02
7.586	45.17470586	270746.11	12230876.08

8.71	59.5533185	208484.45	12415940.8
10	78.5	156928.41	12318880.54
11.482	103.4915143	116067.09	12011958.61
13.183	136.4263189	84006.58	11460708.84
15.136	179.8423194	59879.62	10768889.43
17.378	237.0659839	41847.77	9920683.393
19.953	312.5259341	28803.09	9001711.971
22.909	411.9854906	19462.04	8018076.159
26.303	543.1005301	12902.40	7007300.375
30.2	715.9514	8350.47	5978527.534
34.674	943.7947267	5268.17	4972072.331
39.811	1244.158841	3221.20	4007683.245
45.709	1640.110455	1906.64	3127100.333
52.481	2162.090458	1093.95	2365221.279
60.256	2850.166646	609.61	1737500.194
69.183	3757.235679	332.83	1250513.501
79.433	4953.037169	179.26	887892.211
91.201	6529.333585	95.28	622096.3709
104.713	8607.37771	50.08	431062.8373
120.226	11346.61849	25.74	292010.3991
138.038	14957.77421	13.06	195289.3169
158.489	19718.22905	6.62	130533.9571
181.97	25993.76851	3.31	86128.90037
208.93	34266.61975	1.75	60011.96956
239.883	45171.92515	0.95	43121.4307
275.423	59548.39571	0.54	31866.65805
316.228	78500.11617	0.32	24780.97449

363.078	103483.1228	0.18	18130.01041
416.869	136417.1141	0.10	13534.79237
478.63	179833.0414	0.03	5894.15139
549.541	237066.3189	0.01	2281.595149
Total cross section area of all microcapsules in 1 cm ² of fabric (S _{mc})			209071344.2
Fabric B2 (loop length of 2.83 mm)			
Microcapsule diameter (μm)	Cross section area of one microcapsule (μm ²)	Number of microcapsules in 1 cm ² of fabric	Total cross section area of all microcapsules (μm ²)
1.66	2.163146	89681.43	193994.0241
1.905	2.848784625	830749.10	2366625.26
2.188	3.75806504	1057422.61	3973862.962
2.512	4.95346304	1086969.03	5384260.892
2.884	6.52920296	1026106.09	6699654.924
3.311	8.605735985	915449.22	7878114.31
3.802	11.34733514	791218.28	8978218.958
4.365	14.95678163	660965.57	9885917.691
5.012	19.71931304	544139.27	10730052.55
5.754	25.99018506	443592.74	11529057.43
6.607	34.26717247	354171.17	12136444.67
7.586	45.17470586	278150.59	12565370.9
8.71	59.5533185	214186.16	12755496.85
10	78.5	161220.15	12655782.14
11.482	103.4915143	119241.34	12340466.4
13.183	136.4263189	86304.03	11774140.83
15.136	179.8423194	61517.23	11063401.27
17.378	237.0659839	42992.24	10191998.16
19.953	312.5259341	29590.81	9247894.344

22.909	411.9854906	19994.29	8237357.671
26.303	543.1005301	13255.26	7198938.792
30.2	715.9514	8578.84	6142030.665
34.674	943.7947267	5412.25	5108050.528
39.811	1244.158841	3309.29	4117286.949
45.709	1640.110455	1958.78	3212621.507
52.481	2162.090458	1123.87	2429906.284
60.256	2850.166646	626.29	1785018.035
69.183	3757.235679	341.93	1284713.038
79.433	4953.037169	184.16	912174.6377
91.201	6529.333585	97.88	639109.708
104.713	8607.37771	51.45	442851.7139
120.226	11346.61849	26.44	299996.4148
138.038	14957.77421	13.41	200630.1662
158.489	19718.22905	6.80	134103.8512
181.97	25993.76851	3.40	88484.38754
208.93	34266.61975	1.80	61653.20059
239.883	45171.92515	0.98	44300.73261
275.423	59548.39571	0.55	32738.15999
316.228	78500.11617	0.32	25458.69436
363.078	103483.1228	0.18	18625.83709
416.869	136417.1141	0.10	13904.94721
478.63	179833.0414	0.03	6055.346969
549.541	237066.3189	0.01	2343.993114
Total cross section area of all microcapsules in 1 cm ² of fabric (S_{mc})			214789109.8

Fabric B3 (loop length of 2.87 mm)			
Microcapsule diameter (μm)	Cross section area of one microcapsule (μm^2)	Number of microcapsules in 1 cm^2 of fabric	Total cross section area of all microcapsules (μm^2)
1.66	2.163146	89525.73	193657.2289
1.905	2.848784625	829306.83	2362516.535
2.188	3.75806504	1055586.81	3966963.894
2.512	4.95346304	1085081.93	5374913.217
2.884	6.52920296	1024324.66	6688023.578
3.311	8.605735985	913859.90	7864437.028
3.802	11.34733514	789844.63	8962631.773
4.365	14.95678163	659818.06	9868754.639
5.012	19.71931304	543194.58	10711423.98
5.754	25.99018506	442822.61	11509041.71
6.607	34.26717247	353556.29	12115374.45
7.586	45.17470586	277667.69	12543556.02
8.71	59.5533185	213814.31	12733351.89
10	78.5	160940.26	12633810.3
11.482	103.4915143	119034.32	12319041.98
13.183	136.4263189	86154.19	11753699.61
15.136	179.8423194	61410.43	11044193.97
17.378	237.0659839	42917.60	10174303.72
19.953	312.5259341	29539.43	9231838.972
22.909	411.9854906	19959.58	8223056.703
26.303	543.1005301	13232.25	7186440.634
30.2	715.9514	8563.94	6131367.417
34.674	943.7947267	5402.85	5099182.384
39.811	1244.158841	3303.55	4110138.881

45.709	1640.110455	1955.38	3207044.039
52.481	2162.090458	1121.92	2425687.696
60.256	2850.166646	625.20	1781919.045
69.183	3757.235679	341.34	1282482.633
79.433	4953.037169	183.84	910591.0012
91.201	6529.333585	97.71	638000.1425
104.713	8607.37771	51.36	442082.8741
120.226	11346.61849	26.39	299475.5876
138.038	14957.77421	13.39	200281.8499
158.489	19718.22905	6.79	133871.0321
181.97	25993.76851	3.40	88330.76881
208.93	34266.61975	1.80	61546.16379
239.883	45171.92515	0.98	44223.82161
275.423	59548.39571	0.55	32681.32291
316.228	78500.11617	0.32	25414.49524
363.078	103483.1228	0.18	18593.50057
416.869	136417.1141	0.10	13880.80668
478.63	179833.0414	0.03	6044.834214
549.541	237066.3189	0.01	2339.923682
Total cross section area of all microcapsules in 1 cm ² of fabric (S _{mc})			214416212.1
Fabric B4 (loop length of 2.96 mm)			
Microcapsule diameter (μm)	Cross section area of one microcapsule (μm ²)	Number of microcapsules in 1 cm ² of fabric	Total cross section area of all microcapsules (μm ²)
1.66	2.163146	93106.76	201403.5181
1.905	2.848784625	862479.10	2457017.197
2.188	3.75806504	1097810.28	4125642.45
2.512	4.95346304	1128485.20	5589909.745

2.884	6.52920296	1065297.64	6955544.521
3.311	8.605735985	950414.30	8179014.509
3.802	11.34733514	821438.42	9321137.044
4.365	14.95678163	686210.78	10263504.82
5.012	19.71931304	564922.36	11139880.94
5.754	25.99018506	460535.52	11969403.38
6.607	34.26717247	367698.54	12599989.43
7.586	45.17470586	288774.39	13045298.27
8.71	59.5533185	222366.89	13242685.97
10	78.5	167377.87	13139162.71
11.482	103.4915143	123795.69	12811803.66
13.183	136.4263189	89600.36	12223847.6
15.136	179.8423194	63866.85	11485961.73
17.378	237.0659839	44634.31	10581275.87
19.953	312.5259341	30721.01	9601112.53
22.909	411.9854906	20757.96	8551978.971
26.303	543.1005301	13761.54	7473898.26
30.2	715.9514	8906.50	6376622.114
34.674	943.7947267	5618.97	5303149.68
39.811	1244.158841	3435.69	4274544.436
45.709	1640.110455	2033.60	3335325.801
52.481	2162.090458	1166.79	2522715.204
60.256	2850.166646	650.21	1853195.807
69.183	3757.235679	354.99	1333781.938
79.433	4953.037169	191.20	947014.6413
91.201	6529.333585	101.62	663520.1482
104.713	8607.37771	53.42	459766.1891

120.226	11346.61849	27.45	311454.6111
138.038	14957.77421	13.93	208293.1239
158.489	19718.22905	7.06	139225.8733
181.97	25993.76851	3.53	91863.99956
208.93	34266.61975	1.87	64008.01034
239.883	45171.92515	1.02	45992.77448
275.423	59548.39571	0.57	33988.57583
316.228	78500.11617	0.34	26431.07505
363.078	103483.1228	0.19	19337.24059
416.869	136417.1141	0.11	14436.03895
478.63	179833.0414	0.03	6286.627583
549.541	237066.3189	0.01	2433.520629
Total cross section area of all microcapsules in 1 cm ² of fabric (S _{mc})			222992860.6
Fabric B5 (loop length of 3.05 mm)			
Microcapsule diameter (μm)	Cross section area of one microcapsule (μm ²)	Number of microcapsules in 1 cm ² of fabric	Total cross section area of all microcapsules (μm ²)
1.66	2.163146	94767.53	204996
1.905	2.848784625	877863.34	2500843.591
2.188	3.75806504	1117392.18	4199232.505
2.512	4.95346304	1148614.26	5689618.28
2.884	6.52920296	1084299.61	7079612.205
3.311	8.605735985	967367.06	8324905.515
3.802	11.34733514	836090.61	9487400.358
4.365	14.95678163	698450.89	10446577.37
5.012	19.71931304	574999.02	11338585.62
5.754	25.99018506	468750.20	12182904.44
6.607	34.26717247	374257.27	12824738.4

7.586	45.17470586	293925.33	13277990.32
8.71	59.5533185	226333.30	13478898.87
10	78.5	170363.43	13373529.05
11.482	103.4915143	126003.87	13040330.81
13.183	136.4263189	91198.59	12441887.24
15.136	179.8423194	65006.05	11690839.53
17.378	237.0659839	45430.46	10770016.57
19.953	312.5259341	31268.99	9772369.833
22.909	411.9854906	21128.23	8704522.631
26.303	543.1005301	14007.01	7607211.941
30.2	715.9514	9065.37	6490363.423
34.674	943.7947267	5719.19	5397743.208
39.811	1244.158841	3496.97	4350790.491
45.709	1640.110455	2069.87	3394818.792
52.481	2162.090458	1187.61	2567713.469
60.256	2850.166646	661.80	1886251.697
69.183	3757.235679	361.32	1357572.921
79.433	4953.037169	194.61	963906.7642
91.201	6529.333585	103.43	675355.5132
104.713	8607.37771	54.37	467967.1468
120.226	11346.61849	27.94	317010.1003
138.038	14957.77421	14.17	212008.4974
158.489	19718.22905	7.19	141709.278
181.97	25993.76851	3.60	93502.59933
208.93	34266.61975	1.90	65149.73628
239.883	45171.92515	1.04	46813.15841
275.423	59548.39571	0.58	34594.83805

316.228	78500.11617	0.34	26902.53235
363.078	103483.1228	0.19	19682.1635
416.869	136417.1141	0.11	14693.53797
478.63	179833.0414	0.04	6398.763638
549.541	237066.3189	0.01	2476.927909
Total cross section area of all microcapsules in 1 cm ² of fabric (S _{mc})			226970436.7

2. Application of the microcapsules by the impregnating technique

Fabric B3 (loop length of 2.87 mm)			
Microcapsule diameter (μm)	Cross section area of one microcapsule (μm ²)	Number of microcapsules in 1 cm ² of fabric	Total cross section area of all microcapsules (μm ²)
1.66	2.163146	304854.5803	204996
1.905	2.848784625	2823970.025	2500843.591
2.188	3.75806504	3594502.572	4199232.505
2.512	4.95346304	3694939.847	5689618.28
2.884	6.52920296	3488048.135	7079612.205
3.311	8.605735985	3111891.625	8324905.515
3.802	11.34733514	2689592.684	9487400.358
4.365	14.95678163	2246823.933	10446577.37
5.012	19.71931304	1849695.636	11338585.62
5.754	25.99018506	1507907.27	12182904.44
6.607	34.26717247	1203936.036	12824738.4
7.586	45.17470586	945518.8328	13277990.32
8.71	59.5533185	728084.2173	13478898.87
10	78.5	548036.5685	13373529.05
11.482	103.4915143	405337.7337	13040330.81
13.183	136.4263189	293373.7627	12441887.24

15.136	179.8423194	209115.8615	11690839.53
17.378	237.0659839	146143.7666	10770016.57
19.953	312.5259341	100588.1899	9772369.833
22.909	411.9854906	67966.70533	8704522.631
26.303	543.1005301	45058.67863	7607211.941
30.2	715.9514	29162.0886	6490363.423
34.674	943.7947267	18397.88021	5397743.208
39.811	1244.158841	11249.3021	4350790.491
45.709	1640.110455	6658.503245	3394818.792
52.481	2162.090458	3820.374413	2567713.469
60.256	2850.166646	2128.934966	1886251.697
69.183	3757.235679	1162.323624	1357572.921
79.433	4953.037169	626.0321232	963906.7642
91.201	6529.333585	332.7315552	675355.5132
104.713	8607.37771	174.8948256	467967.1468
120.226	11346.61849	89.8768992	317010.1003
138.038	14957.77421	45.5963376	212008.4974
158.489	19718.22905	23.120064	141709.278
181.97	25993.76851	11.5694304	93502.59933
208.93	34266.61975	6.1183584	65149.73628
239.883	45171.92515	3.3317328	46813.15841
275.423	59548.39571	1.8702816	34594.83805
316.228	78500.11617	1.104312	26902.53235
363.078	103483.1228	0.610896	19682.1635
416.869	136417.1141	0.3477408	14693.53797
478.63	179833.0414	0.1127808	6398.763638
549.541	237066.3189	0.0328944	2476.927909

Total cross section area of all microcapsules in 1 cm ² of fabric (S _{mc})			730133616.2
Fabric B4 (loop length of 2.96 mm)			
Microcapsule diameter (μm)	Cross section area of one microcapsule (μm ²)	Number of microcapsules in 1 cm ² of fabric	Total cross section area of all microcapsules (μm ²)
1.66	2.163146	304854.5803	659444.966
1.905	2.848784625	2823970.025	8044882.388
2.188	3.75806504	3594502.572	13508374.45
2.512	4.95346304	3694939.847	18302747.97
2.884	6.52920296	3488048.135	22774174.21
3.311	8.605735985	3111891.625	26780117.74
3.802	11.34733514	2689592.684	30519709.57
4.365	14.95678163	2246823.933	33605254.92
5.012	19.71931304	1849695.636	36474727.27
5.754	25.99018506	1507907.27	39190789.01
6.607	34.26717247	1203936.036	41255483.79
7.586	45.17470586	945518.8328	42713535.16
8.71	59.5533185	728084.2173	43359831.29
10	78.5	548036.5685	43020870.63
11.482	103.4915143	405337.7337	41949015.88
13.183	136.4263189	293373.7627	40023902.5
15.136	179.8423194	209115.8615	37607881.54
17.378	237.0659839	146143.7666	34645715.83
19.953	312.5259341	100588.1899	31436418
22.909	411.9854906	67966.70533	28001296.44
26.303	543.1005301	45058.67863	24471392.25
30.2	715.9514	29162.0886	20878638.16
34.674	943.7947267	18397.88021	17363822.33

39.811	1244.158841	11249.3021	13995918.66
45.709	1640.110455	6658.503245	10920680.78
52.481	2162.090458	3820.374413	8259995.065
60.256	2850.166646	2128.934966	6067819.432
69.183	3757.235679	1162.323624	4367123.79
79.433	4953.037169	626.0321232	3100760.375
91.201	6529.333585	332.7315552	2172515.318
104.713	8607.37771	174.8948256	1505385.823
120.226	11346.61849	89.8768992	1019798.887
138.038	14957.77421	45.5963376	682019.7228
158.489	19718.22905	23.120064	455886.7176
181.97	25993.76851	11.5694304	300733.0956
208.93	34266.61975	6.1183584	209655.4608
239.883	45171.92515	3.3317328	150500.7846
275.423	59548.39571	1.8702816	111372.2688
316.228	78500.11617	1.104312	86688.62029
363.078	103483.1228	0.610896	63217.42576
416.869	136417.1141	0.3477408	47437.79638
478.63	179833.0414	0.1127808	20281.71427
549.541	237066.3189	0.0328944	7798.15432
Total cross section area of all microcapsules in 1 cm ² of fabric (S _{mc})			730133616.2
Fabric B5 (loop length of 3.05 mm)			
Microcapsule diameter (μm)	Cross section area of one microcapsule (μm ²)	Number of microcapsules in 1 cm ² of fabric	Total cross section area of all microcapsules (μm ²)
1.66	2.163146	301169.7531	204996
1.905	2.848784625	2789836.237	2500843.591
2.188	3.75806504	3551055.23	4199232.505

2.512	4.95346304	3650278.504	5689618.28
2.884	6.52920296	3445887.526	7079612.205
3.311	8.605735985	3074277.682	8324905.515
3.802	11.34733514	2657083.137	9487400.358
4.365	14.95678163	2219666.204	10446577.37
5.012	19.71931304	1827338.062	11338585.62
5.754	25.99018506	1489680.948	12182904.44
6.607	34.26717247	1189383.864	12824738.4
7.586	45.17470586	934090.1918	13277990.32
8.71	59.5533185	719283.7441	13478898.87
10	78.5	541412.3607	13373529.05
11.482	103.4915143	400438.3501	13040330.81
13.183	136.4263189	289827.706	12441887.24
15.136	179.8423194	206588.2438	11690839.53
17.378	237.0659839	144377.303	10770016.57
19.953	312.5259341	99372.36397	9772369.833
22.909	411.9854906	67145.18063	8704522.631
26.303	543.1005301	44514.047	7607211.941
30.2	715.9514	28809.60165	6490363.423
34.674	943.7947267	18175.50202	5397743.208
39.811	1244.158841	11113.32994	4350790.491
45.709	1640.110455	6578.020826	3394818.792
52.481	2162.090458	3774.196922	2567713.469
60.256	2850.166646	2103.202181	1886251.697
69.183	3757.235679	1148.274428	1357572.921
79.433	4953.037169	618.4651704	963906.7642
91.201	6529.333585	328.7097744	675355.5132

104.713	8607.37771	172.7808432	467967.1468
120.226	11346.61849	88.7905424	317010.1003
138.038	14957.77421	45.0452072	212008.4974
158.489	19718.22905	22.840608	141709.278
181.97	25993.76851	11.4295888	93502.59933
208.93	34266.61975	6.0444048	65149.73628
239.883	45171.92515	3.2914616	46813.15841
275.423	59548.39571	1.8476752	34594.83805
316.228	78500.11617	1.090964	26902.53235
363.078	103483.1228	0.603512	19682.1635
416.869	136417.1141	0.3435376	14693.53797
478.63	179833.0414	0.1114176	6398.763638
549.541	237066.3189	0.0324968	2476.927909
Total cross section area of all microcapsules in 1 cm ² of fabric (S _{mc})			721308371.6

Appendix 10

Procedure of calculating the weight percentage of ibuprofen released from the microcapsule-treated fabrics into the receptor fluid

(to investigate the influence of the loop length on the active release capability of the microcapsule-treated fabric)

The content of microcapsule in the fabric M_{mc_fbr} (mg) was calculated by:

$$M_{mc_fbr} = M_6 - M_5 \text{ (mg)} \quad (Eq\ 0.13)$$

with M_5 and M_6 were the weights of the fabric sample before and after the fabric treatment with microcapsules (see the description of applying the microcapsules to the fabric by impregnating).

The content of ibuprofen in the fabric m_{Ibu_fbr} (mg) was calculated by:

$$m_{Ibu_fbr} = M_{mc_fbr} \times \frac{L}{100} \text{ (mg)} \quad (Eq\ 0.14)$$

In which $L(\%)$ was the drug loading ratio of microcapsule.

When the ibuprofen concentration in the receptor fluid was C_{rl} (mg/ml), the correlative content of ibuprofen m_{Ibu_rl} (mg) was calculated by:

$$m_{Ibu_rl} = C_{rl} \times 10 \text{ (mg)} \quad (Eq\ 0.15)$$

And the weight percentage of ibuprofen in microcapsule-treated fabric released into the receptor fluid after 24 hours, coded as $Ibu_{rl}(\%)$, was calculated by:

$$Ibu_{rl}(\%) = \frac{m_{Ibu_rl}}{m_{Ibu_fbr}} \times 100\% \quad (Eq\ 0.16)$$

Since the radius of the microcapsule-treated fabric samples $r_{rl} = 3$ cm, the weight of ibuprofen released per cm^2 of the fabric $Ibu_{rl}(mg/cm^2)$ could be calculated as below:

$$Ibu_{rl}(mg/cm^2) = \frac{m_{Ibu_rl}}{\pi \times r_{rl}^2} \times 100\% = \frac{m_{Ibu_rl}}{28.26} \times 100\% \quad (Eq\ 0.17)$$

Appendix Table 5: Procedure of calculating the weight percentage of ibuprofen released into the receptor fluid

Fabric lot	B3	B4	B5
Loop length (mm)	2.87	2.96	3.05
M_{mc_fbr} (mg) from (Eq 0.13)	166	166	164
m_{Ibu_fbr} (mg) from (Eq 0.14)	11.79	11.79	11.64

C_{rl} (mg/ml) by HPLC	0.064	0.067	0.024
$m_{Ibu_{rl}}$ (mg) from (Eq 0.15)	0.64	0.67	0.24
Ibu_{rl} (%) from (Eq 0.16)	5.43	5.68	2.06
Ibu_{rl} (mg/cm ²) from (Eq 0.17)	0.0226	0.0237	0.0085

Appendix 11

Procedure of calculating the weight percentage of ibuprofen released from the microcapsule-treated fabrics into the receptor fluid

(to investigate the influence of the fabric extension on the active release capability of the fabric)

The content of the microcapsules on the experimental fabric sample ($D_t = 20$ cm) was signed as M_{tt} and calculated by:

$$M_{tt} = m_{af} - m_{bf} \text{ (mg)} \quad (\text{Eq 0.18})$$

With m_{af} and m_{bf} were the weight of the fabric sample before and after the microcapsule treatment. The amount of the microcapsules on the sample E_i ($i=\overline{1,3}$) with the diameter of d_{ri} was signed as M_{ri} and calculated by:

$$M_{ri} = \frac{d_{ri}^2}{D_{tt}^2} \times M_{tt} \text{ (mg)} \quad (\text{Eq 0.19})$$

Then the content of ibuprofen on the sample E_i ($i=\overline{1,3}$), which was signed as m_{ibu} , was calculated by:

$$m_{ibu} = M_{ri} \times \frac{L}{100} \text{ (mg)} \quad (\text{Eq 0.20})$$

With $L(\%)$ was the ibuprofen loading ratio of microcapsules.

Since 15 ml of the receptor fluid was used for each fabric sample, when the concentration of ibuprofen in the receptor fluid determined by HPLC system was C_{ri} (mg/ml), the correlative content of ibuprofen $m_{ibu_{ri}}$ would be calculated by:

$$m_{ibu_{ri}} = C_{ri} \times 15 \text{ (mg)} \quad (\text{Eq 0.21})$$

Therefore the weight percentage of ibuprofen in the microcapsule-treated fabric dissolved into the receptor fluid would be:

$$Ibu_{ri}(\%) = \frac{m_{ibu_{ri}}}{m_{ibu}} \times 100\% \quad (\text{Eq 0.22})$$

Appendix Table 6: Weight percentage of ibuprofen in the microcapsule-treated fabrics released into the receptor fluid Ibu_{ri} according to the fabric extension

Fabric sample	E1	E2	E3
Sample diameter (cm)	5	6	8
M_{ri} (mg) from (Eq 0.19)	72.43	104.3	185.43
m_{ibu} (mg)	4.02	5.79	9.25

from (Eq 0.20)			
C_{ri} (mg/ml)	0.12	0.15	0.25
$m_{Ibu_{ri}}$ (mg) from (Eq 0.21)	1.8	2.25	3.68
Ibu_{ri} (%) from (Eq 0.22)	44.78	38.87	35.76